INVESTIGATION ON EXTRUDED MATERIALS AS HIGH VOLTAGE DIRECT-CURRENT CABLES INSULANTS

A Thesis for the degree of

MASTER OF PHILOSOPHY

submitted to the

UNIVERSITY OF SOUTHAMPTON

by

F.K. AMOURI

B.Sc. Elec. Eng.

September, 1977

CONTENTS

LIST OF FIGURES

UNIVERSITY OF SOUTHAMPTON

ABSTRACT

FACULTY OF ENGINEERING AND APPLIED SCIENCE

ELECTRICAL ENGINEERING

Master of Philosophy

INVESTIGATION ON EXTRUDED MATERIALS AS HIGH VOLTAGE DIRECT CURRENT CABLES INSULANTS

by Farook Khalil Amouri

The values of the resistivity and its dependence on stress and temperature are reported for tests on flat sheet samples of polyethylene, XLPE, EPR and polypropylene. It is found that the time required for steady state conditions to be obtained is so high as to make defined values of resistivity very difficult to obtain.

However computer investigation of the practical significance of this, indicates that with a normal cyclic load on a D.C. cable the variation of resistivity with time does not have a marked effect.

In order to obtain steady-state values of resistivity for polyethylene the use of additives up to 5% by weight is considered. The additives considered are, carbon black, talc and mica and in all cases steady state conduction is reached within a few hours.

Computer design studies are reported which determine steady state stress in the dielectric and transient stresses resulting from impulses and voltage reversal. The design of cables for maximum power capacity is given.

CHAPTER ONE

1-1 GENERAL INTRODUCTION

The growth of the size of the transmitted power in the last few years has increased the complexity of the A.C. transmission systems. This increase has demanded a corresponding increase in the stability and reliability of the whole system. The conditions on which the D.C. system can be adopted are:

a - The economic consideration corresponding to the long distance transmissions.

b - The use of D.C. links or interconnection in the large A.C. systems is to provide the adequate reliability.

c - Submarine D.C. links.

The advantages of D.C. transmission system over the A.C. transmission system from the insulation point of view are:

1 - Breakdown stress of the insulation in D.C. transmission system is higher than that of the A.C. transmission system.

2 - The absence of the charging current in a D.C. cable which obviously becomes of great importance for long cable links.

3 - The D.C. transmission system is rather more economic than the A.C. transmission system.

4 - The size of the partial discharges within the D.C. cable insulation is less than that of the A.C. cable.

5 - The dielectric losses of the D.C. cable is very small compared to that of the A.C. cable.

The properties of oil-impregnated paper used with high-voltage D.C. cables are well known.[1] So, it is useful to investigate the thermoplastics polyethylene and polypropylene as high-voltage extruded D.C.

cable insulants, due to the fact that polyethylene cables could be economically competitive. They are most simpler to instal and for long underwater crossing do not have the restrictions of paper/oil cables.

The thermal conductivity of polyethylene is higher than that of oil-impregnated paper. The electrical resistivity, which varies considerably according to the temperature and electric stress, is the main factor effecting the stress distribution in D.C. cables.

In the CIGRE Report 1958,[12] there is a study of models having polyethylene insulation extruded over a copper conductor. There are carbon paper tapes used as a screen on the conductor and on the sheath. As a result of these tests, it was concluded that the use of polyethylene as insulant for submarine high voltage D.C. cables (200 kV) is possible.

Hawley, Body and Mason in 1966[20] introduced a new manufacturing technique to avoid the partial discharge problem between the conductor and polyethylene insulant by tightly bonding the conductor, core screens and the polyethylene insulant. It was reported that polyethylene will be successful in the future as a high-voltage D.C. cable insulant.

Oudin and Fallou[21] made a special study on several cable models insulated with extruded polyethylene of different thicknesses with aluminium or copper conductors. The results obtained by their tests showed that all the insulated cables failed at their terminals inspite of different design methods of these terminals, after a test duration time ranging from 950 hours and 2100 hours at different loading temperatures. The results of these tests show that the temperature has a very important effect on the life of the polyethylene cables. Oudin and Fallou[21] concluded that the use of extruded polyethylene in submarine cables is possible, but at the shallow depths there were problems due to lower compression.

The use of Ethylene-Propylene-Rubber (EPR) in high temperature cables is more convenient, due to its high working temperature. EPR is used in A.C. cables up to 60 kV.[32] The results obtained by Davini, Consotini and Portinari[32] on the investigation of the EPR insulant show that, the EPR has a partial discharge (corona) resistance better than the polyethylene. EPR shows little crystallinity and its vulcanization are rubber-like.[32] It is well known that saturated rubbers exhibit a very high resistant to deterioration and to cracking induced by ozone.[33] The disadvantages of EPR are that, it has a high thermal resistance and low impulse dielectric strength.

High-voltage extruded D.C. cables can be divided into three main types according to the methods of installation which are:

1 - Submarine cables.

2 - Land cables. This sort of cable can be divided into two types:

a - Naturally cooled cables directly buried in the soil using selected backfills.

b - Internally cooled cables: These cables are used for heavy-duty power transmission.

The D.C. cables are subjected to sudden surges due to: a - polarity reversals, b - switching surges, c - malfunction of the converter, and d - lightning impulse surges.

1-2 SCOPE OF THE PRESENT RESEARCH

The purpose of this work is to study certain types of thermoplastic materials, as polyethylene, polypropylene, and cross-linked polyethylene, and also the elastomer, EPR, as high-voltage extruded D.C. cable insulants. Also to study the design of such cables. The procedure of the research is:

1 - To investigate the conduction mechanism of the current created in the specimen, due to the effect of applying a uniform direct electric field. The important case is the ability of the conduction current to reach steady-state in a short time (few hours) at temperatures less than 50 ^{o}C.

2 - To study the resistivity of the dielectric at different values of stress and temperature, since the resistivity of the dielectric varies with both temperature and stress.

3 - To study the stress distribution in D.C. cables at steady-state voltage and at transient voltages by computer technique.

4 - To study the effect of the environment on high-voltage D.C. cables, specially the effect of the environment on the heat dissipation from the cable.

5 - To use the results from the experimental tests for the best design of high-voltage D.C. cable for each type of the tested materials.

6 - Improvement of the insulation: The problem of the difficulty to get steady-state current in the thermoplastic material is due to the existence of the traps between the crystalline amorphous boundaries, at which the space charge carriers are held. A very long time is needed to reach the steady-state i.e. the state at which the trapping rate is equal to the detrapping rate. The decrease of the resistivity cause a reduction of the time needed to reach the steady-state. This can be achieved by inserting a certain type of additives which has the ability to generate ions or electrons. The generated ions or electrons from the additives, by its activation energy, has the ability to penetrate the potential barriers of the traps. The generation of the ionic or electronic migration in the bulk of the dielectric produce the equilibrium between the injected carriers and the emitted carriers. At the same time

the decrease of the resistivity of the dielectric cause a decrease in the intrinsic electric field. As a result of this, the size of the corona discharges within the micro voids decreases.

7 - To discuss the conduction mechanism of the improved dielectric materials. A general review of theoretical and experimental studies of conduction in dielectric materials is presented in Chapter Two.

Details of the test cell construction and measuring instruments as well as the method of coating the specimens are given in Chapter Three.

The D.C. conduction current measurements and the resistivity investigation of the polyethylene, EPR and polypropylene, over a certain range of applied fields (4 kV/mm - 40 kV/mm) and at temperatures between ambient and 80 ^{o}C, are introduced in Chapter Four.

The D.C. conduction current measurements and the resistivity investigation of the cross-linked polyethylene, polyethylene with a few percent of additives, over a certain range of applied fields (6 kV/mm to 30 kV/mm) and at temperatures between 40 ^{o}C and 80 ^{o}C, are described in Chapter Five.

Discussion of the experimental results is carried out in Chapter Six.

The computation of the steady-state and transient stress distribution in D.C. cable, the computation of the transient temperature rise, and the computation of over-load on the D.C. stress distribution are discussed in Chapter Seven.

In Chapter Eight, the established design for the various dielectric materials, investigated in this work, are carried out.

CHAPTER TWO

REVIEW OF MODELS FOR CONDUCTION IN DIELECTRICS

2-1 INTRODUCTION

The insulation resistance of a material placed between two electrodes is defined as the ratio of the direct voltage applied to the total current flowing between the electrodes, it is composed of the "volume resistance" and the "surface resistance".

The volume resistance is the ratio of the direct voltage applied to that portion of the current passing through the volume of the specimen. The surface resistance is the ratio of the direct voltage applied to the current passing across the surface of the specimen. When the direct voltage is applied to a capacitor with solid dielectric, the current flowing varies in a complex manner with time. It falls from an instantaneous high value at a decaying rate to a constant lower value.

This current is composed of three parts, the normal charging current, the reversible absorption current and the leakage or conduction current. Resistivity can only be defined when steady-state current has been established.

In order to understand the behaviour of dielectrics under direct voltage conditions (high voltage), it is necessary to review previous mechanisms which have been proposed to explain the conduction phenomena.

2-2 TRANSIENT CONDUCTION IN DIELECTRICS AT HIGH FIELDS [> 1.0 kV/mm]

When a certain constant field is applied to any type of dielectric, the current response rises and then falls to an equilibrium (steady-state condition).

The transient current follows the following empirical formula.[1]

$$I_c(t) = C V t^{-n} \qquad \text{- - - (2-1)}$$

where, "C" and "n" are constants and "V" is the applied voltage.

The fact that certain materials are considered as insulants is due to:[22]

a - High metal-insulator contact work function.

b - The existence of the traps in the insulator which attenuate the space-charge-limited current.

The traps have been postulated by many workers.[10] The postulated model depends on the fact that the thermoplastic polyethylene consists of two different conductivity regions (crystalline and amorphous). The potential barriers obtained at the boundaries between the high conductivity crystalline regions and the low conductivity amorphous regions behaves as a trap in which the space charge carriers are held.

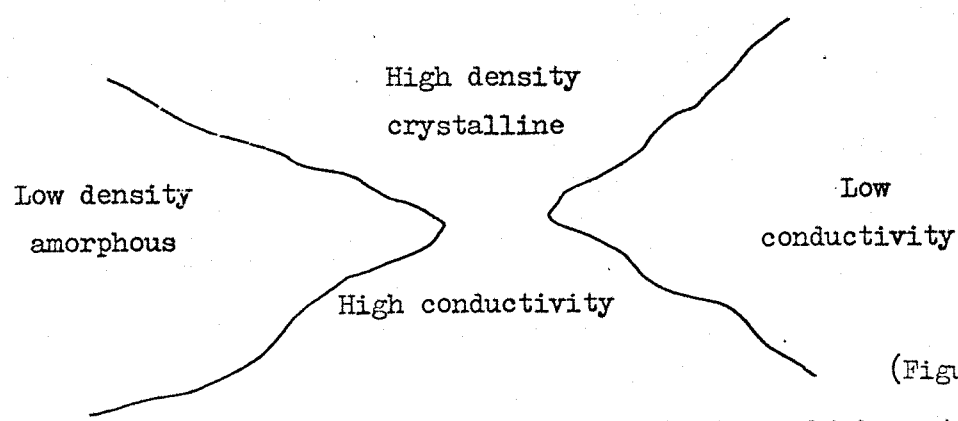

(Figure 2-1)

In addition to this a trap is existent in the lattice which contain impurities. The current follows these conditions, which are designated as trapping, detrapping and steady-state (equilibrium between trapping and detrapping of electron carriers).

In analysis of the transient conduction current at high fields,[2] it was observed that the emission (detrapping) rate of electrons from traps, is small compared to the trapping rate.

At a thermal equilibrium, the conditions of the conduction current can be discussed in two ways.

a - As mentioned above, the initial detrapping rate may be negligible compared to charge trapping rate, but as the space charge of the free electrons builds up the injection current decreases reducing the trapping rate. The field at the leading edge of the trapped charge distribution increases causing an increase in the detrapping rate. Thus both effects act to make an equilibrium between trapping and detrapping rates.

b - Poor injection-contact causes the initial field of electron injected into the insulator to be high enough to cause a significant detrapping immediately. It was found that the detrapping mechanism is exponentially dependent on the field[2] and temperature.[22]

The other mechanisms accounting for the time-dependent conductivity in insulating materials are:[1]

1 - The rotation of dipolar groups.

2 - The surface charge build up at the interface between regions having different conductivities (interfacial polarization), which is either on microscopic scale (molecule) or on submicroscopic scale (atoms).

3 - Ions of opposite sign build up at one or both electrodes.

2-3 STEADY STATE CONDUCTION - TEMPERATURE DEPENDENCE

The temperature dependence of steady state current in dielectrics is similar to that observed in semi-conductors, since the current density usually varies with temperature, according to the Arrhenius relation

$$\text{Log } J = \text{constant} + (W/KT) \qquad \text{- - - (2-2)}$$

where "K" is Boltzmann's constant, and "W" is the activation energy.

Garton and Parkman[7] found that the activation energy of conduction is increased greatly (up to 2.2 eV) by prolonged evacuation at 70 °C. In this case they found that the conductivity is sensitive to extremely small partial pressures of water vapour, and also the well-known temperature-dependence of the crystalline/amorphous volumetric ratio, which is slow enough at 70 °C. At 110 °C a very fast transition occurs forcing the straight line of the Arrhenius to be concaved.

2-4 STEADY STATE CONDUCTION, "CURRENT-STRESS CHARACTERISTICS"

2-4-1 Poole-Frenkel Theory[8]

The first formula discussing the relationship between the conduction current and the stress at high field was obtained by Poole (1916) as[1]

$$\text{Log } J = \text{constant} + \beta E \qquad \text{- - - (2-3)}$$

where J - is the current density,

β - stress coefficient,

E - is the stress.

Poole-Frenkel in 1938 derived a formula which has been described as the current-voltage dependence arising from the field-dependent thermionic emission from traps in the bulk of the insulator. The lowering of the thermionic work-function of the trapped electrons by the effect of the applied field is shown in (Figure 2-2).

As the potential of the trapping is a constant potential "Coulomb potential", then the potential energy to the right of the trap in the presence of the applied field "E" is given by

$$e.\ V_{(X)} = - e.X.E - \frac{e \cdot e}{X \cdot \epsilon} \qquad \text{- - - (2-4)}$$

The condition of the maximum potential is

$$X_o = \left(\frac{e}{\epsilon \cdot E} \right)^{1/2} \qquad \text{- - - (2-5)}$$

$\therefore$ the work-function is reduced by

$$\Delta\Phi = \left(\frac{e^3 E}{\epsilon} \right)^{1/2} \qquad \text{- - - (2-6)}$$

The electrical conductivity is defined by Poole-Frenkel as follows:

a - In the absence of electric field, the number of free electrons present in the conduction band due to thermal ionization from traps is proportional to EXP $(-\Phi/2K_oT)$

b - In the presence of the electric field, the electrical conductivity is proportional to,

$$\sigma \propto e^{\left[\frac{-(\Phi - \Delta\Phi)}{2K_oT} \right]}$$

or

$$\sigma = \sigma_o e^{\left[\frac{\Delta\Phi}{2K_oT} \right]}$$

$$\therefore \quad \sigma = \sigma_o e^{\left[\left(\frac{e^3E}{\epsilon} \right)^{1/2} / K_oT \right]} \qquad \text{- - - (2-7)}$$

2-4-2 Schottky Emission (1914)

Basically it is a thermionic emission from an electrode into the conduction band of the dielectric, with the image force taken into account. The appropriate potential barrier is shown in (Figure 2-3) and the equation of the emission current is[8]

$$J = A\,T^2 e^{\left[- \frac{(\Phi - \Delta\Phi)}{K_oT} \right]}$$

then

$$J = A\,T^2 e^{\left[- \frac{(\Phi - \left(\frac{e^3E}{\epsilon} \right)^{1/2}}{K_oT} \right]} \qquad \text{- - - (2-8)}$$

where '$\Delta\Phi$' is the lowering of the barrier and 'A' is constant.

Equation (2-6) shows that a linear relationship could be obtained by drawing log of current density against the $(\text{field})^{1/2}$.

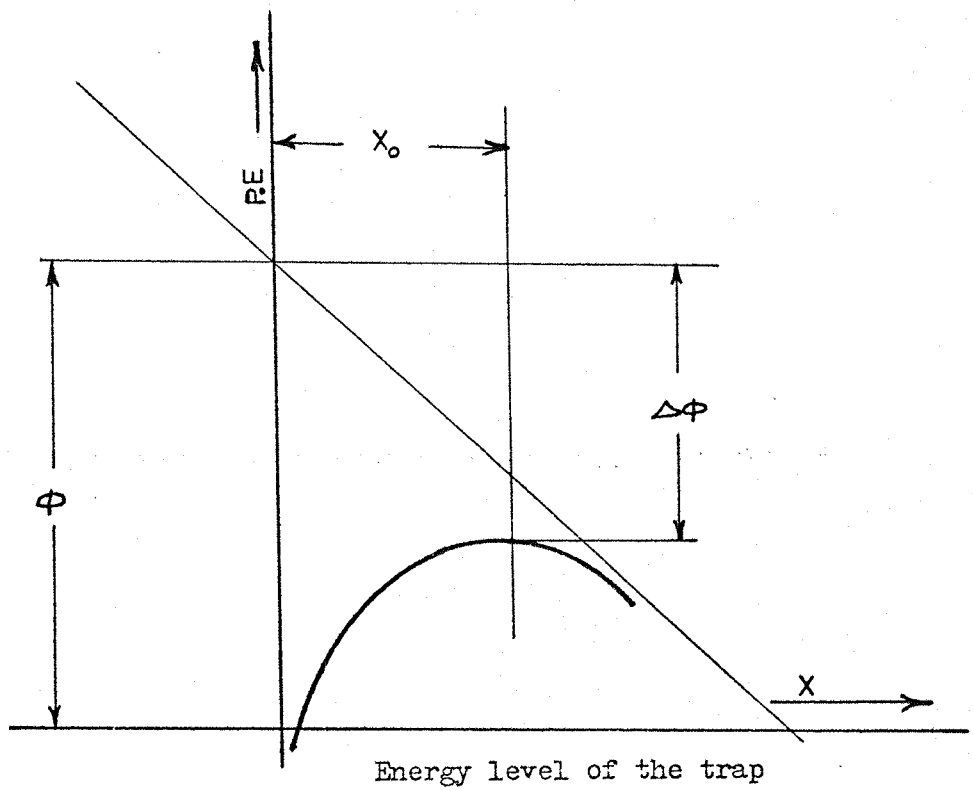

(Figure 2-2) Potential-energy diagram illustrates the Poole-Frenkel effect. 'Φ' is the work function in the absence of the field. '$\Delta\Phi$' is the reduction in the work function due to the applied field.

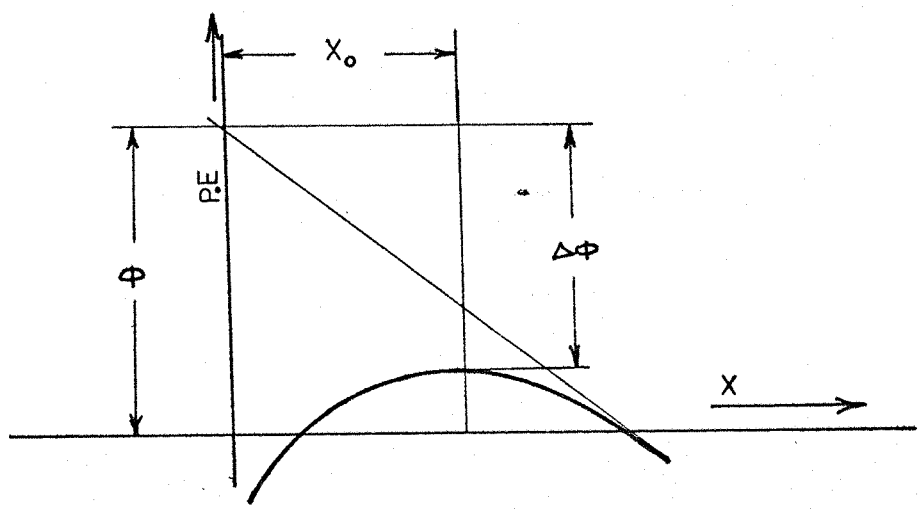

(Figure 2-3) Potential-energy diagram illustrates Schottky effect with the image force taken into consideration.

Comparing equations (2-5) and (2-6) it seems that the temperature-dependence of Poole-Frenkel conductivity differs by factor of two and this is due to the fact that equation (2-5) depends on the position of Fermi-level[8] which is considered to be midway between the trapping level and the bottom of the conduction band.

2-4-3 Space-Charge Limited Conduction

When the cathode is heated sufficiently, a cloud of electrons appears on its surface. In the absence of the electric field it adhers closely to the metal surface due to image force. When the field is applied the electron carriers are pulled towards the anode, and a significant transient current as well as a steady-state current occur. A space charge-limited current is observed when the injected carriers fill the shallow traps completely i.e., when the injected carrier density exceeds the intrinsic carrier density of the insulator. The space charge current depends on the mobility, free charge density, trap density and the field. This can be expressed with the following relationship.

$$J \propto \frac{V^2}{d^3} \qquad \text{- - - (2-9)}$$

2-4-4 Parkman and Garton Theory of Conduction in Polyethylene[7]

Study of the conductivity of purified dry polyethylene in vacuum was carried out by Parkman and Garton. They found that it is necessary to reconsider Poole-Frenkel theory and other hypotheses which have been investigated formerly.

They made a study on the variation of current with respect to field squared i.e., the space charge limited equation and they found that the experimental results differed from those expected theoretically. Also they found that Poole-Frenkel theory failed to cover a wide range of stresses.

The relationship of the conduction current with respect to the applied field obtained from their calculation is ($I \propto E^{3/2}$), which is a combination of Poole-Frenkel and the space charge limited model. In this model, the electrons are injected from the cathode, and their distribution being determined only by the space-charge equation and the traps. The theory takes no account of the material micro-voids, since it is relative only to the electronic conduction in the pure material.

2-5 HIGH FIELD IONIC CONDUCTION

Much work has been done in the field-dependent ionic mobility and on the density of field dependent carrier which is dependent on the degree of dissociation of the divalent impurities and vacancies. All these results which have been mentioned in [1] and [8] show that there is a great identity between the dissociation theory from the point of view of stress dependent with the Schottky or Poole-Frenkel processes.

CHAPTER THREE

EXPERIMENTAL DETAILS

3-1 POLYETHYLENE

The polyethylene produced by polymerisation of ethylene as shown in (Figure 3-1) is a flexible polymer giving good electrical properties.

3-1-1 Low Density Polyethylene

Low density polyethylene is produced under high pressure process giving a polymer of basically single chain type and having short branches of few carbon atoms. The number-average molecular weights range is from 20,000 to 50,000.

Low density polyethylene is generally (50 - 60%) crystalline, the chains in the crystalline region being "straight". The crystallites are platelets about 10 nm thick with the carbon chains being roughly perpendicular to the planes of the platelets, while the molecules themselves are much longer than 10 nm.

The crystal melting point is usually (110 - 115) ^{o}C, softening temperature is (80 - 100) ^{o}C and it is very sensitive to oxidization (with consequent increase in dielectric loss and general deterioration).

The limit of maximum useful temperature is between 70 - 90 ^{o}C. According to these circumstances, polyethylene cables are often designed to run at (< 70 ^{o}C). Polyethylene, above 100 ^{o}C, becomes soluble in many organic solvents. It is very sensitive to sun-light and can not be used out of doors unless loaded with about 2.5% of carbon black. For normal conditions it usually contains antioxidant.

3-1-2 High Density Polyethylene

High density polyethylene is 90% crystalline. It has been produced from ethylene by catalytic process. It is mechanically stable to a higher temperature (crystal melting point 130 - 135 °C). It is stiffer and stronger than the low density polyethylene, and has a better low temperature brittleness. It has a number-average molecular weight of 200,000. A mechanical properties comparison between the high density and low density polyethylene with another polymer is shown in Table 3-1.

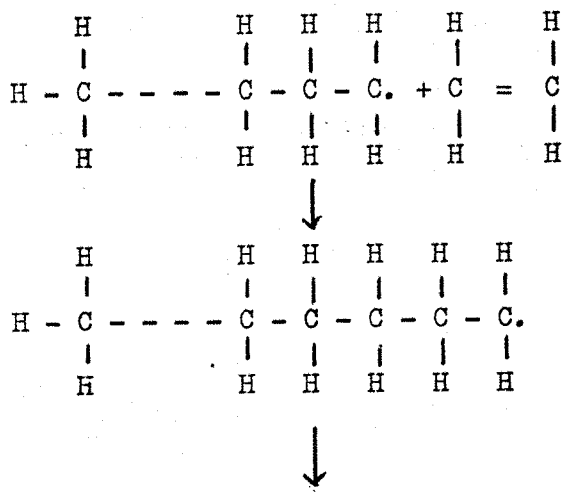

and so on until the chain terminates

(Figure 3-1)

	Density (g/ml)	Hardness (Rockwell)	Tensile strength (N/mm^2)	Compressive strength (N/mm^2)	Tensile modulus elasticity (N/mm^2)	Elongation (%)	Heat (^oC) deflection temp. at $18.5kgF/cm^2$	Crystal melting point Temp. (^oC)	Softening Temp. (^oC)
Polyethylene (Low density)	0.91-0.94	R 3-15	5-20	-	100-300	100-700	33-40	110°C-115°C	80°C-100°C
Polyethylene (High density)	0.94-0.97	R 30-50	15-40	-	500-1200	20-1000	45-55	130°C-135°C	80°C-100°C
Polypropylene	0.9 -0.91	R 90-100	30-40	70	1000-1600	200-700	50-60	165°C	105°C

(Table 3-1)

Mechanical properties of low density polyethylene, high density polyethylene and polypropylene

3-2 TEST CELL

The test cell is constructed from steel. The high-voltage electrode is introduced into the test cell through a P.T.F.E. busing which is profiled to minimize the effect of stress concentration at the test cell wall. The low voltage electrode incorporates a guard ring with 50 μm thickness gap of insulator. The high voltage electrode is movable through an (O) ring and is pressed on the sample with a mechanical pressure of (80.87 gm/cm^2) is obtainable by using a weight of 1051 gm with 537 gm weight of the electrode.

The specimens used are of polyethylene of 125 μm thickness, with one side coated with evaporated aluminium (deposited). It is not easy to use a sample coated on two sides due to the effect of the very small insulation, 50 μm, between the guard ring and the low voltage electrode. An uncoated specimen was used for comparison with the coated one, additionally coating by colloidal graphite is also used.

The tests are performed in the air. An electric heater is used surrounding the test cell. The temperature is controlled by using a thermal controlling device with accuracy of more like $\pm$ 2 ^{o}C. The temperature is measured by a thermo-couple positioned in the guard ring inside the can of the test cell.

3-3 CURRENT MEASUREMENTS

Measurement of current is conducted by using a low range ammeter which is used over a current range 1.2 x 10^{-13}A to 1.2 x 10^{-6}A, in twenty three ranges.

The error percentage of internal meter differs from 1%. at ranges up to 4 x 10^{-8}A, to 2%, at ranges up to 1.2 x 10^{-12}A. The error percentage of external meter which is connected to a chart recorder ranges from 0.25%, at ranges up to 4 x 10^{-8}A, to 1%, at ranges up to 4 x 10^{-12}A.

3-4 STABILITY AND CALIBRATION OF THE AMMETER

It is very important to use a very highly stable ammeter, which needs very high stable generators, because any fluctuations cause relatively large capacitance currents which pass through the tested specimen. By measuring the current from D.C. battery source, for different periods of time through a standard resistor (tolerance $\mp$ 0.1%), it was found that the percentage error is within the limits mentioned in Section (3-3) and Section (3-5).

3-5 HIGH VOLTAGE D.C. SUPPLY

The high voltage D.C. supply used has a maximum output voltage (30 kV) with stability against $\pm$ 10% mains change is 5 p.p.m., the output ripple is 2 parts $10^{\pm 15}$ approximately. The nominal drift after 45 minutes is 25 p.p.m. per 15 minutes, after one hour is 15 p.p.m. per 15 minutes and after a longer time is 5 p.p.m. per 15 minutes.

3-6 RECORDING EQUIPMENT

The potentiometric recorder has a sensitivity of 0-5 mV; 0-10 mV, chart speed 10"/hour. For present purposes i.e., for periods of (24-48) hours and more, a time regulator is used which operates for four minutes every one hour.

3-7 THE METHOD OF TEST

The dielectric specimen which is coated from one side by evaporated aluminium at vacuum (2.0×10^{-5} Torr) is inserted between two plane electrodes, with rounded edges and guard rings according to the following diagram.

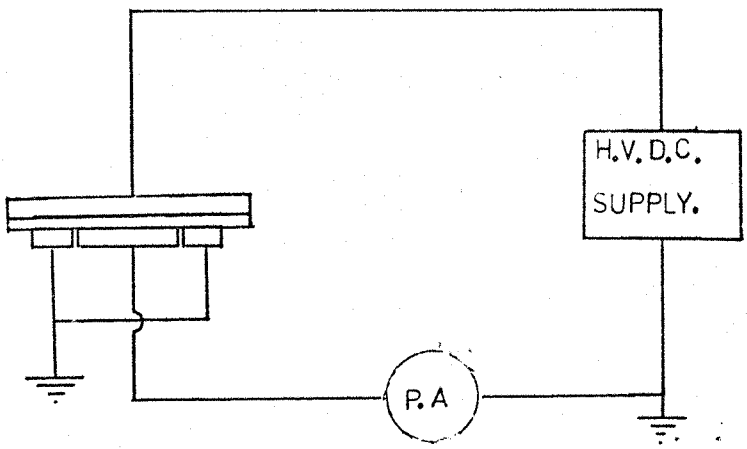

(Figure 3-2)

The high field is obtained by applying the direct voltage from the high voltage D.C. supply.

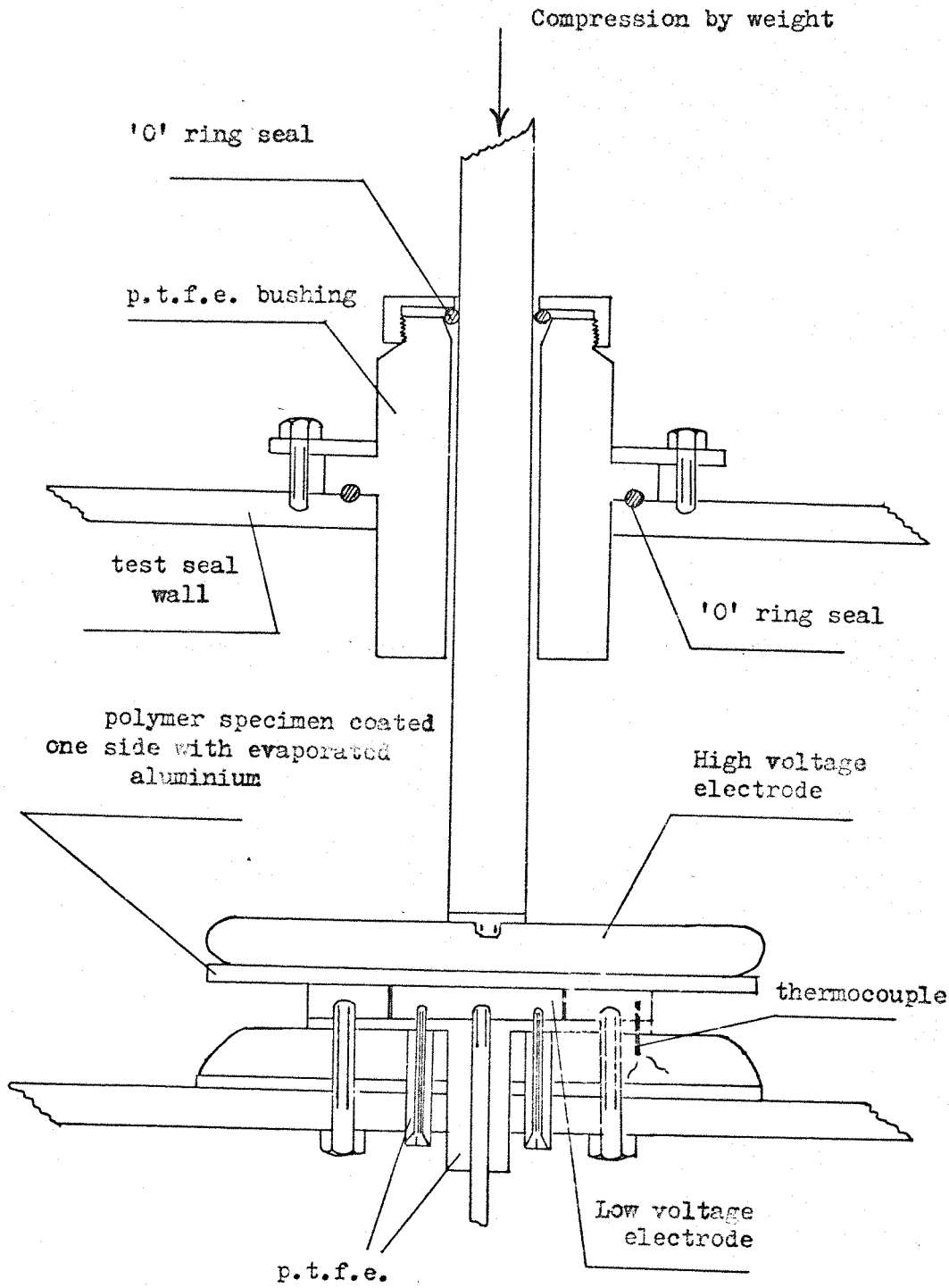

(Figure 3-3)
Diagram of the electrode system

CHAPTER FOUR

RESULTS

4-1 RESULTS FOR POLYETHYLENE

4-1-1 Conduction Current

The measurements of the current show that, the period passing from the instant of voltage application until the current stop decaying takes a long time as shown in (Figures 1-5). At temperatures less than 50 ^{o}C the period needed to reach steady-state is very long ($>$ 10 days).

The decaying percentage of the conduction current is decreased with time. The results obtained (Figure 1) show that the conduction current passing through the volume resistance at constant temperature increases with increase in the stress. At a certain applied field the increase of the temperature increases the magnitude of the conduction current and at the same time decreases the period needed to reach the steady-state.

By plotting the so-called activation plot of log current against the reciprocal of the absolute temperature at different applied fields, it was found that the plot is linear over the temperature range between 50 ^{o}C - 80 ^{o}C and at low stresses in the range of (6-16 kV/mm). At higher stresses a deviation occurs at 80 ^{o}C for the samples of Maker B. The same effect was found with the same polyethylene of Maker B using the uncoated sample. The test was repeated again using polyethylene (Maker C) and the results obtained were different. This conflict is because that, the microcrystalline structures of the two specimens are different due to the two different manufacturing processes.

4-1-2 Transient Current

4-1-2-1 Transient Current at First Applied Field

The transient current obeyed the empirical equation [$I_c(t) = A.t^{-n}$], where A is a constant depending on the temperature and the stress and n is in the range of (0.27 - 0.7) for stresses between 10 kV/mm to 40 kV/mm.

At a temperature of 40 ^{o}C the current decays over a long time which decreases in length as the test temperature is increased from 40 ^{o}C to 80 ^{o}C.

The measurements of conduction current for the fresh specimen show that the amplitude of the charging current is much higher than that of the specimen tested before. The period needed to reach steady-state for the fresh specimen conduction current is much longer than that of the specimen previously subjected to electric field.

4-1-2-2 Discharging at Zero Field : [Short Circuit with Earth]

The discharging current for specimen previously stressed has a rapid initial falling, and then the decay becomes similar to that of the charging current. The discharging current at temperatures more than 60 ^{o}C in a specimen previously stressed with more than 10 kV/mm changes its direction after some time i.e., the decaying current passes the zero limit into the polarity of the original (+) region. The following table shows the dependence of the discharging current on both the temperature and the specimen previously stressed, after 20 minutes of short circuiting the specimen to earth.

Table (4-1) Discharging current after 20 minutes

E (kV/mm) [previous stress]	I_d (A) at 60 °C	I_d (A) at 70 °C	I_d (A) at 80 °C
10	-1.45×10^{-12}	-0.85×10^{-12}	$+0.8\times10^{-12}$
16	-0.2067×10^{-12}	$+0.82\times10^{-12}$	$+2.82\times10^{-12}$
24	-0.25×10^{-12}	-	$+4.65\times10^{-12}$
32	-0.36×10^{-12}	$+0.96\times10^{-12}$	$+6.6\times10^{-12}$

The discharging current takes a long time to reach the zero level at high temperature (in isothermal condition), but it decreases rapidly with decreasing the temperature. It was found for a specimen previously stressed by 32 kV/mm at temperature of 80 °C and a period of 68 hours, that the discharging current was (6.3×10^{-12} A) and then as the temperature decreased to 55 °C the discharging current decreased rapidly to (6×10^{-14} A) and when the temperature increased again the current returned to its value of (6×10^{-12} A) after a few minutes.

The following diagram shows the transient current in 'curve I' at first applied field (usually obtained with fresh samples), curve II shows the discharging current, (during short circuit time), curve III shows the transient current after short circuit.

It was found that it is not easy to obtain the 'curve number I' with a sample previously stressed even if this sample was short circuited to earth for a long time (few days).

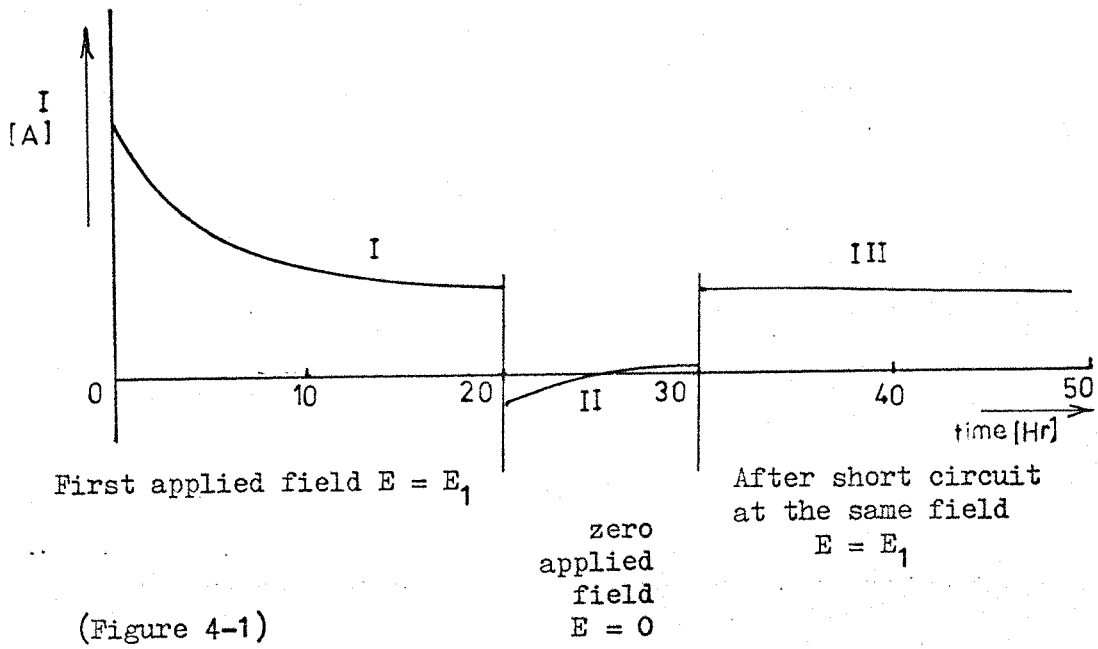

(Figure 4-1)

4-1-3 Resistivity After Twenty Hours

The resistivity of polyethylene varies as a function of both the temperature and the applied field. As shown in (Figure 8), the resistivity of polyethylene at low temperatures is higher than that at high temperatures. As the conduction current continues decaying even after short circuit, the resistivity after short circuit (Figure 11a) differs, i.e. it becomes more than that at first applied field.

The mechanical pressure vibration has no effect on the resistivity in this work, since the mechanical pressure used is more than 50 gm/cm^2. Faraj[11] found that the effect of mechanical pressure vibration on the resistivity was very small at higher values of applied mechanical pressure between 50 gm/cm^2 to 250 gm/cm^2. Since at these pressures there is no vibration due to polyethylene deformation, while the effect was large at low mechanical pressure (0-20 gm/cm^2).

Lawson[1], at high field conduction, found that there is no effect

for the thickness on oil-impregnated paper. Faraj[11], at low fields, found that the resistivity is unaffected by the thickness of the polyethylene.

4-1-4 Effect of Temperature and Stress on Resistivity

Figures (8-11) give the variation of resistivity with applied field for different values of temperature. Figure (10a) gives the variation of resistivity with the reciprocal of the absolute temperature and Figure (10) shows the variation with the temperature in (^{o}C).

Many references give formulae for the variation of resistivity with stress and temperature. In the CIGRE 1958[12], it was found that at a uniform field, the resistivity of the polyethylene is governed by the temperature and the gradient by a formula of the same form, i.e.

$$\rho = \frac{k\, e^{-\alpha\theta}}{E^{\gamma}} \qquad \text{- - - (4-1)}$$

where α - is the value of temperature coefficient appears to be practically independent of the applied voltage. α = constant.

The exponent γ which characterises the variation of the resistance versus voltage.

θ - is the temperature in (^{o}C).

Davey[13] mentioned that the D.C. steady dielectric resistivity for impregnated paper and polyethylene varies with temperature and stress according to the following expression:

$$\rho = \rho_{o}\, e^{-\alpha\theta} \cdot e^{-kE} \qquad \text{- - - (4-2)}$$

where ρ is the dielectric resistivity at temperature θ ^{o}C, and E is the stress in (kV/cm). ρ_{o} - is the dielectric resistivity at a reference temperature e.g. 0 ^{o}C and low stress. α - temperature coefficient of resistivity, k - stress coefficient of resistivity.

Wilkins and Billings[14] mentioned on the conductivity of dielectric of D.C. cable that σ is not constant, it is temperature and stress dependent according to the generally accepted empirical relationship.

$$\sigma = \sigma_o \; e^{\alpha T} \; e^{\beta \, \text{grad } v} \qquad \text{- - - (4-3)}$$

where α and β are constants, T - is the temperature in ^{o}C.

Nobo Ando and Takesh[15] concluded that the resistivity of cable insulation is dependent on both temperature and stress and the dependence is expressed by the following experimental equation.

$$\rho = \rho_o \; e^{[-(\alpha T + \beta E)]} \qquad \text{- - - (4-4)}$$

where T is in ^{o}C.

Eoll[16] assumed that the resistivity of impregnated paper behaves according to the rule.

$$\rho = \rho_o \; e^{-\alpha \theta} \cdot \; e^{-kE} \qquad \text{- - - (4-5)}$$

where θ is in ^{o}C.

Occhini and Maschio[17], mentioned that the conductivity of oil-impregnated paper varies as,

$$\sigma = A \; e^{\left(-\frac{a}{T} + bE\right)} \qquad \text{- - - (4-6)}$$

where T is the absolute temperature.

Chu[18] used the formula for resistivity in oil-impregnated paper which varies as,

$$\rho = \rho_o \; e^{-\alpha \theta} \cdot \; e^{-\beta E} \qquad \text{- - - (4-7)}$$

It is found from Figures (13-15) on Maker B samples that none of the previous theories mentioned in Chapter Two give a linear relation-

ship between the resistivity and stress, within a wide range of stresses (16 - 32 kV/mm).

The results obtained in (Figures 8, 11) on other samples of a different maker (Makers A, and C) show that a linear relationship was observed at resistivity versus the applied stress (First Poole Formula).

The values of the resistivity/temperature coefficient (α) and resistivity/stress coefficient (β) obtained on three different polyethylene samples from different makers, show that, within a wide range of applied field and at a certain temperature, the resistivity/temperature coefficient is slightly increased with the increase of the applied field on samples of Maker B. The results obtained on the samples from Maker A show that the resistivity/temperature coefficient is slightly decreased with the increase of the applied field. The same variation was obtained on the values of the resistivity/stress coefficient (β). The reason of the previous conflict is due to the fact that the values of the resistivity were obtained after twenty hours only, and at this time, the conduction current does not reach the steady-state.

The following tables give the values of the resistivity/temperature coefficient (α), the resistivity/stress coefficient (β), and the values of the corresponding reference resistivity (ρ_o).

Table (4-2-a) Polyethylene, Maker B 125 μm thickness, after twenty hours

α (1/°C)	E (kV/mm)	ρ_o (Ω - cm) (at θ = 40 °C)
0.0700	10	1.6×10^{17}
0.0700	16	3.0×10^{16}
0.0708	24	1.5×10^{16}
0.0743	32	6.6×10^{15}

Table (4-2-b) Polyethylene, Maker B 125μm thickness, after twenty hours

β (cm/kV)	θ (^{o}C)	ρ_o (Ω - cm) (at E = 0.0 kV/mm)
0.0184	50	5.2×10^{17}
0.0179	60	3.1×10^{17}
0.0164	70	1.1×10^{17}

Table (4-3-a) Polyethylene, Maker A 305μm thickness, after twenty hours

α(1/^{o}C)	E (kV/mm)	ρ_o (Ω - cm) (at θ = 40 ^{o}C)
0.0869	9.936	4.5×10^{17}
0.0836	16.40	1.65×10^{17}
0.0733	22.95	7.0×10^{16}
0.0708	29.50	5.3×10^{16}

Table (4-3-b) Polyethylene, Maker A 305μm thickness, after twenty hours

β (cm/kV)	θ (^{o}C)	ρ_o (Ω - cm) (at E = 0.0 kV/mm)
0.01096	40	1.3×10^{18}
0.00274	50	5.3×10^{16}
0.00314	60	3.5×10^{16}
0.00560	80	1.9×10^{16}

The results on polyethylene Maker C (125μm thickness) show that the value of resistivity/stress coefficient (β) is 0.003 cm/kV at 80 ^{o}C temperature and the value of the reference resistivity is 4.5×10^{17} (Ω - cm).

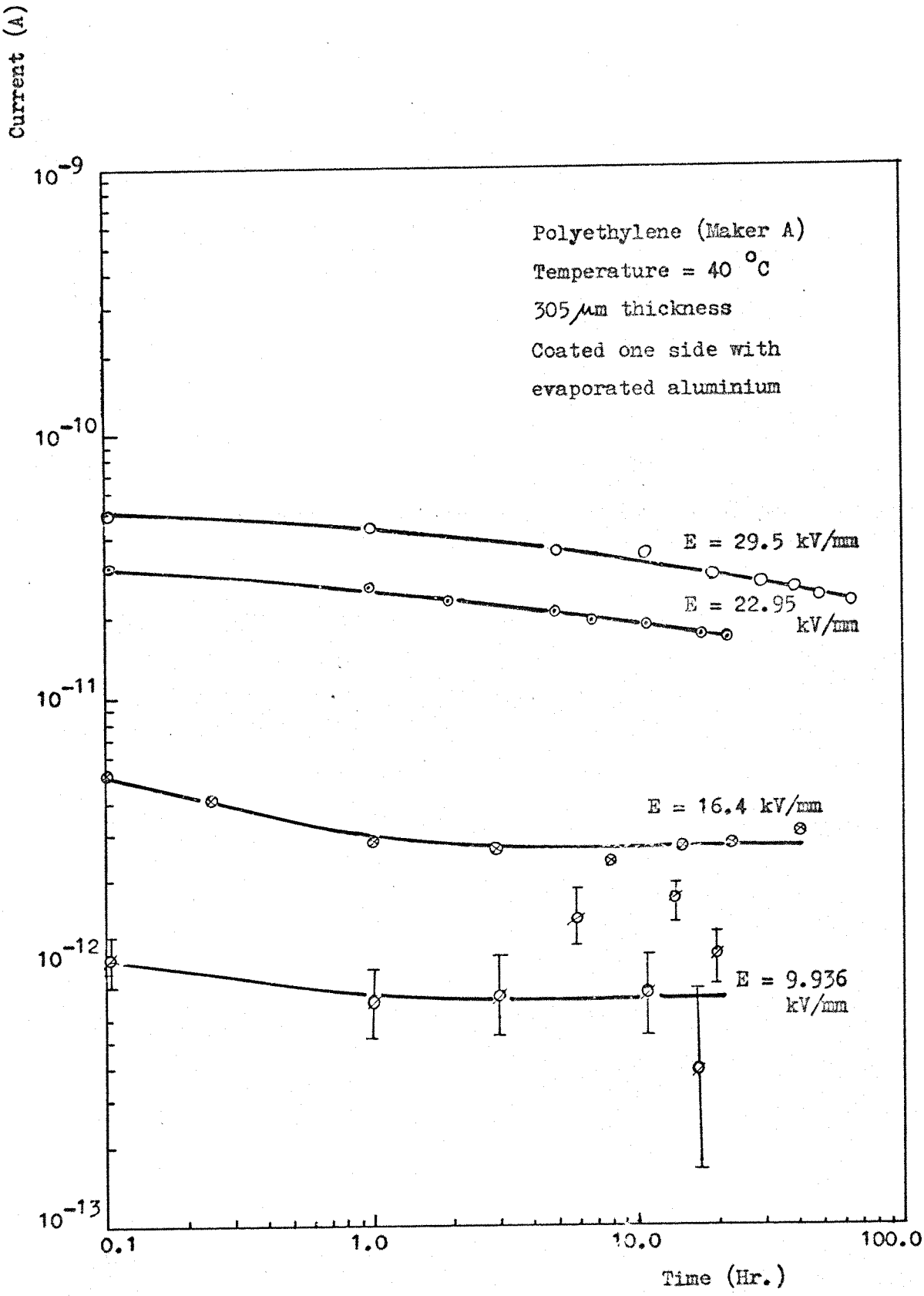

(Figure 1) Plot of conduction current against time

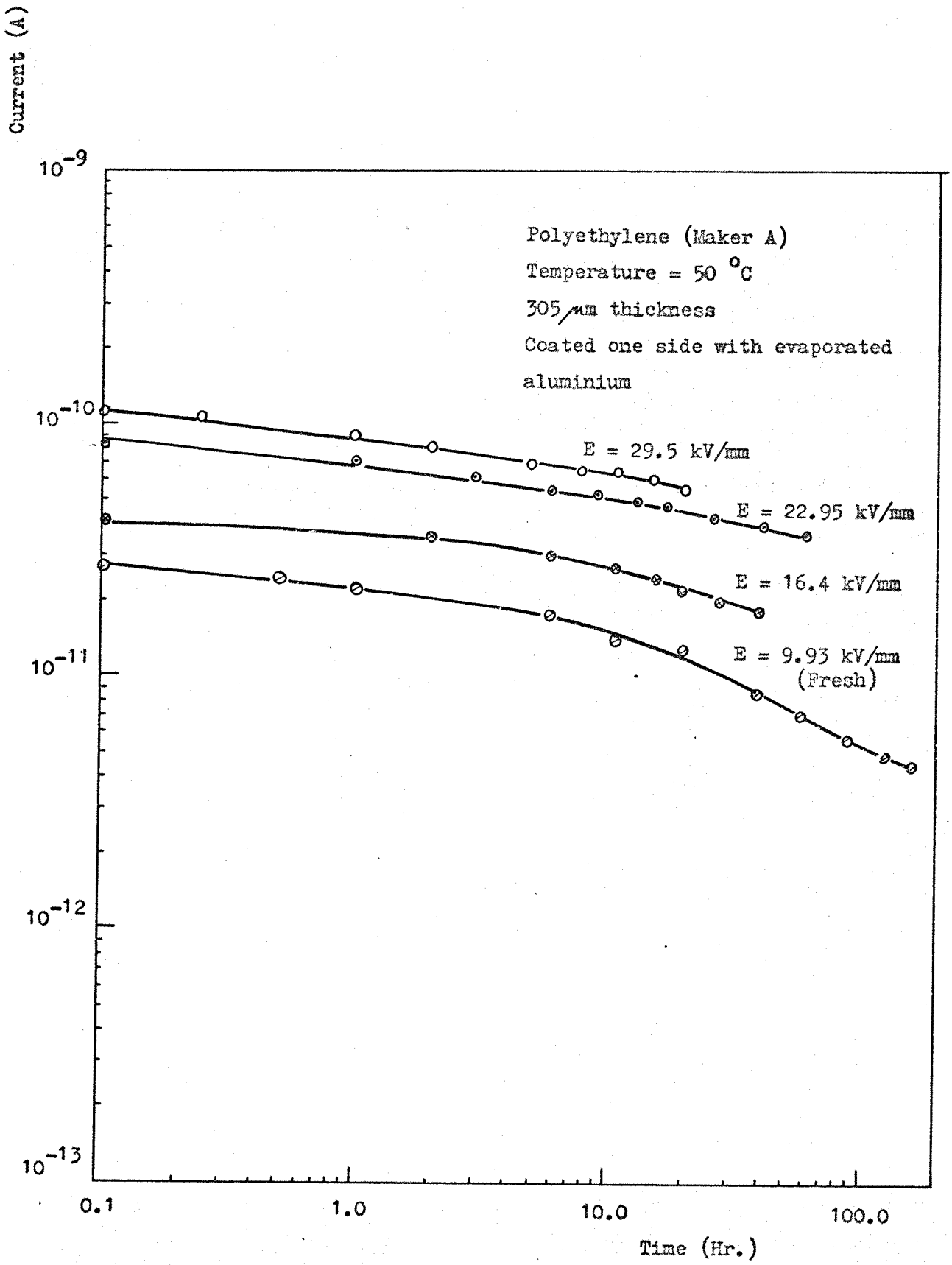

(Figure 2) Plot of conduction current against time

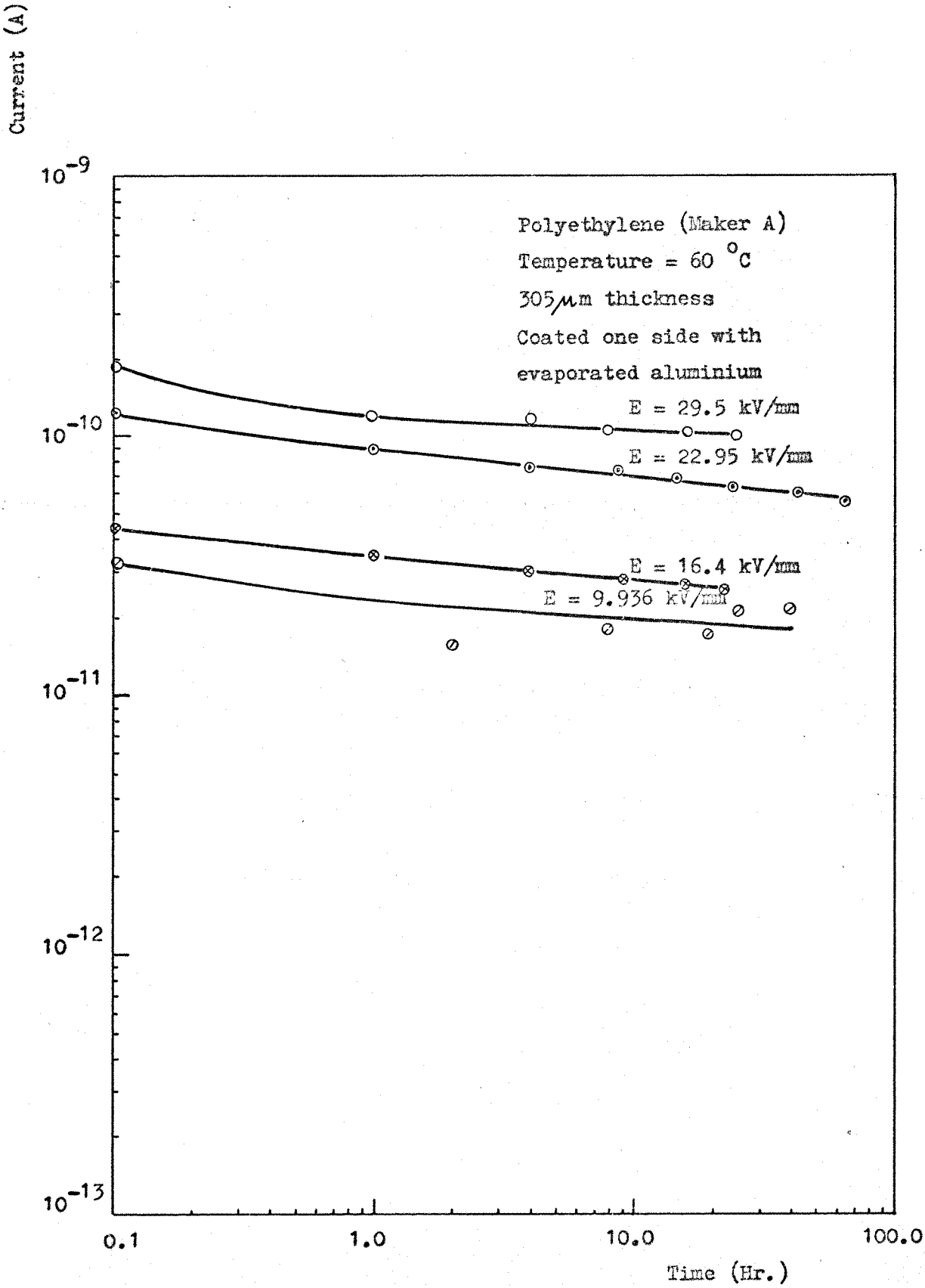

(Figure 3) Plot of the conduction current against time

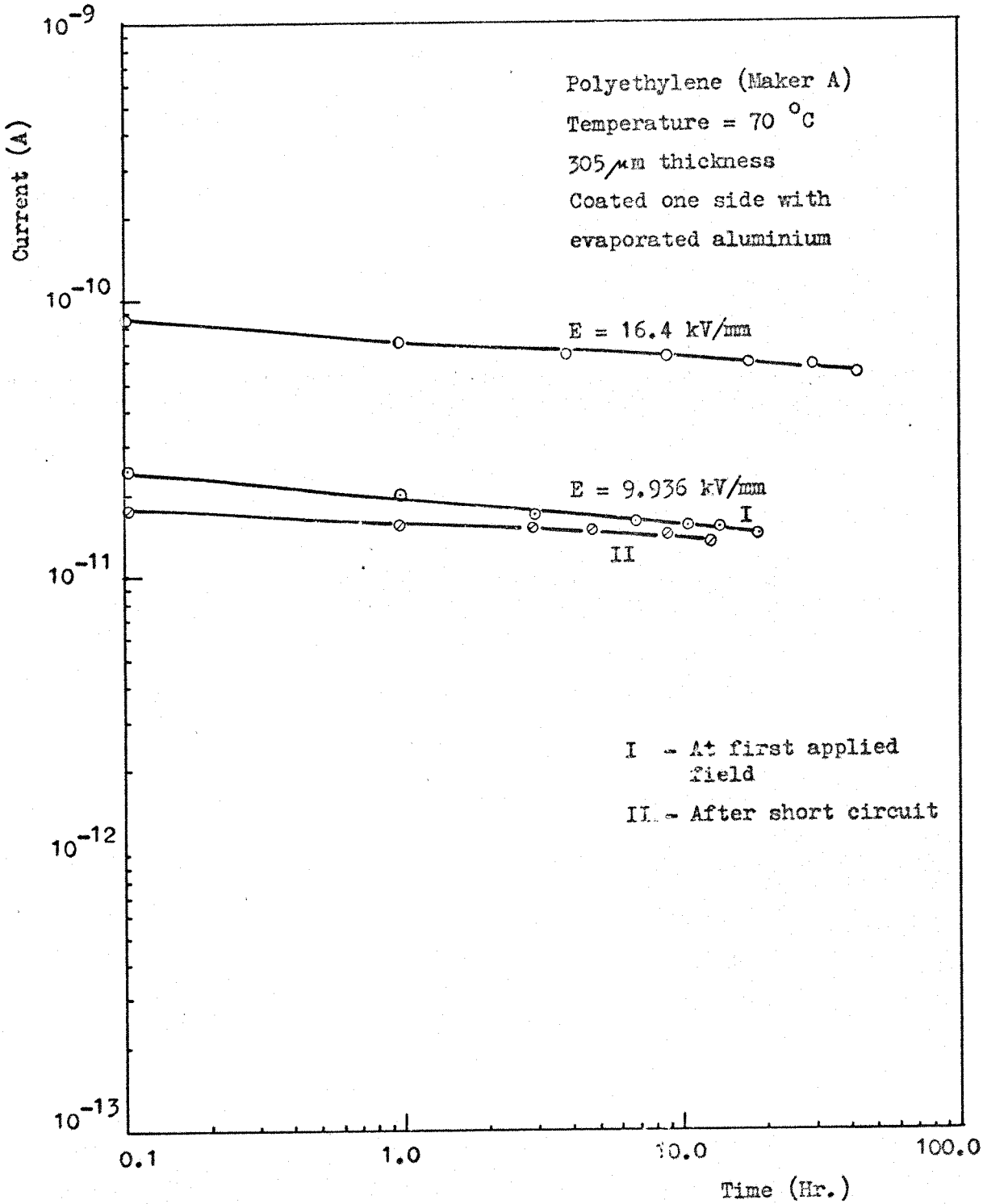

(Figure 4) Plot of conduction current against time

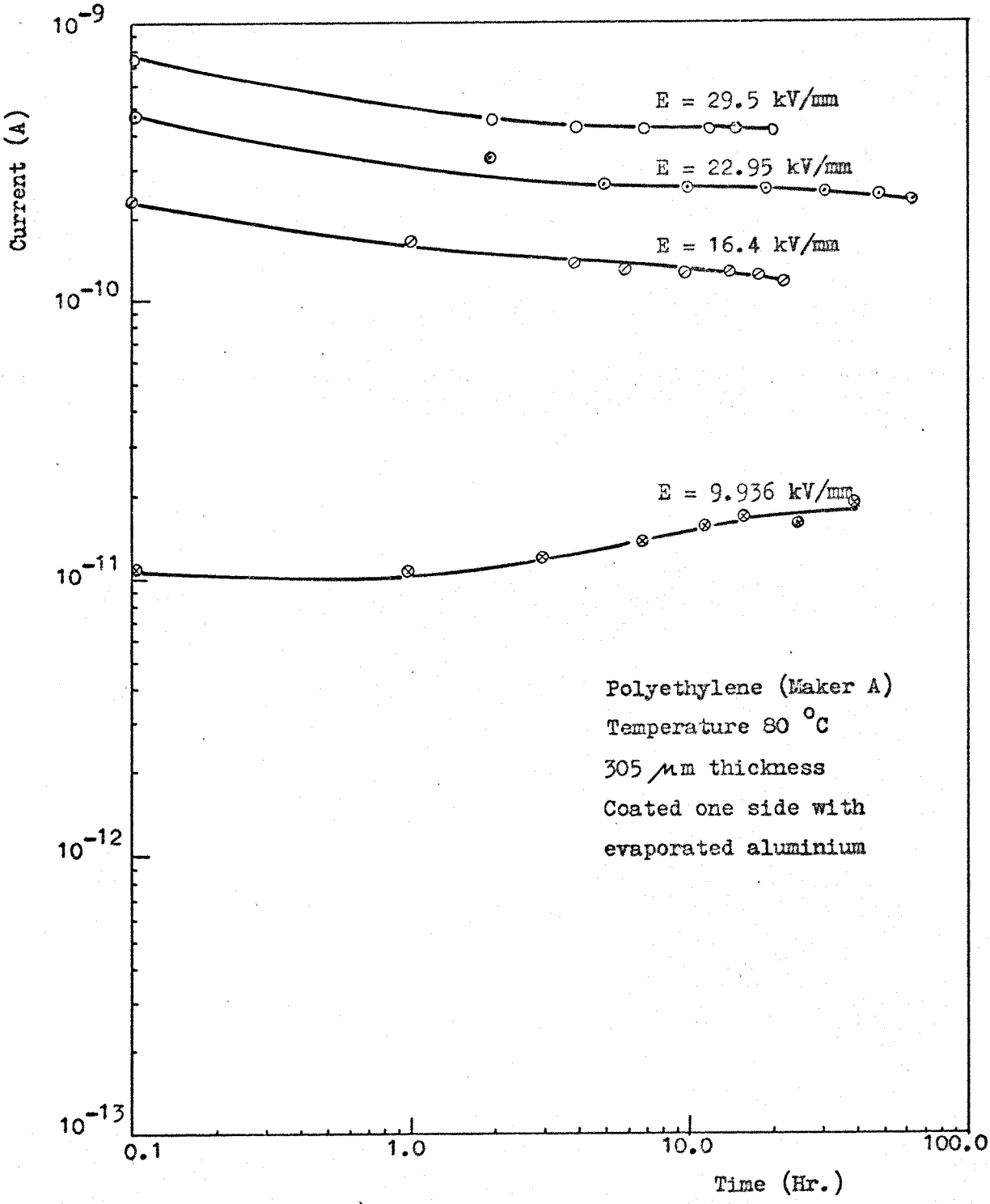

(Figure 5) Plot of conduction current against time

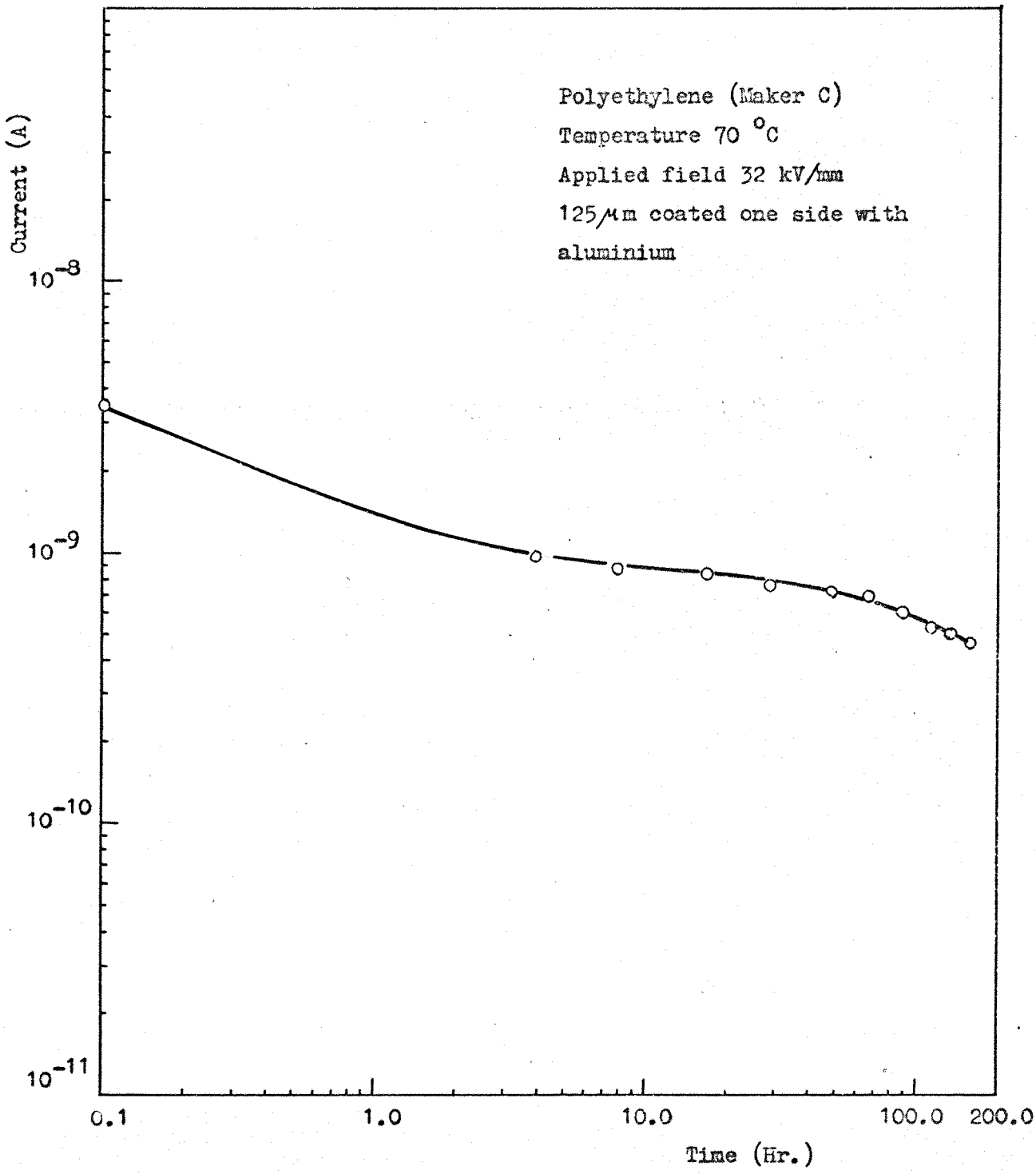

(Figure 6) Plot of conduction current against time

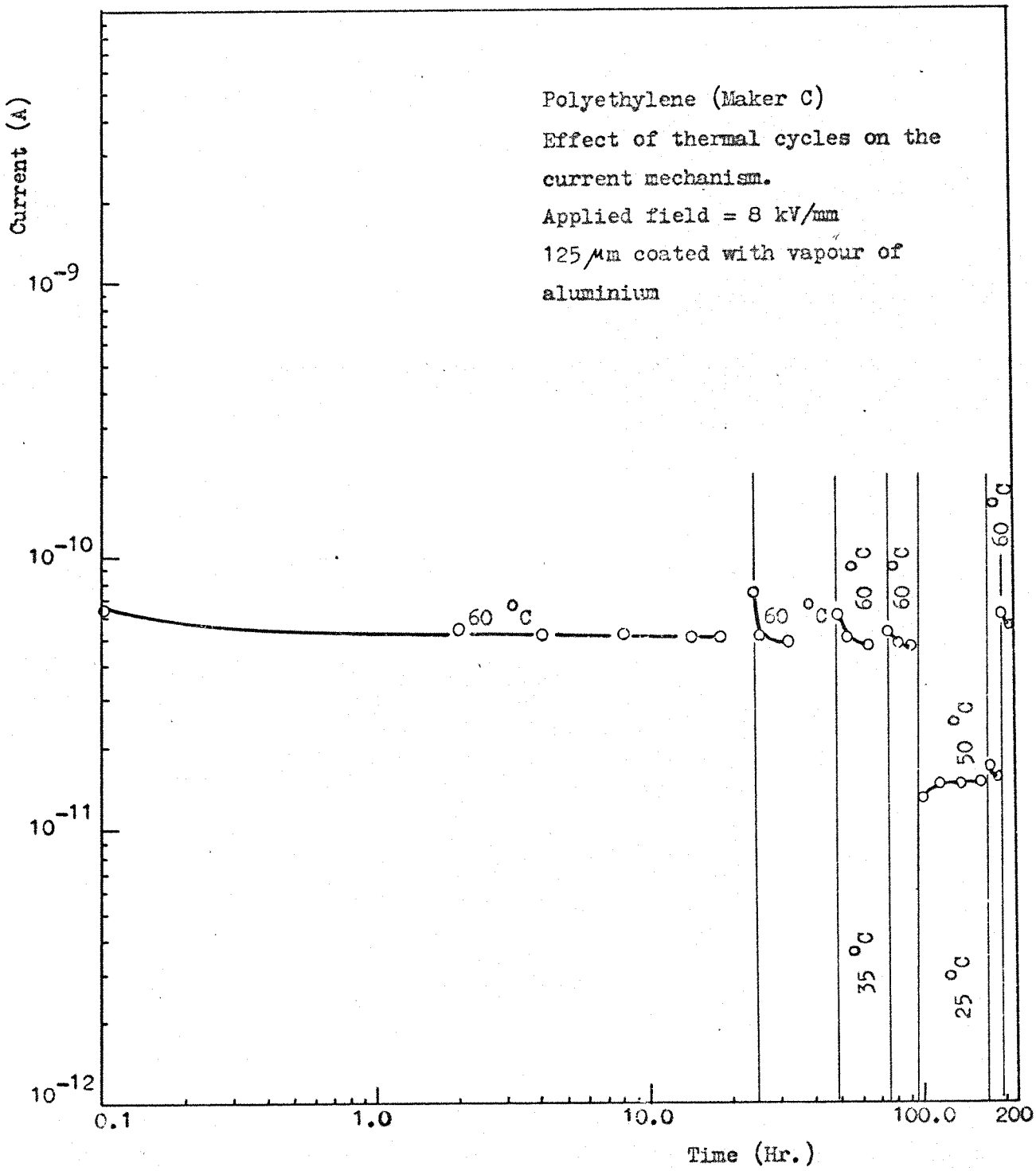

(Figure 7) Plot of conduction current against time at different thermal cycle

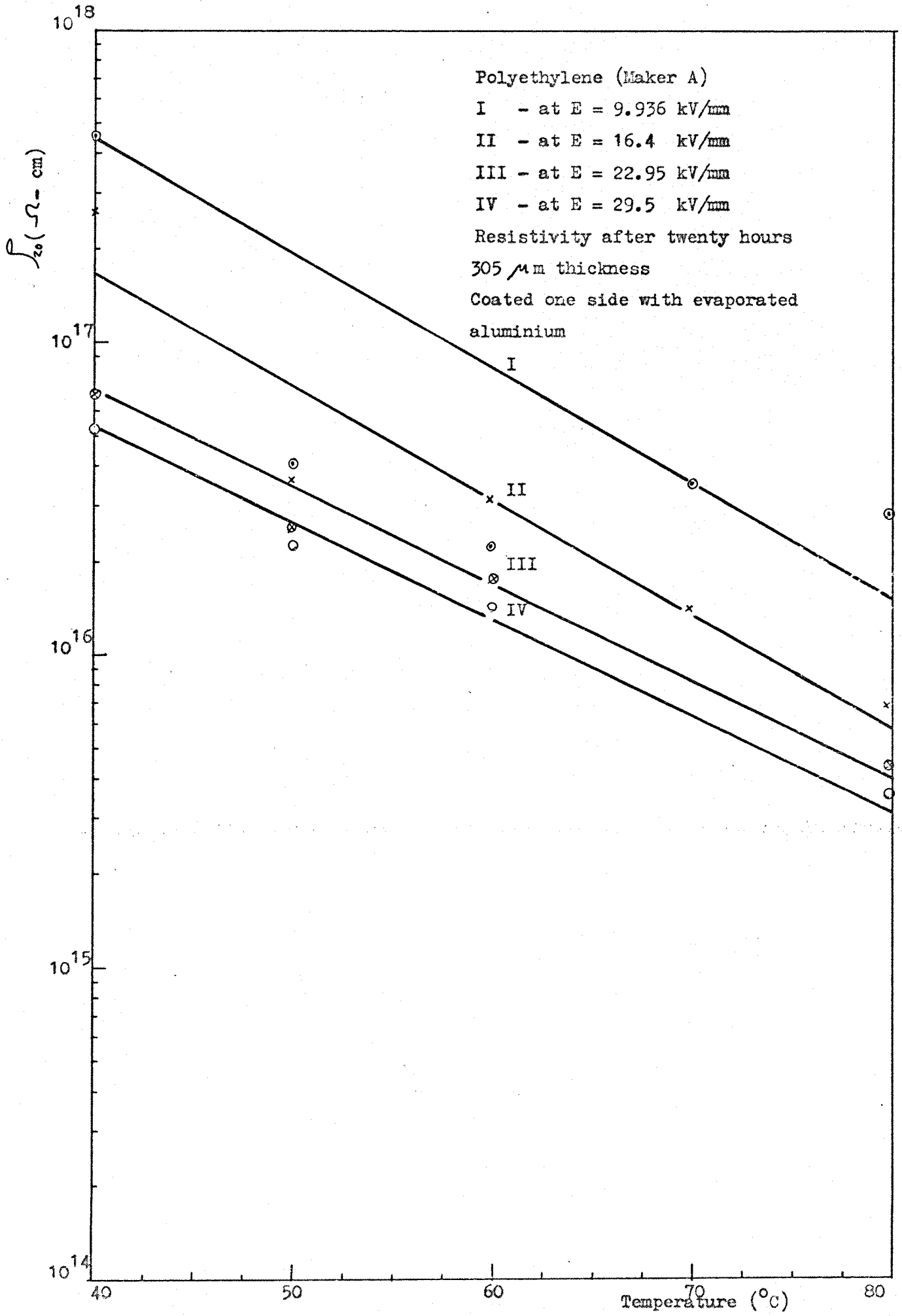

(Figure 8) Plot of resistivity against temperature

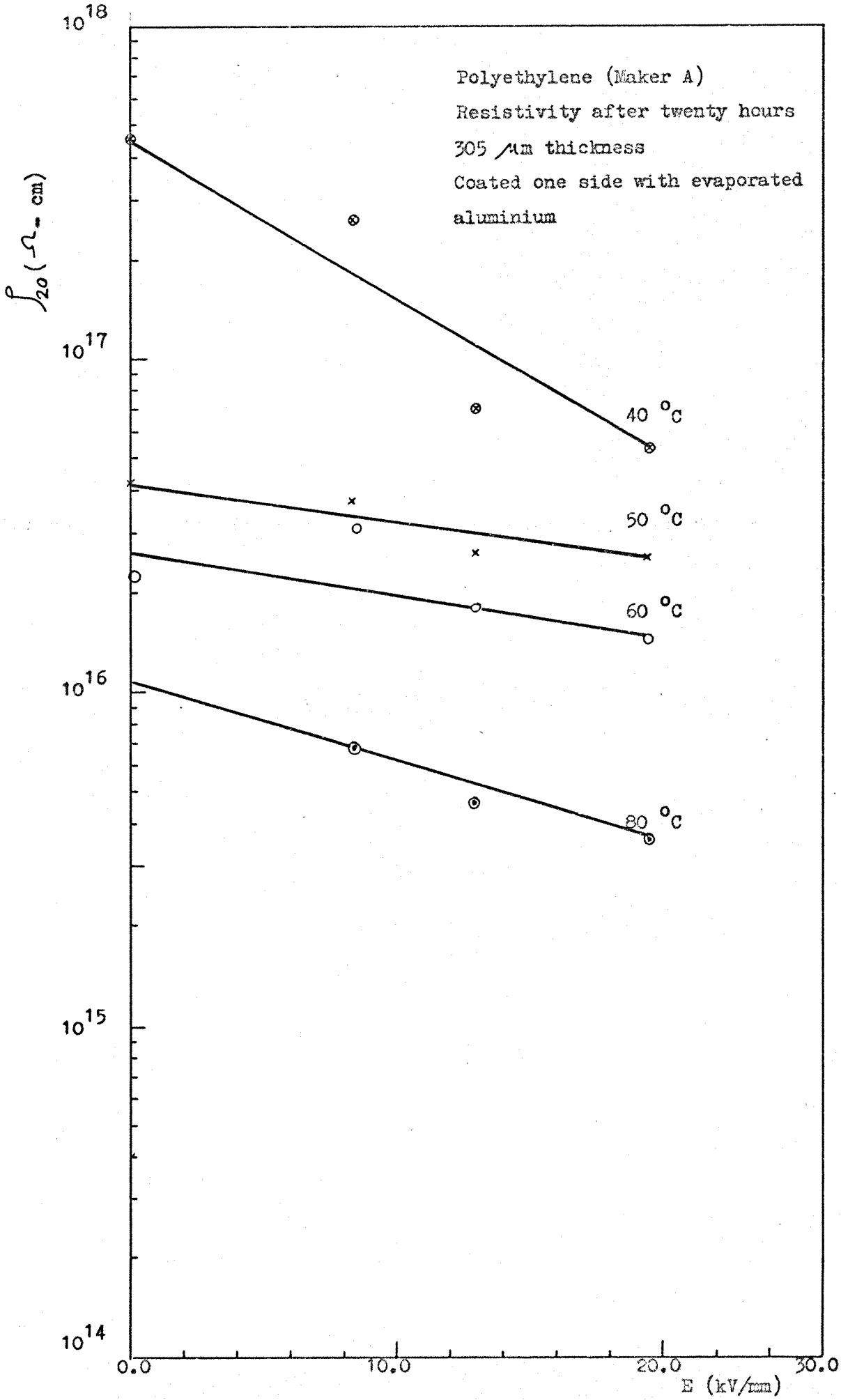

(Figure 9) Plot of resistivity against applied field

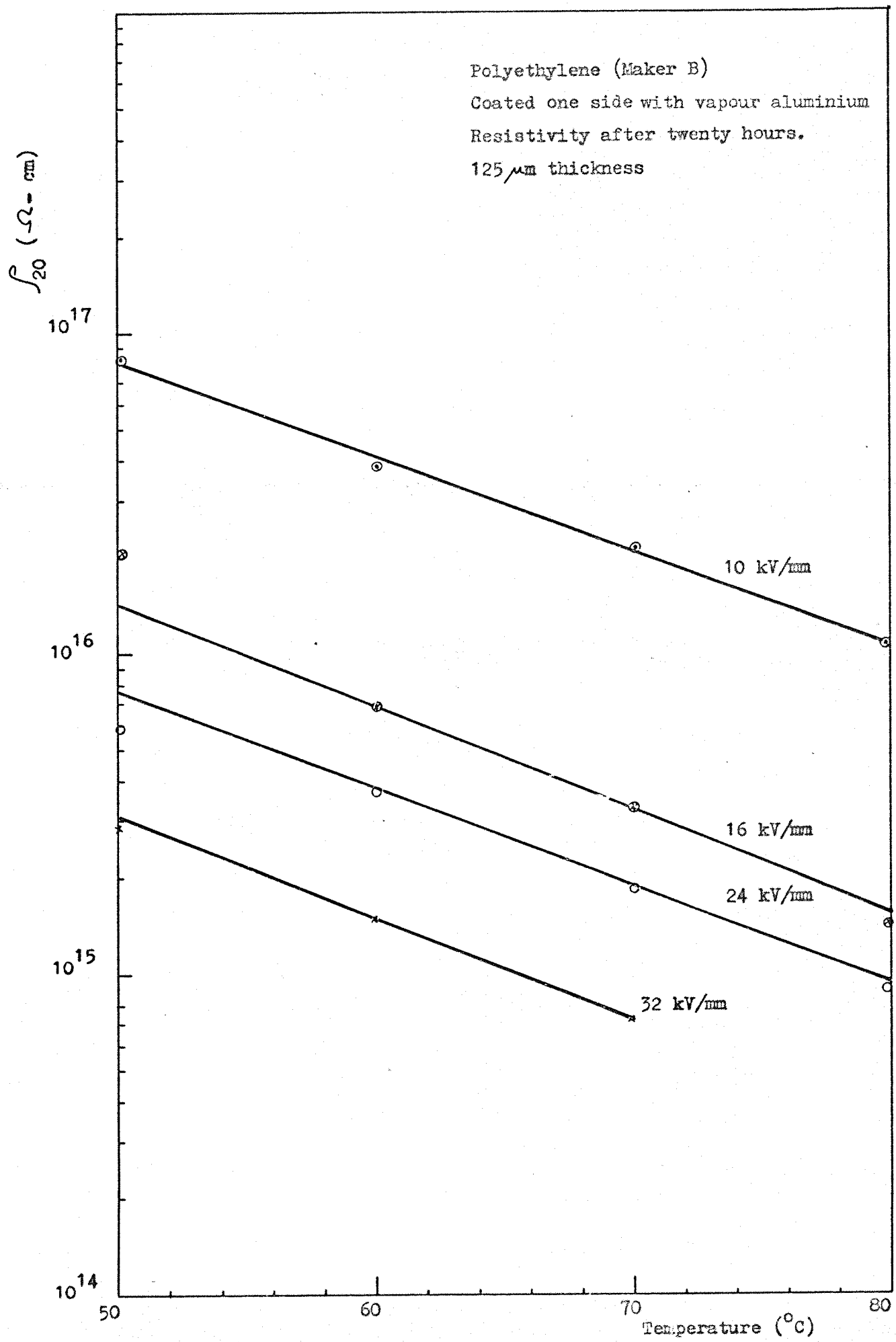

(Figure 10) Plot of resistivity against temperature

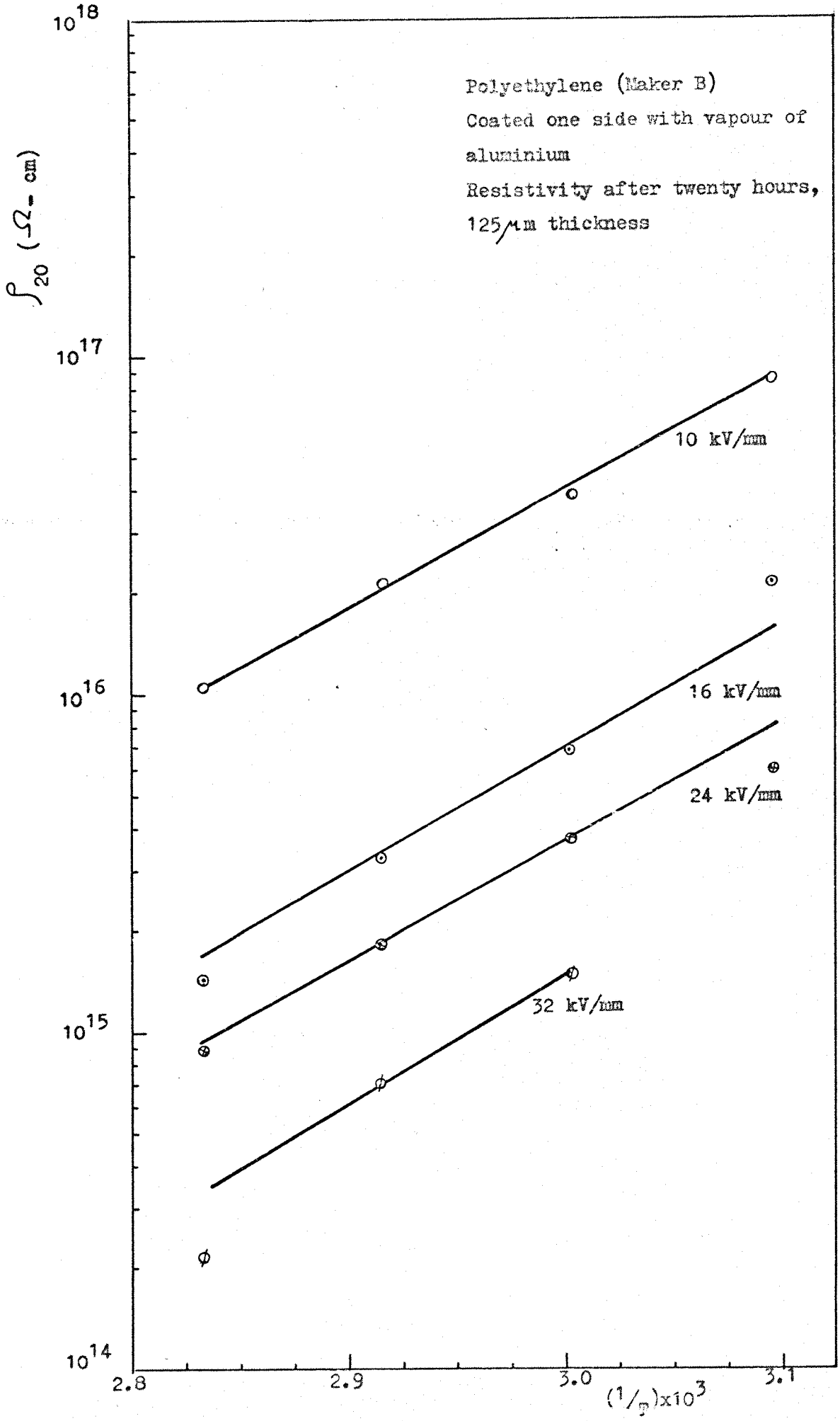

(Figure 10-a) Plot of resistivity against reciprocal absolute temperature

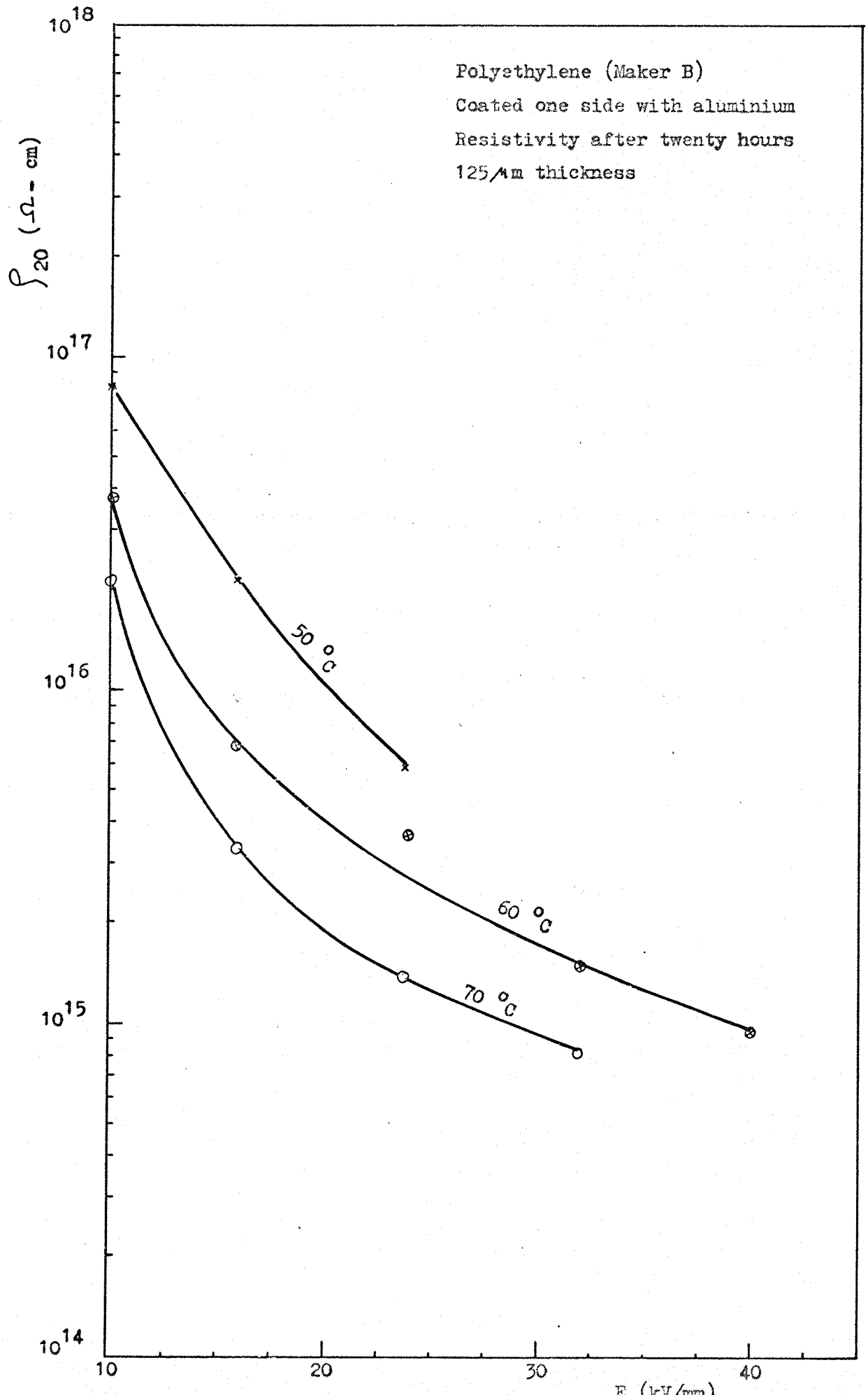

(Figure 11) Plot of resistivity against the applied field

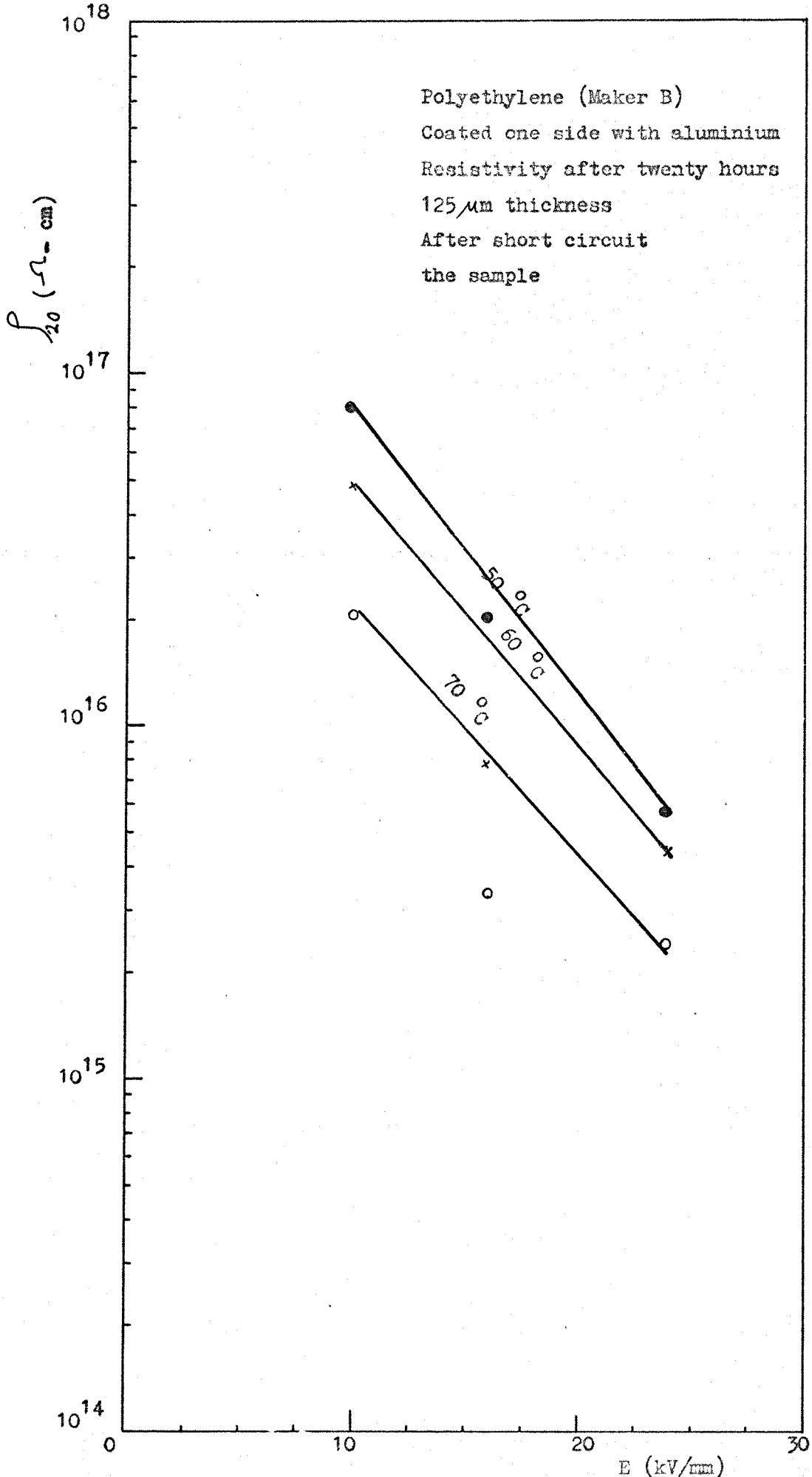

(Figure 11-a) Plot of resistivity against applied field

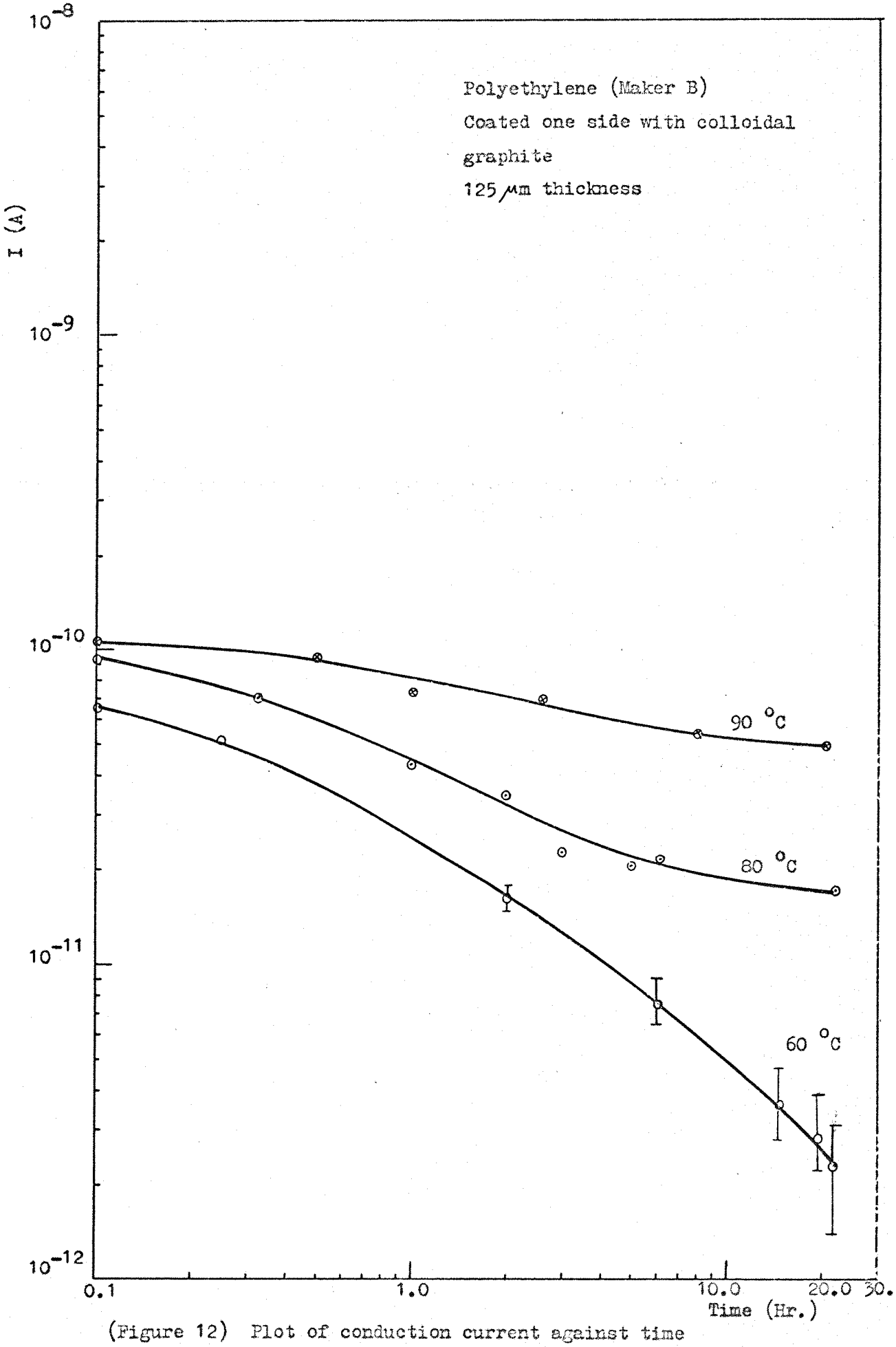

(Figure 12) Plot of conduction current against time

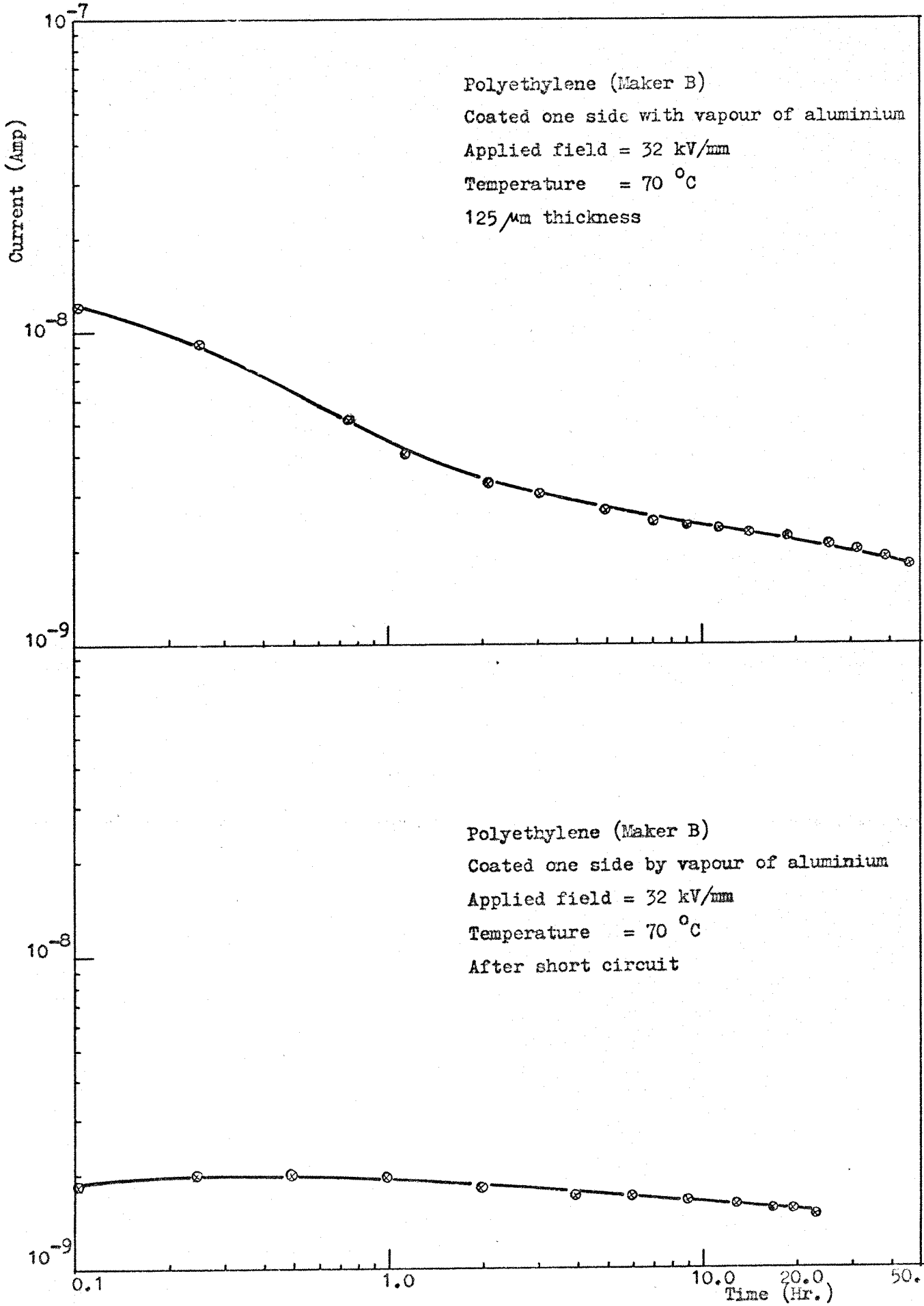

(Figure 13) Plot of conduction current against time

4-1-5 Effect of Manufacturing Process

The results obtained on polyethylene of Maker A and that of Maker B, show that the values of the resistivity/temperature coefficients (α) of Maker A is slightly different than that of Maker B. While the values of the resistivity/stress coefficients and the reference resistivities have a noticeable difference between the values of Maker A and that of Maker B, the value of the resistivity/stress coefficient (β) of Maker C is nearly the same as that of Maker A. The reason for the above conflict is probably due to the different processing methods, which means that the manufacturing process has an important effect on the polyethylene resistivity.

In general the conduction mechanism of the three different Maker samples is the same i.e., conduction mechanism in the three samples face the same difficulty to obtain the steady-state current.

4-2 RESULTS FOR ETHYLENE-PROPYLENE-RUBBER (EPR)

4-2-1 Introduction

The results obtained from the measurements of conduction current in polyethylene show that it is not possible to get the steady-state current and it is difficult to define the resistivity of the polyethylene. Due to the fact that the EPR is a high working-temperature insulant, it is of interest to investigate its D.C. resistivity.

The use of EPR as insulant in high temperature cables seems to be more convenient due to the possibility of a defined resistivity at high temperature.

The mechanical properties of the EPR compared to (XLPE), mineral-filled (XLPE) and butyle rubber are shown in Table (4-4).

	Tensile strength (N/mm^2)	200% modulus (N/mm^2)	Elongation (%)	Stiffness in flexure (N/mm^2) (ASTM D747)	Brittle temperature (^oC) (ASTM D746)	Deformation at 121 ^oC (%)
EPR	5.515-6.205	3.86	350-500	4.413	-75	15
XLPE	12.6174	9.377	440	-	-	-
MFXLPE	15.86	-	350	45.5	-80	10
Butyle	4.55 -5.515	1.793	500-660	4.62	-47	14

Table (4-4) The mechanical properties of EPR, XLPE, MFXLPE and Butyle Rubber

4-2-2 Conduction Current

4-2-2-1 EPR Conduction Current Measurements at Atmospheric Pressure [Contact Effect]

As a result of the test carried out in this work, it was found that it is not possible to measure the conduction current at temperatures less than 80 °C for a specimen of thickness 460 μm and 60 °C for a specimen of thickness 200 μm, since the conduction current goes to the other region of different polarity. This current needs a long time to go back to the region of original positive polarity. This mechanism does not occur in vacuum ($\approx 2.5 \times 10^{-4}$ Torr) which means that the injected carriers from the cathode cause an electric field on the surface of the specimen due to its large thickness. This field ionizes the water molecules existing in the air between the cathode and the specimen's surface, at the same time this field causes a considerable number of the space charge carriers to go back to the cathode producing a negative current.

The above phenomena is due to the low surface tension of the specimen when uncoated, because the effect of the very thin gap (50 μm) between the cathode and the guard ring.

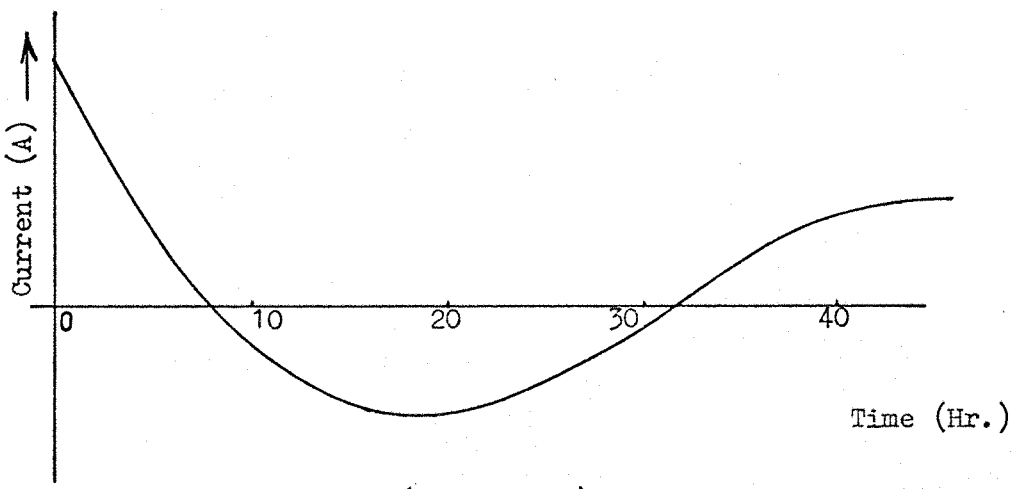

(Figure 4-2)

4-2-2-2 EPR Conduction Current Measurements at Vacuum

As shown in (Figures 14-21) when applying a certain field on a specimen of EPR at a low temperature ($< 70\ ^{o}C$) the conduction mechanism of the current can be divided into four regions. The region I is that at which the current rises at first for a few seconds. In region II the current decays for a few hours, while in region III the current increases again. In region IV the current continues decaying until it reaches the steady state. The above mechanisms are mainly due to the production of the space charge carriers and the ions by the chemical imperfections in the impurity and the physical imperfections in the bulk of the material. The effect of the previous mechanism varies with the temperature and as the temperature increases the effect shown in regions II, III and IV becomes quicker reducing the slope of the curves in regions III and IV causing the current to approach the steady-state.

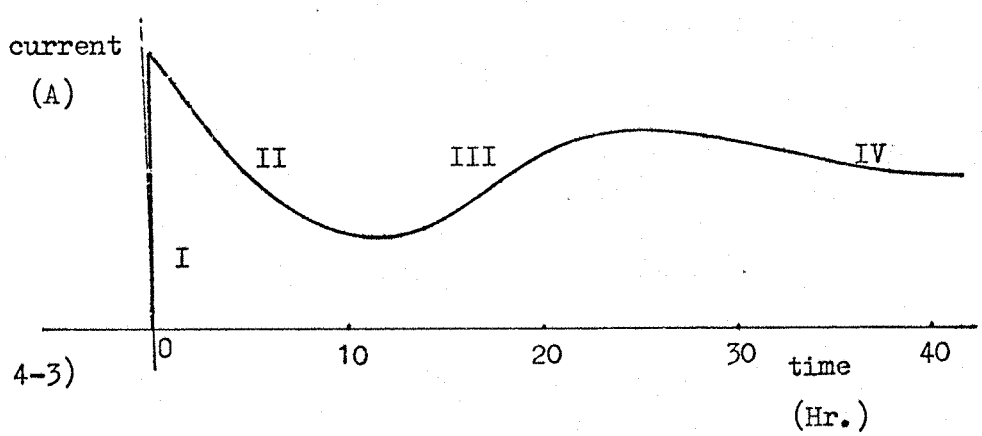

(Figure 4-3)

4-2-2-3 Short Circuit Current to Earth

A study of the short circuit current gives an idea about the space charge motion in the specimen. From the test done in this work on the short circuit current, after a period of applying uniformly electric field at different temperatures, the existence of the ionic conduction is evident. This ionic conduction occurs due to the effect of the

temperature and the previously applied electric stress. From the short circuit current at the atmospheric pressure, the current decreases from the negative region and passes to the positive region at temperatures ($> 80\ ^{o}C$) for 460 μm thickness of specimen, and at ($> 60\ ^{o}C$) for 185 μm thickness of specimen, and after previously applied stresses (> 10 kV/mm). It is well known that the ionic motion depends on the mobility and the density of the carriers which gives a clearer idea why the negative current varies quicker than the positive current. The current in the negative region is due to the stream of the negative ions which has a mobility higher than the mobility of the positive ions. A comparison between the discharging current at the atmospheric pressure and that at vacuum ($\leq 2.5 \times 10^{-4}$ Torr) illustrates the effect of water molecules existing in the air between the cathode and the low voltage (uncoated) side of the EPR specimen.

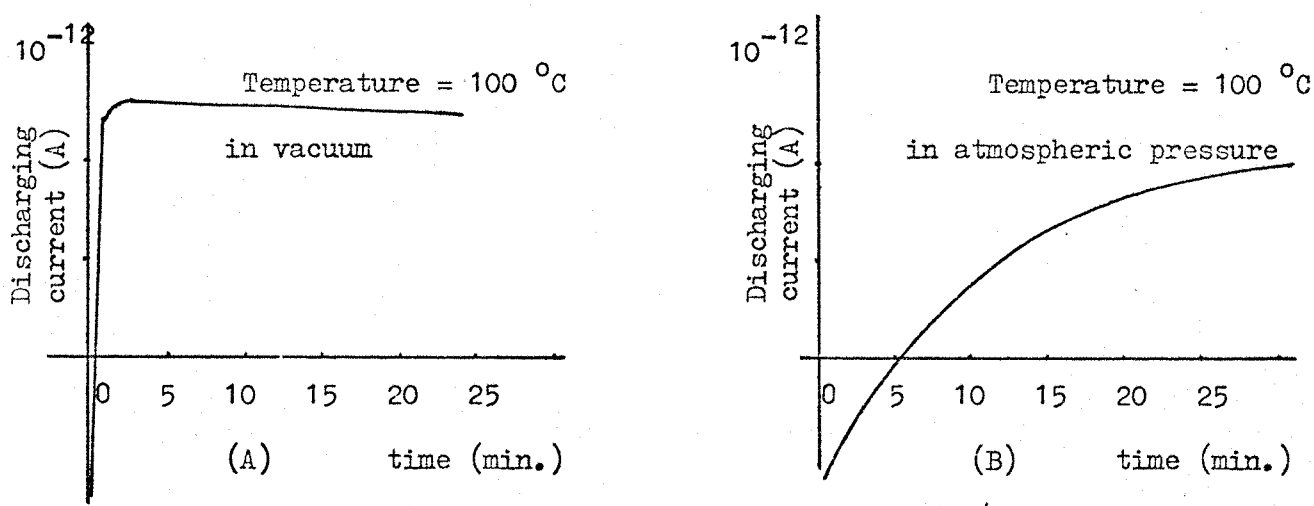

Both A and B are previously stressed with 25 kV/mm
(Figure 4-4)

4-2-2-4 EPR Conduction Current after a Period of Short Circuit

The results obtained in this work show that the conduction current mechanism at second applied field (after a period of short circuiting

the specimen to earth) has lower transient current amplitude than that of the conduction current mechanism at first applied field. This difference in the amplitude is much less than that of the polyethylene, which means that the EPR has less ability to store the electric charges than polyethylene. The above phenomena is shown in the following figure.

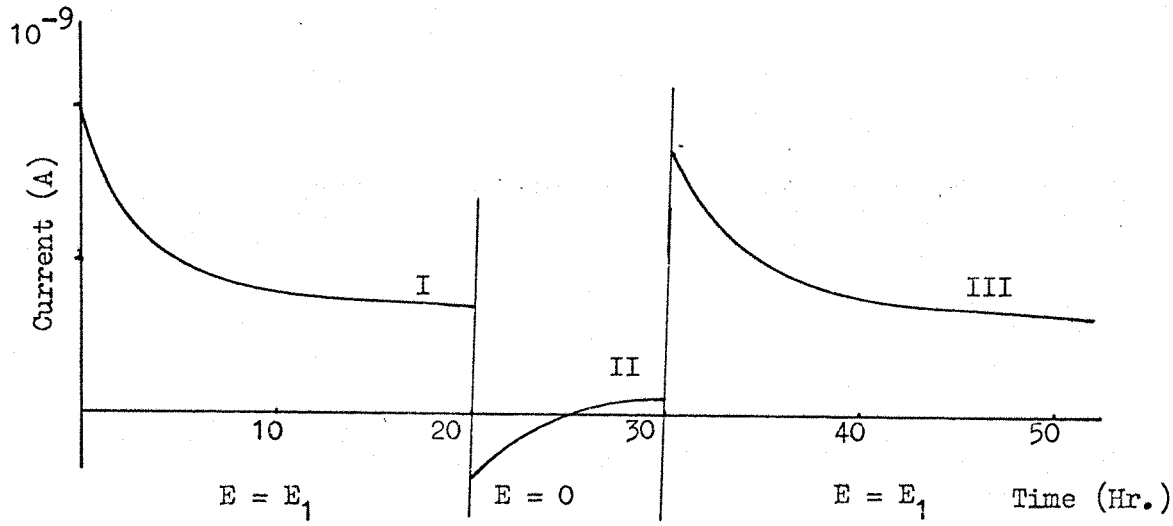

I - At first applied field

II - Discharging current

III - After short circuit

(Figure 4-5)

4-2-2-5 Steady-State Current [Long Time Test]

The study of the conduction current has been carried out at different temperatures (25 °C - 100 °C) and at different stresses (10 kV/mm - 25 kV/mm). The results show that at temperatures between 25 °C and 40 °C it is difficult to get a steady-state current within a time range of 70 hours, since at 25 °C and after 70 hours [in vacuum $\leq 2.5 \times 10^{-4}$ Torr] the conduction current goes to opposite polarity region which needs a very long time [days or weeks] to go back to the original

positive-polarity region. At a temperature of 60 °C and more, it is possible to get a steady-state current within a period of a few days [in vacuum $\leq 2.5 \times 10^{-4}$ Torr]. In air it is possible to get steady-state current within twenty hours at temperature of 80 °C for 460 μm specimen, and at temperature of 60 °C for 185 μm specimen.

The results obtained with a specimen of 185 μm thickness are much better from the steady-state point of view than that with a specimen of 460 μm.

4-2-3 Resistivity Variation of EPR

4-2-3-1 Resistivity/Stress Characteristics

From the results shown in (Figures 23 and 24) it is obvious that the stress-resistivity coefficient (β) does not remain constant as the temperature is increased (Table 4-5-b). In general the resistivity variation with the applied field is linear which gives evidence that the following empirical formula is applicable for EPR insulator.

$$\ln \rho = k + \beta E \qquad \text{- - - (4-8)}$$

where k is constant depending on the temperature.

Table (4-5-a) EPR, 460 μm thickness, resistivity after twenty hours

α (1/°C)	E (kV/mm)	ρ_o (Ω- cm) (at θ = 40 °C)
0.14	10	7.2×10^{18}
0.14	15	7.1×10^{18}
0.14	20	6.9×10^{18}

Table (4-5-b) EPR, 460 μm thickness, resistivity after twenty hours

β (cm/kV)	θ (°C)	(Ω- cm) (at E = 0.0 kV/mm)
0.01	60	8.5×10^{17}
0.0095	70	1.5×10^{17}
0.00036	80	3.8×10^{16}

(Table 4-5-b) shows that the resistivity/stress coefficient decreases as the temperature increases till a certain temperature is reached at which it becomes very small (temp. = 80 °C). After passing this temperature the resistivity/stress coefficient increases again. At temperature of 90 °C the resistivity/stress coefficient in air is the same as that in vacuum.

As the conduction current used in the calculation of the resistivity was taken after twenty hours for all cases, the difference which appeared in the values of β is due to the fact that there is a time lag in reaching the steady-state at different temperatures.

4-2-3-2 Resistivity/Temperature Variation

From the results shown in Figure (25) the slope of resistivity/temperature curve is very high and the resistivity decreases rapidly with the increase in temperature.

Measurements in the atmospheric pressure gave nearly the same slope as that obtained in vacuum.

In general the variation of the resistivity against the temperature is linear and follows the following expirical formula.

$$\ln \rho = k_1 + \alpha \theta \qquad \text{- - - (4-9)}$$

where k_1 is constant depending on the applied field.

4-2-4 Effect of Thickness on Resistivity - EPR

The results obtained show that the resistivity is related to the thickness of the EPR specimen. The relation is not linear since as the temperature increases the effect of thickness decreases as shown in (Table 4-7).

The effect of thickness is very small at low fields at a certain temperature, while at high fields the effect is large as shown in (Table 4-6).

Table (4-6) The applied temperature is 80 °C

Applied field (kV/mm)	Resistivity (ρ_{20}) (Ω - cm) Specimen 185 μm	Resistivity (ρ_{20}) (Ω - cm) Specimen 460 μm	Ratio of ρ_{460}/ρ_{185}
18	1.3×10^{14}	1.42×10^{16}	110
20	1.28×10^{14}	2.87×10^{16}	224
25	1.136×10^{14}	3.36×10^{16}	296
30	9.37×10^{13}	3.57×10^{16}	380

Table (4-7) The applied field is 20 kV/mm

Temperature (°C)	Resistivity (ρ_{20}) (Ω - cm) Specimen 185 μm	Resistivity (ρ_{20}) (Ω - cm) Specimen 460 μm	Ratio of ρ_{460}/ρ_{185}
70	1.75×10^{15}	1.15×10^{17}	65.7
80	9.3×10^{14}	2.82×10^{16}	30.3
90	9.6×10^{14}	1.4×10^{16}	14.6

The large ratio of ρ_{460}/ρ_{185} obtained in the above tables is due to the fact that steady-state has not been reached.

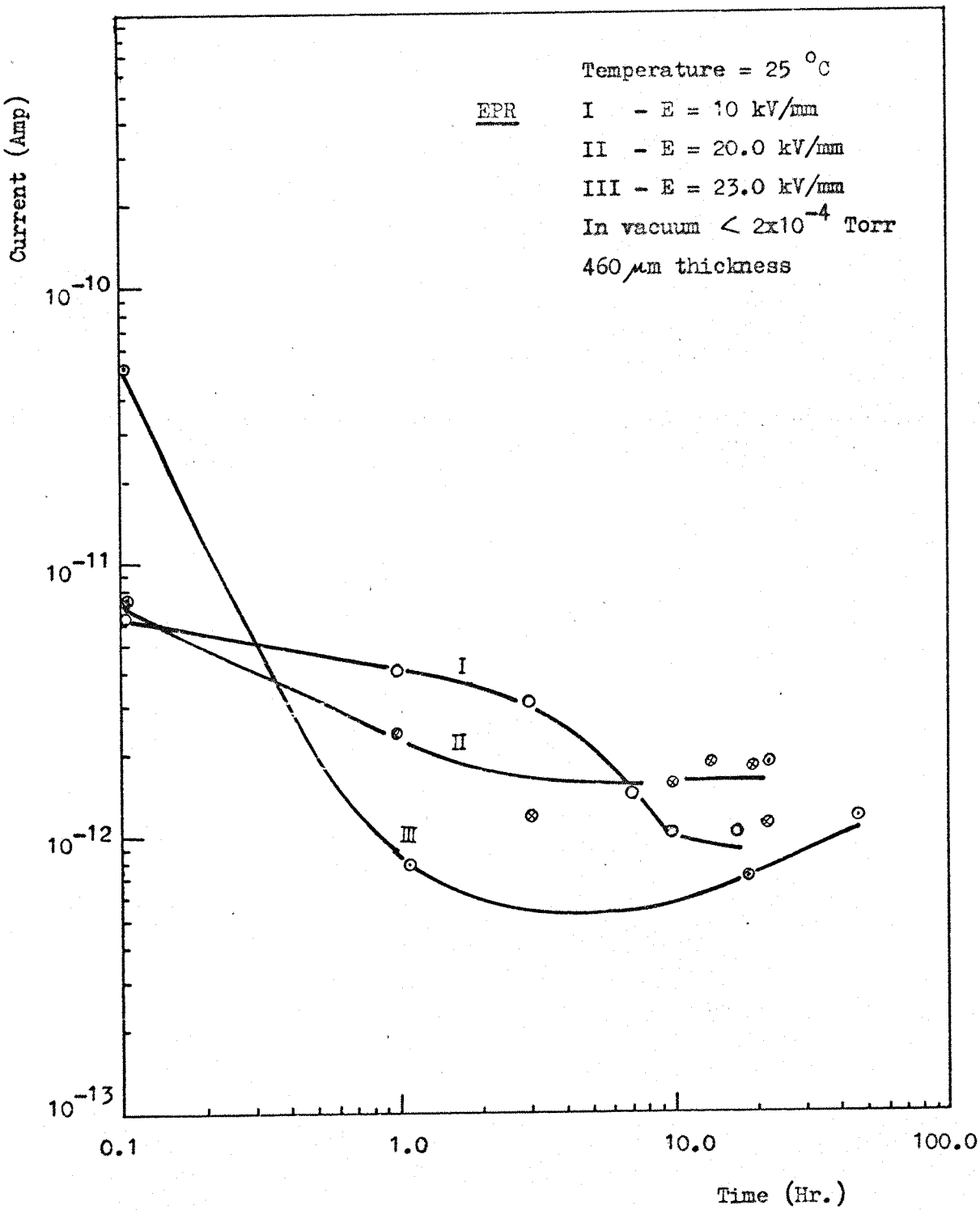

(Figure 14) Plot of conduction current against time

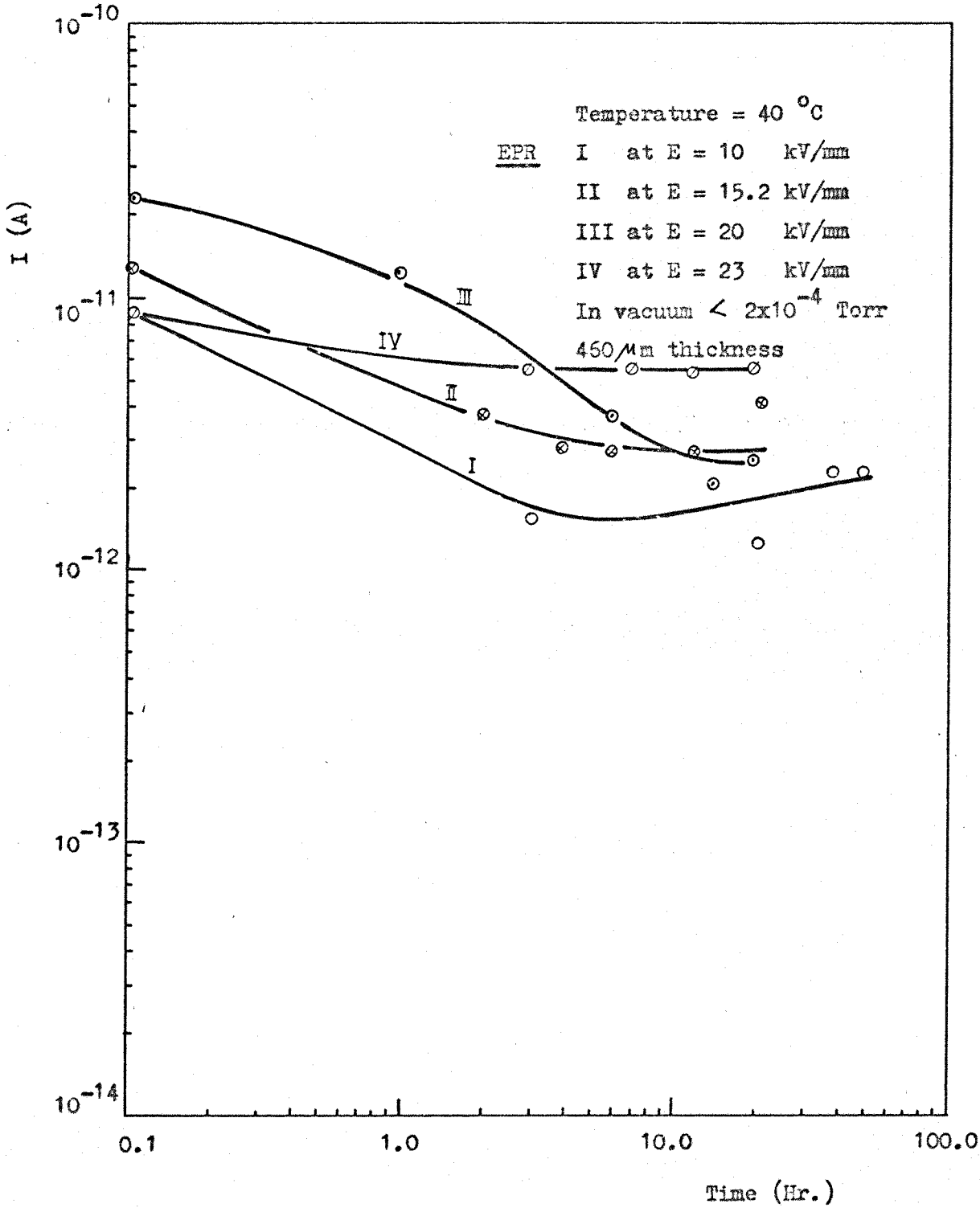

(Figure 15) Plot of conduction current against time

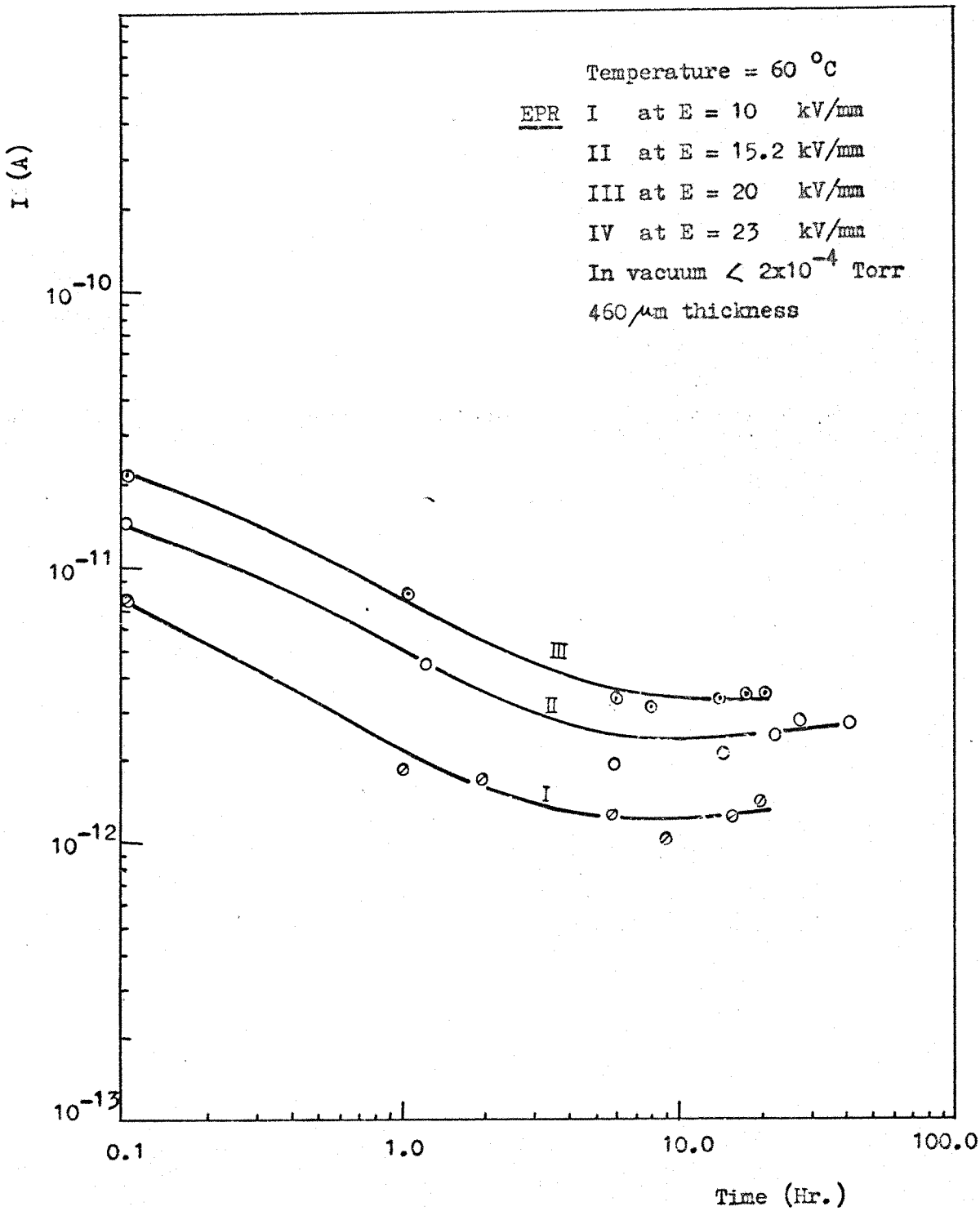

(Figure 16) Plot of conduction current against time

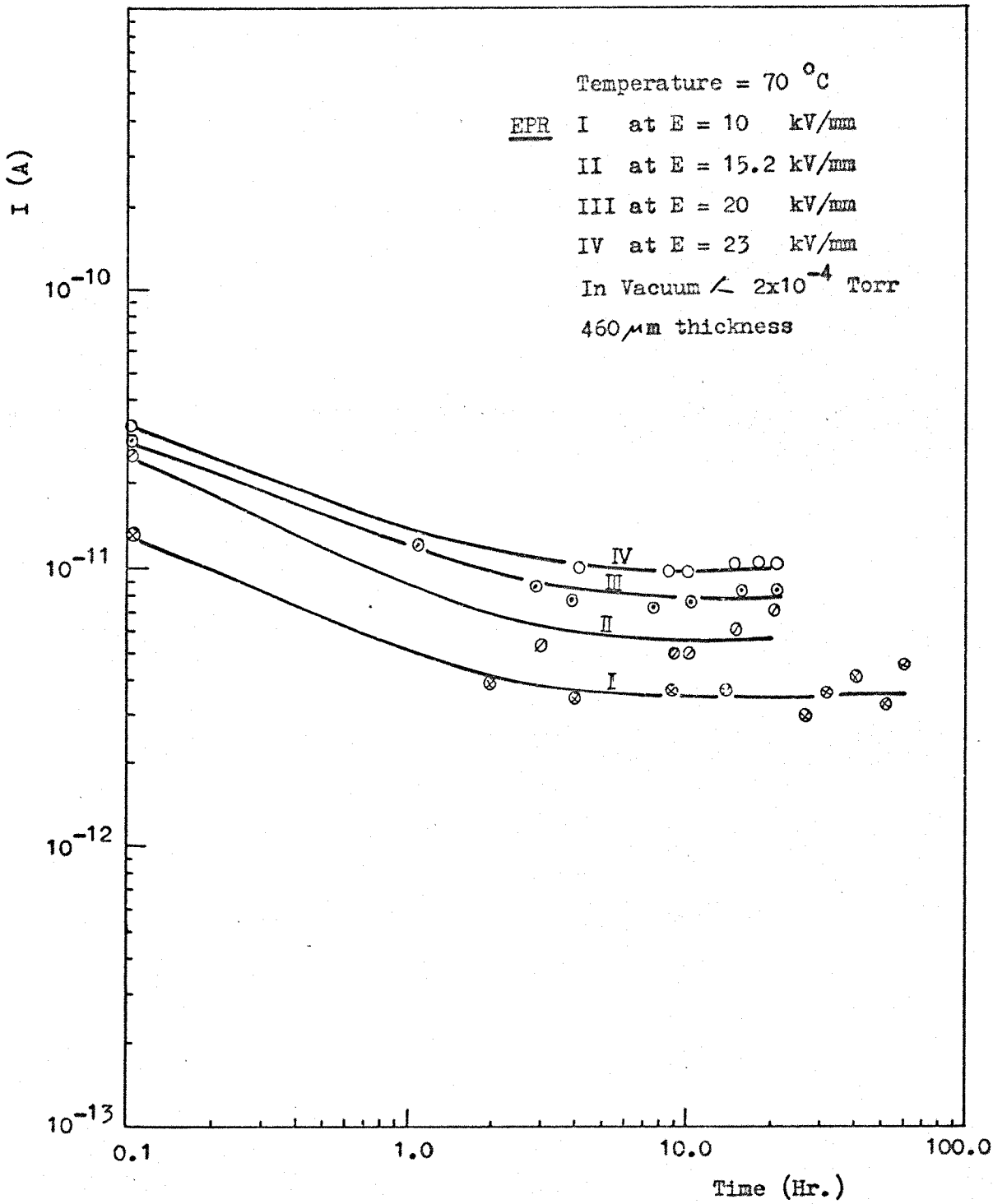

(Figure 17) Plot of conduction current against time

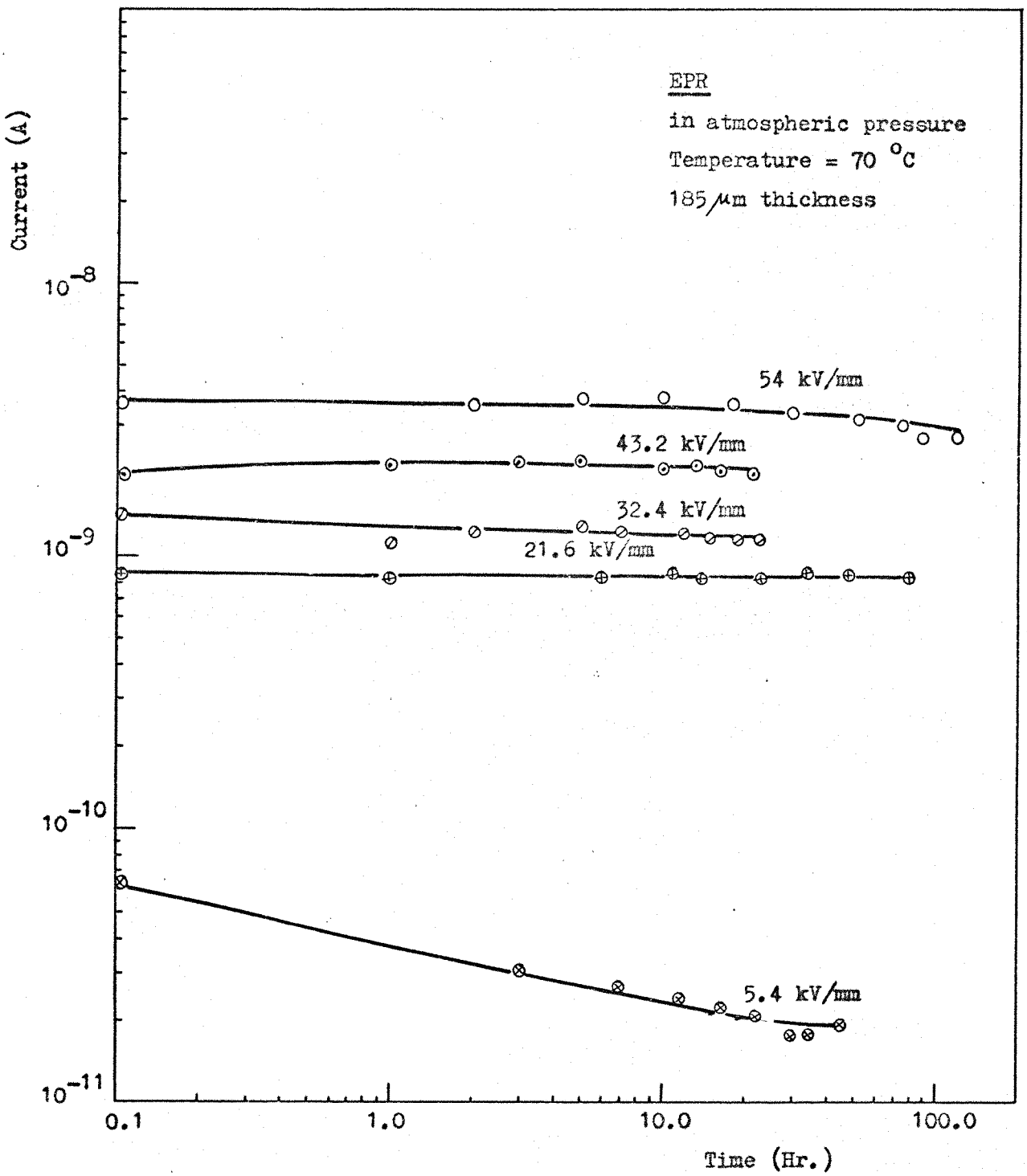

(Figure 17-a) Plot of conduction current against time

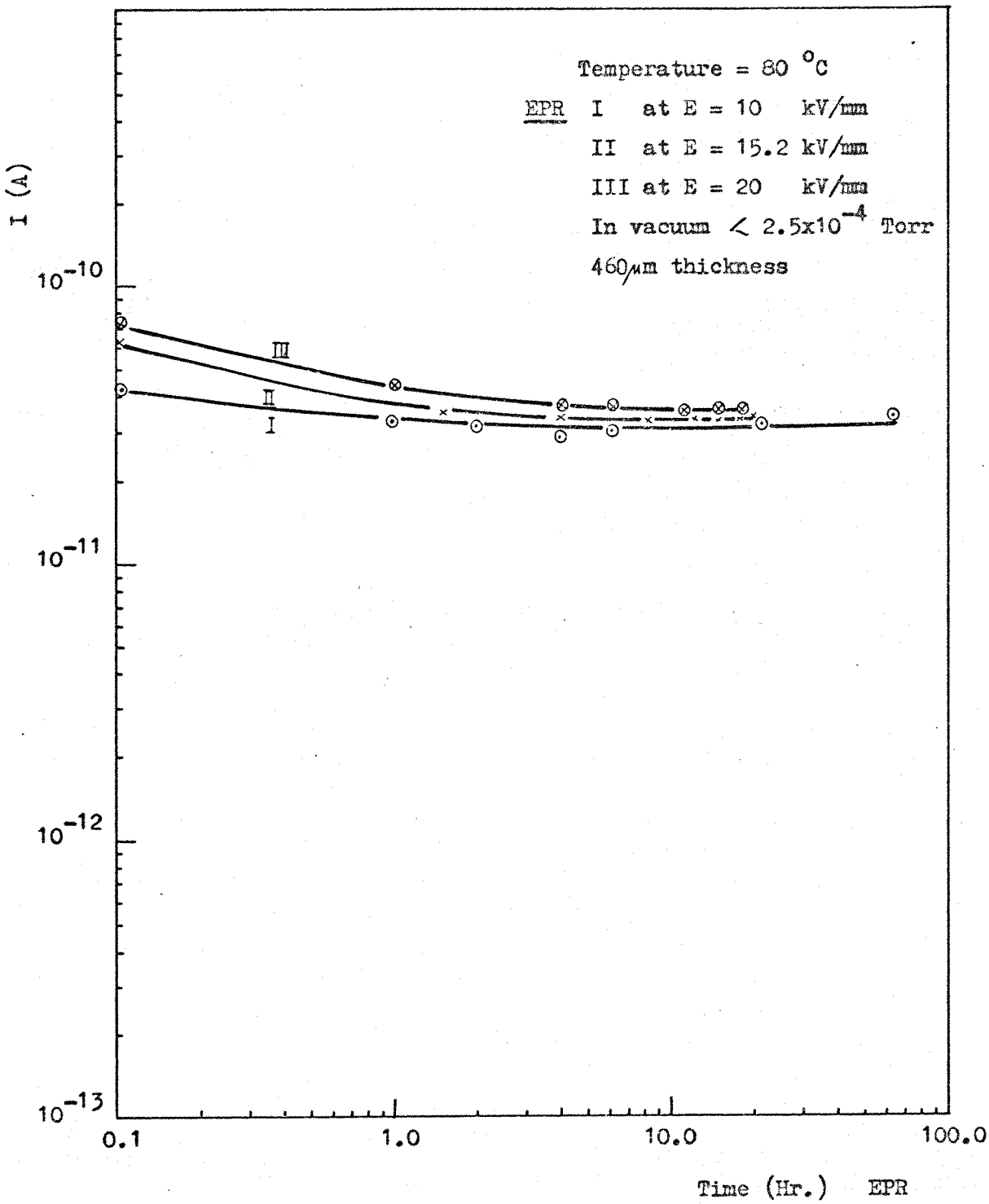

(Figure 18) Plot of conduction current against time

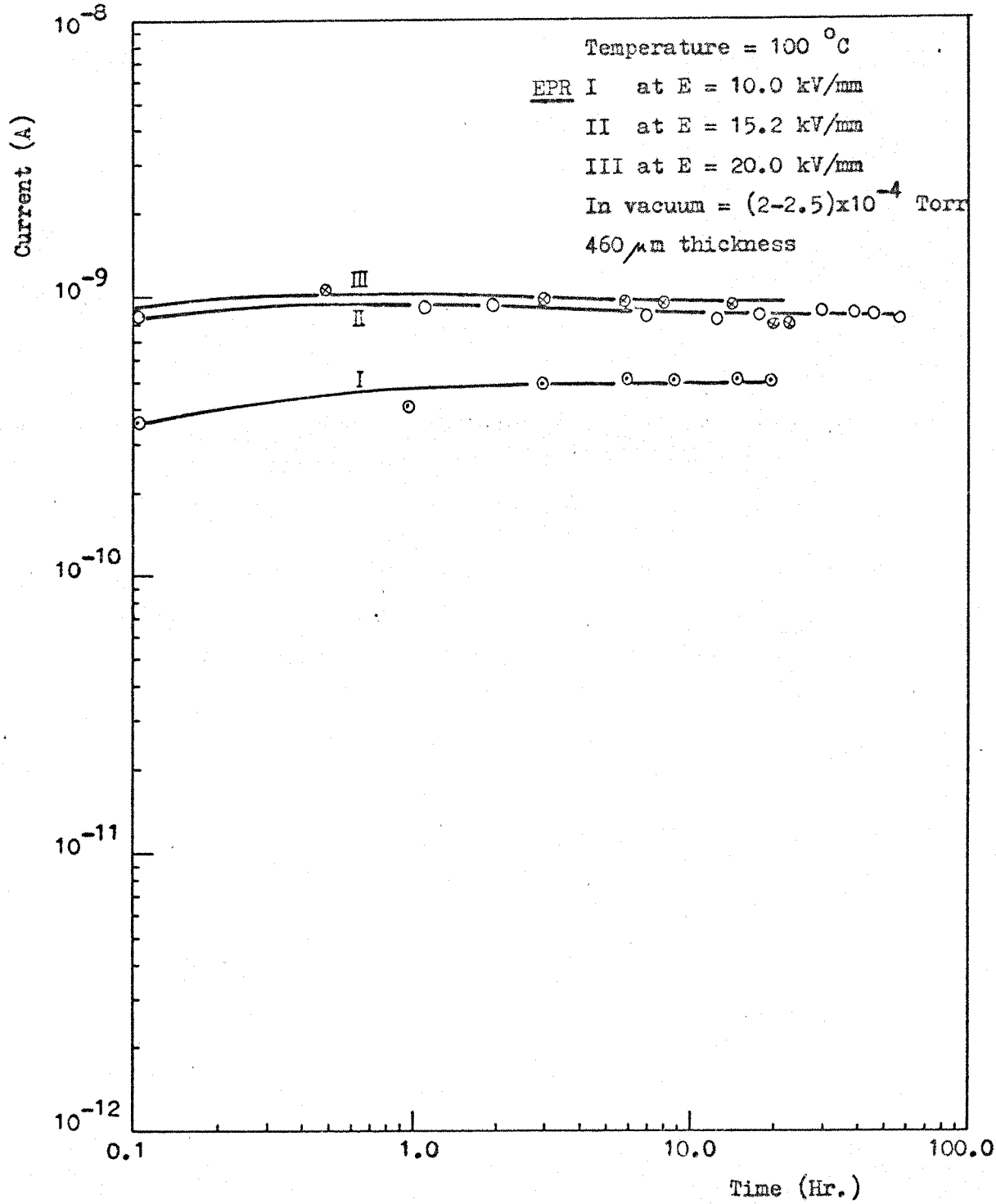

(Figure 19) Plot of conduction current against time

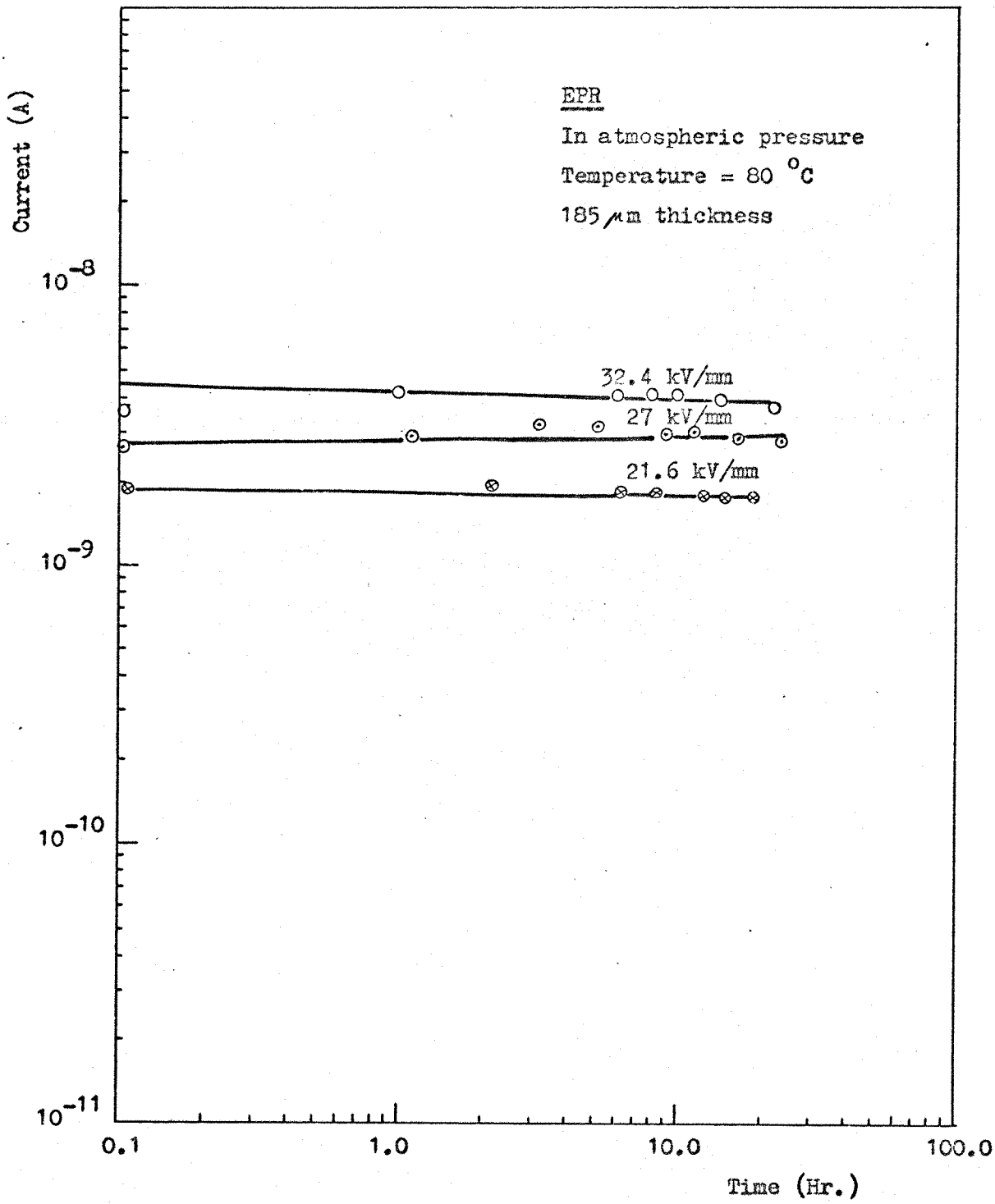

(Figure 20) Plot of conduction current against time

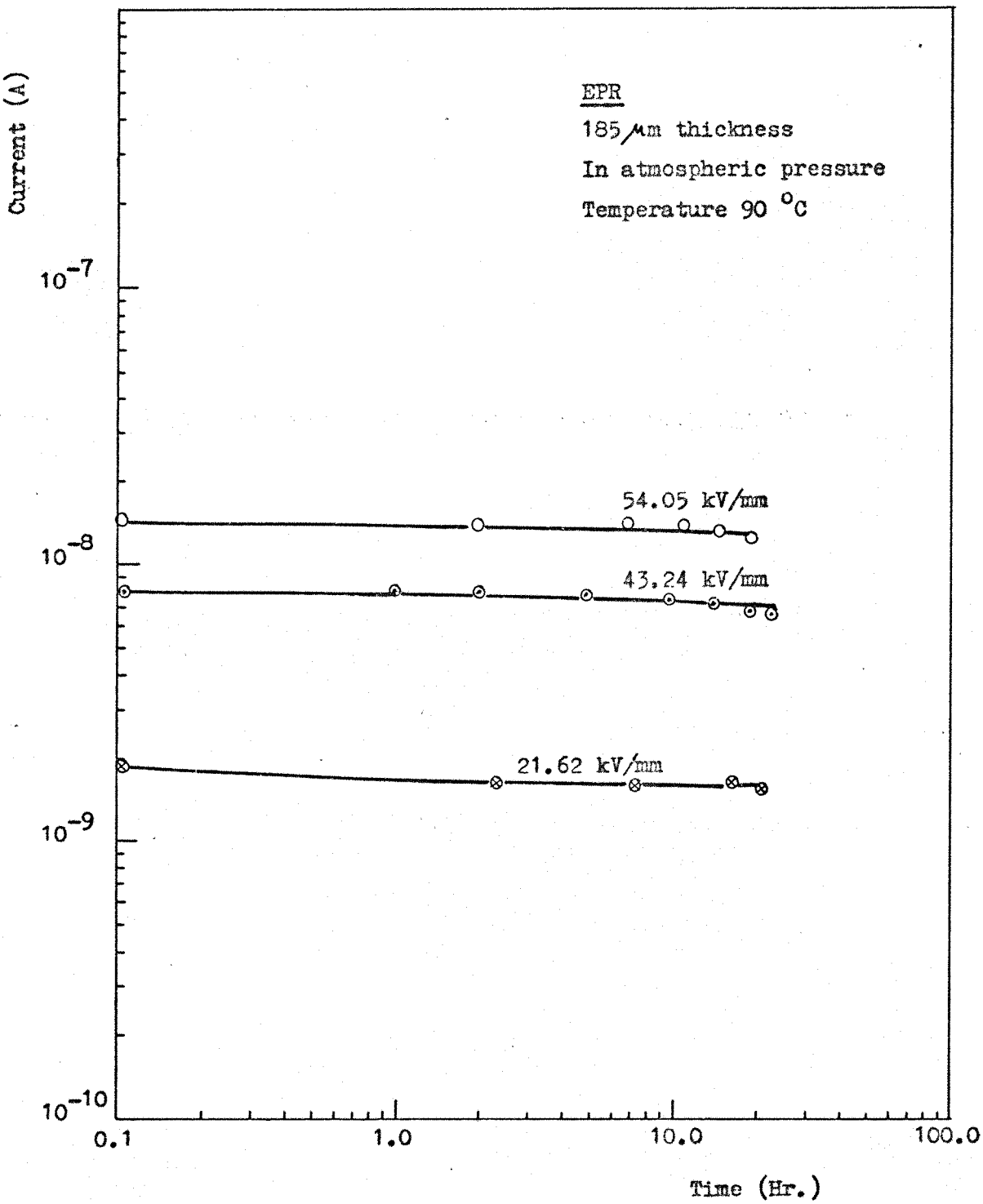

(Figure 21) Plot of conduction current against time

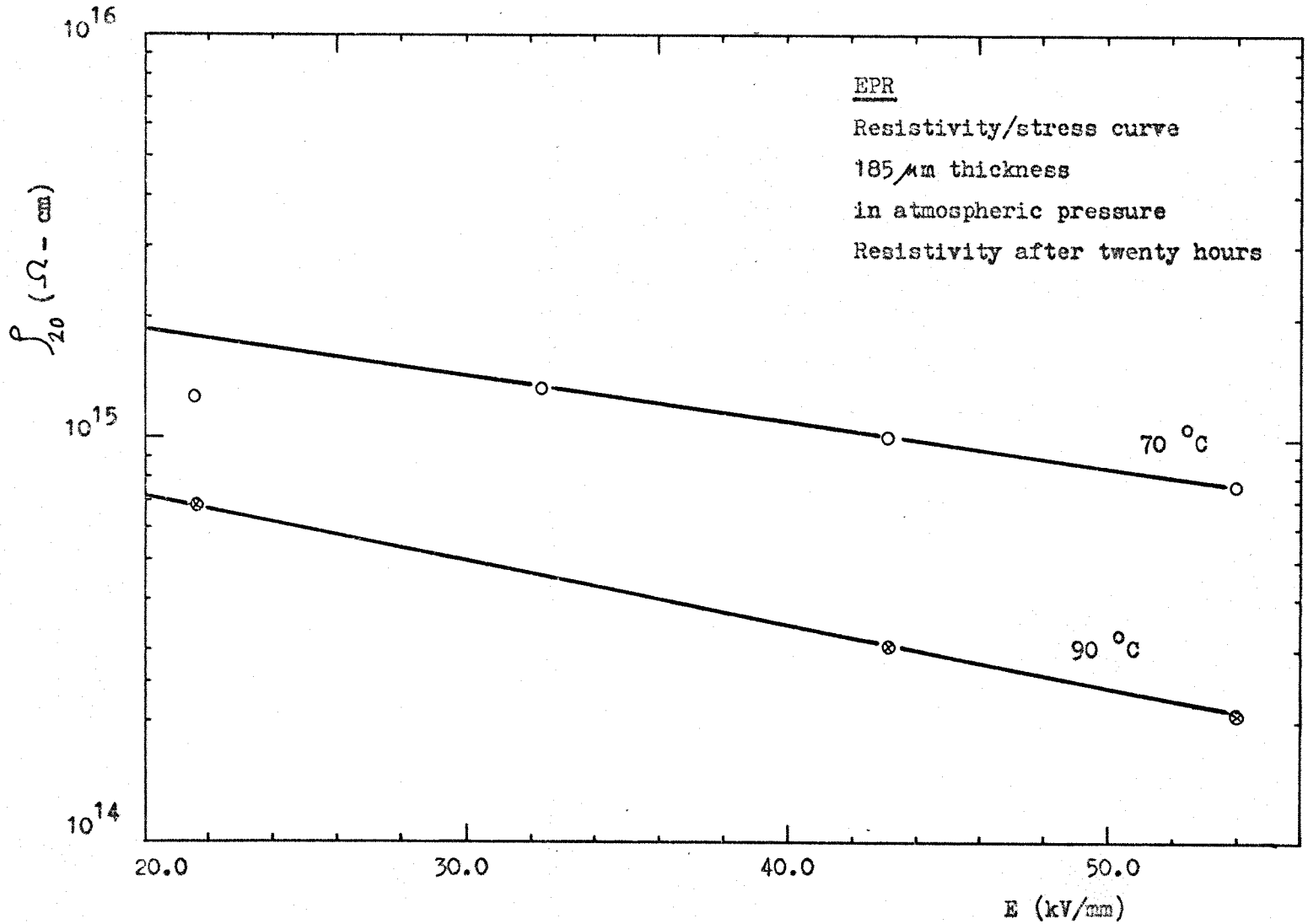

(Figure 22) Plot of resistivity against applied field

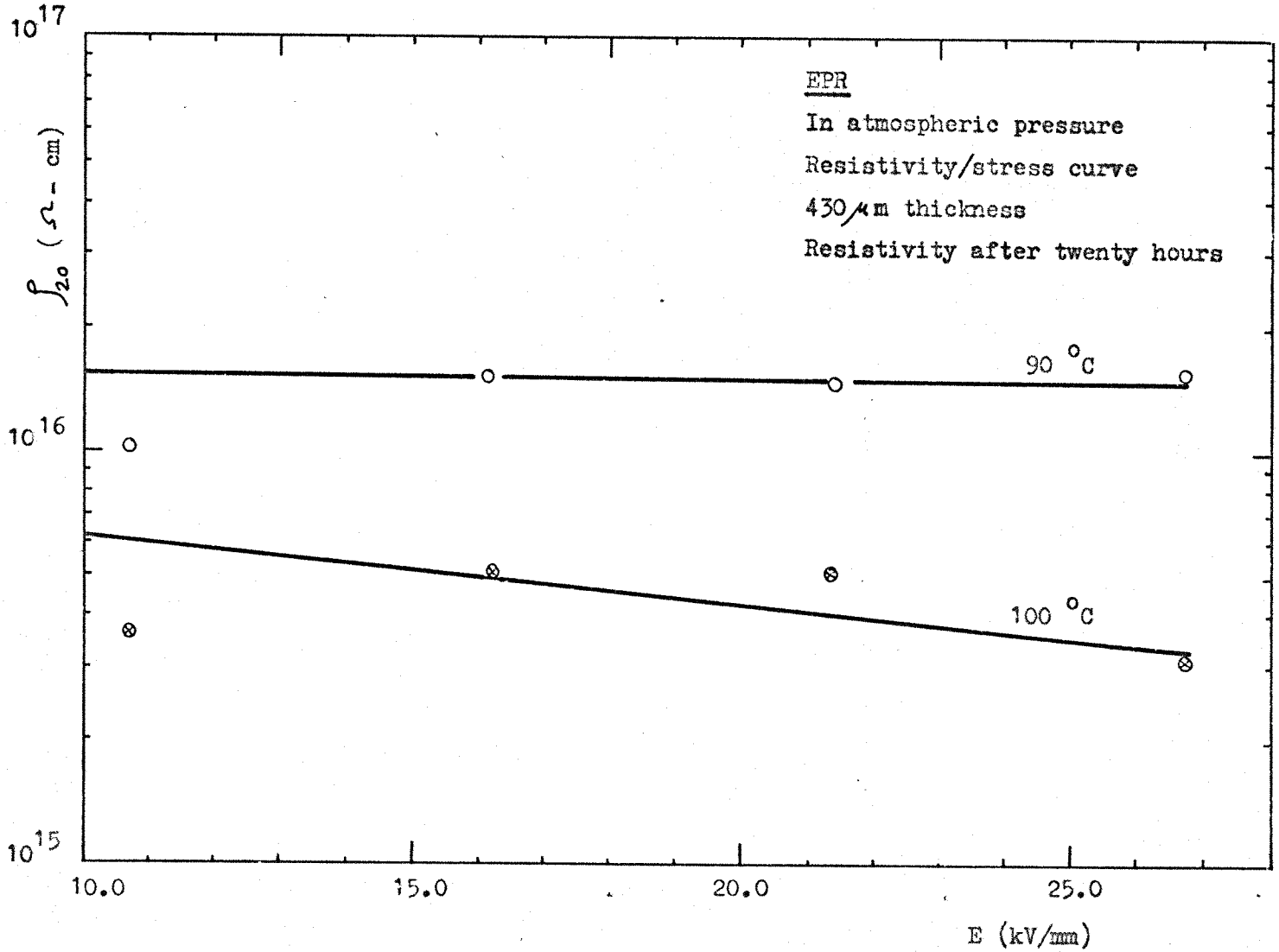

(Figure 23) Plot of resistivity against applied field

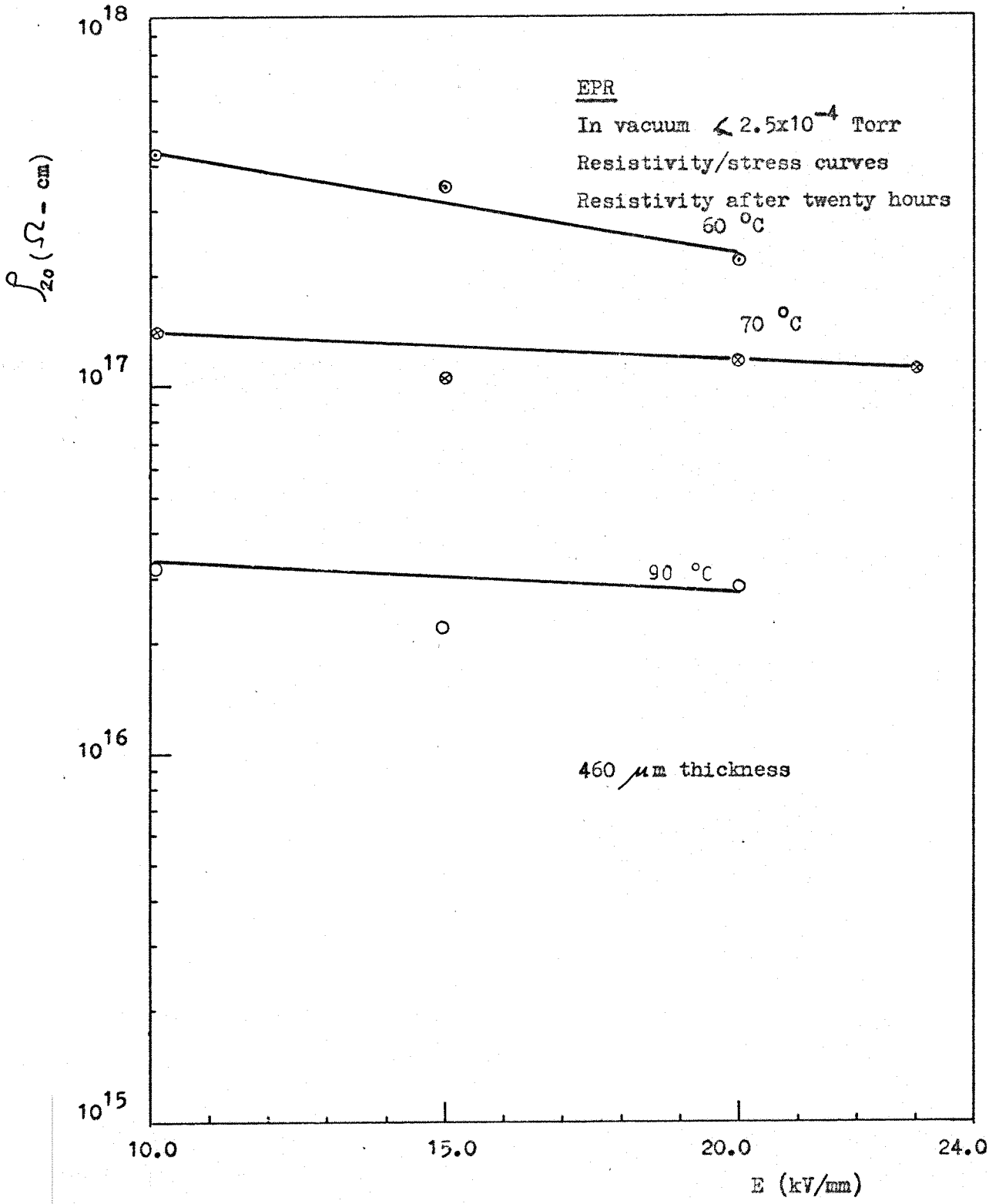

(Figure 24) Plot of resistivity against applied field

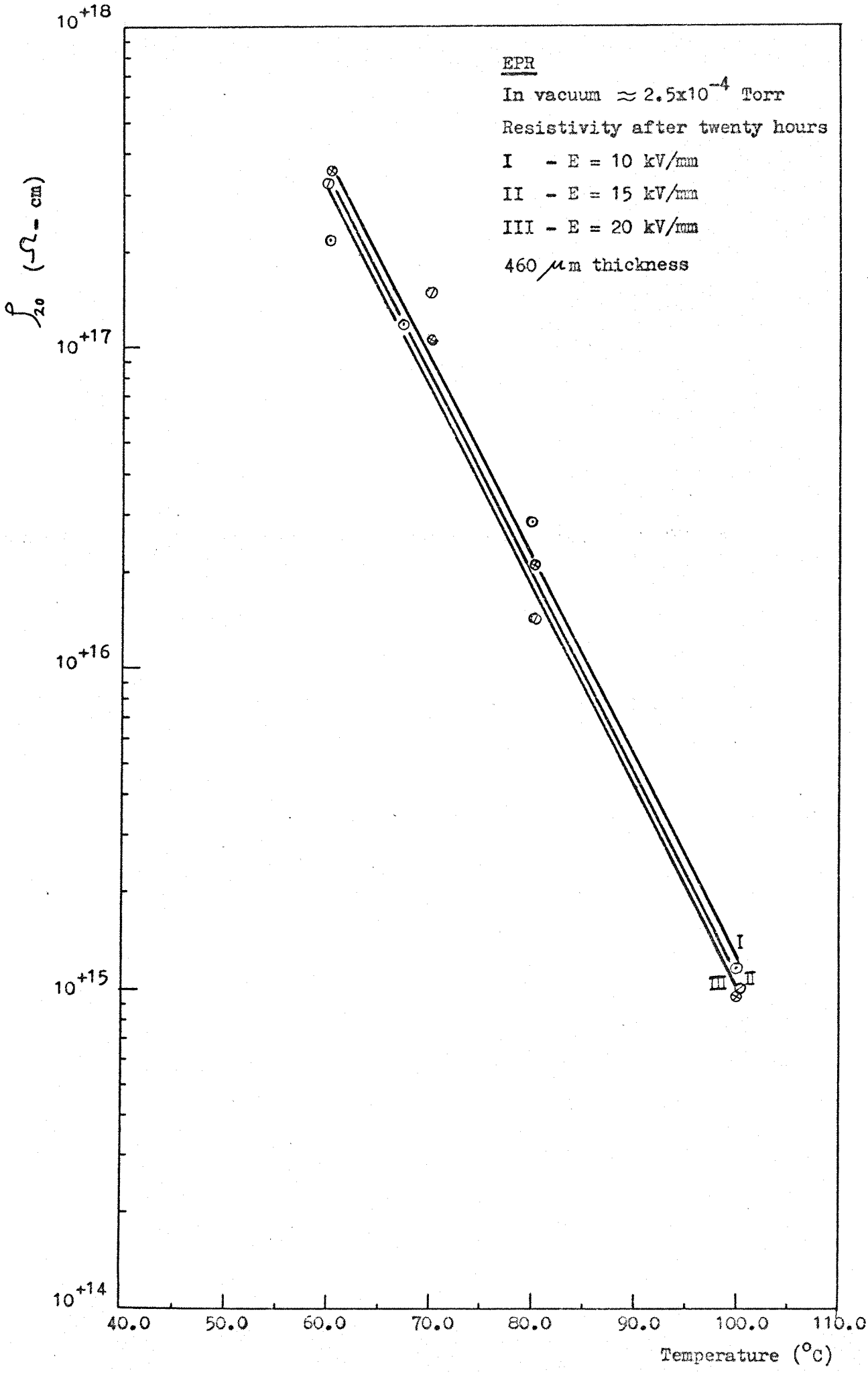

(Figure 25) Plot of resistivity against temperature

4-3 RESULTS FOR POLYPROPYLENE

The polypropylene is a result of polymerizing the propylene [$CH_2 = CH - CH_3$]. Table (3-1) shows the mechanical properties of the polypropylene compared to the polyethylene. The problem encountered when using polypropylene in cables arises from its difficulty of adhering to the surface of the conductor, because it is so hard. This mechanical problem can be solved by special design of the semiconductor layer or by special extrusion technique during the manufacturing process, specially for large size conductor cables as the internally water-cooled cables.

4-3-1 Conduction Current

The results obtained in (Figures 26 - 30) show that the decaying rate of the conduction current at low applied field is very small compared to the decaying rate at high applied field. Within the range of temperatures used in the test (40 ^{o}C - 80 ^{o}C), it is possible to conclude that the conduction current in polypropylene is more steady than the conduction current in the polyethylene.

The mechanism of the conduction current, at first applied field, at short circuit period, and after reapplying the same field gives an evidence that there is much space charge held in the bulk of the polypropylene specimen.

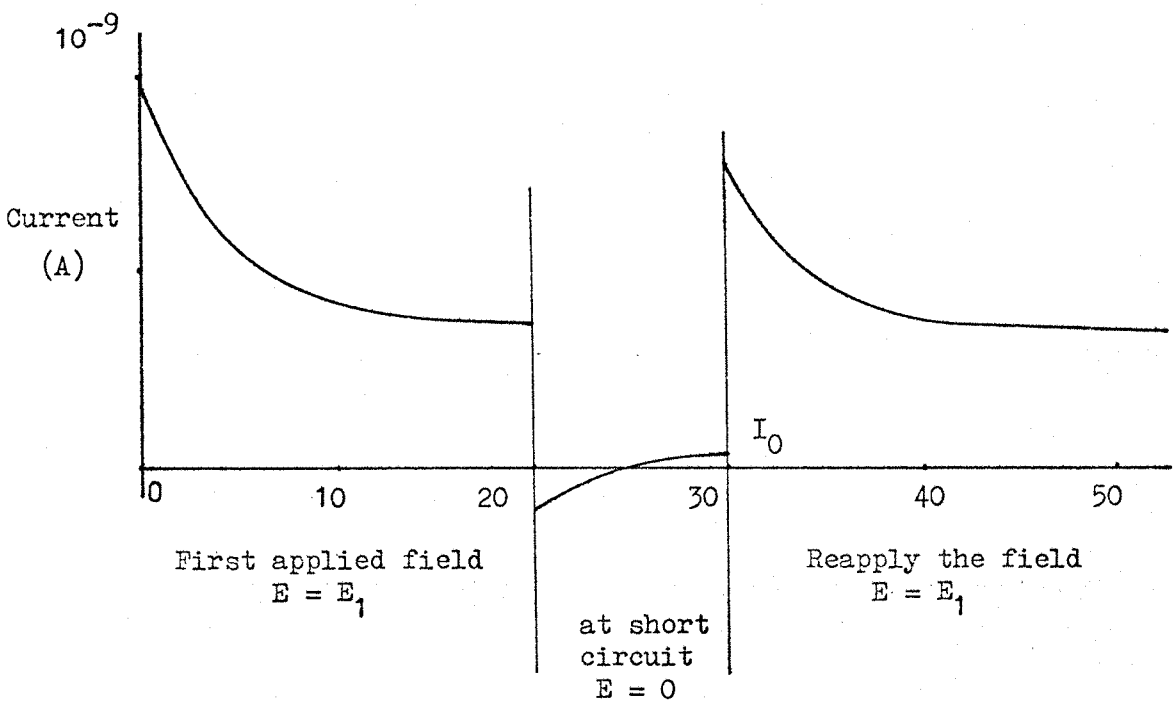

At temperatures ($\lesssim$ 60 °C) $I_0 = 0$. (Figure 4-6)

4-3-2 Resistivity/Stress Variation

At a certain temperature, it was found that the resistivity/stress variation follows the first Poole formula. The different time consumed to reach the steady-state current result in a conflict with Poole theory specially at temperatures more than 50 °C in polypropylene. The values of the resistivity/stress coefficients (β) are shown in Table (4-8-b).

4-3-3 Resistivity/Temperature Variation

The results obtained in Figure (32) show that the resistivity/temperature curves are linear over all the values of the applied fields. The slopes of the curves decrease as the applied field increases. As a result of this the resistivity/temperature coefficient 'α' decreases.

Table (4-8-a) Polypropylene resistivity after twenty hours, specimen thickness 160/μm

α (1/°C)	E (kV/mm)	ρ_o (Ω - cm) (at θ = 40 °C)
0.12	6.25	3.2×10^{17}
0.11	16.75	2.17×10^{17}
0.073	31.25	4.2×10^{17}

Table (4-8-b) Polypropylene resistivity after twenty hours, specimen thickness 160/μm

β (cm/kV)	θ (°C)	ρ_o (Ω - cm) (at E = 0.0 kV/mm)
0.00767	40	5.3×10^{17}
0.00720	50	2.3×10^{17}
0.00630	60	1.0×10^{16}
0.00220	80	4.5×10^{15}

4-3-4 The Effect of Thickness on the Resistivity of the Polypropylene

The results obtained (Figure 30) show that the effect of smaller thickness decreases the time consumed to reach the steady-state current. The results shown in Table (4-9) give the values of the polypropylene resistivity (after twenty hours) for different thicknesses.

Table (4-9)

Thickness (μm)	Resistivity (Ω - cm)
160	1.87×10^{15}
185	9.1×10^{15}
255	1.21×10^{16}

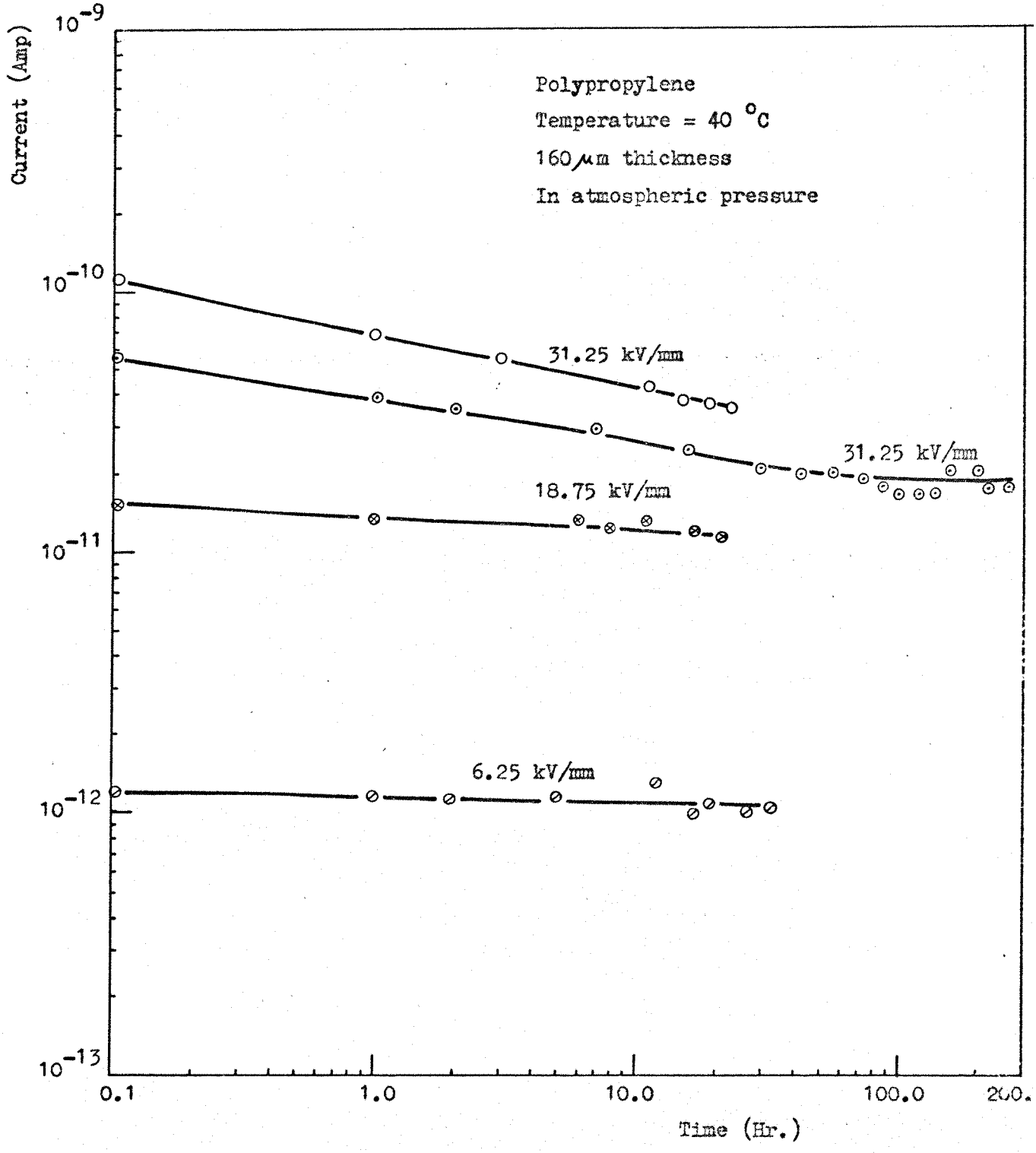

(Figure 26) Plot of conduction current against time

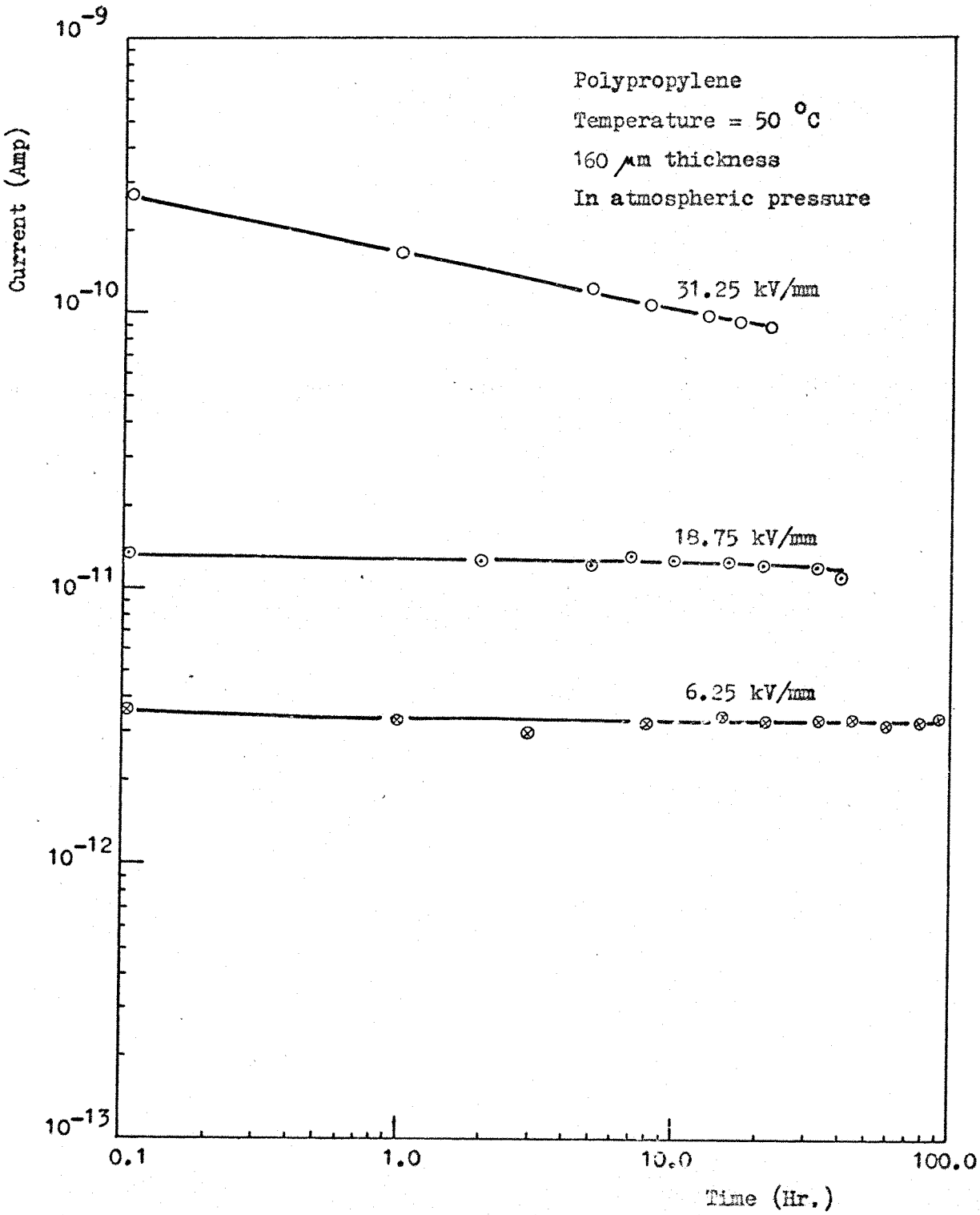

(Figure 27) Plot of conduction current against time

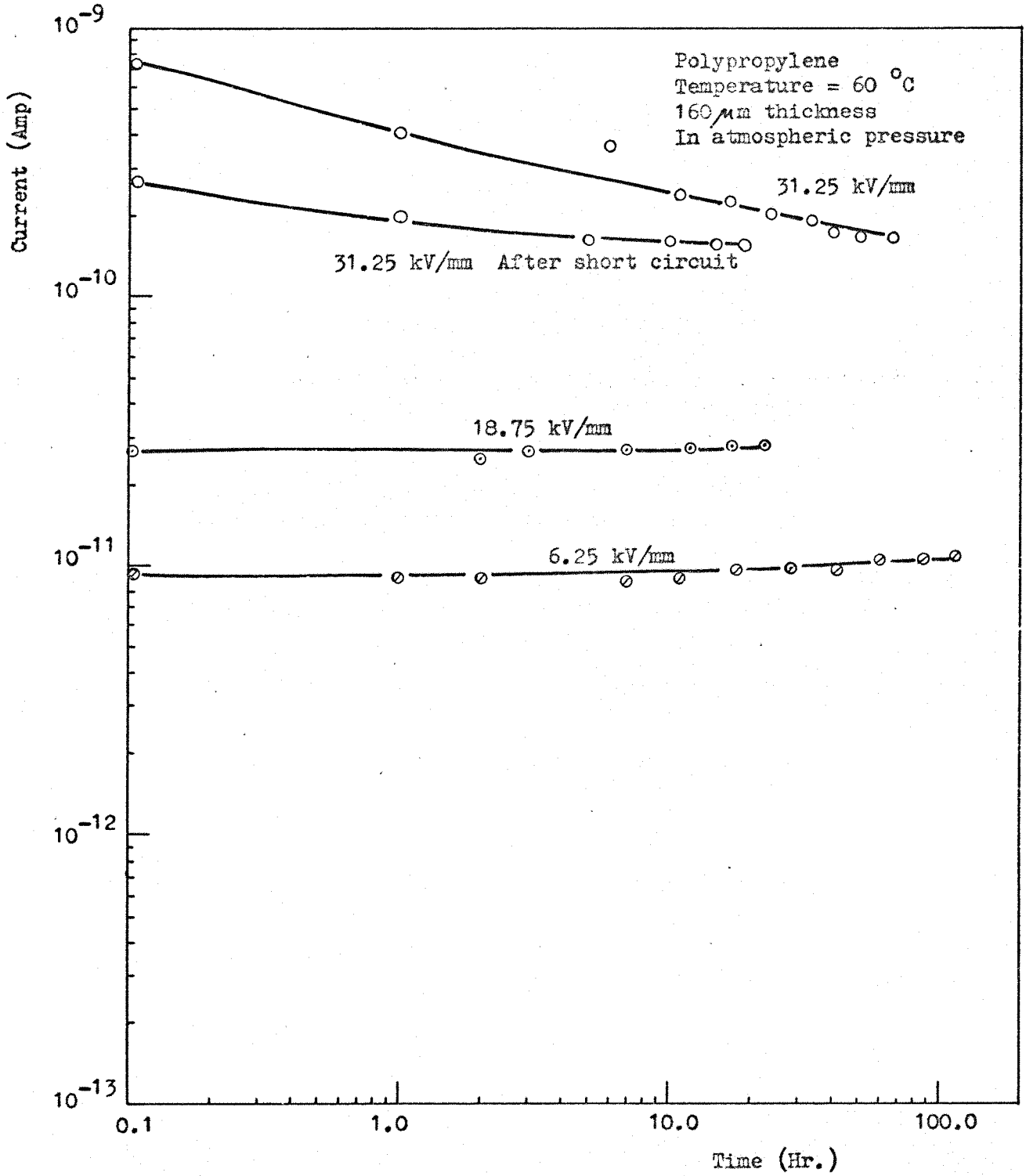

(Figure 28) Plot of conduction current against time

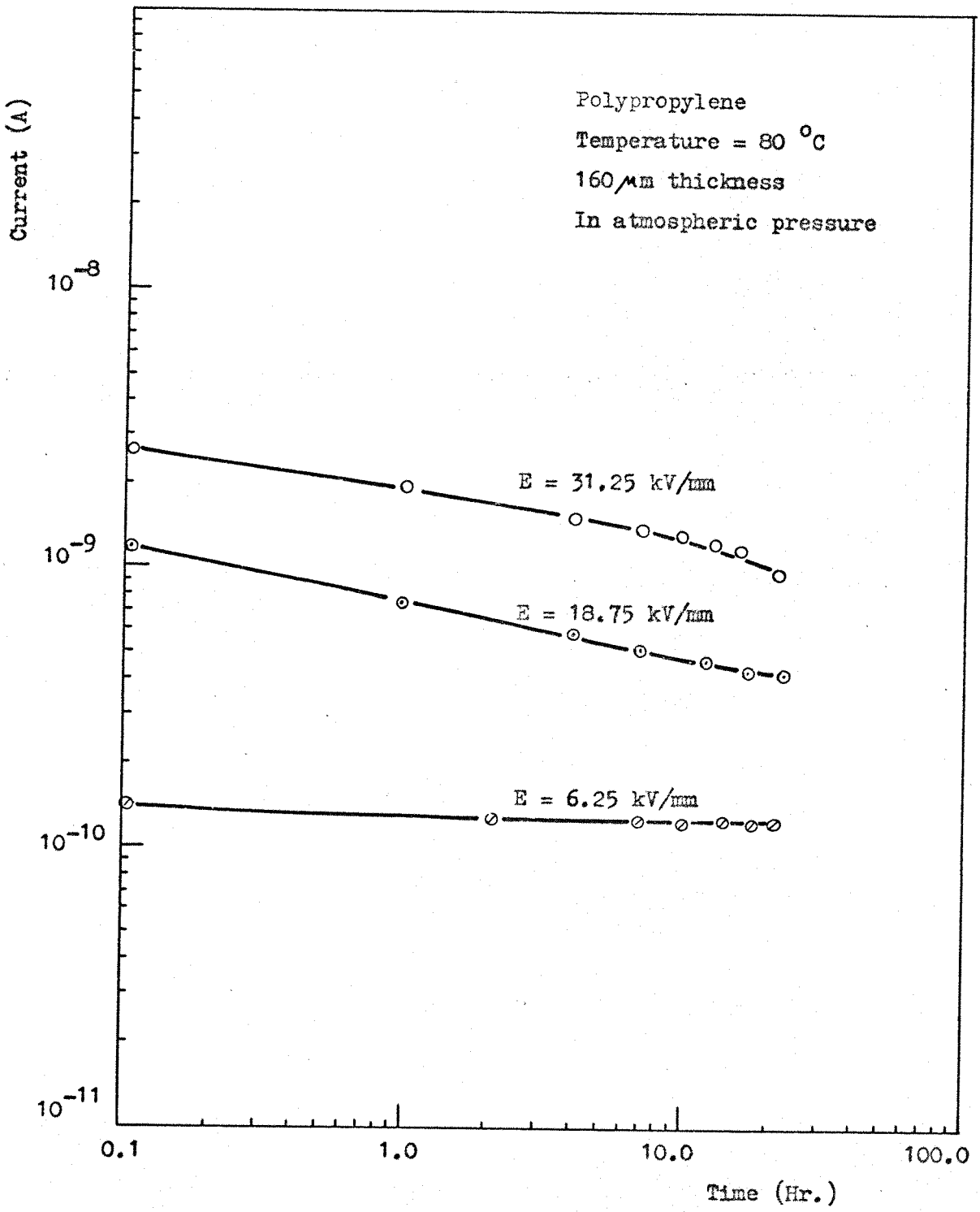

(Figure 29) Plot of conduction current against time

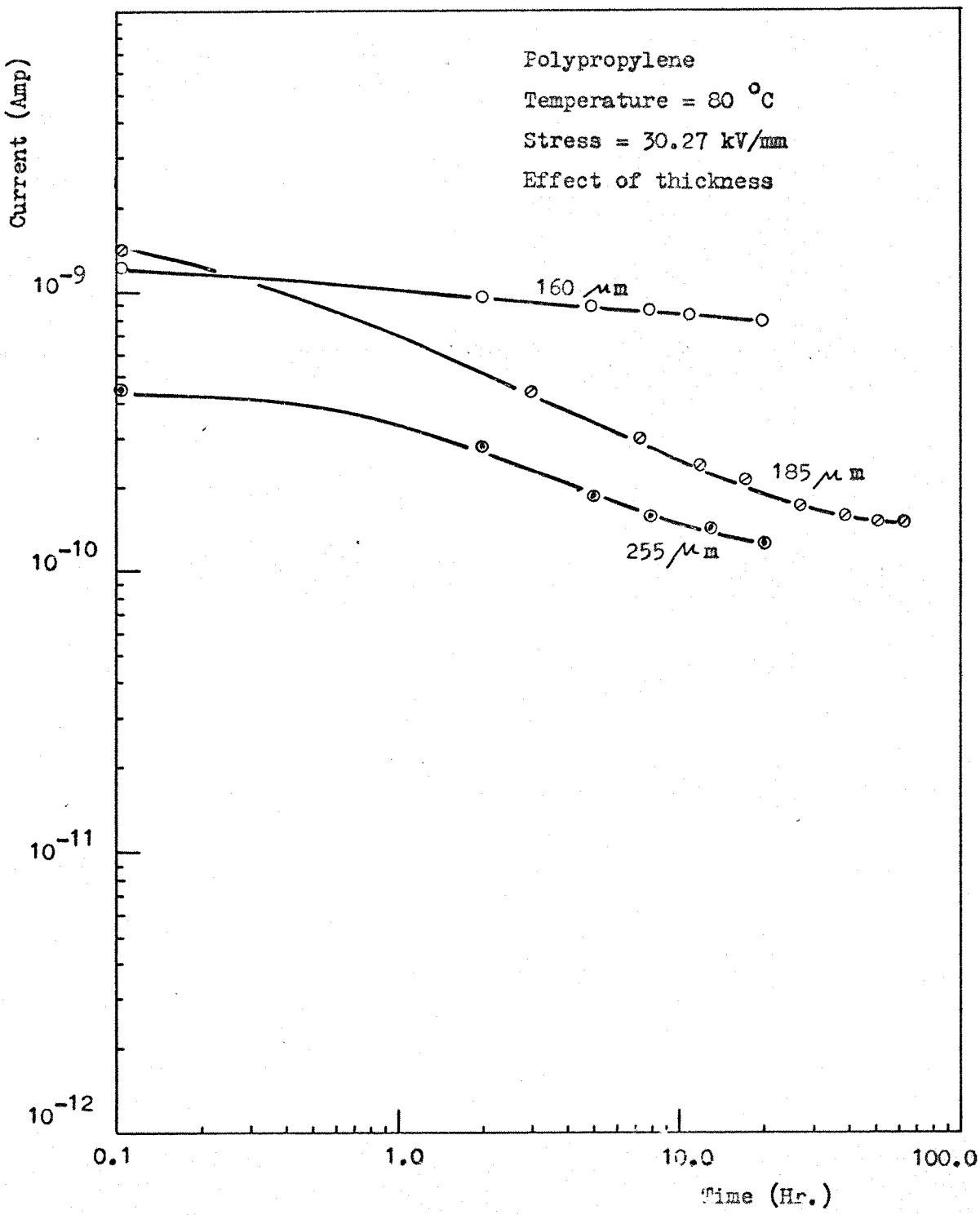

(Figure 30) Plot of conduction current against time

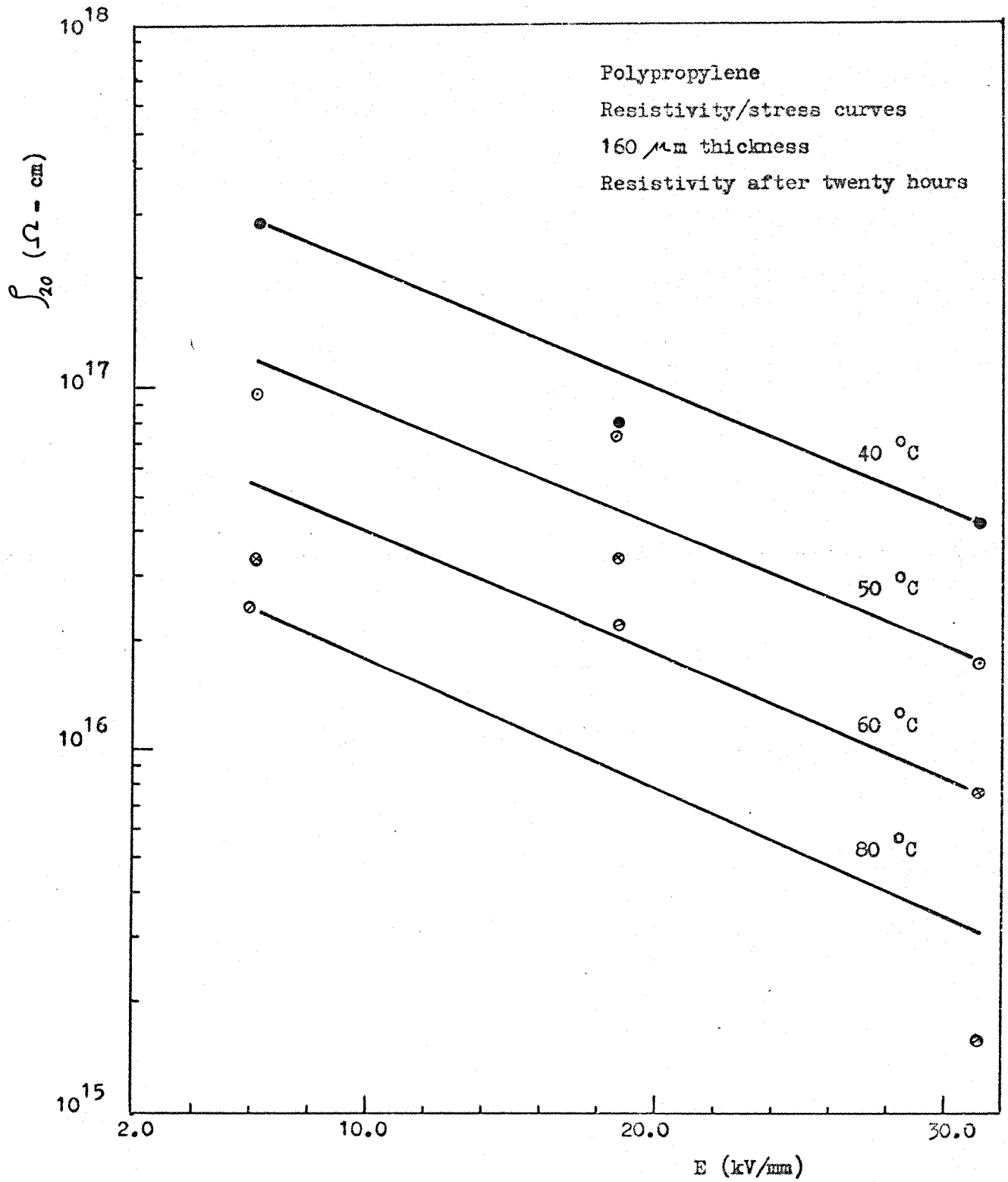

(Figure 31) Plot of resistivity against applied field

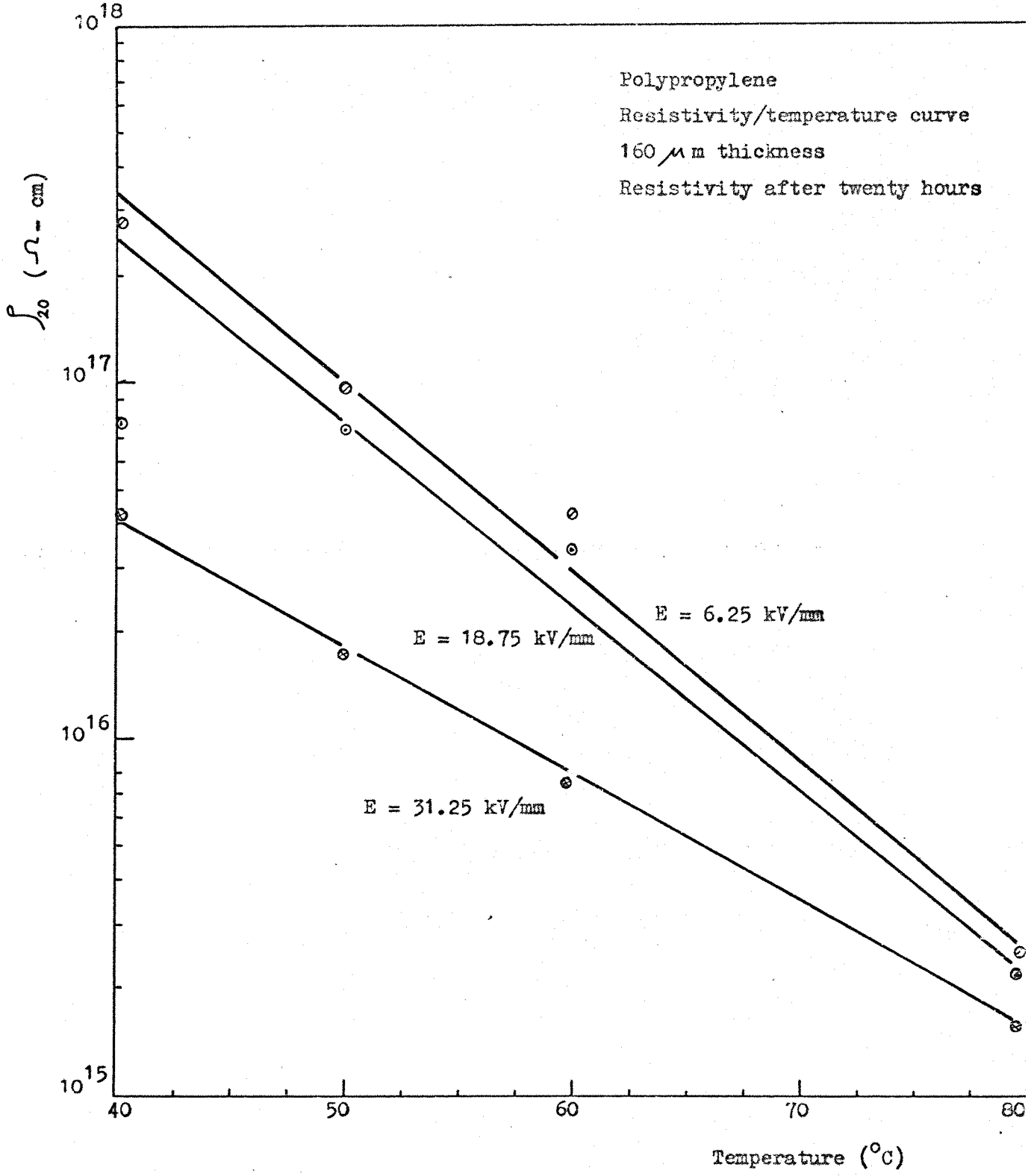

(Figure 32) Plot of resistivity against temperature

CHAPTER FIVE

RESULTS FOR CROSS-LINKED POLYETHYLENE AND POLYETHYLENE WITH ADDITIVES

5-1 INTRODUCTION

The results obtained from the previous work on the polyethylene show that, it is not possible to define the resistivity of the polyethylene due to the difficulty obtained to get the steady-state current. Opinion in the present investigation is that, the reason of the above difficulty is due to the fact that the injected space charge carriers and the carriers from inside the bulk of the polyethylene needs a very long time "days" to achieve equilibrium, i.e. between the trapped carriers and the emitted carriers.

The study on the tree-initiation associated with space charge formation in polyethylene by Ieda and Nawata[40] shows that, the effect of the space charge accumulation has a great influence on the increase of the microscopic electric fields and then on the breakdown strengths of the plastic materials operating under direct fields. The complete dissipation time of the trapped carriers obtained[40] on the polarity-reversal test above room temperature is quite long.[40]

Opinions on the effects of certain types of additives in polyethylene are as follows: first to reduce the electrical resistivity of the polyethylene, secondly, to obtain a steady-state current, while the third is that, the existence of the additive (which has higher conductivity) in the matrix of the polyethylene has great effect to sweep-out the space charge accumulation held by the potential barriers.

The resistivity of the cross-linked-polyethylene and the resistivity of the polyethylene with different types of additives has been investigated in this work.

5.2 CROSS-LINKED-POLYETHYLENE

5-2-1 Introduction

Cross-linking of the linear thermoplastics as polyethylene can be done either by X-rays or chemically, in order to produce a sort of thermosetting material which has good thermal properties. Cross-linked-polyethylene is used for A.C. cables up to 110 kV with average designed stresses less than 5.9 kV/mm and a working temperature of (90 ^{o}C).[35] Singh and Bruhin[27] studied cross-linked polyethylene, their suggestion is that the mineral-filled cross-linked polyethylene is useful for high voltage D.C. cables. The results obtained by Singh and Bruhin[27] are mainly dependant on the values of conductivity after a few minutes (10 minutes), while such materials as cross-linked polyethylene under D.C. field needs longer time for the conduction current to reach the steady-state. The decrease of the thermal resistivity of the cross-linked polyethylene, was achieved by using the mineral fillers.[27] Investigation of the cross-linked polyethylene's resistivity at different temperatures, and at different stresses has been done experimentally in this work. The cross-linked polyethylene used in the present experimental work was formed by, a chemical cross-linking of the polyethylene with a few Dicumyl-Peroxide

5-2-2 Experimental Results

5-2-2-1 Conduction Current in XLPE

The results obtained in this work show that, it is possible to get steady-state current at temperature 40 ^{o}C and at atmospheric pressure, specially at fields less than 10 kV/mm. The probability for obtaining steady-state current within 10 hours is decreased as the applied field increased. At field (E = 12.5 kV/mm) and at temperature (60 ^{o}C) steady-

state current was obtained after twenty hours, while at fields (6.25 kV/mm, 4.167 kV/mm) steady-state current was obtained within twenty hours. At stresses less than 10 kV/mm, the probability for obtaining steady-state current is increased as the temperature increased.

The application of high fields of more than 10 kV/mm, results many space charge carriers being injected and superimposed with the carriers from the bulk, the accumulation needs a long time to be trapped and emitted in order to get the equilibrium between the injected and the emitted carriers.

5-2-2-2 Resistivity/Temperature Variation

The results obtained in (Figure 7) show that the resistivity is decreased as the temperature is increased in the same manner as polyethylene, EPR and polypropylene which follows the well known empirical formula.

$$\log \rho = k + \alpha \theta \qquad \text{- - - (5-1)}$$

where k is constant depends on the applied field.

The following table shows the values of the resistivity/temperature coefficients (α) at different applied stresses.

Table (5-1-a) (XLPE) 240 μm thickness

α (1/°C)	E (kV/mm)	ρ_o (Ω - cm) (at θ = 40°C)
0.180	4.167	1.95×10^{16}
0.180	6.25	1.5×10^{16}
0.1783	12.5	1.3×10^{16}
0.162	20.834	8.1×10^{15}

5-2-2-3 Resistivity/Stress Variation

The results obtained (Figure 6) show that the resistivity is decreased as the applied field is increased. The variation of ($\log \rho$) with (E) is quite linear for a wide range of fields (4.1 kV/mm - 33.3 kV/mm). The resistivity/stress characteristics are following the first Poole formula as,

$$\log \rho = k1 + \beta E \qquad - - - (5\text{-}2)$$

where k1 is a constant depends on the temperature of the specimen.

The following table shows that 'β' is decreased due to the increase of the temperature.

Table (5-1-b) (XLPE) 240 μm thickness

β (cm/kV)	θ (^{o}C)	ρ_o (Ω - cm) (at E = 0.0 kV/mm)
0.004380	40	2.4×10^{16}
0.00315	50	7.3×10^{15}
0.00275	60	2.85×10^{15}
0.00178	80	4.6×10^{14}

5-2-2-4 Discharging Current [Short Circuit Current with Earth]

The short circuit current to earth of the specimen after applying an electric field, decay with time and needs long time to reach zero (months). At high temperature and at previously positive high field the decaying current changes its sign from negative to positive. The mechanism of the short circuit current depends on the quantity of the space charge carriers and the previous period of the applied electric field. At high temperature, more than 60 ^{o}C, the positive current

obtained indicates the presence of positive ions in the specimen.

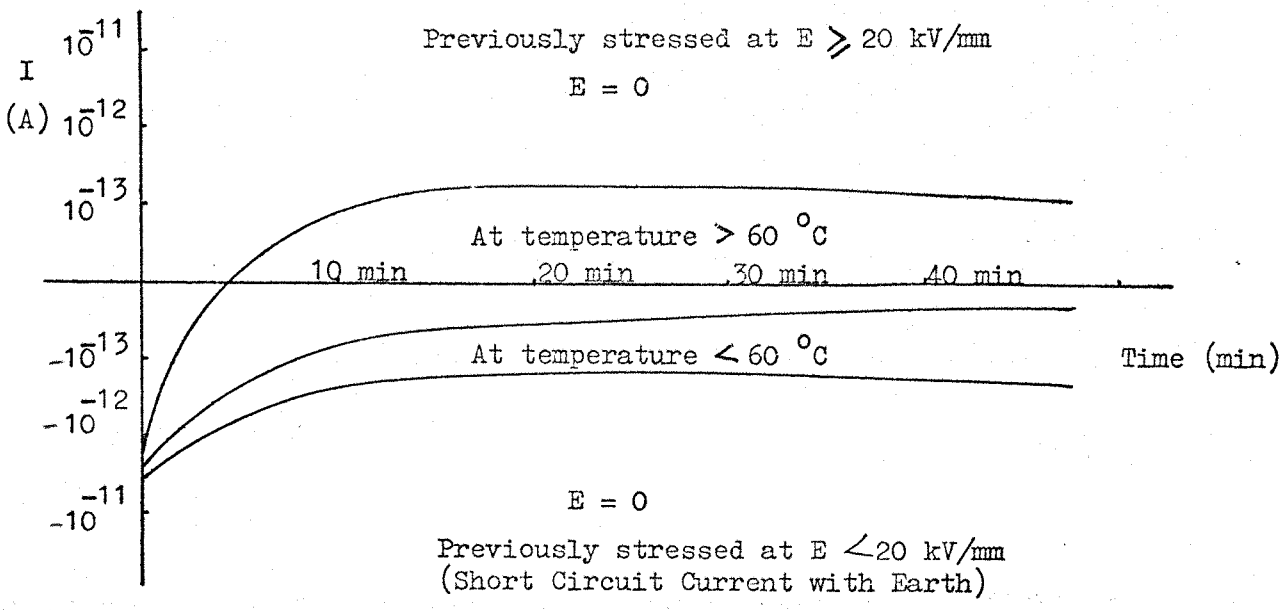

(Figure 5-1)

5-2-2-5 Conduction Current After Short Circuit

The results obtained in this work show that the current at second applied field i.e., after short-circuit is approximately the same as that at the first applied field, which give evidence, that the cross-linked-polyethylene has less ability to store space charge carriers than polyethylene. This is because it is mostly amorphous material. For a fresh specimen the decaying current takes longer time than that of the old specimen (previously tested) with higher amplitude of the transient current.

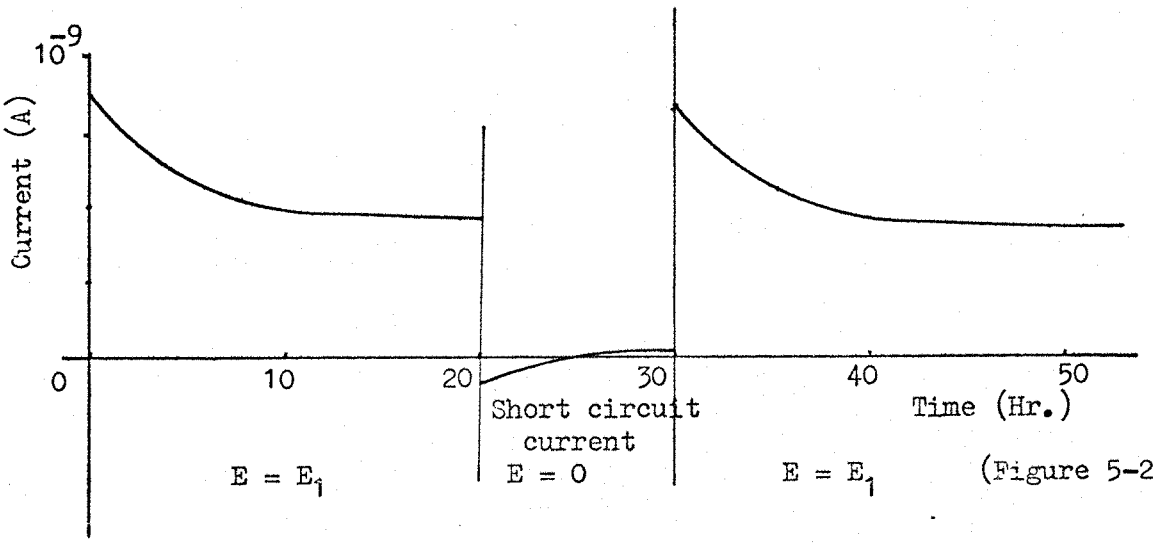

(Figure 5-2)

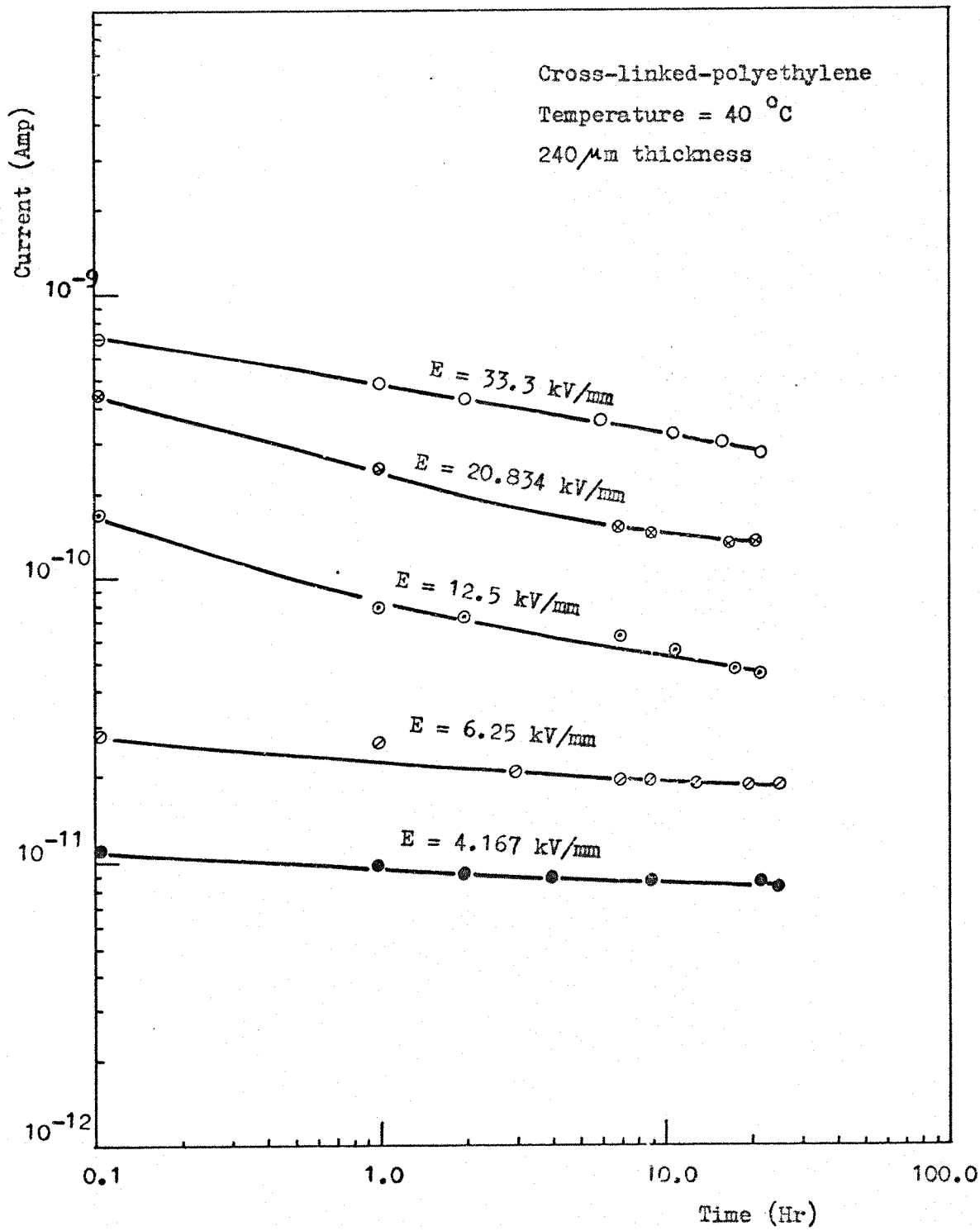

(Figure 1) Plot of conduction current against time

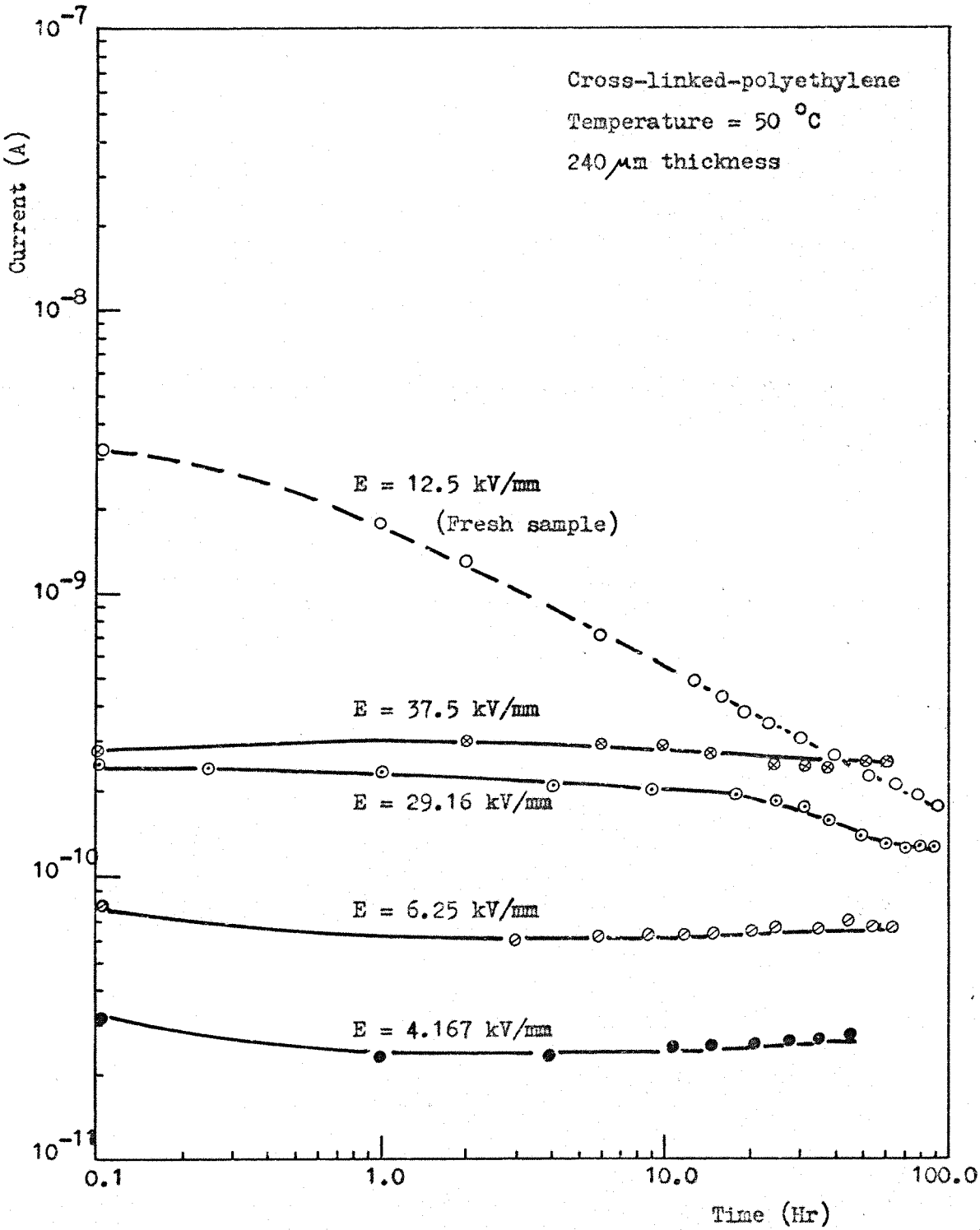

(Figure 2) Plot of conduction current against time

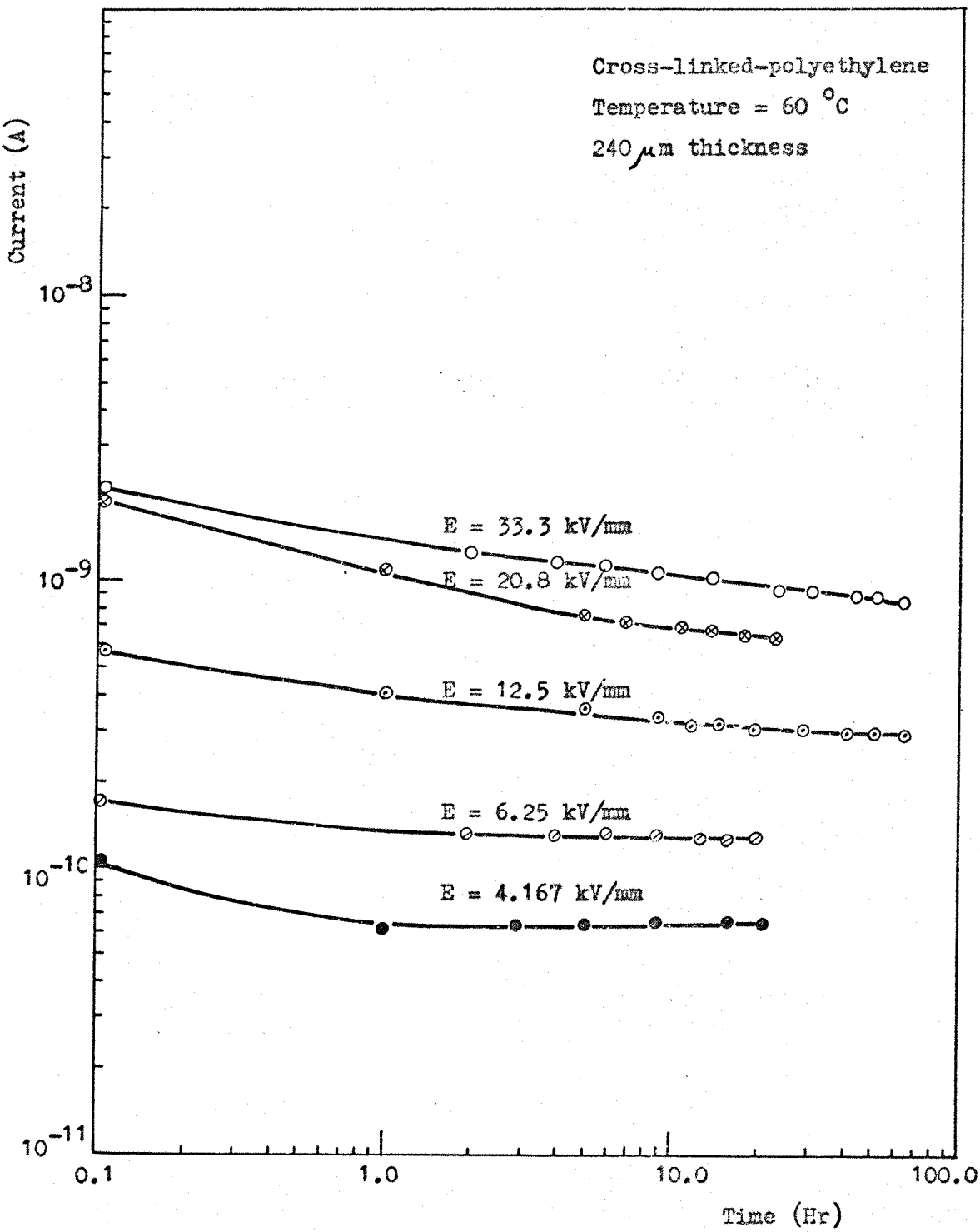

(Figure 3) Plot of conduction current against time

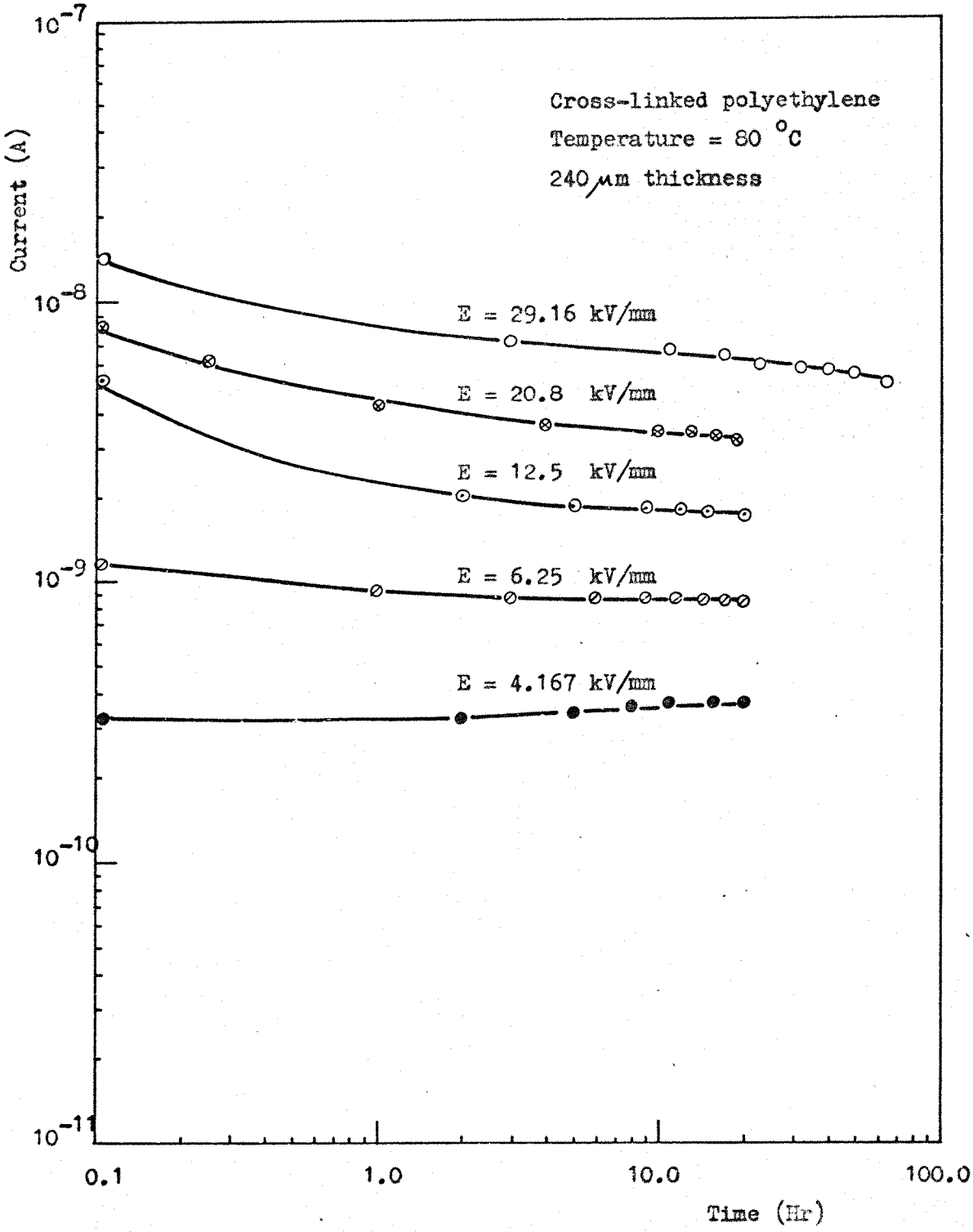

(Figure 4) Plot of conduction current against time

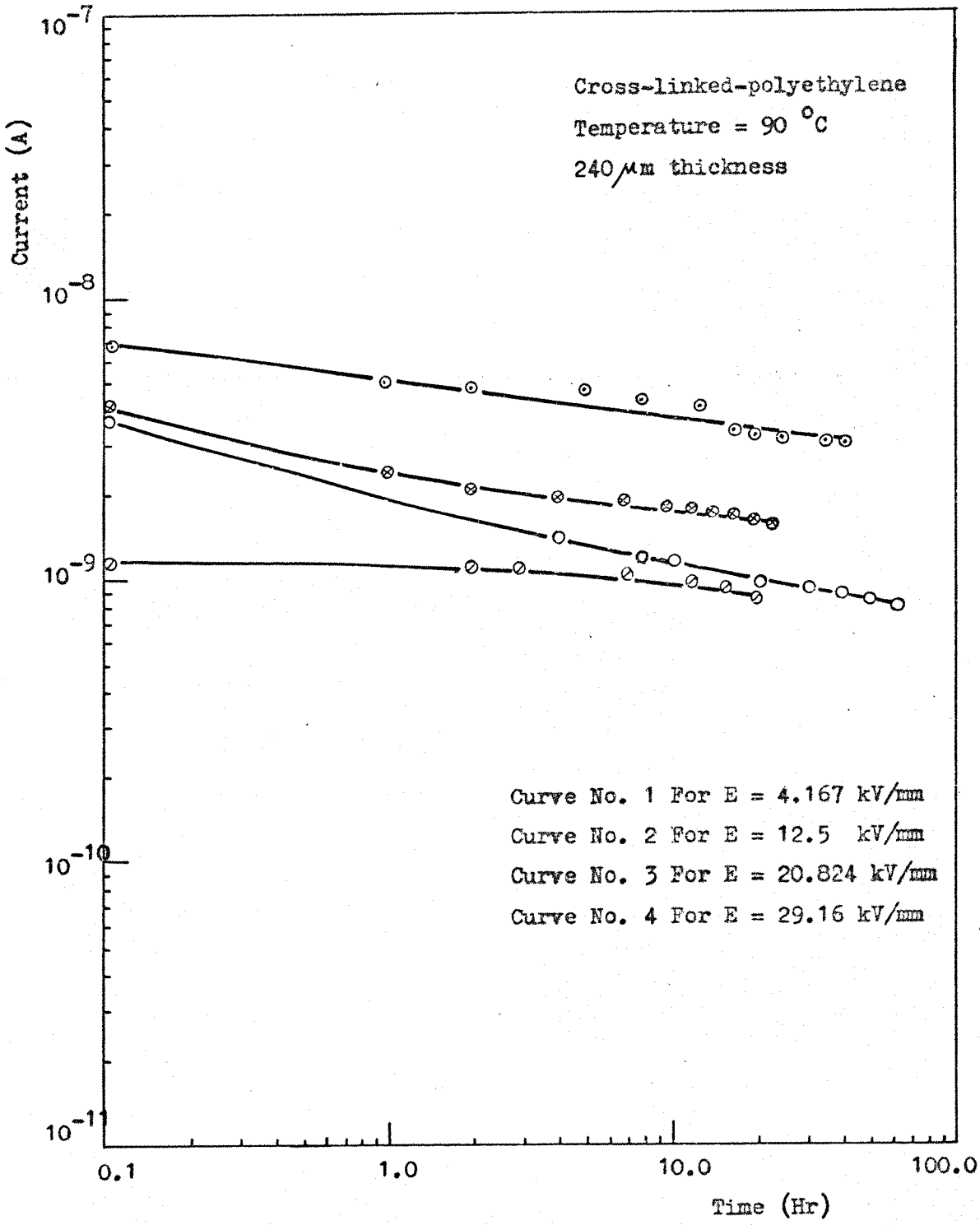

(Figure 5) Plot of conduction current against time

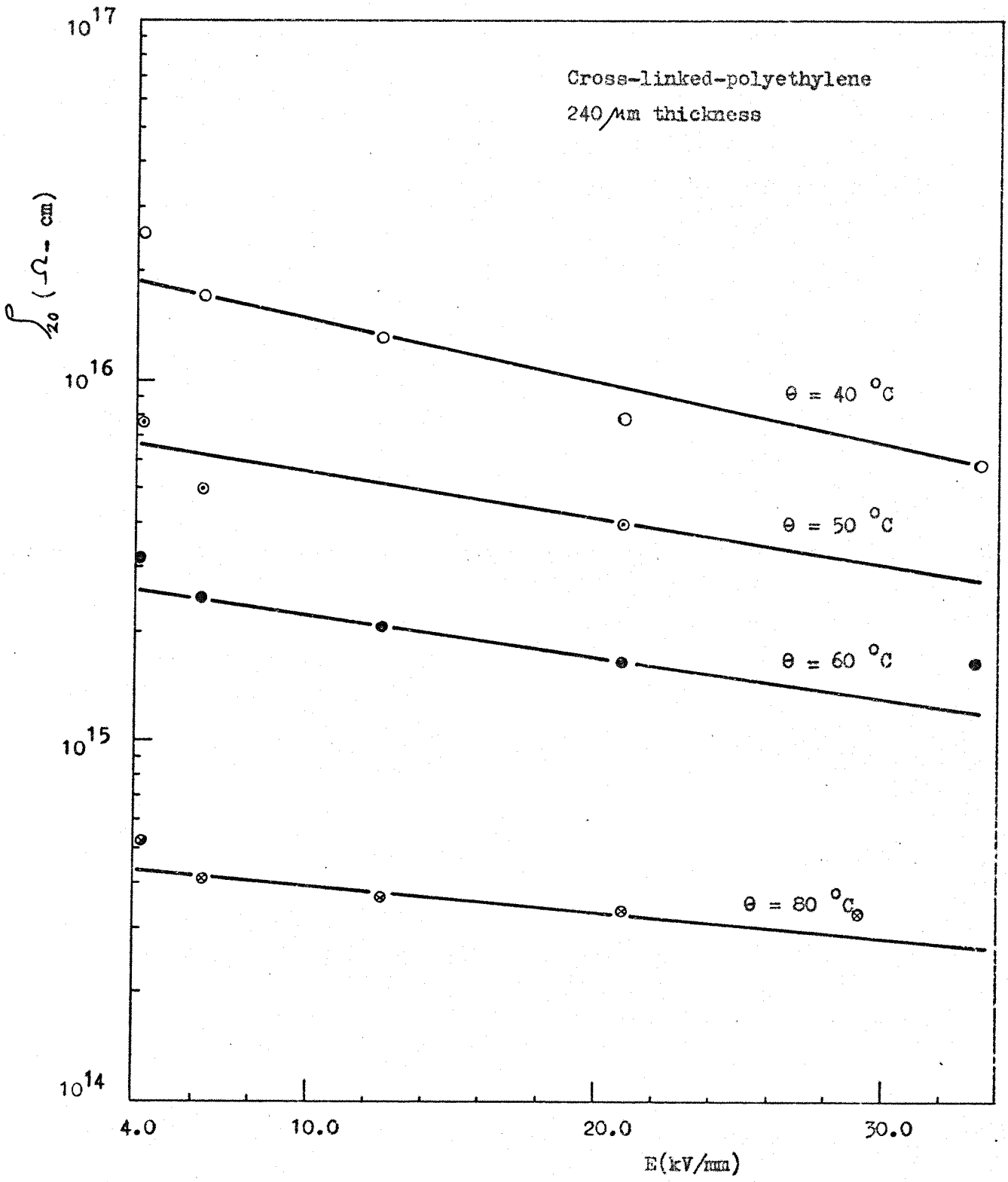

(Figure 6) Plot of resistivity against applied field

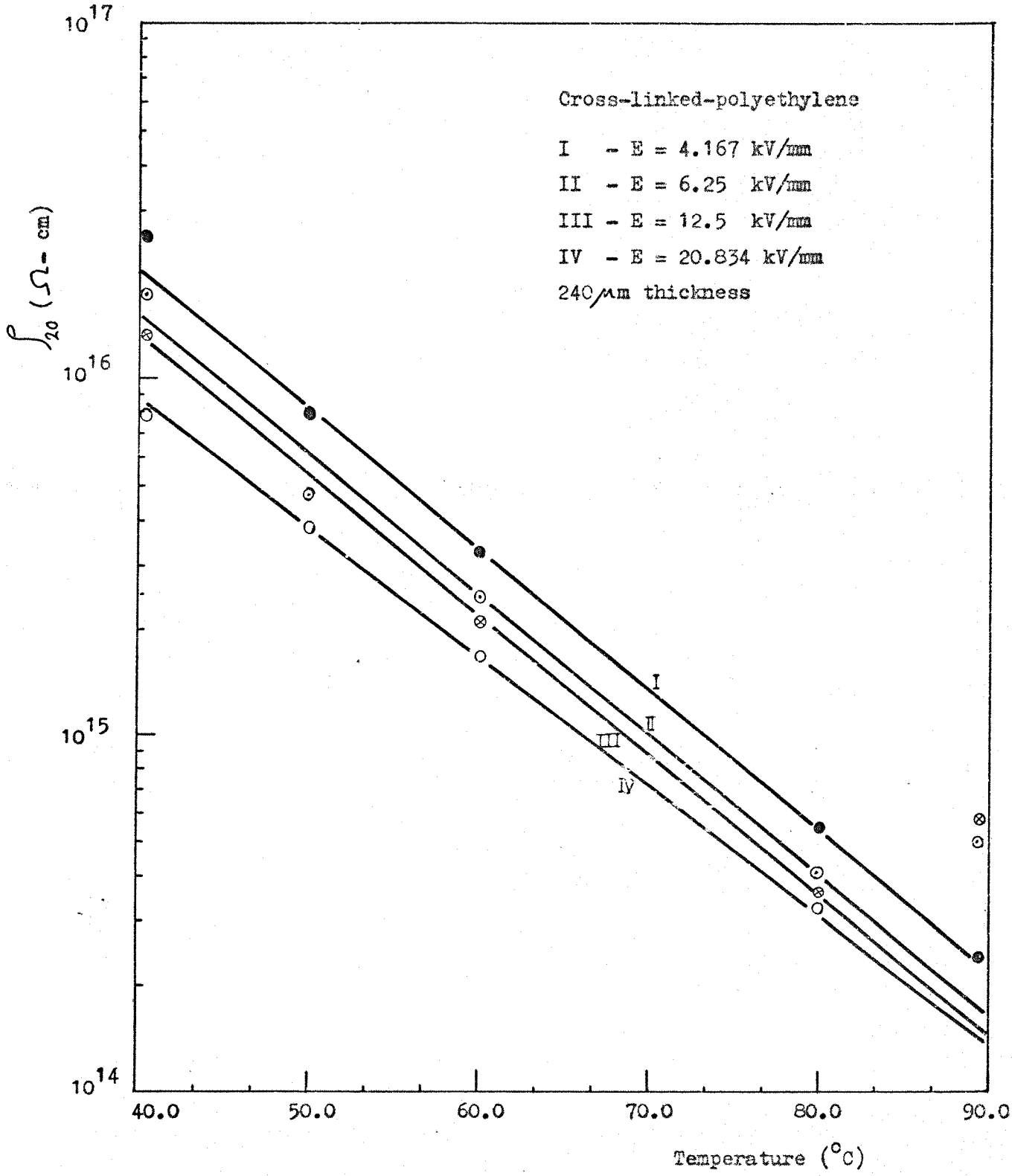

(Figure 7) Plot of resistivity against temperature

5-2-2-6 Effect of Acetophenone

During the processing of the cross-linked polyethylene a small quantity of volatile acetophenone was produced as a by-product, which increases the conductivity at the first applied field. The acetophenone is easily evaporated during the application of the electric field, even at low temperature.

5-3 POLYETHYLENE WITH ADDITIVES

5-3-1 Introduction

The conduction mechanism in the polymers at high electric fields can be described in the same manner as in semiconductors. The electronic conduction in semiconductors are generally described in terms of, either the band theory, or by the hopping type. In the band theory the charge carriers are generated by displacing an electron from the valence band to the conduction band. While in the hopping type the situation is that, the charge carriers jump from one localized state (one) to another localized state (two) at a distance (x), over an energy barrier (ΔW). The jump probability P_j is then given as[42]

$$P_j = V.P(x).e^{\left[-\left[\Delta W + {}^1/_2(W1 + W2)\right]/kT\right]} \qquad - - - (5\text{-}3)$$

where V is the phonon frequency,

P(x) is the tunnelling factor,

W1 and W2 are the energies of polarization around localized-state one and two.

The existence of the impurities in the polymer matrix increases the hopping probability, as it increases the number of the localized sites.

The study of the conduction mechanism of the carbon filled polymers done by Forster[42] shows that, the carbon filled polymers do not conduct

by any single classical conduction mechanism. A reasonable postulation, is that the band conduction as well as conduction by hopping and possible ion diffusion occurs.[41, 42] The concentration of the additives, the degree of dispersion as well as the thermal and mechanical history of the sample and the manufacturing process, all have an effect on the conduction mechanism.

The study of polyethylene immersed in hexane for several hours prior to measurements done by Hugues[41] shows that the small concentration of the residual ionic species is responsible for the electrical transport. The assumed ionic mechanism by Hugues[41] is that, the ionic migration is usually envisaged as an activated diffusion process, in which an ion jumps from one position to another each time overcoming an energy barrier. In the previous model, the electrical conductivity is envisaged to be thermally activated.[41]

5-4 SPECIMEN MANUFACTURE

The general processing method of polyethylene specimen including certain types of additives has the following procedures:

1 - Polyethylene pellets about 3.5 mm in diameter can be introduced into a mill at temperature 150 ^{o}C.

2 - After fusion of the polyethylene to a homogeneous mass, the additive particles should be added slowly and blended into the polymer.

3 - A total milling time of about (30 - 40) minutes is necessary to obtain a uniform mixture of the two components.

4 - The test samples can be obtained by pressing the milled sheets for (30 - 40) minutes at about 75 ^{o}C temperature, and at about 800 psi pressure, pressed sheet thickness of (0.3 - 1) mm is expected.

5 - The temperature of the fusion and that of the pressing must be adopted to obtain a flexible sheet and to avoid the cracking.

5-5 POLYETHYLENE WITH CARBON BLACK COMPOSITE

5-5-1 Introduction

The electrical behaviour of carbon-filled polymers have been investigated by several workers at different percentage of carbon-black in the polymer.[41,42,43] The general well-known idea is that, the existence of the high percentage, more than 10%, of carbon particle dispersion in the matrix of the polymer can substantially decrease the resistivity of the various polymers.[41] The percentage 10% is the critical percent, and above this percentage a sharp decrease of the polymer's resistivity is obtained. The above combination was considered as a semi-conducting material, which is used as a shield extruding semiconducting layers in the high voltage power cables.

At low percentage, less than 10%, a very small attention has been given. The results obtained by Hugues[41] on 3% carbon in polyethylene at low fields, less than 1 kV/mm, show that, the existence of 3% carbon dispersed in polyethylene give no noticeable decrease of the polyethylene resistivity. The results obtained by Forster[2] at low percentages show that the low percent carbon-black increases the resistivity of the polyethylene at low fields.

The idea of using (3% and 5%) carbon-black in polyethylene is that, the dispersion of the carbon-black in the polyethylene matrix can increase the ability to sweep out the space charge carriers which are held by the potential barriers at the interfaces between the crystalline and the amorphous regions of the polyethylene. The electrical resistivity of the polyethylene with two different percentages of carbon (3% and 5%) have been investigated at different temperatures and at different high stresses. The conduction current was measured at very long time and at different conditions.

5-5-2 Method of Manufacturing

The manufacturing process of 3% and 5% carbon-black in polyethylene has been done by two stages. The first stage was done by Cabot Carbon Ltd. with a master-batch consisting of 30% of carbon-black in the polyethylene. The second stage was done at Pirelli General Cable Works Ltd., in which the percentage of carbon-black was reduced to 3% and 5% by a two-roll mill machine. Later on the batch was compressed under high temperature [$\simeq$ 175 ^{o}C] and high pressure [$\simeq$ 800 psi] in the form of sheets.

5-5-3 Results

5-5-3-1 Conduction Current

The results obtained (Figures 8 - 11) show that the current was settled down to steady-state at a period of time within (20 hours) at 3% carbon in polyethylene and within (10 hours) at 5% carbon black in the polyethylene. Furthermore the amplitude of the transient current above the steady-state is less than that for the unfilled polyethylene. Hence the injected carriers which are trapped in the unfilled polyethylene are more numerous than that of polyethylene + carbon-black, since the effect of the carbon-black is to sweep out most of the space charge carriers.

At a certain applied field, increase of the temperature reduces the period needed to reach the steady-state.

5-5-3-2 Resistivity/Stress and Temperature Variation

The results obtained (Figures 16 - 17) show that the resistivity of the polyethylene + carbon-black at low fields and at a certain temperature is higher than that of the unfilled polyethylene. At high fields (with a certain temperature) the resistivity of the polyethylene

+ carbon black is lower than that of the unfilled polyethylene. The reasons of the above results are as follows: First the resistivity of the unfilled polyethylene is not a real resistivity since the conduction current at low temperatures and at low fields was not at steady-state even after more than 10 days. As the carbon black is sweeping out most of the space charge carriers, the period of the transient current is reduced, while with the unfilled polyethylene the space charge carriers trapped cause a high amplitude of the transient current. The second probable reason is that, the existence of the carbon black particles in the matrix of the polyethylene during the manufacturing process interrupt the crystallization in the polyethylene, which decreases the percentage of the crystalline part and increases the amorphous part which has a higher resistivity than the crystalline part.

At a certain temperature, the resistivity-stress variation is applicable to the first Poole formula as in equation (5-2). At a certain field, the resistivity varies with the temperature by the empirical formula of equation (5-1).

As in Table (5-2-a) and Table (5-2-b), the effect of the carbon black increases the values of both the resistivity-stress coefficient (β) and the resistivity-temperature coefficient. The increase of the slope of resistivity against temperature means that the activation energy of the composite is increased.

5-5-3-3 Conduction Current After Short Circuit

The results obtained in (Figures 7 - 11) show that the conduction current after a period of few hours short circuiting the specimen to earth has the same mechanism as that at first applied field with little decrease in the amplitude of the transient current.

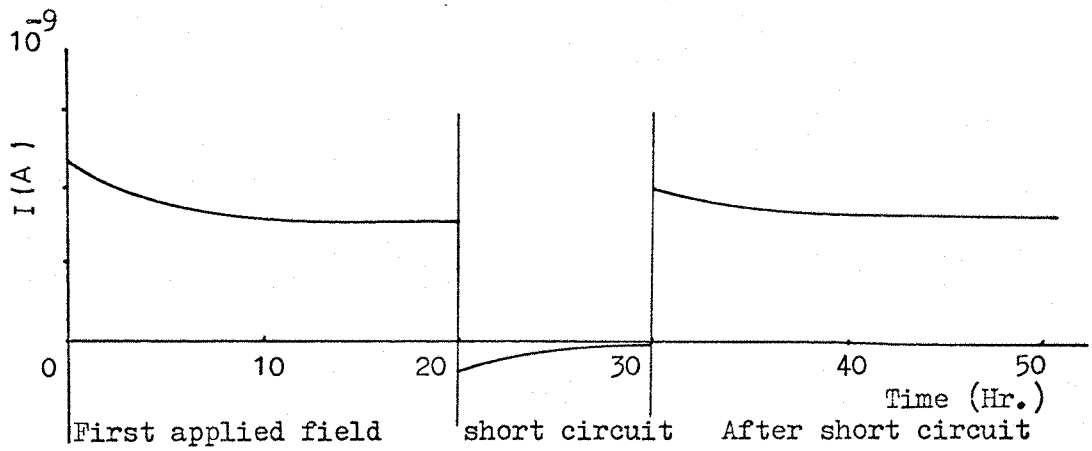

Conduction Current Before and After Short Circuit (Figure 5-3)

Table (5-2-a) Resistivity after twenty hours

Composite	Specimen thickness (μm)	α(1/°C)	E (kV/mm)	ρ_o (Ω - cm) (at θ = 40 °C)
unfilled PE	305	0.0869	10.0	4.3×10^{17}
PE + 3% C.B.	372	0.0886	10.75	1.25×10^{17}
PE + 5% C.B.	286	0.0940	10.5	1.75×10^{17}

Table (5-2-b) Resistivity after twenty hours

Composite	Specimen thickness (μm)	β (cm/kV)	θ (°C)	ρ_o (Ω - cm) (at E = 0.0 kV/mm)
unfilled PE	305	0.00274	50	5.3×10^{16}
PE + 3% C.B.	372	0.003436	50	8.2×10^{16}
PE + 5% C.B.	286	0.0064	50	1.35×10^{17}

5-6 COMPOSITE OF POLYETHYLENE AND MINERAL FILLERS

5-6-1 Introduction

The effect of the inorganic-filler particles in the polyethylene matrix have been investigated.[45,35] The results on the conductivity obtained show that there is no noticeable increase of the conductivity at percentages less than a critical value. The results obtained[46] show that the critical percentage depends on the size of the dispersion particle through the polyethylene matrix. The corona initiation and breakdown characteristics of mica-filled polyethylene plaques show that the composite molding has greatly improved breakdown characteristics.[46] At high fields the effect of the fillers on the resistivity and conduction current mechanism is not clear yet. The reason for using some inorganic fillers as talc and mica in different percentages is to decrease the polyethylene resistivity and at the same time decrease the initial transient current in order to get the steady-state parameters of the composite.

The conduction current and the resistivity at different temperatures and stresses of the composite (polyethylene + 3% and 5% talc) has been investigated. Also the conduction current and the resistivity at different temperatures and at different stresses of the polyethylene plus 5% mica composite.

5-6-2 Results for Polyethylene Plus Talc Composite

5-6-2-1 Conduction Current

The results obtained with 3% talc in polyethylene (Figures 12 - 13) show that the conduction current settled down to steady-state at a period of time within twenty hours at different temperatures and at different stresses.

The results obtained (Figures 14 - 15) on polyethylene plus 5% talc composite show that the conduction current was settled down to steady-state after a period of time within ten hours.

The results on the fresh samples show that the amplitude of the initial transient current is higher than that of the same sample which is previously tested under a D.C. electric field. There are two invisaged reasons of the above conflict. The first is the existence of some by-product ions which increase the amplitude of the transient current until it is swept out by the conduction mechanism. The second is that, the traps of the potential barriers are empty, so that the injected carriers and the carriers from inside the bulk of the polyethylene are held in the deep traps and when the sample is short-circuited to earth, the carriers of the shallow traps discharge, while those at the deep traps need a very long time to be swept out.

The existence of the talc in the matrix of the polyethylene increase the probability of conduction by hopping, which overcomes the potential barriers of the traps and leads to an equilibrium between the injected and the emitted carriers i.e., the steady-state current is obtained.

5-6-2-2 Resistivity/Temperature and Stress Variation

The resistivity of the (polyethylene plus talc) composite is less than that of the unfilled polyethylene as shown in (Figures 16 - 17). The results shown in Table (5-3-a) give evidence that the existence of the talc particles in the polyethylene matrix has a noticeable effect on the values of the resistivity/temperature coefficient (α) but very small effect on resistivity/stress coefficient (β). From the above results one can say that the existence of the talc particles in the polyethylene matrix has no noticeable effect on the energy of activation.

The results obtained (Figure 16) show that the resistivity/stress variation is exactly applicable to the first Poole formula as in equation (5-2).

Table (5-3-a) Resistivity after twenty hours

Composite	Specimen thickness (μm)	α(1/°C)	E (kV/mm)	ρ_0 (Ω- cm) (at θ = 40 °C)
unfilled PE	305	0.0869	10.0	4.3×10^{17}
PE + 3% talc	438	0.0840	10.3	6.9×10^{16}
PE + 5% talc	444	0.0880	10.2	5.0×10^{16}

Table (5-3-b) Resistivity after twenty hours

Composite	Specimen thickness (μm)	β (cm/kV)	θ (°C)	ρ_0 (Ω- cm) (at E = 0.0 kV/mm)
unfilled PE	305	0.00274	50	5.3×10^{16}
PE + 3% talc	438	0.00260	50	3.6×10^{16}
PE + 5% talc	444	0.00286	50	3.0×10^{16}

5-6-2-3 Current After Short Circuit

The measurements of the conduction current after a period of a few hours short circuiting the sample to earth shows that the transient current has the same amplitude as the transient current of the first applied field. The exceptional transient current is only obtained at the fresh samples, which has amplitude of transient current greater than that of the previously tested.

5-6-3 Results of Polyethylene plus Mica Composite

5-6-3-1 Conduction Current

The results obtained (Figures 18 - 19) on the composite of polyethylene with 5% mica show that it is possible to obtain steady-state current within a period of time much less than that of the unfilled polyethylene. The mechanism of the conduction current is the same as that of the (polyethylene talc) composite. The measurements show that the conduction current settles down to steady-state within twenty hours.

5-6-3-2 Steady-State Resistivity

The results obtained in (Figures 16 - 17) show that the resistivity varies with the temperature and the applied field in the same manner as the composite of the polyethylene plus talc with no effect on the value of the resistivity. The values of the resistivity/temperature coefficient (α), the resistivity/stress coefficient (β), and the values of the corresponding reference resistivity (ρ_o) are shown in the following tables.

Table (5-4-a) Resistivity after twenty hours

Composite	Specimen thickness (μm)	α ($1/^{o}C$)	E (kV/mm)	ρ_o (Ω - cm) (at θ = 40 ^{o}C)
unfilled PE	305	0.0869	10.0	4.3×10^{17}
PE + 5% mica	500	0.0708	10.0	1.2×10^{18}

Table (5-4-b) Resistivity after twenty hours

Composite	Specimen thickness (μm)	β (cm/kV)	θ (°C)	ρ_o (Ω - cm) (at E = 0.0 kV/mm)
unfilled PE	305	0.00274	50	5.3×10^{16}
PE + 5% mica	500	0.0088	50	1.2×10^{18}

5-6-4 Effect of the Additives on the Mechanical Properties of the Composite

The tensile strength of the polyethylene is increased by using carbon in proportion up to (10%) by weight.[41] At high percentages (>10%) the tensile strength of the composite decrease rapidly. Generally the effect of the additives increases the stiffness of the polymers but the effect of small percentages up to 5% is small.

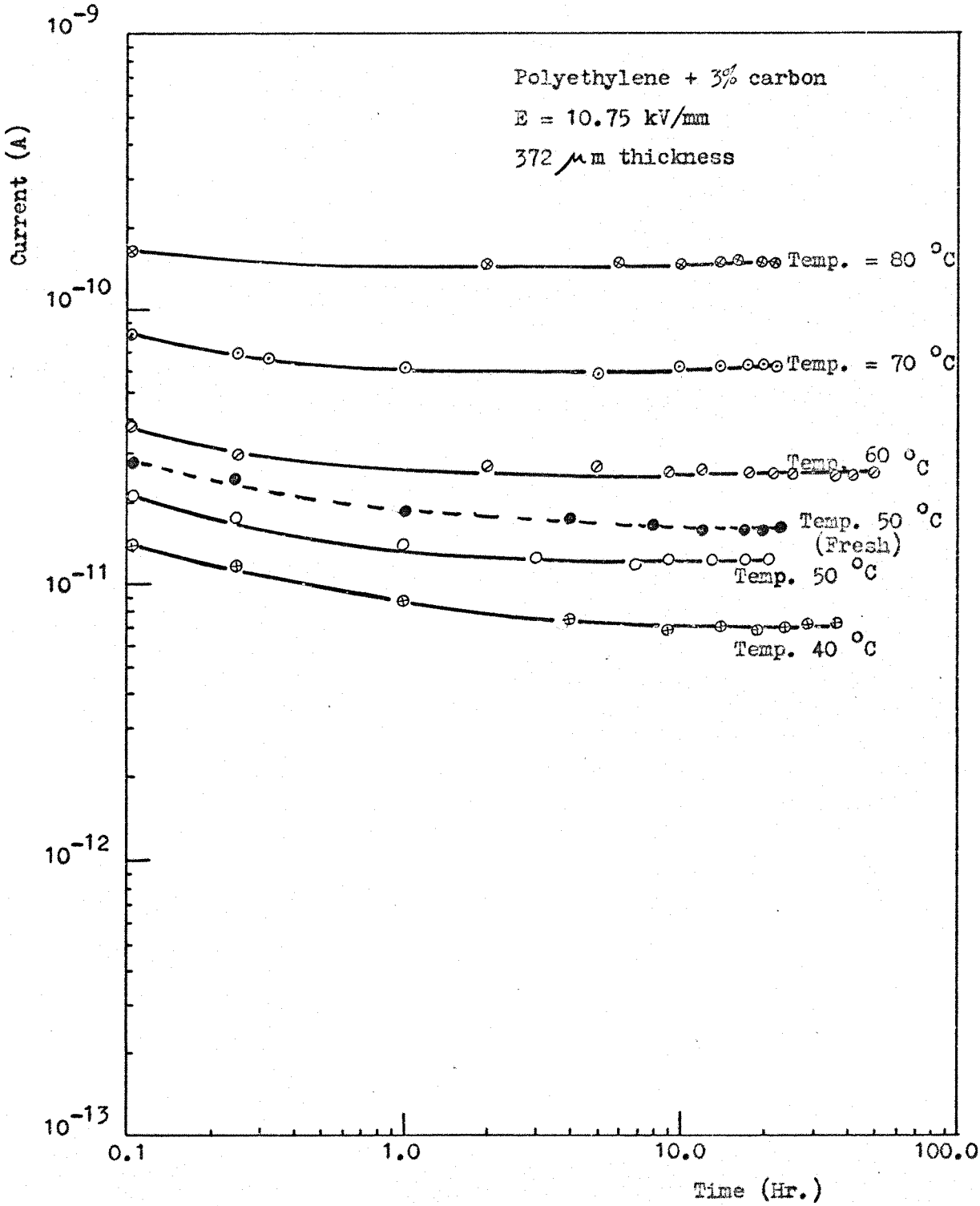

(Figure 8) Plot of conduction current against time

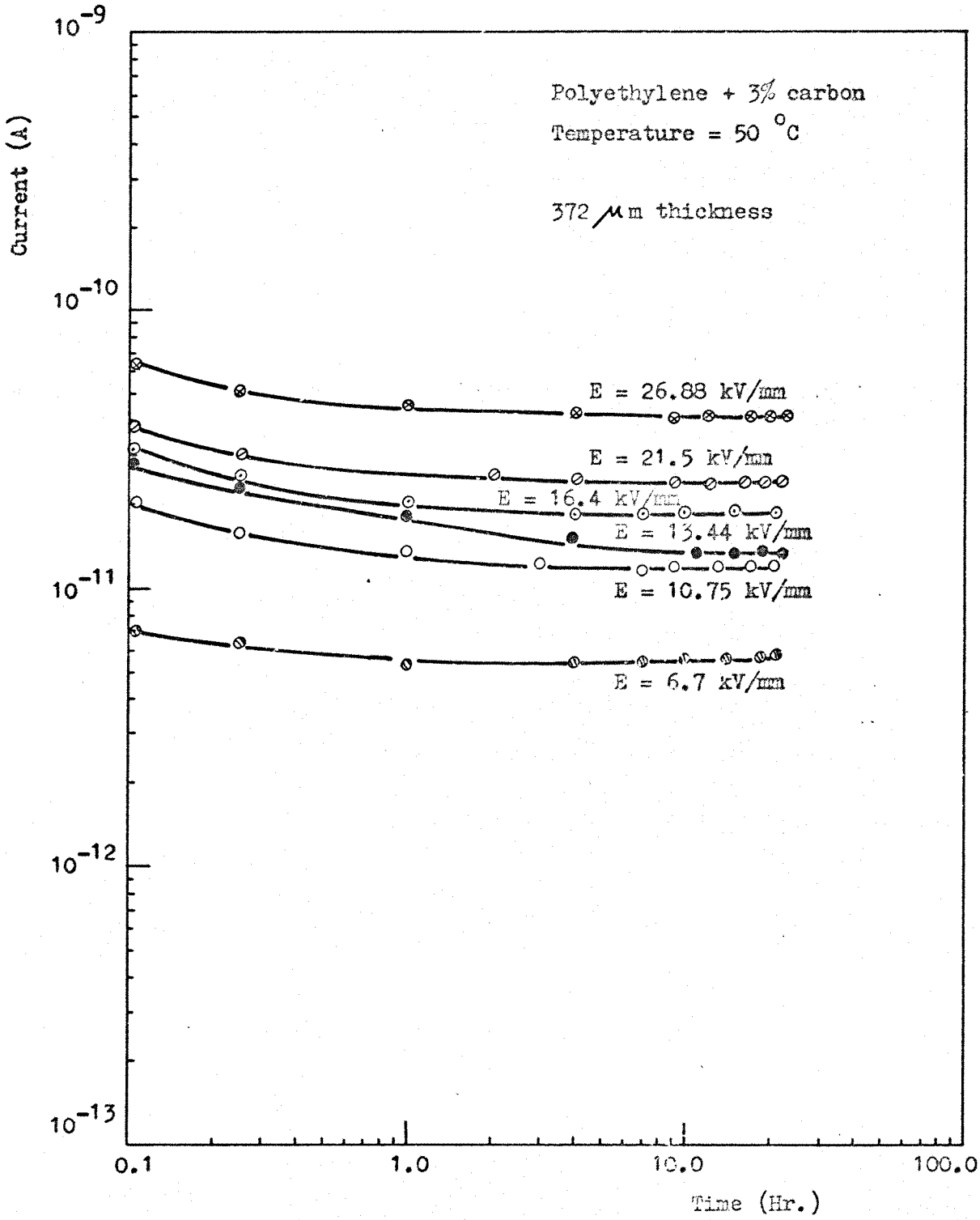

(Figure 9) Plot of conduction current against time

considering that the lightning arresters have an ignition voltage V_{ar} and as the working voltage of the D.C. cable is $V_{d.c}$, the D.C. cable could experience a voltage summation from $-V_{d.c}$ to $-V_{ar}$, or a reversal from $-V_{d.c}$ to V_{ar}.

The transients caused by the mal-function and the switching surges can be limited by the lightning arresters in the system as the arrester voltage level V_{ar} is sufficiently low.[47] As the necessary criteria for selecting the insulation levels in the D.C. cable depends on the subjected transient stresses based on $V_{d.c}$ and V_{ar}, the computation of the transient stresses due to the previous sudden effects will be more important in order to choose the right lightning arrester voltage level.

As the D.C. operating voltage of the cable stay on, the initial condition of the surge is considered to be zero and the solution of the rising potentials became as:

$$X = \Phi^{-1} \cdot \int_0^{t_p} \Phi(t) \cdot F(t)\, dt \qquad \text{- - - (7-26)}$$

where t_p is the period of the surge.

As the surge switched off in a period of t_p, the equation of the falling potentials is:

$$X = \Phi(0) \cdot \Phi^{-1} \cdot X_0 \qquad \text{- - - (7-27)}$$

where X_0 represents the node potentials of the disappeared surge.

The above transient solution was done by a computer program and the results obtained are shown in (Figure 7-10).

The results shown in Figures (7-6 to 7-10) are for polyethylene submarine cable which has the following dimensions:

$r = 1.42$ (cm) is the conductor radius

$R = 4.22$ (cm) is the sheath radius

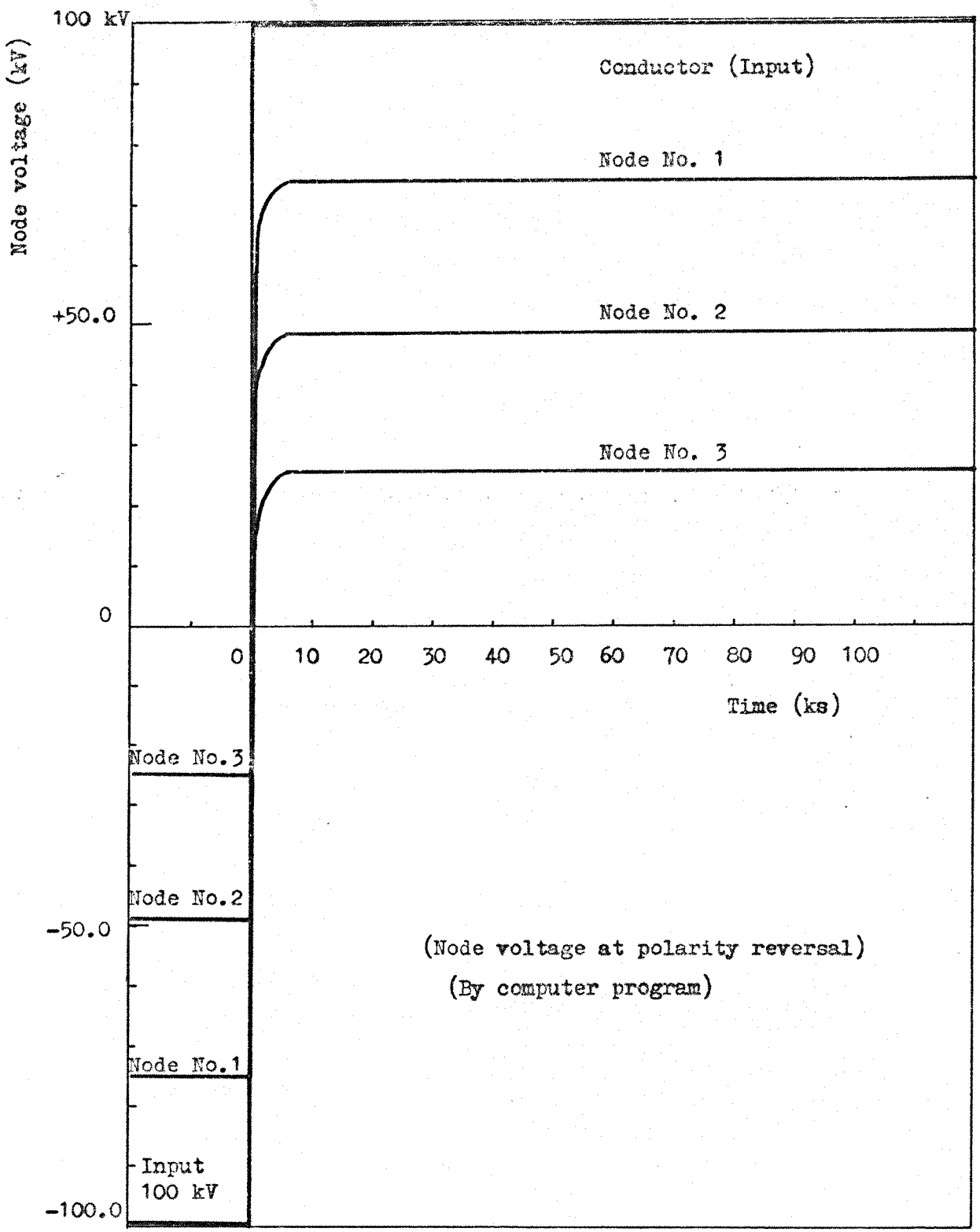

(Figure 7-6) Plot of node voltage against time

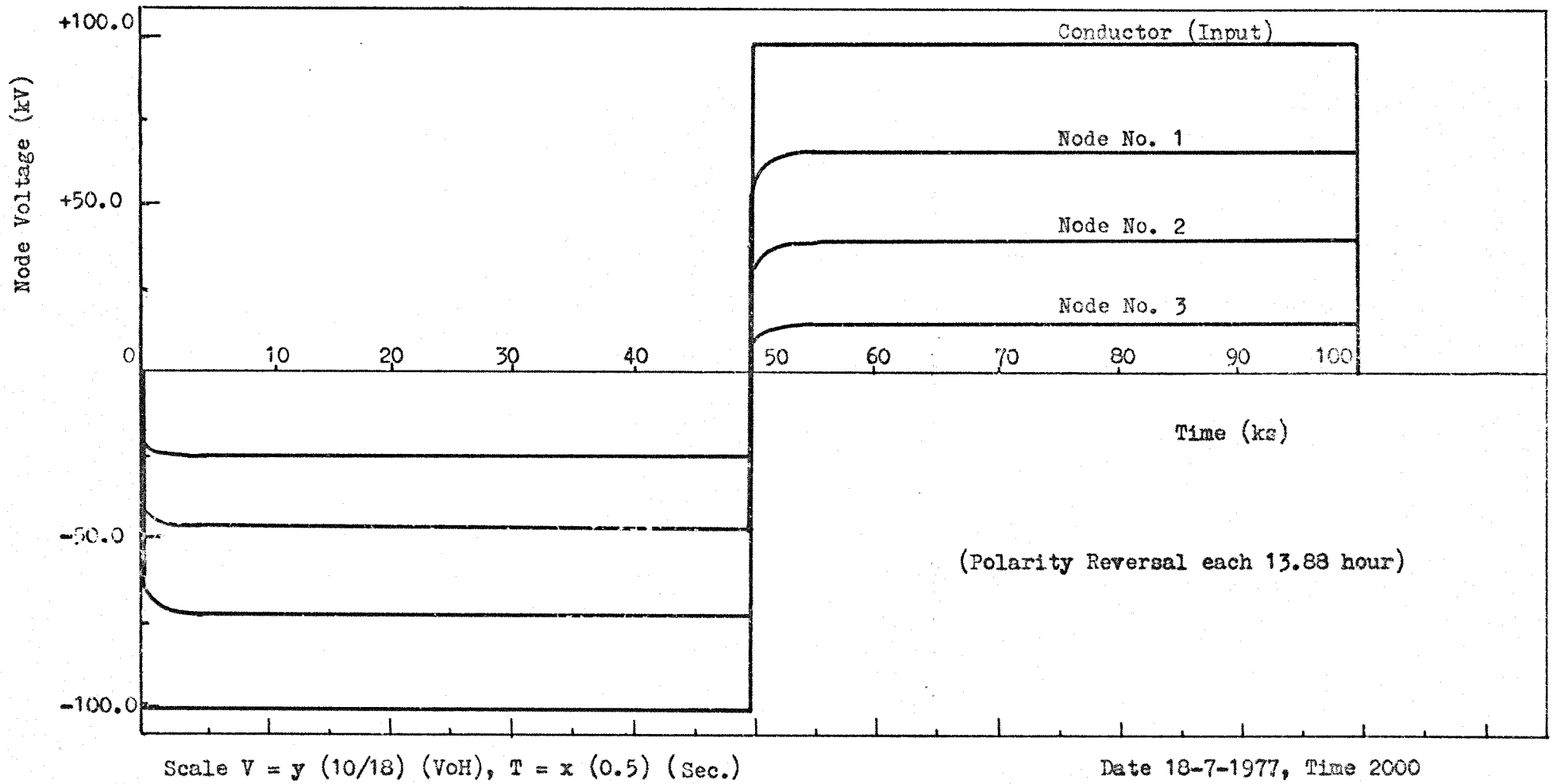

(Figure 7-7) Plot of node voltage against time

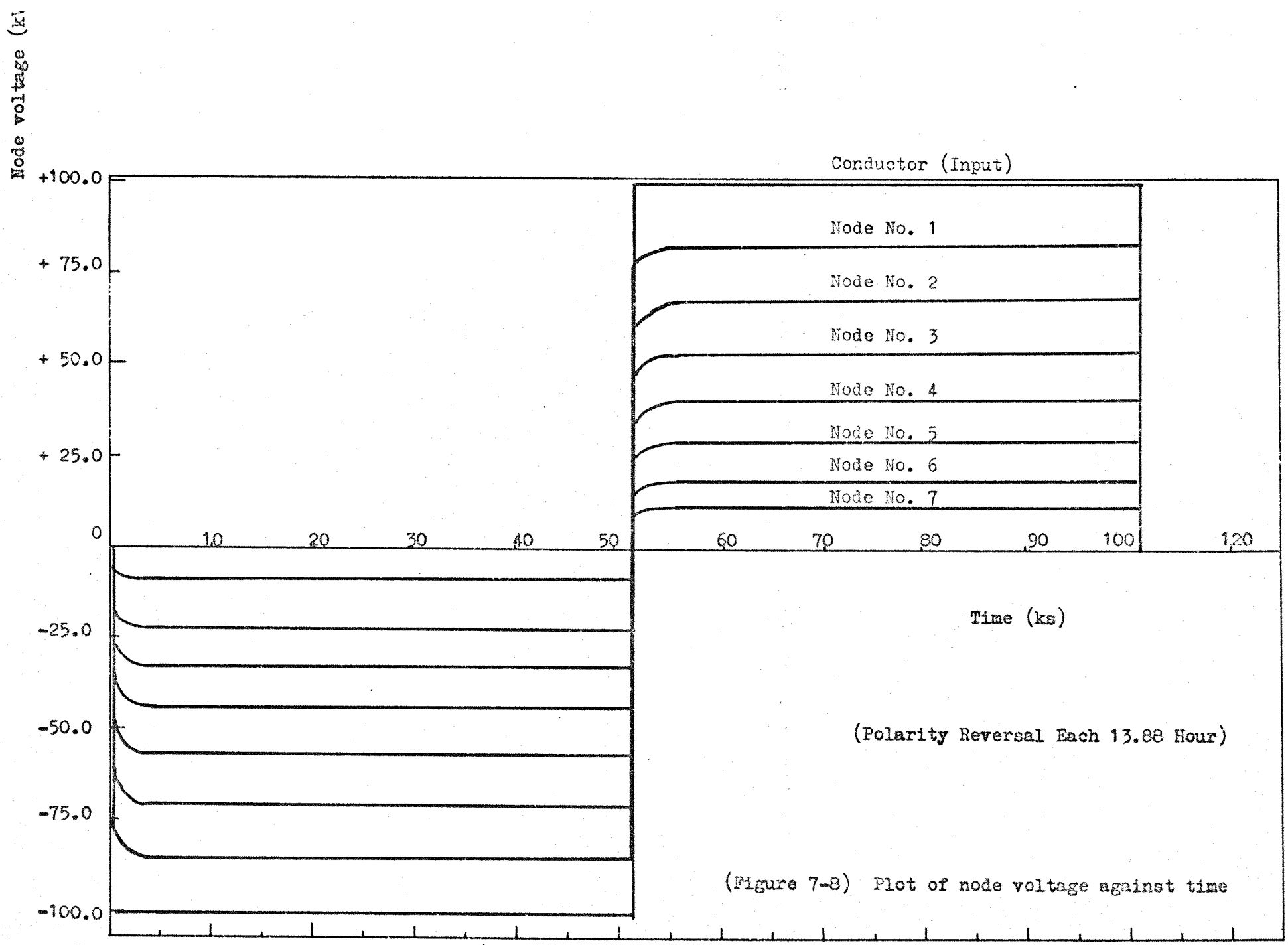

(Figure 7-8) Plot of node voltage against time

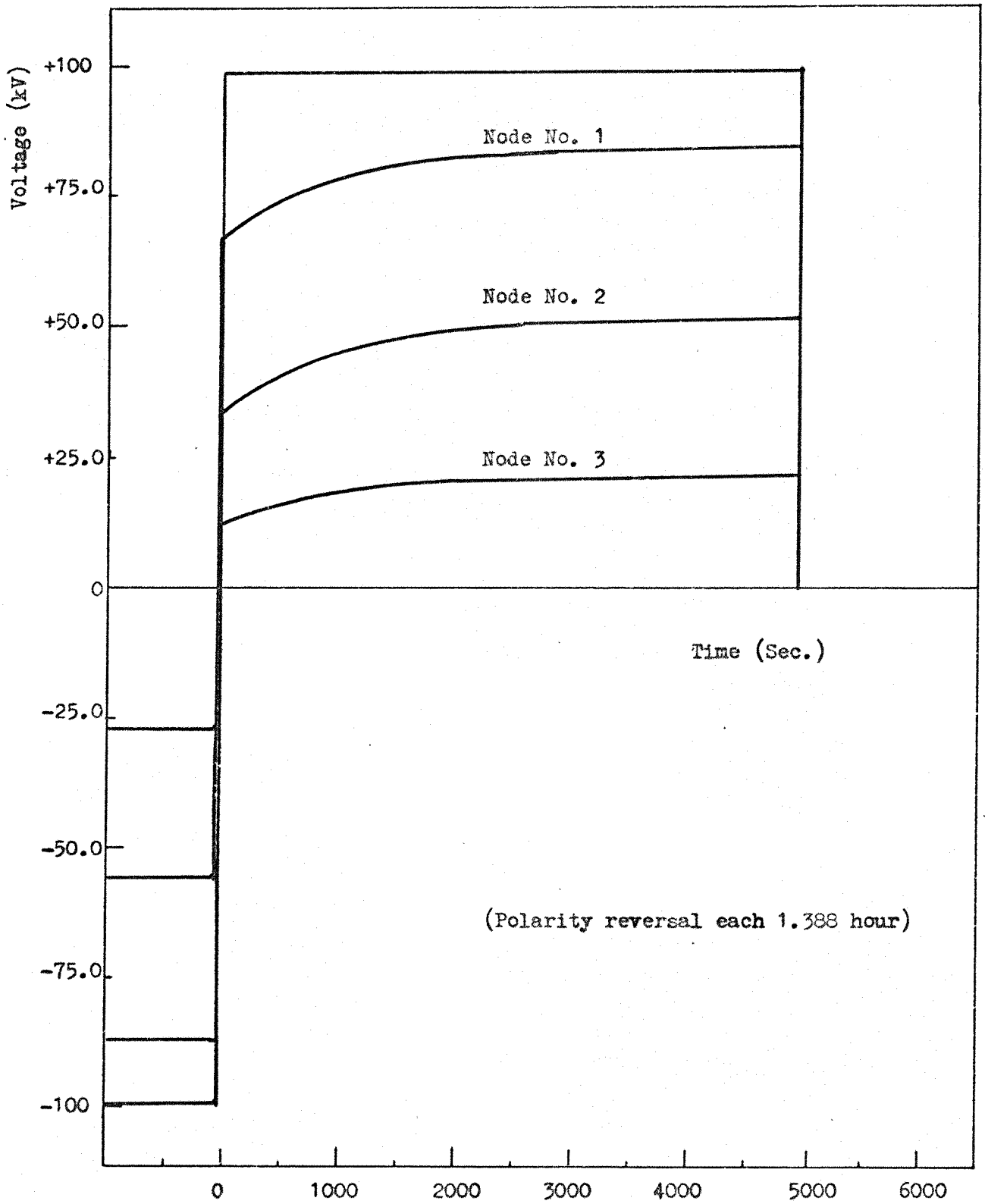

(Figure 7-9) Plot of node voltage against time

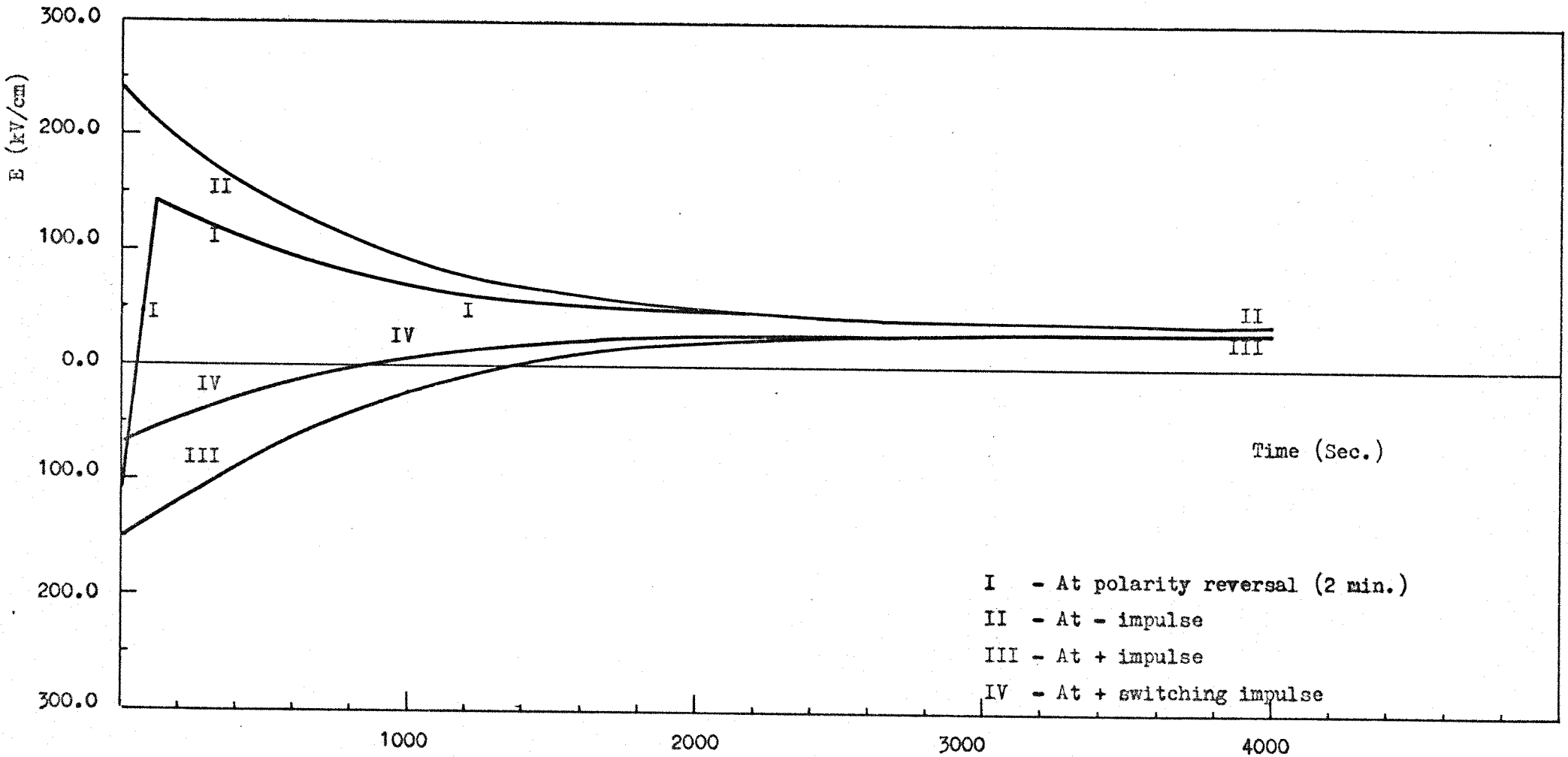

(Figure 7-10) Plot of transient stress against time

CHAPTER EIGHT

DESIGN OF EXTRUDED HIGH VOLTAGE D.C. CABLES

8-1 INTRODUCTION

The calculation of the stress distribution in the D.C. cable insulant as shown in Chapter Seven depends on the resistivity of the insulant. The experimental results show that it is difficult to define the right resistivity of the polyethylene.

The use of polyethylene as high voltage D.C. cable insulant with maximum conductor stress more than 10 kV/mm is not possible, due to the effect of the high intrinsic electric field obtained by the space charge accumulation which needs a very long relaxation time to vanish and this decreases the dielectric strength of the polyethylene. This effect is worse at polarity reversal, at switching surges and at impulse lightning surges. For oil-impregnated paper Lawson[33] found that the effect of polarity reversal is to increase the probability of breakdown due to the formation and growth of vapour bubbles in the butt gap spaces adjacent to the electrode and not due to the macroscopic polarization under direct voltage conditions.

The results obtained by Oudin and Fallou[21] (1965) on many cable samples using polyethylene as insulant show that the average design D.C. stress for samples of proposed submarine cables using polyethylene is about 3.5 kV/mm. For land cables the average design stress would be less than that of submarine cables due to the fact that the dielectric strength underwater is improved by the compressive force.

As the dielectric strength and the impulse withstand level of the EPR are relatively low,[32] the design average A.C. stress of the EPR cables is about 4.0 kV/mm.

To date there is no complete International Recommendations for the insulation test of the D.C. cables. The recommendation of CIGRE Study Committee No. 2 (presented in Electra No. 24, October 1972) was used in testing the high-voltage D.C. cable of the Cross-Skagerrak Sea between Denmark and Norway, each cable samples include two flexible joints.[37]

The following procedure of the insulation test are useful in the high voltage D.C. cable design.[37]

1 - Thirty days thermal cycles (8 hours on full load and 16 hours on no load) with the maximum working conductor temperature plus 5 ^{o}C. The procedure of the thirty days thermal cycles are:

a - First ten days thermal cycles are at voltage (2 $V_{d.c}$), at positive polarity.

b - Second ten days thermal cycles at voltage (2 $V_{d.c}$), at negative polarity.

c - Third ten days thermal cycles at voltage (1.5 $V_{d.c}$) with polarity reversal every four hours (reversal time must not exceed two minutes).

2 - Hot impulse test at voltage (3 x $V_{d.c}$) of positive polarity and at voltage (3 x $V_{d.c}$) of negative polarity.

It was found from the tests done on the Cross-Skagerrak D.C. cable[37] that, the parts near the joints in the cable are the most effected by the recommended CIGRE test procedure.

8-2 LIMITS OF HIGH VOLTAGE D.C. CABLE INSULATION DESIGN

The main criteria for dimensioning the D.C. cable are:

1 - The stress at the conductor with no load.

$$E_{r0} = \frac{V}{r \ln (R/r)} \leqq E \qquad \text{- - - (8-1)}$$

where E_{rO} is the stress at the conductor with no load.

V is the working D.C. voltage.

r, R are the conductor and sheath radius.

E is the working stress of the dielectric, which is limited by the dielectric strength of the insulant.

2 - The stress at the sheath with full-load is:

$$E_R \leqslant E \qquad \text{- - - (8-2)}$$

E_R can be found from the following equation.

$$\ln E_R + \beta . E_R = \ln E_r + \beta \cdot E_r + \left(\frac{q . g . \alpha}{2\pi} - 1 \right) \ln \left(\frac{R}{r} \right)$$

3 - The stress at the conductor at nominal load is:

$$E_r' = 2 E_{rO} - E_r \lessapprox E' \qquad \text{- - - (8-3)}$$

where E_r is the steady-state stress at the conductor with a loaded cable. Since E' only appears temporarily, it has a higher value than E.

The stress factor which represents the ratio between the no load stress at the conductor and the full load stress at the sheath is:

$$D = \frac{E_{rO}}{E_R} \approx 1.$$

4 - Basic Impulse Insulation Level:

The contribution D.C. voltage (k) is equal,

$$k = \frac{V_{B.d} - Vr}{V} \qquad \text{- - - (8-4)}$$

and $V_{B.d} = E_{B.d} \cdot r \cdot \ln (R/r)$

where $E_{B.d}$ is the effective breakdown stress

Vr is the reversal breakdown voltage

V · is the working D.C. voltage

and R,r are the sheath and conductor radius

k depends on the temperature different across the insulation and on the type of insulation usually used ($k \lessapprox 1$).

The basic criteria for the selection of the insulation level for a D.C. cable is:[47]

$$V_{BiL} \geqslant M\,(V_{PI} + k \cdot V) \qquad \text{- - - (8-5)}$$

where M - is the margin factor

V_{PI} - is the lightning arrester protection level

V - is the working D.C. voltage

k - is the D.C. voltage contribution factor.

5 - The maximum temperature at the conductor:

The temperature at the conductor is limited by the maximum stress at the sheath. This maximum stress on the sheath is a result of the temperature drop in the insulation.

8-3 DESIGN PROCEDURE OF NATURALLY COOLED EPR D.C. LAND CABLE

1 - The maximum stress on the conductor can be defined according to the design stress limits mentioned in (Section 8-2). The impulse dielectric strength of the EPR cable is considered ($\approx$ 80 kV/mm).

2 - The maximum conductor temperature is limited by the maximum stress on the sheath and the maximum sheath temperature. For naturally cooled cables the sheath temperature must be not more than 50 ^{o}C.

3 - The working voltage of the cable is defined by the basic insulation level of the cable and the lightning arrester protection level.

For EPR high voltage D.C. cable the maximum stress on the conductor

that can be used is ($\lesssim$ 10 kV/mm). The conductor temperature that can be used is in the limits of 50 °C to 60 °C for the naturally cooled direct buried EPR D.C. cables.

4 - The current rating: The rated current is defined by the cross-sectional area of the conductor and the maximum transmitted power. The effect of the cyclic rating factor (1.13 I rated current), the copper losses, the conductor temperature, the thermal resistance of the insulation and the thermal resistance of the surrounding soil are defined the maximum transmitted power of the EPR D.C. cable.

5 - The insulation thickness: The thickness of insulation can be adopted by taking into account the thermal resistance of the insulant, the maximum stress on the conductor and the maximum thickness which can be extruded (for extruded cables the recommended maximum thickness is about 2.6 cm).

6 - The thermal resistance of the insulant: As the thermal resistivity of the EPR is relatively high (610 $\frac{°C}{w}$ cm),[32] the thicker insulation give a high thermal resistance of the insulant. A series calculation can be done to compromise between the designed average stress and the thermal resistance of the insulant.

7 - The soil thermal resistance: The external thermal resistance in two cable system can be found by the image method as:

The temperature rise in cable A due to the losses q in cable B is:

$$\theta_1 = \frac{q\, g_s}{2\pi} \ln \left(\frac{\sqrt{4h^2 + a^2}}{a} \right) \qquad - - - (8\text{-}6)$$

where g_s is the effective thermal resistivity of the soil.

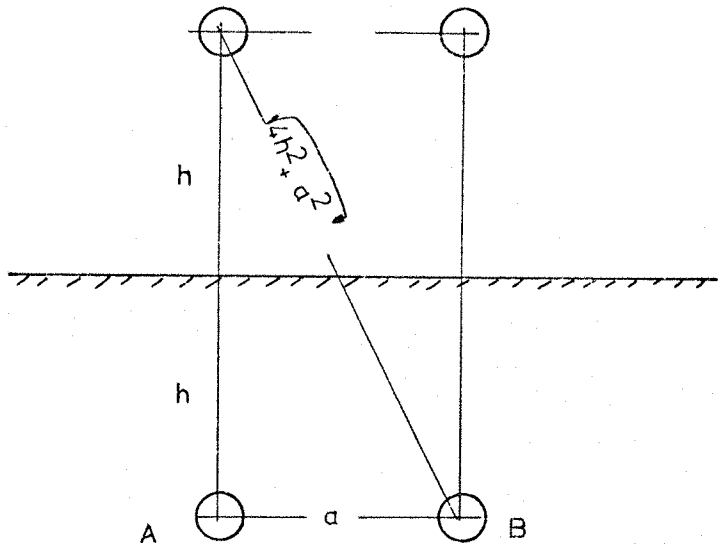

(Figure 8-a)

The temperature rise in cable A due to the losses q in cable A is:

$$\theta_2 = \frac{q\, g_s}{2\pi} \ln (2h/R) \qquad \text{- - - (8-7)}$$

The total external thermal resistance is

$$G_e = \frac{\theta_1 + \theta_2}{q} \quad [\ ^{\circ}C/_{w}\ ]$$

$$\therefore \quad G_e = \frac{g_s}{2\pi} \left[\ln \left(\frac{2h}{R} \right) + \ln \left(\frac{\sqrt{4h^2 + a^2}}{a} \right) \right] \qquad \text{- - - (8-8)}$$

Table (8-1) shows the relation between the thermal resistance and the spacing between the two cables. The effective thermal resistivity of the backfill and the soil is used as $g = 120 \left[\frac{^{\circ}C}{w} \text{ cm} \right]$ and the depth ($h = 100$ cm).

Table (8-1) $R = 4$ cm, $h = 100$ cm

a (cm)	G_{soil} ($^{\circ}C/_{w}$)
5	145.55
10	132.33
20	119.16
30	111.54
40	106.75
50	102.15

8 - The electrical resistivity of the dielectric: The electrical resistivity which varies with the temperature and the stress is the main factor affecting the stress distribution in the D.C. cable. From the experimental work on EPR it was obtained that:

a - The temperature coefficient of the EPR $\alpha = 0.14\ (1/^{o}C)$

b - The stress coefficient of the EPR $\beta = 0.01$ (cm/kV)

c - The reference resistivity, $\rho_{o} = 8.5 \times 10^{17}$ at 60 ^{o}C

9 - The technical problems:

a - The field produced by the stranded copper conductor can be reduced 20% by using semiconductor tapes, at the same time it is improving the contact with the cable insulant.

b - Some of the troubles in the D.C. cables are due to the corona discharges at the outer surface of the insulation, since at the loaded cables the maximum stresses are on the sheath. It is very important to design a method of coating the outer surface of the insulation with a semiconductor layer sticking hard and improving the contact.

c - The mechanical and chemical protection jacket. The mechanical properties of the EPR insulation (Table 4-4) shows that the EPR needs a mechanical protection and at the same time a chemical protection is necessary.

Within the limits of the design, a study of the variation of the maximum power with the rated voltage, conductor cross sectional area, dielectric thickness and the soil thermal resistivity are shown in (Figure 8-1 to Figure 8-4).

8-3-1 Specification of EPR Cable

From the graphs of the maximum power variation, a more realistic single D.C. EPR cable can be designed with the following specification:

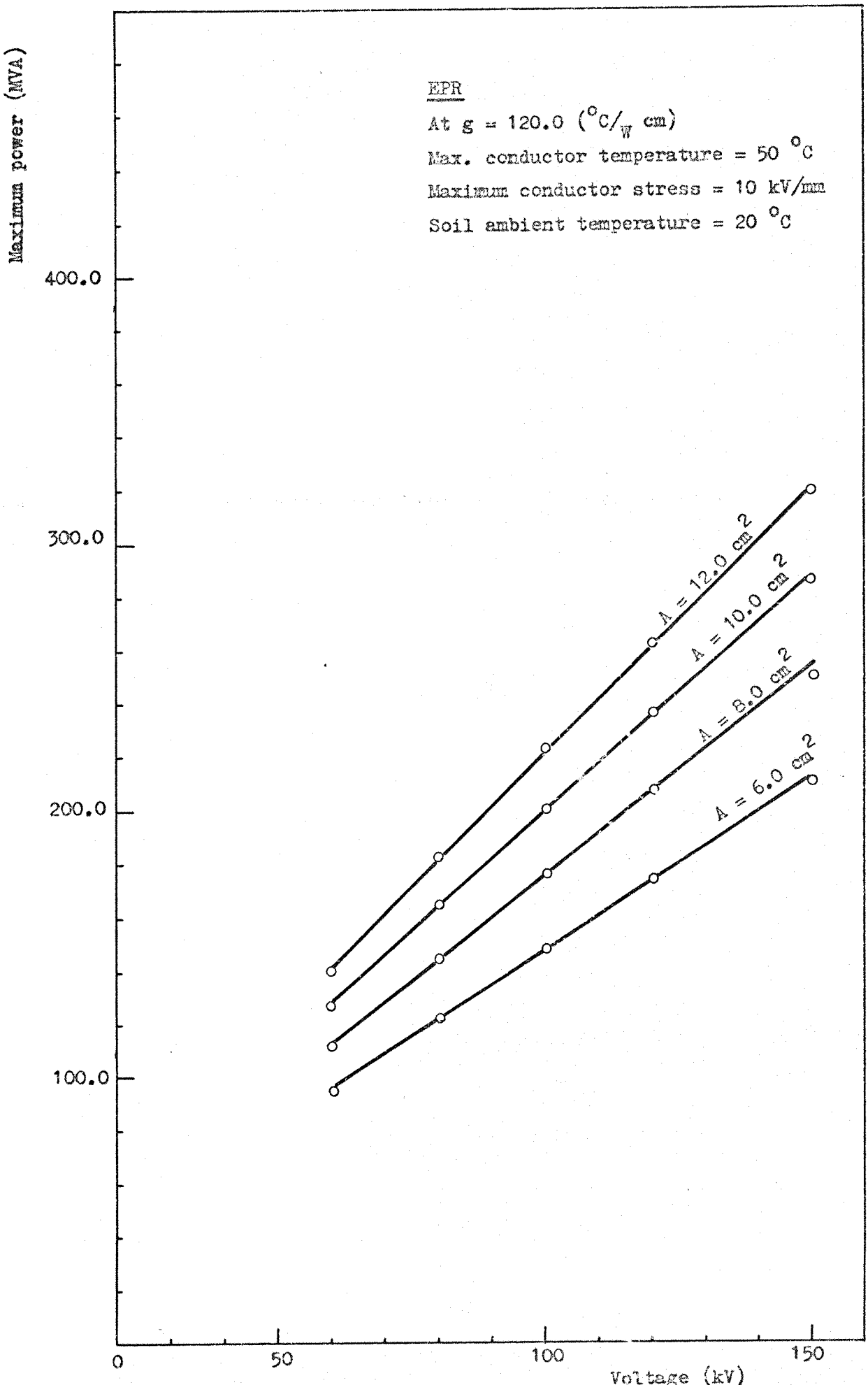

(Figure 8-1) Plot of maximum power against voltage

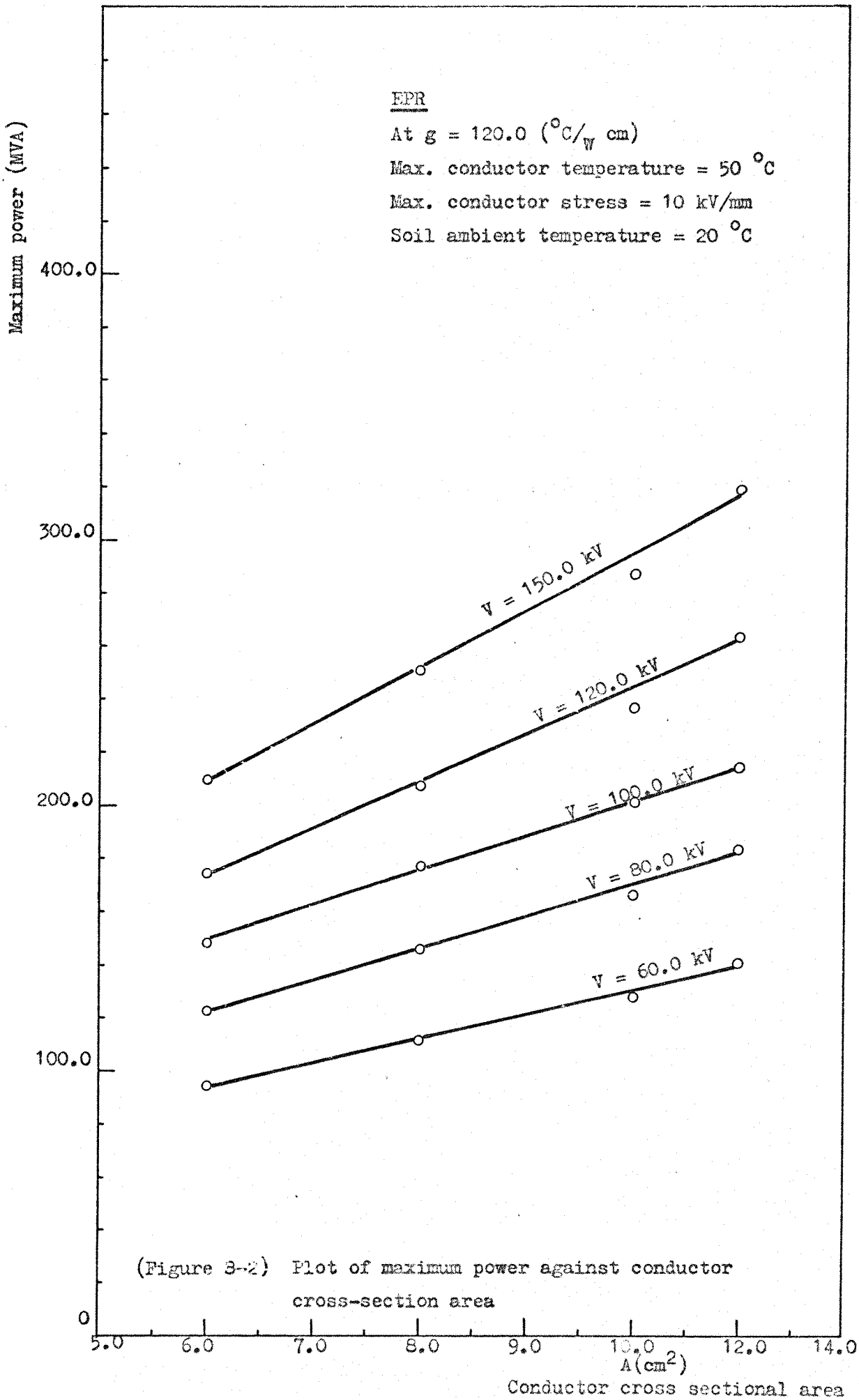

(Figure 3-2) Plot of maximum power against conductor cross-section area

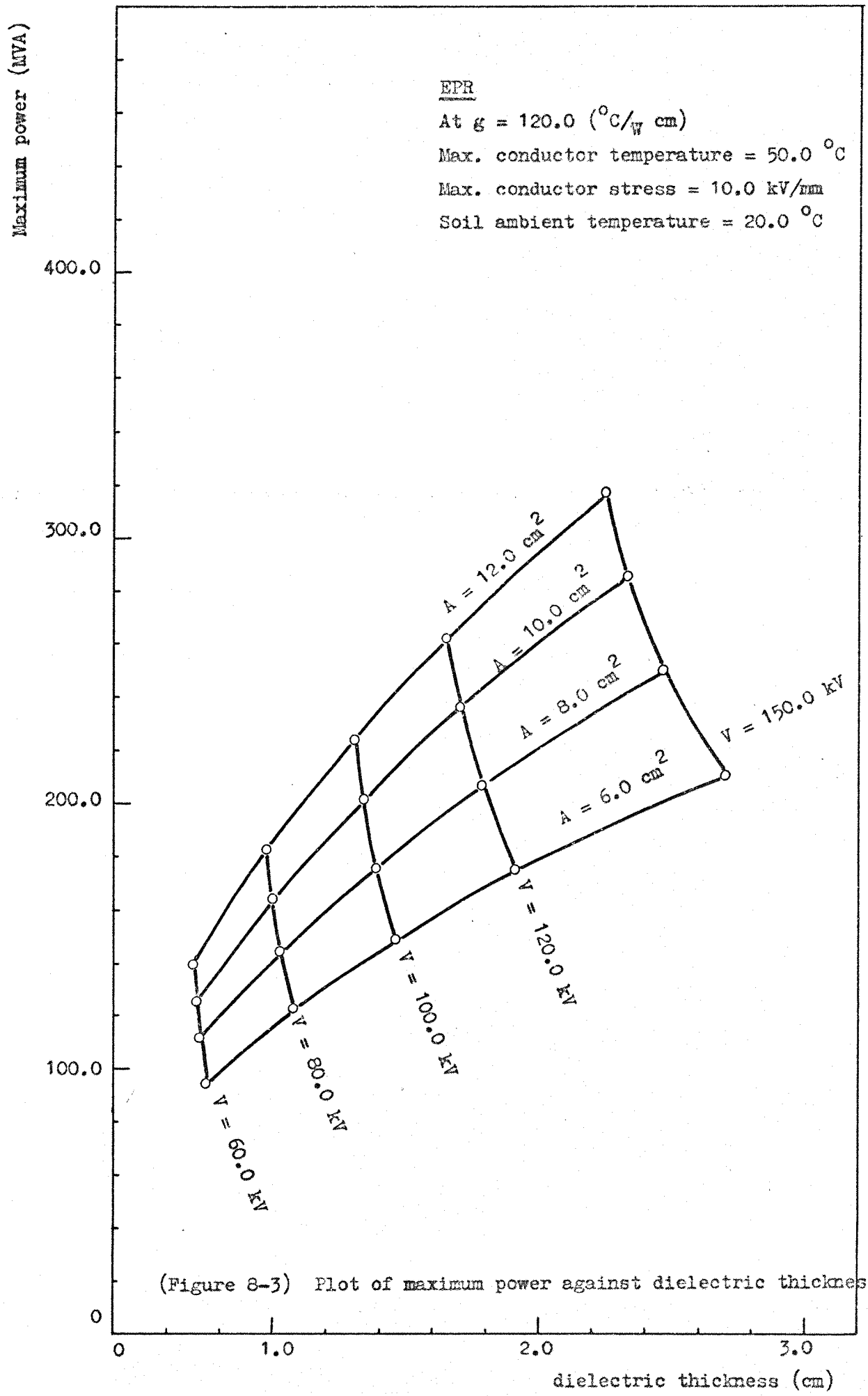

(Figure 8-3) Plot of maximum power against dielectric thickness

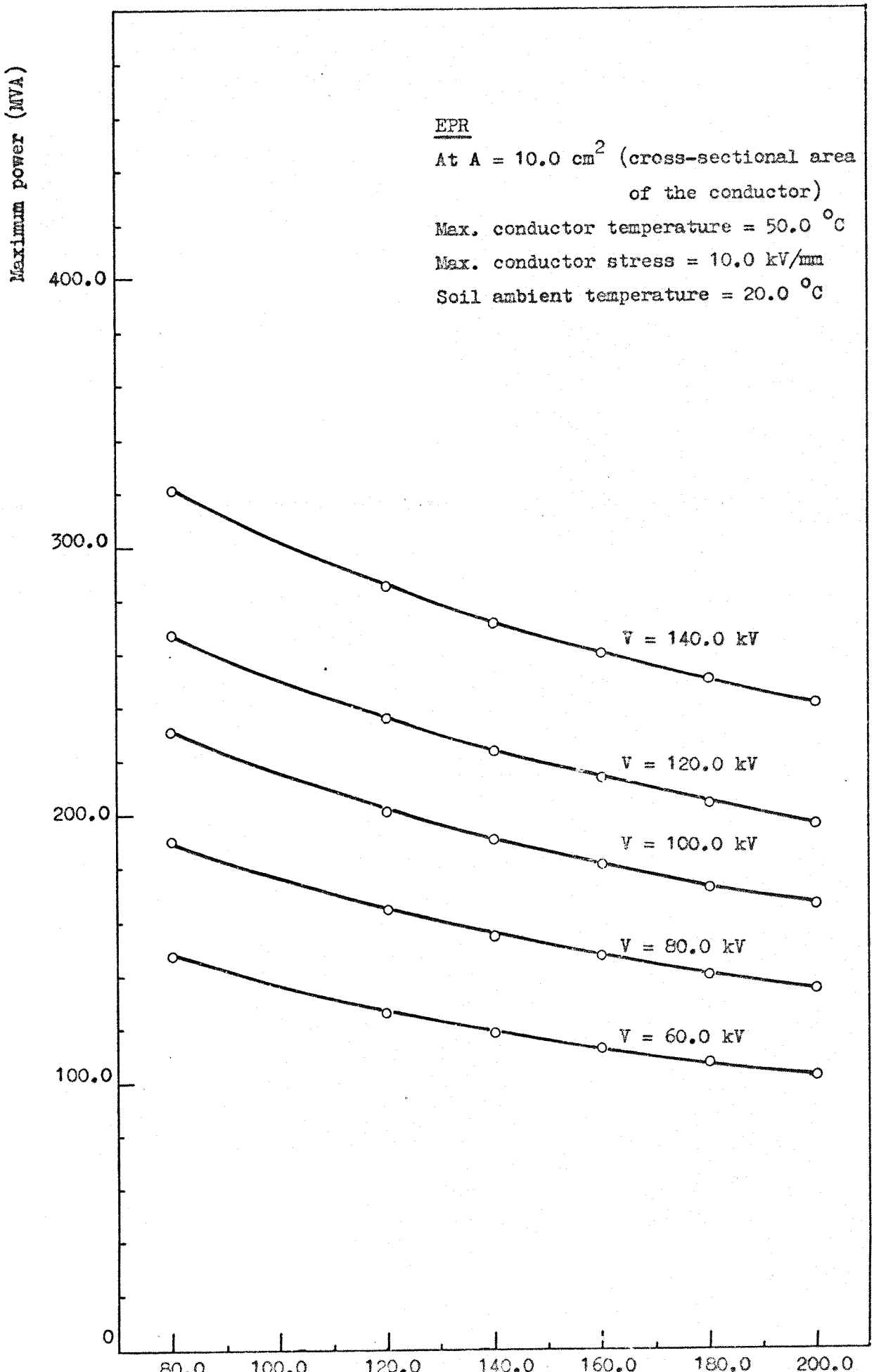

(Figure 8-4) Plot of maximum power against soil thermal resistivity

1 - The rated voltage is ± 100 kV.

2 - The maximum transient conductor stress is 10 kV/mm.

3 - The cross sectional area is 10 cm^2.

4 - The conductor radius is 1.784 cm.

5 - The semiconducting layer on the conductor and on the sheath is 0.02 cm.

6 - The outer sheath radius of the dielectric is 3.14 cm.

7 - The maximum transient stress on no load, at the sheath is 5.7 kV/mm, and at the conductor is 9.9 kV/mm.

8 - The dielectric thermal resistance is 53.816 $(\frac{^oC}{w})$ using the thermal resistivity of EPR 610 $(\frac{^oC}{w}$ cm).

9 - The soil thermal resistance is 136.57 $(\frac{^oC}{w})$ using the thermal resistivity of the soil 120 $(\frac{^oC}{w}$ cm).

10 - The temperature drop in the dielectric is 8.48 ^oC.

11 - The conductor temperature is 50 ^oC.

12 - The soil ambient temperature is 20 ^oC.

13 - The conductor losses is 0.15757 (w/cm).

14 - The maximum conductor current is 1000A.

15 - The maximum power is 200 MW.

16 - The stress on the conductor at full load is E_r = 6.07 kV/mm.

17 - The stress on the sheath at full load is E_R = 8.7 kV/mm.

8-4 DESIGN PROCEDURE OF POLYETHYLENE SUBMARINE HIGH VOLTAGE D.C. CABLE

The use of polyethylene as insulant for the submarine cable is more convenient than the oil impregnated paper, since at great depth the compression force on the cable increase the dielectric strength of the insulation. The main procedure of the design of the polyethylene cable under water is:

1 - The maximum stress on the conductor can be defined according to the limits of the D.C. cable design mentioned in (Section 8-2).

2 - In submarine cable, the maximum temperature is limited by the maximum current carrying capacity and the maximum stress on the sheath.

3 - The working voltage of the cable is defined by the basic insulation level of the cable and the lightning arrester protection level.

4 - The current rating: The conductor current is defined by the maximum current carrying capacity of the cable and by the stress factor (D).

5 - The insulation thickness is used within the limits of the maximum stress on the conductor and the maximum thickness which can be extruded.

6 - The effect of the dielectric thermal resistance and the thermal resistance of the surrounding mud is much less than that of the land cables. The thermal resistivity of the surrounding mud used as 30 $(\frac{^{o}C}{W}\ cm)$. The thermal resistivity of the polyethylene used as 330 $(\frac{^{o}C}{W}\ cm)$, $\rho_{40^{o}C} = 1.3 \times 10^{18}\ (\Omega\text{-cm})$.

7 - The electrical resistivity of the polyethylene which varies considerably with the applied electric field and the temperature. The values of the resistivity/temperature coefficient and the resistivity/stress coefficient can be used as $\alpha = 0.07\ (1/^{o}C)$, $\beta = 0.003\ (cm/kV)$.

8 - The technical problems: The technical problems need special design procedure for the submarine cable which are:

a - Chemical protection is used to prevent the penetration of the sea water through the polyethylene insulant.

b - Mechanical protection. The design of the armour winding must be out of the British Standard, due to the effect of water compression force and the water tide.

8-4-1 Specification of a Submarine D.C. Cable

The following specification gives an example of the possible polyethylene submarine cable which can be designed:

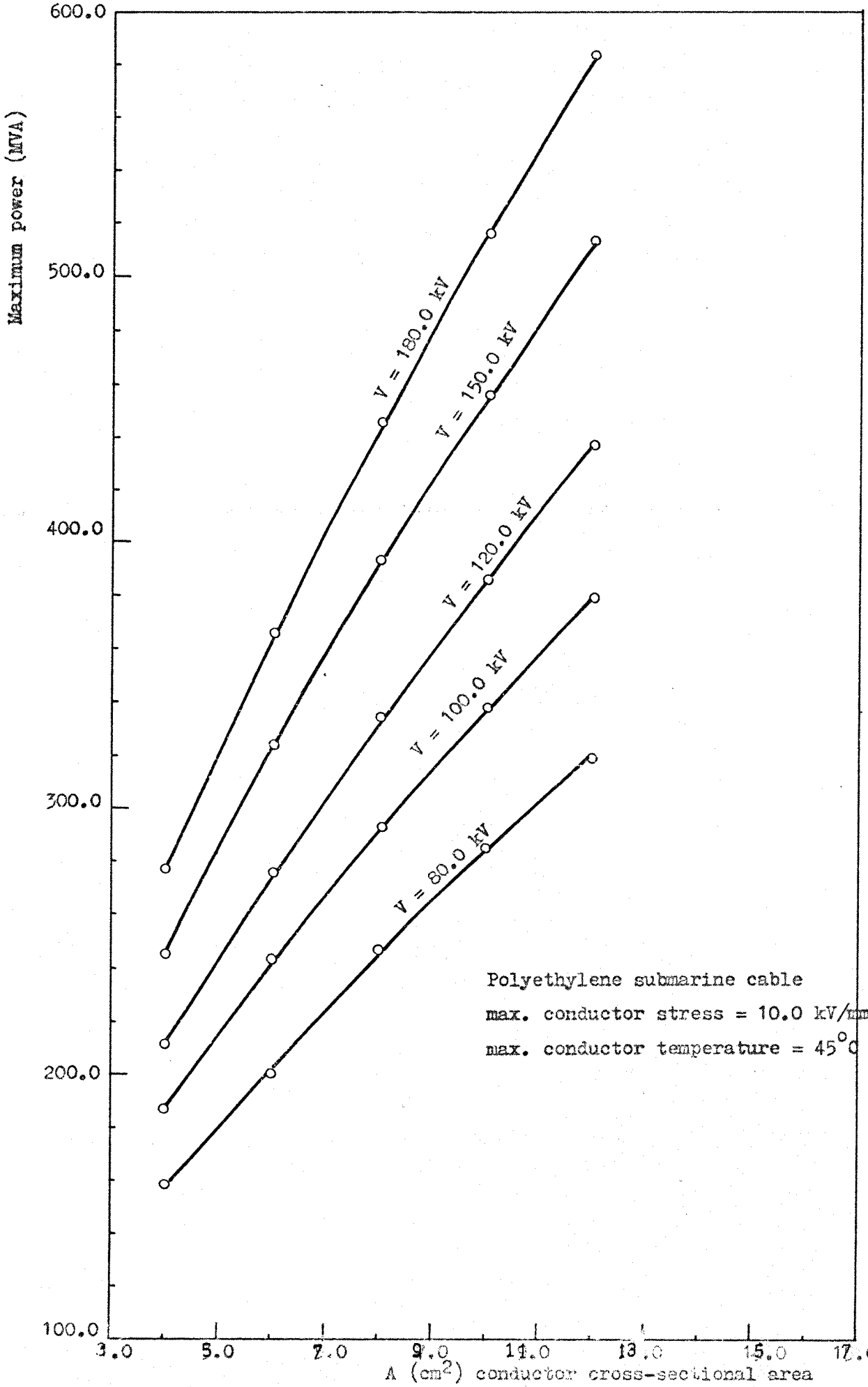

(Figure 8-5) Plot of maximum power against conductor cross-sectional area

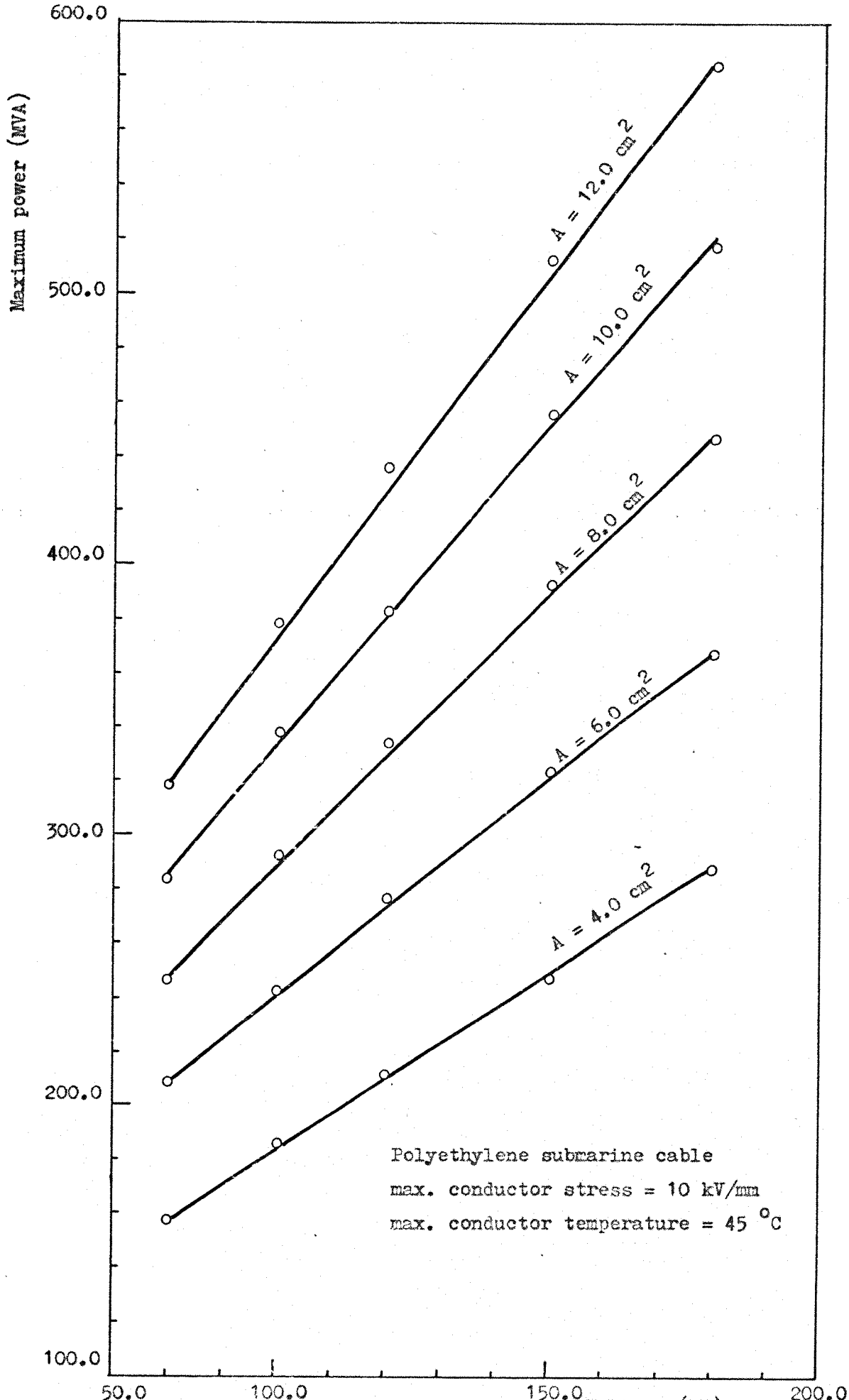

(Figure 8-6) Plot of maximum power against applied voltage

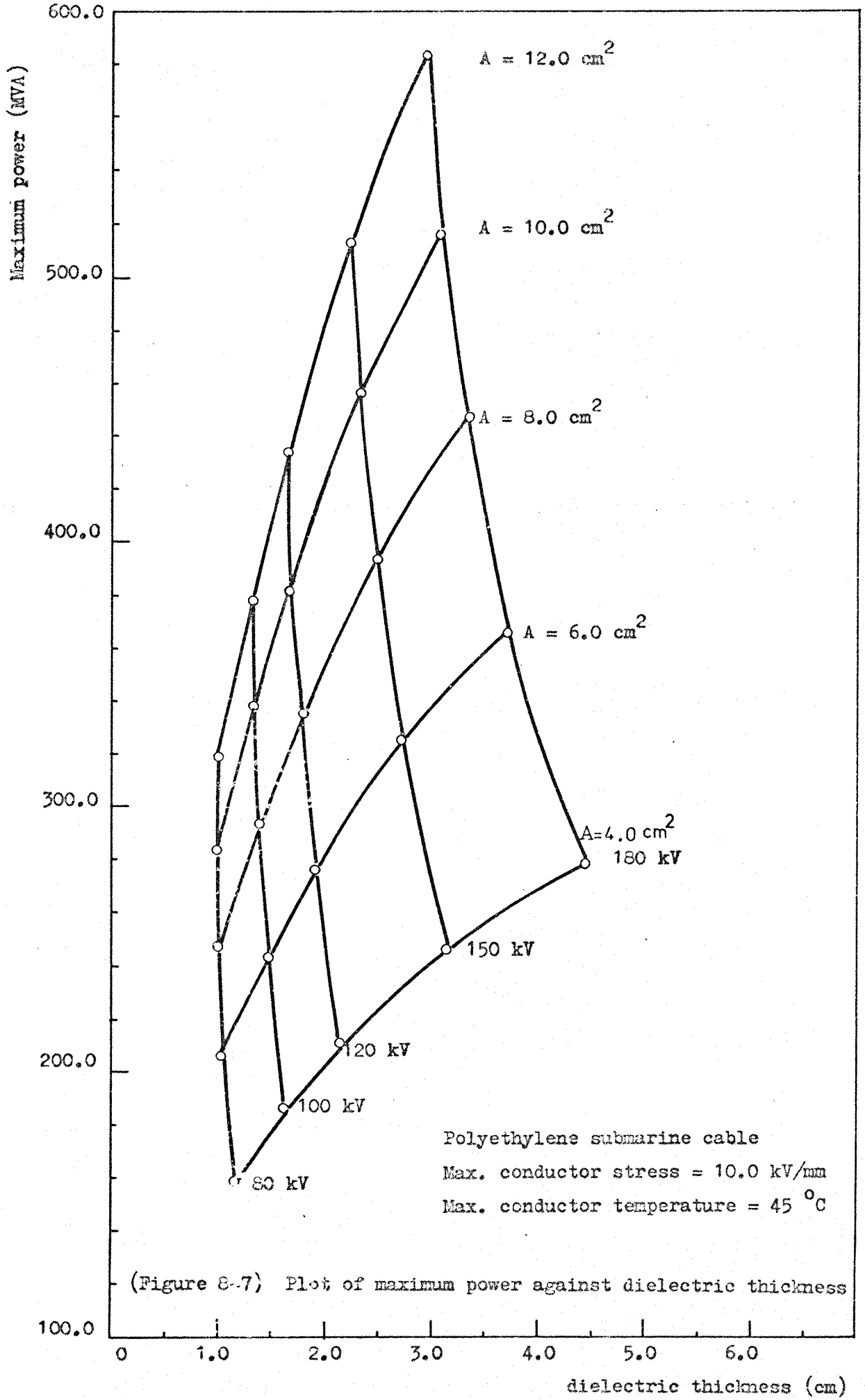

(Figure 8-7) Plot of maximum power against dielectric thickness

The cross sectional area = 10 cm^2.

The maximum no load stress on the conductor is 10 kV/mm.

The insulation thickness is 2.35 cm.

The rated D.C. working voltage is ± 150 kV.

The maximum power is 455 MW.

The maximum conductor current is 1520A.

The maximum stress on the sheath at full-load is 7.7 kV/mm.

The stress on the conductor at full-load is 4.87 kV/mm.

8-4-2 Investigation of Polyethylene with Additive as High Voltage D.C. Cable Insulant

The design study of extruded D.C. cables using polyethylene with few percent of additive is possible after defining the dielectric strength and the thermal resistivity of the composite. The effect of the additives is expected to decrease the thermal resistivity of the polyethylene which prcbably decrease the thermal gradient in the dielectric.

8-5 DESIGN OF XLPE CABLE AND POLYPROPYLENE CABLE

Design of XLPE cable and polypropylene cable can be done after defining the dielectric strength and the thermal resistivity of the dielectric.

8-6 DESIGN PROCEDURE OF POLYETHYLENE CABLE (INTERNALLY WATER COOLED)

8-6-1 Heat Distribution

The heat distribution through the water channel and the cable insulation can be represented as shown:

$$q\,dx = q_e dx + q_w dx \qquad - - - (8\text{-}9)$$

$$\left[Tc - Ta \right] = G_1 q_e \qquad - - - (8\text{-}10)$$

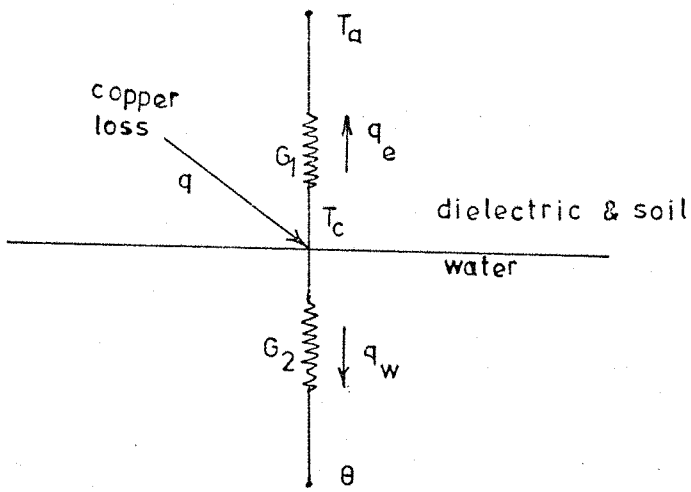

(Figure 8-b)

$$[\ Tc - \theta\ ] = G_2\ q_w \qquad \text{- - - (8-11)}$$

$$q_w\ dx = C\ W\ d\theta \qquad \text{- - - (8-12)}$$

$$\therefore \quad q_w = C\ W \frac{d\theta}{dx}$$

and $$\frac{Tc - \theta}{G_2} = q_w = C\ W \frac{d\theta}{dx}$$

$$\therefore \quad Tc = G_2\ C\ W \frac{d\theta}{dx} \qquad \text{- - - (8-13)}$$

From equation (8-10)

$$\frac{Tc - Ta}{G_1} = q_e = q - q_w = q - C\ W \frac{d\theta}{dx}$$

$$\therefore \quad Tc = G_1\ (q - C\ W \frac{d\theta}{dx}\ ) + Ta \qquad \text{- - - (8-14)}$$

From equation (8-13) and equation (8-14)

$$\therefore \quad G_2\ C\ W \frac{d\theta}{dx} + \theta = G_1 q - C\ W\ G_1 \frac{d\theta}{dx} + Ta$$

Finally,

$$C\,W\,(G_1 + G_2)\,\frac{d\theta}{dx} + \theta - (G_1 q + Ta) = 0 \qquad \text{- - - (8-15)}$$

where q is the copper losses (W/cm)

q_e is the heat through the insulant and soil (W/cm)

q_w is the heat dissipated in the water (W/cm)

Tc is the temperature at the conductor (^oC)

C is the heat capacity of the coolant. For water

$C = 4.2\ (J/cm^3\ .\ ^oC)$

$W = V.A.\ (cm^3/sec.)$ water flow

$G_2\ (^oC/W)$ is the thermal resistance between the conductor and the coolant center axis

$G_1\ (^oC/W)$ is the thermal resistance of the insulation and the surrounding soil

$G_1 = G_{dielectric} + G_{soil}$

Ta is the ambient temperature of the ground.

Suppose that

$$\left.\begin{aligned} C\,W\,(G_1 + G_2) &= A \\ G_1 q + Ta &= B \end{aligned}\right] \quad \text{are constant}$$

$$A\,\frac{d\theta}{dx} + (\theta - B) = 0$$

$$\int \frac{A}{\theta - B}\,d\theta = \int -\,dx$$

$$A \ln (\theta - B) = -x + K$$

$$A_t \quad x = 0 \quad , \quad \theta = \theta_i$$

$$\therefore \qquad A \ln (\theta_i - B) = K$$

$$A \ln (\theta - B) = - X + A \ln (\theta_i - B)$$

$$\ln (\theta - B) = - \frac{X}{A} + \ln (\theta_i - B)$$

$$(\theta - B) = e^{-X/A} (\theta_i - B)$$

$$\frac{\theta - B}{\theta_i - B} = e^{-X/A} \qquad - - - (8\text{-}16)$$

θ_i - (^oC) is the input temperature of the coolant

θ - (^oC) is the temperature of the coolant at distance (X) from the input point.

8-6-2 Specification of the Designed Cable

Design of internally water cooled cable for a maximum power of 0.9 GW:

The water channel diameter used is (5.0 cm) in order to transmit a high electric power of 9 GW.

The pipe wall thickness used is 0.2 cm.[34]

The conductor radius is designed as 4.0 cm.

The outer sheath radius is 5.80 cm.

Semiconducting layer on the conductor and on the sheath are of 0.02 cm thickness.

The copper area is 27.5 cm^2.

The insulation thickness is 1.80 cm.

The rated D.C. working voltage is ± 150 kV.

The maximum stress on the conductor (no load) is 10.0 kV/mm.

The maximum conductor current is 3000A.

The maximum power is 0.9 GW.

8.6.3 The Dielectric and the Surrounding Soil Thermal Resistance

The dielectric thermal resistance is:

$$G_d = \frac{g_d}{2\pi} \ln (R/r)$$

$$G_d = 19.43 \ \left(\frac{^oC}{W} \text{ cm} \right)$$

The soil thermal resistance is

$$G_{soil} = \frac{g_s}{2\pi} \left[\ln \left(\frac{2h}{R} \right) + \ln \left(\frac{\sqrt{4h^2 + a^2}}{a^2} \right) \right]$$

$$G_{soil} = 95.15 \ \left(\frac{^oC}{W} \text{ cm} \right)$$

$$G_1 = G_d + G_{soil}$$

$$\therefore \quad G_1 = 114.60 \ \left(^oC/_W \right)$$

8-6-4 The Thermal Resistance of the Water (G_2)

In order to find the heat dissipated in the water channel, it is necessary to find the thermal resistance of the coolant:

as

$$\left[G_2 = \frac{1}{h \cdot A} \right] \qquad - - - (8\text{-}17)$$

where h is the heat transfer coefficient of the coolant ($W/cm^2\text{-}^oC$)

A is the cross-sectional area of the coolant (cm^2)

To find the heat transfer coefficient the following empirical formula can be used:[28]

$$\left[\frac{h \cdot d}{K} = 0.03 \left[\frac{d \cdot V \cdot \rho}{\eta} \right]^{0.8} \cdot \left[\frac{C \cdot \eta}{K} \right]^{0.4} \right] \quad \text{---} \quad (8\text{-}18)$$

where

h - heat transfer coefficient (W/m^2-^oC)

d - mean hydraulic diameter (m)

K - thermal conductivity of the coolant ($W/^oC$ m)

ρ - density of the coolant (kg/m^3)

C - specific heat of the coolant (water) = 4.2 (J/g_m ^oC)

η - viscosity of the coolant (for water $\eta = 0.544 \times 10^{-3}$ (kg/m-sec.))

V - velocity of the coolant (m/sec.).

To find the velocity the following empirical formula can be used.

$$\left[V^{1.8} = \Delta P \cdot \frac{d^{1.2}}{0.092 \cdot L \cdot (\rho)^{0.8} \cdot (\eta)^{0.2}} \right] \quad \text{---} \quad (8\text{-}19)$$

where

ΔP - the pressure of the coolant at the input (N/m^2)

d - mean hydraulic diameter (m)

η - viscosity of the coolant (kg/sec. m)

ρ - density (kg/m^3) of the coolant

V - velocity of the coolant (m/sec.)

L - distance between the cable section (m).

Suppose that:

ΔP = 30 atmosphere = $30 \times 1 \times 10^5$ (N/m^2)

ρ = 988 (kg/m^3)

η = 0.544×10^{-3} (kg/m sec.)

L = 5.6 km

d = 0.05 meter

From equation (8-19) the velocity is:

$$\therefore \quad V = 1.8 \ (M/sec.)$$

The flow (m^3/sec.) is

$$W = V.A$$

$$= 1.8 \times (2.5)^2 \times \quad \times 10^{-4}$$

$$\therefore \quad \left[W = 3.5343 \times 10^{-3} \right] \ (m^3/sec)$$

$$\left[W = 3.5343 \times 10^{3} \right] \ (cm^3/sec)$$

To find the heat transfer coefficient use K = 0.643 (W/m ^{o}C) thermal conductivity of the water.

From equation (8-18) the heat transfer coefficient is:

$$\left[h = 0.7277 \ \left(\frac{W}{cm^2 \ ^{o}C} \right) \right]$$

$$\therefore \quad G_2 = \frac{1}{h \ . \ A}$$

$$\left[G_2 = 0.07 \right] \ \left({}^{o}C/_{W} \right)$$

From equations (8-9) to (8-13) and as the input temperature of the water is 30 ^{o}C, the ambient ground temperature considered is 20 ^{o}C, the temperature rise and the heat distribution are shown in (Table 8-2), the distance between the cooling stations considered is 5.6 (km).

Table (8-2)

Node	Water temperature (^{o}C)	Heat in the water q_w (W/cm)	Heat in the dielectric + soil q_e (W/cm)	Conductor temperature Tc (^{o}C)	Distance (km)
1	30	0.42996	0.0805	30.033	0
2	35	0.38934	0.12067	35.-314	1.811
3	40	0.349707	0.1608	40.03086	3.82
4	44	0.31766	0.193	44.022	5.6
5	45	0.3096	0.2009	45.0286	6.07
6	50	0.26945	0.24105	50.027	8.637
7	52.387	0.25066	0.25984	52.368	10.0
8	55	0.22933	0.2812	55.026	11.62
9	60	0.1892	0.322	60.0243	15.2
10	65	0.149	0.36146	65.023	19.6
11	70	0.10906	0.40144	70.0076	25.4
12	75	0.06894	0.442	75.005	33.85
13	80	0.02883	0.482	80.002	49.97

Table (8-2) shows that the distance between each cooling station which has a maximum temperature (50 ^{o}C) is (L = 8.6 km).

Table (8-3) gives the heat distribution as the distance between each cooling station is considered 6 (km).

Table (8-3)

Node	Water temperature θ (°C)	Heat in the water q_w (W/cm)	Heat in (soil + dielectric) q_e (W/cm)	Conductor temperature Tc (°C)	Distance in (km) (L)
1	30	0.429983	0.8052	30.03	0
2	35	0.3899	0.12064	35.028	1.811
3	40	0.34975	0.16075	40.025	3.82
4	44.85	0.31083	0.19967	44.87	6.0
5	45	0.30963	0.20087	45.0224	6.072
6	50	0.269505	0.240895	50.0083	8.64

The D.C. stress distribution of this cable is different from one position to the other, Table (8-4) gives the stress at different positions in each section of the cable.

Table (8-4)

Node	Stress on the conductor E_r (kV/mm)	Stress on the sheath E_R (kV/mm)	Average stress E_{ar} (kV/mm)	Losses in insulant + soil q_e (W/cm)	Distance in kilometer L (km)
1	9.57	8.0	8.785	0.08056	0
2	9.17	8.3	8.74	0.12065	1.811
3	8.82	8.305	8.585	0.16075	3.82
4	8.5	8.31	8.405	0.1997	6

8-7 DESIGN OF D.C. CABLES AT MAXIMUM CONDUCTOR AREA

The following cables are designed at maximum conductor area, maximum insulation thickness which can be extruded:

A - Polyethylene Land Cable

The specification of this cable are:

1 - The rated voltage is ∓ 100 kV.

2 - The cross-sectional area of the conductor is 25 cm^2.

3 - The insulation thickness is 2.6 cm.

4 - The sheath radius is 5.44 cm.

5 - The maximum stress on the conductor at no load is 5.4 kV/mm.

6 - The dielectric thermal resistance is 54 ($\frac{^{o}C}{W}$).

7 - The soil thermal resistance is 160 ($\frac{^{o}C}{W}$).

8 - The conductor temperature is 45 ^{o}C.

9 - The maximum stress on sheath at full-load is 5.25 kV/mm.

10 - The maximum power is 315 MVA.

B - EPR Land Cable:

Specification of this cable are:

1 - The rated voltage is ∓ 100 kV.

2 - The cross-sectional area of the conductor is 25 cm^2.

3 - The insulation thickness is 2.6 cm.

4 - The sheath radius is 5.44 cm.

5 - The maximum stress on the conductor is 5.4 kV/mm.

6 - The dielectric thermal resistance is 63.1 ($\frac{^{o}C}{W}$).

7 - The surrounding soil thermal resistance is 159.5 ($\frac{^{o}C}{W}$).

8 - The conductor temperature is 60 ^{o}C.

9 - The stress on the sheath at full load is 6.0 kV/mm.

10 - The maximum power is 360 MVA.

CONCLUSIONS

A - POLYETHYLENE

1 - It is not possible to define the steady state resistivity of the polyethylene due to the difficulty obtained in getting steady-state current. The steady-state current was not obtained in polyethylene at temperatures less than 50 °C and at different stresses (8 kV/mm - 40 kV/mm). At temperature 70 °C and under stress 32 kV/mm, steady-state current was not obtained after 170 hours.

2 - At a certain temperature, the conduction current mechanism under applied field depends on the previous history of the polyethylene specimen.

3 - The value of the polyethylene resistivity after a period of short circuiting the specimen is slightly different to that at first applied field (just before short circuiting the specimen to earth). This difference depends on the period of the short circuit.

4 - The resistivity of polyethylene varies with stress according to the first Poole Theory. The plot of resistivity against stress is linear over the stress range from 10 kV/mm to 32 kV/mm. The resistivity/temperature characteristics is linear over a wide range of temperature (40 °C - 80 °C). The empirical formula which give the relation between the resistivity/stress and resistivity/temperature in polyethylene is over the probably working range.

$$\rho = \rho_0 \; e^{-\alpha\theta} \cdot e^{-\beta E}$$

where ρ_0 is the reference resistivity.

5 - The manufacturing process has a great effect on the conduction

mechanism in the polyethylene specimen, which reflects the difference in the physical structure of the polyethylene specimen.

6 - The values of the resistivity/stress coefficient (β), resistivity/temperature coefficient (α) and the reference resistivity (ρ_0) for the stress and temperature range likely in a D.C. cable are:

$\alpha = 0.087$ (1/°C)

$\beta = 0.003$ (cm/kV)

ρ_0 at 40 °C = 1.3×10^{18} (Ω - cm)

B - ETHYLENE-PROPYLENE-RUBBER (EPR)

1 - At temperatures less than 50 °C, it is difficult to get steady-state current within a few days.

2 - The time consumed to reach steady-state is decreased with the decrease of the specimen thickness.

3 - At temperature 70 °C and at stresses less than 32 kV/mm, steady-state current was obtained within ten hours.

4 - At a certain temperature, the conduction current mechanism under applied field is rarely effected by the previous history of the EPR specimen.

5 - The resistivity of the EPR varies with the stress and with the temperature by the same empirical formula of the polyethylene (within a certain range of temperature and stress).

6 - The values of the resistivity/stress coefficient (β), the resistivity/temperature coefficient (α) and the reference resistivity (ρ_0) for the stress and temperature range likely in a D.C. cable are:

$\alpha = 0.14$ (1/°C)

$\beta = 0.01$ (cm/kV)

ρ_0 at 40 °C = 8.5×10^{17} (Ω - cm)

C - POLYPROPYLENE

1 - With a temperature range of (40 °C - 50 °C) and at applied fields (6.25 kV/mm - 19 kV/mm), steady-state current was obtained within twenty hours.

2 - At a certain temperature, the conduction mechanism under applied field depends on the previous history of the polypropylene specimen.

3 - The resistivity of the polypropylene varies with the stress and with the temperature according to a formula similar to that for polyethylene and EPR (within a certain range of temperature and stress).

4 - The resistivity of the polypropylene specimen increases with increase in the specimen thickness.

5 - With a wide range of stress (6.25 kV/mm - 31.25 kV/mm), the resistivity/temperature coefficient (α) is decreased with the increase of the applied field. At a certain applied field and with a wide range of temperature (40 °C - 80 °C), the increase of the temperature causes a decrease in the value of the resistivity/stress coefficient (β). This wide range of temperature and stress is not found in the high-voltage D.C. cable. The above changes in 'α' and 'β' are also found in polyethylene and EPR.

6 - The values of the resistivity/stress coefficient (β), the resistivity/temperature coefficient (α) and the reference resistivity (ρ_o) for the stress and temperature range likely in a D.C. cable are:

$\alpha = 0.11 \ (1/^{\circ}C)$

$\beta = 0.0076 \ (cm/kV)$

ρ_o at 40 °C $= 5.3 \times 10^{17} \ (\Omega - cm)$

D - CROSS-LINKED POLYETHYLENE (XLPE)

1 - At 40 °C, the steady-state current was obtained within twenty hours specially at values of applied field less than 10 kV/mm.

2 - At a certain temperature, the time consumed for the current to reach steady-state is increased as the applied field is increased. At a certain applied field, the time consumed to reach the steady-state is decreased as the temperature is increased.

3 - The resistivity of XLPE varies with the stress and with the temperature by a formula of the type found for polyethylene, EPR and polypropylene.

4 - At a wide range of stress and at a certain temperature, the resistivity/temperature coefficient (α) is decreased as the applied field is increased. At a certain applied field, the resistivity/stress coefficient (β) is increased as the temperature is increased.

5 - The values of the resistivity/stress coefficient (β), the resistivity/temp. coefficient (α) and the reference resistivity (ρ_0) for the stress and temperature range likely in a D.C. cable are:

$\alpha = 0.18 \ (1/^{o}C)$

$\beta = 0.0032 \ (cm/kV)$

ρ_0 at 40 $^{o}C = 2.4 \times 10^{15} \ (\Omega - cm)$

E - POLYETHYLENE WITH A LOW PERCENTAGE OF ADDITIVES

1 - Carbon black content of 3% and 5% in polyethylene has no effect on the resistivity of the polyethylene.

2 - Steady-state current can be obtained within twenty hours for composite of polyethylene with (3-5%) of carbon black.

3 - Talc of content 3% and 5% in polyethylene gives a smaller resistivity than that of unfilled polyethylene.

4 - Steady-state current can be obtained within twenty hours for the composite of polyethylene with 5% talc and within thirty hours for the composite of polyethylene with 3% talc.

5 - Mica content of 5% in polyethylene gives a small increase of the composite resistivity.

6 - Steady-state current can be obtained within twenty hours for the composite of polyethylene with 5% mica.

7 - The following table shows the values of the resistivity/temperature, resistivity/stress on the reference resistivity of the polyethylene with additives.

Composite	α (1/°C)	β (cm/kV)	ρ_0 at 50 °C (Ω- cm)
Unfilled P.E	0.0869	0.00274	5.3×10^{16}
PE + 3% C.B	0.0886	0.00344	8.2×10^{16}
PE + 5% C.B	0.0940	0.00640	1.35×10^{17}
PE + 3% talc	0.0840	0.00260	3.6×10^{16}
PE + 5% talc	0.0880	0.00286	3.0×10^{16}
PE + 5% mica	0.0708	0.0088	1.2×10^{18}

F - DESIGN STUDIES

1 - The dielectric loss of a D.C. cable is very small and can normally be ignored. The dielectric loss is still very small after decreasing the dielectric resistivity to about 10^{12} (Ω- cm).

2 - By assuming that the polyethylene resistivity increase with time, a computer program shows that the stresses created by the cyclic loading can be ignored in the design procedure of the D.C. cable.

3 - The use of externally cooled high voltage extruded D.C. cables is not convenient due to the high D.C. electric stress obtained by the thermal gradient at the sheath on full-load.

4 - For high voltage D.C. land cables of extruded insulation (which has

relatively low average stress), the largest capacity is obtained with internally water cooling.

5 - The use of a relatively high working temperature insulant such as EPR, XLPE (conductor temperature more than 60 ^{o}C) is limited by the high stress at the sheath on full-load.

G - GENERAL

The nature of the conduction mechanism and the possible theoretical models have been discussed in Chapters 2, 4, 5 and 6. From the practical point of view it has been seen that although it is preferable to quote a steady-state value of the resistivity for a D.C. cable with a normal cyclic load, the contained use in resistivity with time is not a major design problem. However the very slow change in resistivity with time has a marked effect on the transient performance e.g., impulse lightning surges, switching surges and polarity reversal. Also the effect of the space charge accumulation effectively reduces the breakdown strength of the dielectric.

To overcome these problems the use of additives has been investigated and it has been shown that the insertion of small amounts of either carbon black, talc or mica to the polyethylene decreases the time consumed to reach the steady-state and hence are beneficial. However the long term effects of these additives require further investigation along with the resultant mechanical and thermal properties.

Investigation into the maximum capacity of a polyethylene extruded cable indicate the following; (assuming $E_{b.d}$ of 100 kV/mm on impulse and 80 kV/mm on D.C.)

Land cable, P_{max} = 306 MVA, V = 100 kV.

Land internally cooled cable with length 6 km between the cooling stations, P_{max} = 900 MVA, V = 150 kV.

Submarine cable, P_{max} = 580 MVA, V = 180 kV.

It is not anticipated that a voltage higher than 200 kV will be used for extruded plastic cables without increase in the value of average designed stress. Up to date the values quoted above are conservative.

Investigation into the maximum capacity of EPR extruded cable indicate the following; (assuming $E_{b.d}$ of 80 kV/mm on impulse and 60 kV/mm on D.C.)

Land cable, P_{max} = 400 MVA, V = 100 kV.

EPR is commonly used as A.C. cable insulant.

The polyethylene material is more economic than that of EPR. The above appraisal is purely technical and obviously the ultimate requirement for the use of extruded plastic cables is economic, furthermore, considerable advantages exist because of the absence of an impregnant such as gas or oil.

REFERENCES

1. Lawson, W.G. - "High-field electrical conduction in oil-impregnated paper dielectric". Ph.D. Thesis, March 1972, University of Southampton.

2. Arnett, P.C. - "Transient conduction in insulators at high fields" J. Applied Physics Vol. 46, No. 12, Dec. 1975.

3. Van Trunhout, J. - "Thermally stimulated discharge of polymer electrics", 1975.

4. ASTM Designation - D150 -50T, "Tentative methods of test for A.C. capacitance dielectric constant, and loss characteristics of electrical insulating materials."

5. Bradwell, A. and Cooper, R. - "Conduction in polyethylene with strong electric fields and the effect of prestressing on the electric strength". Proc. IEE Vol. 118, No. 1, Jan. 1971.

6. Auckland, D.W. and Prof. Cooper, R. - "Investigation of water absorption by electrically stressed polyethylene". Paper 7489, Proc. IEE, Vol. 122, No. 8, August 1975.

7. Garton, C.G. and Parkman, N. - "Experimental investigation of conduction in polyethylene from 4 MV/mm up to intrinsic breakdown". Proc. IEE, Vol. 23, No. 3, March 1976.

8. Odwyer, J.J. - "The theory of electrical conduction and breakdown in solid dielectrics" (1973).

9. Sillars, R.W. - "Electrical insulating materials and their application", IEE monograph series 14, (1973).

10. Parkman, N. - "High-field conduction in polyethylene". Oct. 1967, Ph.D. Thesis, University of London.

11. Faraj, A. - "The volume resistivity of polyethylene" 1964, Ph.D. Thesis, University of Leeds.

12. CIGRE, 1958, Part 1, - "Research work in dielectric working conditions of D.C. cables".

13. Davey, E.L. - "The testing of high voltage D.C. power cables".

14. Wikins, R., Storey, J.T. and Billings, M.J. - "Numerical determination of the electrical and thermal fields in a D.C. cable".

15. Nobuo, Ando. and Takeshi, Endo. - "Insulation performance of extra high-voltage D.C. oil-filled cable". Hitachi Review Vol. 22, No. 7.

16. Eoll, C.K. - "Theory of stress distribution in insulation of high voltage D.C. cables". IEE Tran. on electrical insulation, Vol. E1-10, No. 2, June 1975.

17. Occhini, E and Maschio, G. - "Electrical characteristics of oil-impregnated paper as insulation for H.V. D.C. cables". IEE Tran. of power apparatus, March 1967.

18. Chu, S.C. - "Design stresses and current rating of impregnated paper insulated cables for H.V. D.C." Paper No. 31P, 66-37, May 1966.

19. Oudin, J.M. and Thevenon, H. - CIGRE, 1966 "Theory of D.C. cables. Calculation of gradient and its correlation with breakdown gradient".

20. Hawley, W.G., Body, R.S. and Mason, - "Polyethylene as a possible H.V.D.C. cable insulant". I.E.E. High Voltage D.C. Transmission. Tk 311, PT. 1, September 1966, p. 338.

21. Oudin, J.M. and Fallou, M. - "Some consideration on the design of D.C. cables" I.E.E. High Voltage D.C. Transmission. Tk 311, PT. 1, September 1966, p. 318.

22. Rose, A. - "Space-charge-limited currents". The molecular designing of materials and devices. By Von Hippel, p. 178.

23. Lawson, W.G. - "High-field conduction and breakdown in polythene". J. Appl. Phy. 1965.

24. British Patent No. 1257920 - "Insulated electrical conductors".

25. United State Patent No. 3655,565, April 11, 1972.

26. Williams, A.L. - "D.C. Power Transmission". Electrical Journal, March 1960.

27. Singh, N. and Bruhin, A.C. - "Application of extrudable insulants to D.C. cables". General Electric Company, Bridgeport, Connecticut.

28. Weedy, B.M. - "Electric Power Systems", Chapter 8.

29. Blodgett, R.B. and Fisher, G. - "Present status of the Corona - and Heat-Resistant Cable Insulation Based on Ethylene-Propylene-Rubber". I.E.E. Trans. of Power and Apparatus, Vol. PAS-87, No. 4, April 1968.

30. Weedy, B.M. - "Effect of environment on transient thermal performance of underground cables". Proc. I.E.E. Vol. 119, No. 2, Feb. 1972.

32. Davini, G., Consortini, G. and Portinari, G. - "Recent Developments in EPR-Insulated High-Voltage Cables". I.E.E. Trans. of Power and Apparatus, Vol. PAS 86, No. 11, November 1967.

33. Blodgett, R.B. and Fisher, R.G. - "A New Corona-and Heat-Resistant Cable Insulation Based on Ethylene Propylene Rubber". I.E.E. Trans. of Power and Apparatus, Dec. 1963, p. 980

34. Lawson, W.G., Rolandin, L.M. and Head, J.G. - "The effect of polarity reversals on the dielectric strength of oil-impregnated paper insulation for D.C. cables."

35. Birnbreier, H., Fisher, W. and Rasquin, W. - "Higher power cables with internal water cooling". CIGRE 1974, 21-09 p. 2.

36. Schmill, J.V. - "Variable Soil Thermal Resistivity - Steady-State Analysis". I.E.E. Transactions on Power Apparatus and Systems, Vol. PAS-86, No. 2, Feb. 1967.

37. Hange, O. and Johnsen, J.N. - "HVDC cable for crossing the Skagerrak Sea between Denmark and Norway". CIGRE, 1974, Session 21-29 August.

38. Huges, K.E.L. and Nicholson, J.A. - "Design Features of High Voltage D.C. band cables". I.E.E. High Voltage D.C. Transmission Conference 19th - 23rd September 1966, p. 315.

39. Tanaka, T. - "Charge injection by voltage application into polymer dielectrics - new proposal for D.C cable polymer insulation system. I.E.E. Trans., May 5, 1976.

40. Noto, F. and Yoshimura, N. - "Tree initiation in polyethylene by application of D.C. and impulse voltage". I.E.E. Trans., Vol. E1-12 No. 1, Feb. 1977.

41. Hugues, St-Onge, - "Electrical Conduction in 3 Percent Carbon-Filled Polyethylene - Part 1". I.E.E. Trans. Vol. E1-11, No. 1, March 1976.

42. Forster, E.O. - "Electrical conduction mechanism in carbon filled polymers". I.E.E. Trans. Power App. Syst., Vol. PAS-90, pp. 913-916, May/June 1971.

43. Bahder, G. and Garcia, F.G. - "Electrical Characteristics of Extruded Semi-Conducting Shields in Power Cables". I.E.E. Trans. Power App. System, Vol. PAS-90, pp. 917-925, May/June 1971.

44. Bueche, F. - "Electrical Properties of Carbon Black in an SBR-Wax Matrix". J. of Applied Polymer-Science, Vol. 11, 1319-1330 (1973).

45. Wertheimer, M.R., Paquin, L., Schreiber, H.P. and Boggs, S.A. - "Dielectric Permittivity, Coductivity, and Breakdown Characteristics of Polymer-Mica Composites". I.E.E. Trans. on E.I., Vol. E1-12, No. 2, April 1977.

46. Malliaris, A. and Turner, D.T. - "Influence of Particle Size on the Electrical Resistivity of Compacted Mixtures of Polymeric and Metallic Powders". J. of Applied Physics, Vol. 42, No. 2, Feb. 1971.

47. Bahder, G., Garcia, F.G. and Brooks, A.S. - "Insulation Co-ordination in high voltage D.C. cables". CIGRE, No. 21-03, 1972.

48. Ieda and Nawata - "DC TREEING breakdown associated with space charge formation in polyethylene". I.E.E. Trans. Vol. E1-12, No. 1, Feb. 1977.

49. Ritchie, - "Physics of Plastics". Plastics Institute London Ilife Books Ltd.

50. Fujiki, S., Furusawa, H., Kuhara, T. and Matsuba, H. - "The research in discharge suppression of the high voltage cross-linked-polyethylene insulated power cables". I.E.E. of Power and Appar. System, Dec. 1970, pp. 2703-2708.

51. Hochstadt, H. - "Differential Equations, A Modern Approach". Holt, Rinehart and Winston.

ACKNOWLEDGEMENTS

The author would like to thank the Ministry of Higher Education - Republic of Iraq for the award of the scholarship. Thanks are also due to Mr. S. Swingler, Mr. M. Burdy and Mr. R. Lazimour for the practical assistance. The author would like to thank Dr. M. Rechowicz, Pirelli General Work, for providing the various samples of polyethylene, EPR, XLPE and polypropylene. The author would like to thank Dr. W.G. Lawson, Pirelli General Work, for the useful technical discussion. Finally the author would like to thank Dr. B.M. Weedy for helpful advice received during the course of this work and for acting as Academic Supervisor, and Professor P. Hammond for providing facilities in the Department of Electrical Engineering.

APPENDIX

1 - Program No. 1

Input data:

V1 - Working D.C. voltage (kV)

R - Radius of the conductor (cm)

R1 - Radius of the sheath (cm)

A1 - Resistivity/temperature coefficient ($1/^{o}C$)

B1 - Resistivity/stress coefficient (cm/kV)

G - Thermal resistivity ($\frac{^{o}C}{W}$ cm)

Q - Conductor losses (W/cm)

Subroutine D01ABF for numerical integration

Subroutine E01AAF for Aitken interpolation.

Program No. 1

```
£FXF/S910/AMOURI/FORT/ST=4000/T=30/L=6000/PR=1//
      LIST(LP)
      PROGRAM(A591)
      INPUT 5=CPU
      OUTPUT 6=LPO
      COMPACT DATA
      COMPRESS INTEGER AND LOGICAL
      TRACE
      END
      MASTER CALC
      DIMENSION S0(6),V0(6),C(15),G1(6),S1(6)
      EXTERNAL S
      COMMON/ANOR/Y,A1,B1,G,R,Q
      READ(5,15) V1,P,R1,A1,B1,G
      WRITE(6,10)V1,P,R1,A1,B1,G
 10   FORMAT(1H ,6F10.5)
      S0(1)=15.0
      DO 20 I=2,6
 20   S0(I)=S0(I-1)+5.0
 30   READ(5,15) Q
      WRITE(6,10)Q
 15   FORMAT(6F10.5)
C FIND V0 FOR EACH S0
      DO 40 I=1,6
      Y=S0(I)
      CALL DO1AHF(R,R1,S,1.E-8,64,N,V,0)
      V0(I)=V
      WRITE(6,45) S0(I),V0(I)
 40   CONTINUE
      CALL E01AAF (V0,S0,C,6,15,5,V1)
      Y=C(15)
      CALL DO1AHF(R,R1,S,1.E-8,64,N,V,0)
      WRITE(6,45) V,Y
 45   FORMAT(1H ,2F10.4)
      STOP
      END
      FUNCTION S(X)
      DIMENSION S1(6),G1(6),C(15)
      COMMON/ANOR/Y,A1,B1,G,R,Q
      PI=3.14159
      F=B1*Y+ALOG(Y)+(A1*G*S/PI-1.0)*ALOG(X/R)
      S1(1)=30.0
      DO 55 I=2,6
 55   S1(I)=S1(I-1)+5.0
      DO 65 I=1,6
      G1(I)=R1*S1(I)+ALOG(S1(I))
 65   WRITE(6,75) G1(I),S1(I),F
      CALL E01AAF(G1,S1,C,6,15,5,F)
      S=C(15)
      WRITE(6,75) S
 75   FORMAT(1H ,4F10.4)
      RETURN
      END
      FINISH
£DATA
 150.0      1.784      4.135      0.0869     0.003      350.0
 0.36
END
```

2 - Program No. 2

Input data

SD - D.C. stress on the conductor (kV/cm)

R - Radius of the conductor (cm)

A1 - Resistivity/temperature coefficient ($1/^{o}C$)

B1 - Resistivity/stress coefficient (cm/kV)

G - Thermal resistivity ($\frac{^{o}C}{W}$ cm)

V1 - D.C. working voltage

D - Reference resistivity of the dielectric (Ω - cm)

TR - is the temperature (^{o}C)

Q1 - Conductor losses (W/cm)

RTH - Total thermal resistance of the dielectric and the soil

Program No. 2

```
$EXEC/591F/AMOURT/FORT/ST=7000/T=160/L=7000/PR=1//
      LIST(LP)
      PROGRAM(A591)
      INPUT 5=CRD
      OUTPUT 6=LPD
      COMPACT DATA
      COMPRESS INTEGER AND LOGICAL
      TRACE 2
      END
      MASTER CALC
      DIMENSION X(41),S1(41),TD(41),QQ(41),Q1(41),T1(41),X1(41),S4(41),
     1TD1(41),SD1(41),T2(41),Q2(41),T3(41),Q3(41),TP(10),Q(10),Q1(10),SA
     1(10)
      READ(5,10)SO,R,A1,B1,G,V1
      D=10.0E-18
      TP(1)=50.0
      DO 100 N=2,10
      Q(1)=0.1575
      Q2(1)=0.0
      Q(N)=Q(N-1)+Q2(N-1)+0.05
      RTH=190.4
      TP(N)=RTH*Q(N)+20.0
 10   FORMAT(6F10.5)
      WRITE(6,15)SO,R,A1,B1,G,V1,Q(N),TP(N)
      S1(2)=63.4222
      DO 11 I=3,10
 11   S1(I)=S1(I-1)+1.5
C FIND X FOR EACH S1
      PI=3.141592654
      PJ=6.283185307
      DO 20 I=2,10
      X(I)=R*EXP((ALOG(S1(I))+B1*S1(I)-ALOG(SO)-B1*SO)/(Q(N)*G*A1/PJ-1))
 15   FORMAT(1H ,9F10.5)
C FIND TD FOR EACH X
      TD(I)=TP(N)-(Q(N)*G*(ALOG(X(I)/R))/PJ)
C FIND QQ FOR EACH TD
      QQ(I)=D*PI*((SA(I))**2)*((X(I))**2-R**2)*EXP(A1*TD(I)+B1*S1(I))
      SA(I)=(S1(I)+SO)/2
C FIND T1 FOR EACH QQ
      QQ(1)=0.0
      T1(I)=TP(N)-(Q(N)+((QQ(I)+QQ(I-1))/2))*G*(ALOG(X(I)/R))/PJ
C FIND Q1 FOR EACH T1
      Q1(I)=D*PI*((SA(I))**2)*((X(I))**2-R**2)*EXP(A1*T1(I)+B1*S1(I))
C FIND X1 FOR EACH S1
      Q1(1)=0.0
      Q2(I)=Q(N)+((Q1(I)+Q1(I-1))/2)
      X1(I)=R*EXP((ALOG(S1(I))+B1*S1(I)-ALOG(SO)-B1*SO)/(Q2(I)*G*A1/PJ-1
     1))
C FIND TD1 FOR EACH X1
      TD1(I)=TP(N)-Q(N)*G*(ALOG(X(I)/R))/PJ
```

```
C FIND Q01 FOR EACH T01
      Q01(I)=D*PI*((SA(I))**2)*((X1(I))**2-R**2)*EXP(A1*T01(I)+B1*S1(I))
C FIND T2 FOR EACH Q01
      Q01(1)=0.0
      T2(I)=TR(N)-(Q(N)+((Q01(I)+Q01(I-1))/2))*G*(ALOG(X1(I)/R))/PJ
C FIND Q2 FOR EACH T2
      Q2(I)=D*PI*((SA(I))**2)*((X1(I))**2-R**2)*EXP(A1*T01(I)+B1*S1(I))
C FIND T3 FOR EACH Q2
      Q2(1)=0.0
      T3(I)=TR(N)-(Q(N)+((Q2(I)+Q2(I-1))/2))*G*(ALOG(X1(I)/R))/PJ
 20   CONTINUE
      DO 50 I=2,10
 50   WRITE(6,17)X(I),S1(I)
 17   FORMAT(1H ,2F20.6)
      WRITE(6,60)
 60   FORMAT(////////////////)
      DO 51 I=2,10
 51   WRITE(6,25)S1(I),T0(I),Q0(I),T1(I),Q1(I)
 25   FORMAT(1H ,5F20.10)
      WRITE(6,67)
 67   FORMAT(////////////////)
      DO 57 I=2,10
 57   WRITE(6,39)X1(I),S1(I)
 39   FORMAT(1H ,2F20.8)
      WRITE(6,68)
 68   FORMAT(////////////////////)
      DO 61 I=2,10
 61   WRITE(6,35)Q3(I),X1(I),T01(I),Q01(I),T2(I)
 35   FORMAT(1H ,5F22.6)
      WRITE(6,69)
 69   FORMAT(////////////////)
      DO 71 I=2,10
 71   WRITE(6,45)Q2(I),X1(I),T3(I),S1(I)
 45   FORMAT(1H ,4F20.6)
      DO 150 I=2,10
      D1(I)=1/(D*(EXP(A1*(T3(I)-TR(N)))*(EXP(B1*S1(I)))))
 130  WRITE(6,150)D1(I),Q2(I)
 150  FORMAT(1H ,2E30.5)
 100  CONTINUE
      STOP
      END
      FINISH
$DATA
 60.7       1.804       0.14        0.01        610.0       100.0
$END
```

3 - Program No. 3

Input data

SPHL - Specific heat of the copper ($J/g_m\ ^oC$)

DNSTL - Density of the copper (gm/cm^3)

Current - Conductor current (A)

Resistance - is the resistance of the copper (Ω)

DT - Time interval for the iteration of the dielectric (second)

DT1 - Time interval for the iteration of the soil (second)

NIT - Number of iteration

NITT - Number of print out iteration

N - Number of nodes in the dielectric

N1 - Number of nodes in the soil

GTH - Thermal resistivity of the dielectric ($\frac{^oC}{W}$ cm)

SPH - Specific heat of the dielectric ($J/g_m\ ^oC$)

DNST - Density of the dielectric (gm/cm^3)

GTH1 - Thermal resistivity of the soil ($\frac{^oC}{W}$ cm)

SPH1 - Specific heat of the soil ($J/g_m\ ^oC$)

DNST1 - Density of the soil (gm/cm^3)

R - Radius of the conductor (cm)

DD - is the space between the two cables (cm)

H - is the depth of the cable (cm)

R1 - is the radius of the sheath

THETA - is the angle between the x-axis of the first cable and the diagonal between the x-axis and image of the second cable.

Program No. 3

```
£FXE/591H/AMOPRI/FORT/ST=6500/T=900/L=9000/PR=2//
      LIST(LP)
      PROGRAM(A591)
      INPUT 5=CRD
      OUTPUT 6=LPD
      COMPACT DATA
      COMPRESS INTEGER AND LOGICAL
      TRACE 2
      END
      MASTER CARLES
      DIMENSION A(9),B(9),C(9),T(9),TA(9),G(9),TS(20),RTH(9),CAP(9),
     1R(9),R1(20),A1(20),B1(20),C1(20),T1(20),RTH1(20),CAP1(20),AA(20),G
     1G(20),RD(20)
      PI=3,141592654
      PJ=6,283185308
      SPHI=0,39
      DNSTL=7,7
      CURRENT=1000,0
      RESISTANCE=1,56E-7
      W=RESISTANCE*(CURRENT)**2
      DT=100,0
      DT1=100,0
      MIT=180
      MITT=10
      N=4
      N1=4
      READ(5,20)GTH,SPH,DNST,GTH1,SPH1,DNST1
20    FORMAT(1H ,6F10,5)
      WRITE(6,18)GTH,SPH,DNST,GTH1,SPH1,DNST1
18    FORMAT(1H ,6F14,8)
      WRITE(6,62)Q
62    FORMAT(1H ,F10,6)
      M=N-1
      R(1)=1,804
      CAP(1)=PI*((R(1))**2)*SPHI*DNSTL
      DO 21 J=2,N
21    R(J)=R(J-1)+0,4454456667
      DO 25 J=2,M
      RTH(J-1)=(GTH/PJ)*ALOG(R(J)/R(J-1))
      RTH(J+1)=(GTH/PJ)*ALOG(R(J+1)/R(J))
      CAP(J)=PI*((R(J))**2-(R(J-1))**2)*SPH*DNST
      A(J-1)=DT/(RTH(J-1)*CAP(J))
      B(J+1)=DT/(RTH(J+1)*CAP(J))
      C(J)=1-(A(J-1)+B(J+1))
25    CONTINUE
      DO 19 J=2,M
19    WRITE(6,24)R(J),RTH(J-1),RTH(J+1),CAP(J),A(J-1),B(J+1),C(J)
24    FORMAT(1H ,7F16,6)
      DD=10,0
      H=100,0
28    R1(1)=3,140337
      THETA=1,52084
      DO 50 K=2,N1
50    R1(K)=R1(K-1)+3,0
      DO 51 K=1,N1
51    RD(K)=SQRT((R1(K)*SIN(THETA))**2+(DD-(R1(K)*COS(THETA)))**2)
      DO 53 K=1,N1
53    GG(K)=(GTH1/PJ)*(ALOG((2*H-R1(K))/R1(K))+ALOG((SQRT(4*H**2+DD**2)-
     1R1(K))/(RD(K))))
      DO 55 K=2,N1-1
      RTH1(K-1)=GG(K-1)-GG(K)
      RTH1(K+1)=GG(K)-GG(K+1)
```

```
      CAP1(K)=PI*SPH1*DUST1*((R1(K))**2-(R1(K-1))**2)
      A1(K-1)=DT1/(RTH1(K-1)*CAP1(K))
      B1(K+1)=DT1/(RTH1(K+1)*CAP1(K))
      C1(K)=1-(A1(K-1)+B1(K+1))
55    CONTINUE
      DO 17 K=2,N1-1
      WRITE(6,67)
67    FORMAT(/////)
      WRITE(6,66)GG(K),RO(K)
66    FORMAT(1H ,2F10.6)
17    WRITE(6,60)R1(K),RTH1(K+1),RTH1(K-1),CAP1(K),A1(K-1),B1(K+1),C1(K)
60    FORMAT(1H ,7F16.6)
      DO 30 J=1,N
      G(J)=0.0
30    T(J)=0.0
      DO 70 K=1,N1
70    T1(K)=0.0
      IT=0.0
110   I=0.0
111   IT=IT+1
11    I=I+1
      G(2)=QO*DT*(1.0+0.0041*(T(2)))/CAP(1)
      DO 12 J=2,N
12    TA(J)=A(J-1)*T(J-1)+B(J+1)*T(J+1)+C(J)*T(J)+G(J)
      TA(1)=TA(2)
      IF(TA(N)-100.0)8,77,77
8     DO 222 K=2
      A(K-1)=B(K+1)
222   C(K)=1-(A(K-1)+A1(K-1))
29    TA(N)=A(N-1)*T(K-1)+C(N)*T(N)+G(N)
44    DO 93 J=1,N
93    T(J)=TA(J)
      T1(1)=TA(N)
      DO 85 K=2,N1-1
85    TS(K)=A1(K-1)*T1(K-1)+B1(K+1)*T1(K+1)+C1(K)*T1(K)
      TS(1)=TS(2)
90    DO 96 K=1,N1
96    T1(K)=TS(K)
      IF (IT-I)9,9,11
9     WRITE(6,115)NIT
115   FORMAT(7H AFTER ,I5,44H ITERATION,THE CABLE NODE TEMPERATURE,ARE :
     1 /)
      AAA=TS(N-1)
      WRITE(6,119)AAA
119   FORMAT(1X,F10.4/)
      WRITE(6,116)(J,TA(J),J=1,N)
114   FORMAT(I5,5X,F20.10,/)
      WRITE(6,250)TA(N),A(K-1),C(N),G(2)
250   FORMAT(1H ,4E20.5)
      WRITE(6,130)NIT
130   FORMAT(7H AFTER ,I5,44H ITERATIONS,THE SOIL NODE TEMPERATURE,ARE :
     1 ,/)
      WRITE(6,134)TS(N1-1)
134   FORMAT(1H ,F30.5)
      WRITE(6,135)(K,TS(K),K=1,N1-1)
135   FORMAT(I5 ,5X,E30.5,/)
      WRITE(6,61)
61    FORMAT(///)
      IF(NITT-IT)0,0,111
77    STOP
      END
      FINISH
£DATA
 610.0      2.5         1.200      120.0      0.5         1.6
£END
```

4 - Program No. 4

Input data

T - Time in hours

DT1, DT2 - Time periods during the daily thermal cycle (hours)

W, H - Factors of the resistivity/temperature coefficient decaying with time

ALPHO - Resistivity/temperature coefficient at the first hour ($1/^{o}C$)

In subroutine NAILOVER and subroutine NASSIM the dimensions are:

V1 - D.C. working voltage (kV)

R - Radius of the conductor (cm)

R1 - Radius of the sheath (cm)

B1 - Resistivity/stress coefficient (cm/kV)

G - Thermal resistivity ($\frac{^{o}C}{W}$ cm)

Q - Conductor losses (W/cm)

Program No. 4

```
£EXF/591Y/AMOUR1/FORT/ST=9000/T=1500/L=9000/PR=2//
      PROGRAM(A591)
      INPUT 5=CRD
      OUTPUT 6=LPD
      COMPACT DATA
      COMPRESS INTEGER AND LOGICAL
      TRACE
      END
      MASTER CABLES
      DIMENSION T(90),ALPH(90),W(90),ALPH1(90),ALPH2(90),W1(90),W2(90)
      COMMON/AMOR/Y,AA,B1,G,R,Q
      COMMON/DMOR/P,BB,B2,E,U,Q1
      COMMON/CMOR/M
      T(2)=24.0
      DT1=8.0
      DT2=16.0
      H=0.2
      W0=0.75
      ALPH0=0.15
      DO 11 M=3,60
      T(M)=T(M-1)+24.0
      W(M)=W0/(T(M))**H
      ALPH(M)=ALPH0/(T(M))**W(M)
      W1(M)=W(M)/(DT1)**H
      W2(M)=W(M)/(DT2)**H
      ALPH1(M)=ALPH(M)/(DT1)**W1(M)
 16   ALPH2(M)=ALPH(M)/(DT2)**W2(M)
      AA=ALPH1(M)
      CALL NAILOVER
      BB=ALPH2(M)
      CALL NASSIM
 11   CONTINUE
      STOP
      END
      SUBROUTINE NAILOVER
      DIMENSION S0(6),V0(6),C(15),G1(6),S1(6)
      EXTERNAL S
      COMMON/AMOR/Y,AA,B1,G,R,Q
      COMMON/CMOR/M
      V1=100.0
      R=1.42
      R1=4.22
      B1=0.015
      G=330.0
      Q=0.197
      WRITE(6,10)V1,R,R1,AA,B1,G
 10   FORMAT(1H ,6F10.3)
      S0(1)=30.0
      DO 20 I=2,6
 20   S0(I)=S0(I-1)+10
      WRITE(6,10)Q
C FIND V0 FOR EACH S0
      DO 40 I=1,6
      Y=S0(I)
      CALL E01ABF(R,R1,S,1.E-8,64,N,V,Q)
      V0(I)=V
 40   CONTINUE
      CALL E01AAF (V0,S0,C,6,15,5,V1)
      Y=C(15)
      WRITE(6,130)M
 130  FORMAT(7H AFTER ,I5,45H DAYS,THE STRESS ON THE CONDUCTOR EQUAL TO
     1 ,/)
```

```
      CALL D01AMF(R,R1,S,1.E-8,64,N,V,0)
      WRITE(6,45) V,Y
      WRITE(6,60)
 60   FORMAT(/////)
 45   FORMAT(1H ,2F10.4)
      RETURN
      END
      FUNCTION S(X)
      DIMENSION S1(6),G1(6),C(15)
      COMMON/AMOR/Y,AA,B1,S,R,Q
      COMMON/CMOR/M
      PI=3.28318
      F=B1*Y+ALOG(Y)+(AA*Q*G/PI-1.0)*ALOG(X/R)
      S1(1)=35.0
      DO 55 I=2,6
 55   S1(I)=S1(I-1)+10
      DO 65 I=1,6
 65   G1(I)=B1*S1(I)+ALOG(S1(I))
      CALL E01AAF(G1,S1,C,6,15,5,F)
      S=C(15)
      RETURN
      END
      SUBROUTINE NASSIM
      DIMENSION S0(6),V0(6),C(15),G1(6),S1(6)
      EXTERNAL SS
      COMMON/DMOR/P,B0,B2,E,U,Q1
      COMMON/CMOR/M
      V1=100.0
      U=1.42
      R1=4.22
      B2=0.015
      E=330.0
      Q1=0.35
      WRITE(6,10)V1,U,R1,B0,B2,E
 10   FORMAT(1H ,6F10.3)
      S0(1)=30.0
      DO 20 I=2,6
 20   S0(I)=S0(I-1)+10
      WRITE(6,10)Q1
C FIND V0 FOR EACH S0
      DO 40 I=1,6
      P=S0(I)
      CALL D01AMF(U,R1,SS,1.E-8,64,N,V,0)
      V0(I)=V
 40   CONTINUE
      CALL E01AAF (V0,S0,C,6,15,5,V1)
      P=C(15)
      CALL D01AMF(U,R1,SS,1.E-8,64,N,V,0)
      WRITE(6,130)M
 130  FORMAT(7H AFTER ,I5,45H DAYS,THE STRESS ON THE CONDUCTOR EQUAL TO
     1: ,/)
      WRITE(6,45) V,P
      WRITE(6,60)
 60   FORMAT(////////////)
 45   FORMAT(1H ,2F10.4)
      RETURN
      END
      FUNCTION SS(X)
      DIMENSION S1(6),G1(6),C(15)
      COMMON/DMOR/P,B0,B2,E,U,Q1
      COMMON/CMOR/M
      PI=3.28318
      F=B2*P+ALOG(P)+(B0*Q1*E/PI-1.0)*ALOG(X/U)
      S1(1)=35.0
      DO 55 I=2,6
 55   S1(I)=S1(I-1)+10
      DO 65 I=1,6
 65   G1(I)=B2*S1(I)+ALOG(S1(I))
      CALL E01AAF(G1,S1,C,6,15,5,F)
      SS=C(15)
      RETURN
      END
      FINISH
$END
```

5 - Program No. 5

Input data

V - D.C. working voltage (kV)

R, R1, - Conductor and sheath radius (cm)

W - Factor of the resistivity/temperature coefficient decaying with time

B - Resistivity/stress coefficient (cm/kV)

EP - Dielectric constant

A_O - Reference resistivity/temperature coefficient ($1/^oC$)

M - Number of time division during the first polarity reversal

L - Number of series reversal of the polarity

RESO - Reference resistivity (Ω - cm)

Q - Conductor losses (W/cm)

G - Thermal resistivity of the dielectric ($\frac{^oC}{W}$ cm)

TMC - Temperature at the conductor (^oC)

T - Time (hours)

SDC - D.C. stress cable insulation (kV/cm)

X - is distance at any point in the insulation (cm)

SR - is the transient stress due to the polarity reversal (kV/cm)

Program No. 5

```
£EXE/5912/AMOURI/FORT/ST=18200/T=80/L=1000/CST=19000/PR=1//
      LIST(LP)
      PROGRAM(A591)
      INPUT 5=CRD
      OUTPUT 6=LPD
      COMPRESS INTEGER AND LOGICAL
      TRACE 2
      END
      MASTER CARLES
      DIMENSION T(20,10),A(20,10),TM(10),X(10),SA(10),SDC(10),RES(20,10,
     110),TU(20,10,10),SR(20,10,10)
      READ(5,10)V,R,R1,J,R,EP,AO
 10   FORMAT(1H ,7F10.5)
      WRITE(6,90)V,R,R1,,,R,EP,AO
 90   FORMAT(1H ,7F10.5)
      M=8
      L=20
      RESO=1.0E+18
      G=0.197
      G=330.0
      TMC=34.066
      ED=R.85E-12
      T(1,1)=0.5
      T(1,M)=4.0
      SDC(1)=29.3791
      SDC(2)=34.25
      SDC(3)=37.74
      SDC(4)=40.53
      PJ=6.2831853D8
      X(1)=R
      DO 11 I=2,4
 11   X(I)=X(I-1)+0.933
      DO 12 I=1,4
 12   SA(I)=V/X(I)*ALOG(R1/R)
      A(1,1)=AO
      TM(1)=TMC
      DO 16 J=2,M
      N=1
 13   T(N,J)=T(N,(J-1))+0.5
 16   A(N,J)=AO/(T(N,J))**W
      DO 14 N=2,L
      J=M
      T(N,J)=T((N-1),J)+T(1,M)
 14   A(N,J)=AO/(T((N-1),J))**W
      DO 17 I=2,4
 17   TM(I)=TMC-(D*G/PJ)*ALOG(X(I)/R)
      DO 100 N=1,L
      J=M
      DO 18 I=1,4
      RES(N,J,I)=RESO/(EXP(A(N,J)*(TM(I)))*EXP(R*SDC(I)))
 18   TU(N,J,I)=EP*RES(N,J,I)*ED/3600
100   CONTINUE
      DO 150 J=1,M
      N=1
      DO 28 I=1,4
      RES(N,J,I)=RESO/(EXP(A(N,J)*(TM(I)))*EXP(R*SDC(I)))
 28   TU(N,J,I)=EP*RES(N,J,I)*ED/3600
150   CONTINUE
      DO 200 I=1,4
      DO 19 J=1,M
      N=1
```

```
19    SP(N,J,I)=(2*SA(I)/EXP(T(N,J)/TU(N,J,I)))-(2*(SDC(I)/EXP(T(N,J)/TU
     1(N,J,I)))-SDC(I))
      DO 20 N=2,L
      J=M
20    SP(N,J,I)=(2*SA(I)/EXP(T(1,M)/TU(N,J,I)))-(2*(SP((N-1),J,I)/EXP(T(
     11,A)/TU(N,J,I)))-SP((N-1),J,I))
200   CONTINUE
      DO 31 N=1,L
      J=M
31    WRITE(6,32)(N,RES(N,J,I),TU(N,J,I),T(N,J),A(N,J),I=1,4)
32    FORMAT(I5, 5X ,4E20.5,/)
      WRITE(6,60)
60    FORMAT(////////////)
      DO 33 J=1,M
      N=1
33    WRITE(6,34)(J,RES(N,J,I),TU(N,J,I),T(N,J),A(N,J),I=1,4)
34    FORMAT(I5, 5X ,4E20.5,/)
      WRITE(6,61)
61    FORMAT(//////////)
      DO 21 I=1,4
      J=M
21    WRITE(6,22)(N,SP(N,J,I),T(N,J),N=1,L)
22    FORMAT(I5, 5X ,2F20.5,/)
      WRITE(6,62)
62    FORMAT(//////////)
      DO 29 J=1,M
      N=1
29    WRITE(6,23)(J,SP(N,J,I),T(N,J),I=1,4)
23    FORMAT(I5, 5X ,2F20.5,/)
      STOP
      END
      FINISH
$DATA
 100.0      1.42       4.22       0.000      0.015      2.3        0.14
$END
```

6 - Programs No. 6, No. 7 and No. 8

Input data

a - Program No. 6

M - Number of nodes in the cable insulation

V_0 - D.C. working voltage (kV)

X_0 - Radius of the conductor (cm)

X - is the radius of the rings at node points in the insulation (cm)

R - is the dielectric resistance per node (Ω)

D - is the capacitance per node (F/cm)

V_{10}, V_{20}, --- V_{NO} - are the D.C. node voltages before the reverse of the polarity

Subroutine F02AGF used to find the solution of the matrix 'A'

K - is the number of time intervals during the polarity reversal

T - is the time in seconds

DT - is the time interval (second)

b - Program No. 7

This program has the same dimensions as that in program No. 6.

VD - is the impulse voltage (kV)

c - Program No. 8

This program has the same dimensions as that in program No. 6.

Subroutine F01AAF was used to find the inverse of matrix 'H'

7 -

Polyethylene Makers A and B are kindly supported by Pirelli General Work Ltd.

Polyethylene Maker C is kindly supported by the Central Electricity Generating Board.

Program No. 6

```
£FXE/591W/AMOURT/FORT/CST=22000/ST=22000/T=80/L=1000/PR=1//
      LIST(LP)
      PROGRAM(W591)
      INPUT 5=CRD
      OUTPUT 6=LPO
      COMPACT DATA
      COMPRESS INTEGER AND LOGICAL
      TRACE 2
      END
      MASTER CARLES
      DIMENSION A(3,3),R(3,3),Y(3),U(3),RR(3),RI(3),UR(3,3),UI(3,3),INT(
     13),UA(4,4),BU(4,4),VT1(60),VT2(60),VT3(60),T(60),AT(3,3),R(3,3),AH
     1T(3,3),AH(3,3),AA(3,3),SS101(60),SS12(60),SS13(60),SS1(60),SS201(6
     10),SS21(60),SS22(60),SS23(60),SS2(60),SS301(60),SS31(60),SS32(60),
     1SS33(60),SS3(60),VT21(60),VT22(60),VT23(60),SS11(60),AI11(60),AI12
     1(60),AI13(60),AI21(60),AI22(60),AI23(60),AI31(60),AI32(60),AI33(60
     1),VT11(60),VT12(60),VT13(60),S11(60),S12(60),S13(60),S21(60),S22(6
     10),S23(60),S31(60),S32(60),S33(60),S1(60),S2(60),S3(60),VTT1(60),V
     1TT2(60),VTT3(60),VST1(60),VST2(60),VST3(60),HH11(60),HH12(60),HH13
     1(60),HH21(60),HH22(60),HH23(60),HH31(60),HH32(60),HH33(60),BU11(60
     1),BU21(60),BU31(60),Z1(60),Z2(60),Z3(60),Z4(60),VP(60)
      N=3
      V0=100.0
      X0=1.42
      X1=2.12
      X2=2.82
      X3=3.52
      X4=4.22
      R1=2.1E+14
      D1=3.193E-12
      R2=1.9663E+14
      D2=4.485E-12
      R3=1.73E+14
      D3=5.77E-12
      R4=1.5E+14
      D4=7.055E-12
      V10=-75.0
      V20=-50.0
      V30=-25.0
20    DD=((D2*D3)+(D2*D4)+(D3*D4))
      W1=(DD/R1)
      W2=((DD*(R1+R2)/(R1*R2))-(((D2*D3)+(D2*D4))/R2))
      W3=((DD/R2)+(D2*D3/R3)-(D3*(R2+R3)/(R2*R3)))
      W4=((D2*D3*(R3+R4)/(R3*R4))-(((D2*D3)+(D2*D4))/R3))
21    G1=((((D2)**2)*(D3+D4))-(DD*(D1+D2)))
      UA(2,1)=W1/G1
      UA(2,2)=W2/G1
      UA(2,3)=W3/G1
      UA(2,4)=W4/G1
22    UA(3,1)=(((D1+D2)*UA(2,1)/D2)+(1/(R1*D2)))
      UA(3,2)=(((D1+D2)*UA(2,2)/D2)+((R1+R2)/(D2*R1*R2)))
      UA(3,3)=(((D1+D2)*UA(2,3))+(1/R2))/D2
      UA(3,4)=((D1+D2)*UA(2,4))/D2
23    UA(4,1)=(D3*UA(3,1)/(D3+D4))
      UA(4,2)=(D3*UA(3,2)/(D3+D4))
      UA(4,3)=((D3*UA(3,3))-(1/R3))/(D3+D4)
24    UA(4,4)=((D3*UA(3,4))-((R3+R4)/(R3*R4)))/(D3+D4)
      A(1,1)=UA(2,2)
      A(1,2)=-UA(2,3)
      A(1,3)=UA(2,4)
      A(2,1)=+UA(3,2)
      A(2,2)=-UA(3,3)
```

```
      A(2,3)=-UA(3,4)
      A(3,1)=UA(4,2)
      A(3,2)=-UA(4,3)
      A(3,3)=UA(4,4)
      AA(2,1)=-UA(2,1)
      AA(3,1)=-UA(3,1)
      AA(4,1)=-UA(4,1)
      AT(1,1)=-A(1,1)
      AT(1,2)=-A(2,1)
      AT(1,3)=-A(3,1)
      AT(2,1)=-A(1,2)
      AT(2,2)=-A(2,2)
      AT(2,3)=-A(3,2)
      AT(3,1)=-A(1,3)
      AT(3,2)=-A(2,3)
      AT(3,3)=-A(3,3)
      DO 10 I=1,3
      WRITE(6,11)(AT(I,J),J=1,3)
11    FORMAT(1H ,3E20.3,/)
10    CONTINUE
      IFAIL=0
      IV=3
      CALL F02AGF(AT,IV,M,RR,RI,UP,IV,UI,IV,INT,IFAIL)
      WRITE(6,60)
60    FORMAT(//////)
      DO 12 I=1,3
12    WRITE(6,13)RR(I),RI(I)
13    FORMAT(1H ,2E30.5,/)
      WRITE(6,61)
61    FORMAT(/////////)
      DO 14 I=1,3
      WRITE(6,15)(UP(I,J),UI(I,J),J=1,3)
15    FORMAT(1H ,6E20.3,/)
14    CONTINUE
      WRITE(6,63)
63    FORMAT(///////)
      F1=((UR(1,1)/UR(1,3))-(UR(2,1)/UR(2,3)))
      F2=((UR(1,2)/UR(1,3))-(UR(2,2)/UR(2,3)))
      F3=((V10/UR(1,3))-(V20/UR(2,3)))
      F4=((UR(2,1)/UR(2,3))-(UR(3,1)/UR(3,3)))
      F5=((UR(2,2)/UR(2,3))-(UR(3,2)/UR(3,3)))
      F6=((V20/UR(2,3))-(V30/UR(3,3)))
      BA=((F2*F6)-(F3*F5))/((F2*F4)-(F1*F5))
      HB=(F3-(BA*F1))/F2
      BC=(V10-(BA*UR(1,1))-(BB*UR(1,2)))/UR(1,3)
      K=10
      T(1)=12.0
      DO 50 N=2,K
50    T(N)=T(N-1)+12.0
      DO 91 N=(K+1),50
91    T(N)=T(N-1)+0.1
      DT=120.0
      WP=2*VU/DT
      H(1,1)=BA*UR(1,1)
      H(1,2)=BA*UR(1,2)
      H(1,3)=BA*UR(1,3)
      H(2,1)=BB*UR(2,1)
      H(2,2)=BB*UR(2,2)
      H(2,3)=BB*UR(2,3)
      H(3,1)=BC*UR(3,1)
      H(3,2)=BC*UR(3,2)
      H(3,3)=BC*UR(3,3)
      AHT(1,1)=((H(2,2)*H(3,3))-(H(2,3)*H(3,2)))
      AHT(1,2)=-((H(2,1)*H(3,3))-(H(2,3)*H(3,1)))
      AHT(1,3)=((H(2,1)*H(3,2))-(H(2,2)*H(3,1)))
      AHT(2,1)=-((H(1,2)*H(3,3))-(H(1,3)*H(3,2)))
      AHT(2,2)=((H(1,1)*H(3,3))-(H(1,3)*H(3,1)))
```

```
      AHT(2,3)=-((H(1,1)*H(3,2))-(H(1,2)*H(3,1)))
      AHT(3,1)=((H(1,2)*H(2,3))-(H(1,3)*H(2,2)))
      AHT(3,2)=-((H(1,1)*H(2,3))-(H(1,3)*H(2,1)))
      AHT(3,3)=((H(1,1)*H(2,2))-(H(1,2)*H(2,1)))
      AH(1,1)=AHT(1,1)
      AH(1,2)=AHT(2,1)
      AH(1,3)=AHT(3,1)
      AH(2,1)=AHT(1,2)
      AH(2,2)=AHT(2,2)
      AH(2,3)=AHT(3,2)
      AH(3,1)=AHT(1,3)
      AH(3,2)=AHT(2,3)
      AH(3,3)=AHT(3,3)
      PHI=(H(1,1)*((H(2,2)*H(3,3))-(H(2,3)*H(3,2))))-(H(1,2)*((H(2,1)*H(
     13,3))-(H(2,3)*H(3,1))))+(H(1,3)*((H(2,1)*H(3,2))-(H(2,2)*H(3,1))))
      VO1=0.0
      VO2=0.0
      VO3=0.0
      DO 77 N=1,50
      AI11(N)=AH(1,1)/(PHI*EXP(RR(1)*T(N)))
      AI12(N)=AH(1,2)/(PHI*EXP(RR(2)*T(N)))
      AI13(N)=AH(1,3)/(PHI*EXP(RR(3)*T(N)))
      AI21(N)=AH(2,1)/(PHI*EXP(RR(1)*T(N)))
      AI22(N)=AH(2,2)/(PHI*EXP(RR(2)*T(N)))
      AI23(N)=AH(2,3)/(PHI*EXP(RR(3)*T(N)))
      AI31(N)=AH(3,1)/(PHI*EXP(RR(1)*T(N)))
      AI32(N)=AH(3,2)/(PHI*EXP(RR(2)*T(N)))
      AI33(N)=AH(3,3)/(PHI*EXP(RR(3)*T(N)))
101   HH11(N)=(H(1,1)*AI11(N))+H(1,2)*AI21(N)+H(1,3)*AI31(N))
      HH12(N)=(H(1,1)*AI12(N)+H(1,2)*AI22(N)+H(1,3)*AI32(N))
      HH13(N)=(H(1,1)*AI13(N)+H(1,2)*AI23(N)+H(1,3)*AI33(N))
102   HH21(N)=(H(2,1)*AI11(N)+H(2,2)*AI21(N)+H(2,3)*AI31(N))
      HH22(N)=(H(2,1)*AI12(N)+H(2,2)*AI22(N)+H(2,3)*AI32(N))
      HH23(N)=(H(2,1)*AI13(N)+H(2,2)*AI23(N)+H(2,3)*AI33(N))
103   HH31(N)=(H(3,1)*AI11(N)+H(3,2)*AI21(N)+H(3,3)*AI31(N))
      HH32(N)=(H(3,1)*AI12(N)+H(3,2)*AI22(N)+H(3,3)*AI32(N))
      HH33(N)=(H(3,1)*AI13(N)+H(3,2)*AI23(N)+H(3,3)*AI33(N))
      VT11(N)=(VO1*HH11(N)+VO2*HH12(N)+VO3*HH13(N))
      VT12(N)=(VO1*HH21(N)+VO2*HH22(N)+VO3*HH23(N))
      VT13(N)=(VO1*HH31(N)+VO2*HH32(N)+VO3*HH33(N))
77    CONTINUE
      DO 90 N=1,K
      VP(N)=(VM*T(N))-VO
      SS101(N)=((((WM*T(N)-VO)*(EXP(RR(1)*T(N))))/RR(1))+(VO/RR(1)))-((WM
     1/(RR(1))**2)*((EXP(RR(1)*T(N)))-1)))
      SS11(N)=H(1,1)*AA(2,1)*SS101(N)
      SS12(N)=H(1,2)*AA(3,1)*SS101(N)
      SS13(N)=H(1,3)*AA(4,1)*SS101(N)
      SS1(N)=SS11(N)+SS12(N)+SS13(N)
      SS201(N)=((((WM*T(N)-VO)*(EXP(RR(2)*T(N))))/RR(2))+(VO/RR(2)))-((WM
     1/(RR(2))**2)*((EXP(RR(2)*T(N)))-1)))
      SS21(N)=H(2,1)*AA(2,1)*SS201(N)
      SS22(N)=H(2,2)*AA(3,1)*SS201(N)
      SS23(N)=H(2,3)*AA(4,1)*SS201(N)
      SS2(N)=SS21(N)+SS22(N)+SS23(N)
      SS301(N)=((((WM*T(N)-VO)*(EXP(RR(3)*T(N))))/RR(3))+(VO/RR(3)))-((WM
     1/(RR(3))**2)*((EXP(RR(3)*T(N)))-1)))
      SS31(N)=H(3,1)*AA(2,1)*SS301(N)
      SS32(N)=H(3,2)*AA(3,1)*SS301(N)
      SS33(N)=H(3,3)*AA(4,1)*SS301(N)
      SS3(N)=SS31(N)+SS32(N)+SS33(N)
      VT21(N)=(SS1(N)*AI11(N)+SS2(N)*AI12(N)+SS3(N)*AI13(N))
      VT22(N)=(SS1(N)*AI21(N)+SS2(N)*AI22(N)+SS3(N)*AI23(N))
      VT23(N)=(SS1(N)*AI31(N)+SS2(N)*AI32(N)+SS3(N)*AI33(N))
      VT1(N)=VT11(N)+VT21(N)
      VT2(N)=VT12(N)+VT22(N)
```

```
      VT3(N)=VT13(N)+VT23(N)
   90 CONTINUE
      BU11(K)=-UA(2,1)*VU
      BU21(K)=-UA(3,1)*VU
      BU31(K)=-UA(4,1)*VU
      WRITE(6,17)V10,V20,V30,BU11(K),BU21(K),BU31(K)
   17 FORMAT(1H ,6E15.3,/)
      DO 100 N=(K+1),50
      S11(N)=B(1,1)*BU11(K)*(EXP(RR(1)*T(N))-EXP(RR(1)*T(K)))/RR(1)
      S12(N)=B(1,2)*BU21(K)*(EXP(RR(1)*T(N))-EXP(RR(1)*T(K)))/RR(1)
      S13(N)=B(1,3)*BU31(K)*(EXP(RR(1)*T(N))-EXP(RR(1)*T(K)))/RR(1)
      S21(N)=B(2,1)*BU11(K)*(EXP(RR(2)*T(N))-EXP(RR(2)*T(K)))/RR(2)
      S22(N)=B(2,2)*BU21(K)*(EXP(RR(2)*T(N))-EXP(RR(2)*T(K)))/RR(2)
      S23(N)=B(2,3)*BU31(K)*(EXP(RR(2)*T(N))-EXP(RR(2)*T(K)))/RR(2)
      S31(N)=B(3,1)*BU11(K)*(EXP(RR(3)*T(N))-EXP(RR(3)*T(K)))/RR(3)
      S32(N)=B(3,2)*BU21(K)*(EXP(RR(3)*T(N))-EXP(RR(3)*T(K)))/RR(3)
      S33(N)=B(3,3)*BU31(K)*(EXP(RR(3)*T(N))-EXP(RR(3)*T(K)))/RR(3)
      S1(N)=S11(N)+S12(N)+S13(N)
      S2(N)=S21(N)+S22(N)+S23(N)
      S3(N)=S31(N)+S32(N)+S33(N)
      VTT1(N)=AI11(N)*S1(N)+AI12(N)*S2(N)+AI13(N)*S3(N)
      VTT2(N)=AI21(N)*S1(N)+AI22(N)*S2(N)+AI23(N)*S3(N)
      VTT3(N)=AI31(N)*S1(N)+AI32(N)*S2(N)+AI33(N)*S3(N)
      VST1(N)=+(VTT1(N)+VT11(N))
      VST2(N)=+(VTT2(N)+VT12(N))
      VST3(N)=+(VTT3(N)+VT12(N))
  100 CONTINUE
      DO 201 N=1,K
      Z1(N)=(VP(N)-VT1(N))/(X1-X0)
      Z2(N)=(VT1(N)-VT2(N))/(X2-X1)
      Z3(N)=(VT2(N)-VT3(N))/(X3-X2)
      Z4(N)=VT3(N)/(X4-X3)
  201 CONTINUE
      DO 202 N=K+1,50
      Z1(N)=(V0-VST1(N))/(X1-X0)
      Z2(N)=(VST1(N)-VST2(N))/(X2-X1)
      Z3(N)=(VST2(N)-VST3(N))/(X3-X2)
      Z4(N)=VST3(N)/(X4-X3)
  202 CONTINUE
      WRITE(6,62)
   62 FORMAT(/////////)
      WRITE(6,30)DA,DB,DC,
   30 FORMAT(1H ,3E30.5)
      WRITE(6,64)
   64 FORMAT(/////)
   55 WRITE(6,80)(N,T(N),VT1(N),VT2(N),VT3(N),N=1,K)
   80 FORMAT(I5 ,5X, 4E20.3,/)
      WRITE(6,95)(N,T(N),VST1(N),VST2(N),VST3(N),N=(K+1),50)
   95 FORMAT(I5 ,5X, 4E20.3,/)
      WRITE(6,70)
   70 FORMAT(/////)
      DO 66 N=(K+1),50
   66 WRITE(6,81)(N,T(N),VTT1(N),VTT2(N),VTT3(N),N=(K+1),50)
   81 FORMAT(I5 ,5X, 4E20.3,/)
      WRITE(6,133)
  133 FORMAT(////)
      WRITE(6,122)(N,VT11(N),VT12(N),VT13(N),N=1,50)
  122 FORMAT(I5 ,5X, 3E20.3,/)
      WRITE(6,199)
  199 FORMAT(/////)
      WRITE(6,203)(N,T(N),Z1(N),Z2(N),Z3(N),Z4(N),N=1,50)
  203 FORMAT(I5 ,5X, 5E15.5,/)
      STOP
      END
      FINISH
$END
```

Program No. 7

```
£FXE/5910/AMOURI/FORT/CST=22000/ST=22000/T=80/L=1000/PR=2//
      LIST(LP)
      PROGRAM(U591)
      INPUT 5=CRD
      OUTPUT 6=LPD
      COMPACT DATA
      COMPRESS INTEGER AND LOGICAL
      TRACE 2
      END
      MASTER CABLES
      DIMENSION A(3,3),B(3,3),Y(3),U(3),RP(3),RI(3),UP(3,3),UI(3,3),INT(
     13),UA(4,4),DU(4,4),VT1(60),VT2(60),VT3(60),T(60),AT(3,3),U(3,3),AH
     1T(3,3),AH(3,3),AA(3,3),SS101(60),SS12(60),SS13(60),SS1(60),SS201(6
     10),SS21(60),SS22(60),SS23(60),SS2(60),SS301(60),SS31(60),SS32(60),
     1SS33(60),SS3(60),VT21(60),VT22(60),VT23(60),SS11(60),AI11(60),AI12
     1(60),AI13(60),AI21(60),AI22(60),AI23(60),AI31(60),AI32(60),AI33(60
     1),VT11(60),VT12(60),VT13(60),S11(60),S12(60),S13(60),S21(60),S22(6
     10),S23(60),S31(60),S32(60),S33(60),S1(60),S2(60),S3(60),VTT1(60),V
     1TT2(60),VTT3(60),VST1(60),VST2(60),VST3(60),HH11(60),HH12(60),HH13
     1(60),HH21(60),HH22(60),HH23(60),HH31(60),HH32(60),HH33(60),RU11(60
     1),RU21(60),RU31(60),Z1(60),Z2(60),Z3(60),Z4(60),PP(60),VS11(60),VS
     112(60),VS13(60)
      V0=100.0
      V0=+100.0
      M=3
      X0=1.42
      X1=2.12
      X2=2.82
      X3=3.52
      X4=4.22
      R1=2.1E+14
      D1=3.193E-12
      R2=1.9663E+14
      D2=4.465E-12
      R3=1.75E+14
      D3=5.77E-12
      R4=1.5E+14
      D4=7.055E-12
      V10=+75.0
      V20=+50.0
      V30=+25.0
20    D=((D2*D3)+(D2*D4)+(D3*D4))
      W1=(D5/R1)
      W2=((D5*(R1+R2)/(R1*R2))-(((D2*D3)+(D2*D4))/R2))
      W3=((D5/R2)+(D2*D3/R3)-(D5*(R2+R3)/(R2*R3)))
      W4=((D2+D3*(R3+R4)/(D3*R4))-(((D2*D5)+(D2*D4))/R3))
21    G1=((((D2)**2)*(D3+D4))-(D5*(D1+D2)))
      UA(2,1)=W1/G1
      UA(2,2)=W2/G1
      UA(2,3)=W3/G1
      UA(2,4)=W4/G1
22    UA(3,1)=(((D1+D2)*UA(2,1)/D2)+(1/(R1*D2)))
      UA(3,2)=(((D1+D2)*UA(2,2)/D2)+((R1+R2)/(D2*R1+R2)))
      UA(3,3)=(((D1+D2)*UA(2,3))+(1/R2))/D2
      UA(3,4)=((D1+D2)*UA(2,4))/D2
23    UA(4,1)=(D3*UA(3,1)/(D3+D4))
      UA(4,2)=(D3*UA(3,2)/(D3+D4))
      UA(4,3)=(((D3*UA(3,3))-(1/R3))/(D3+D4)
24    UA(4,4)=((D3*UA(3,4))-((R3+R4)/(R3*R4)))/(D3+D4)
      A(1,1)=UA(2,2)
      A(1,2)=-UA(2,3)
      A(1,3)=UA(2,4)
```

```
      A(2,1)=+UA(3,2)
      A(2,2)=-UA(3,3)
      A(2,3)=+UA(3,4)
      A(3,1)=UA(4,2)
      A(3,2)=-UA(4,3)
      A(3,3)=UA(4,4)
      AA(2,1)=-UA(2,1)
      AA(3,1)=-UA(3,1)
      AA(4,1)=-UA(4,1)
      AT(1,1)=A(1,1)
      AT(1,2)=A(2,1)
      AT(1,3)=A(3,1)
      AT(2,1)=A(1,2)
      AT(2,2)=A(2,2)
      AT(2,3)=A(3,2)
      AT(3,1)=A(1,3)
      AT(3,2)=A(2,3)
      AT(3,3)=A(3,3)
      DO 10 I=1,3
      WRITE(6,11)(AT(I,J),J=1,3)
   11 FORMAT(1H ,3E20.3,/)
   10 CONTINUE
      IFAIL=0
      IV=3
      CALL FO2AGF(AT,IV,N,RR,RI,UP,IV,UI,IV,INT,IFAIL)
      WRITE(6,60)
   60 FORMAT(//////)
      DO 12 I=1,3
   12 WRITE(6,13)RR(I),RI(I)
   13 FORMAT(1H ,2E30.5,/)
      WRITE(6,61)
   61 FORMAT(/////////)
      DO 14 I=1,3
      WRITE(6,15)(UP(I,J),UI(I,J),J=1,3)
   15 FORMAT(1H ,6E20.3,/)
   14 CONTINUE
      WRITE(6,62)
   62 FORMAT(////////)
      F1=((UR(1,1)/UR(1,3))-(UR(2,1)/UR(2,3)))
      F2=((UR(1,2)/UR(1,3))-(UR(2,2)/UR(2,3)))
      F3=((V10/UR(1,3))-(V20/UR(2,3)))
      F4=((UR(2,1)/UR(2,3))-(UR(3,1)/UR(3,3)))
      F5=((UR(2,2)/UR(2,3))-(UR(3,2)/UR(3,3)))
      F6=((V20/UR(2,3))-(V30/UR(3,3)))
      BA=((F2*F6)-(F3*F5))/((F2*F4)-(F1*F5))
      BB=(F3-(BA*F1))/F2
      BC=(V10-(BA*UR(1,1))-(BB*UR(1,2)))/UR(1,3)
      K=10
      T(1)=0.5E-3
      DO 50 N=2,K
   50 T(N)=T(N-1)+0.5E-3
      DO 91 N=(K+1),50
   91 T(N)=T(N-1)+0.1
      H(1,1)=BA*UR(1,1)
      H(1,2)=BA*UR(1,2)
      H(1,3)=BA*UR(1,3)
      H(2,1)=BB*UR(2,1)
      H(2,2)=BB*UR(2,2)
      H(2,3)=BB*UR(2,3)
      H(3,1)=BC*UR(3,1)
      H(3,2)=BC*UR(3,2)
      H(3,3)=BC*UR(3,3)
      AHT(1,1)=((H(2,2)*H(3,3))-(H(2,3)*H(3,2)))
      AHT(1,2)=-((H(2,1)*H(3,3))-(H(2,3)*H(3,1)))
      AHT(1,3)=((H(2,1)*H(3,2))-(H(2,2)*H(3,1)))
      AHT(2,1)=-((H(1,2)*H(3,3))-(H(1,3)*H(3,2)))
```

```
      AMT(2,2)=((H(1,1)*H(3,3))-(H(1,3)*H(3,1)))
      AMT(2,3)=-((H(1,1)*H(3,2))-(H(1,2)*H(3,1)))
      AMT(3,1)=((H(1,2)*H(2,3))-(H(1,3)*H(2,2)))
      AMT(3,2)=-((H(1,1)*H(2,3))-(H(1,3)*H(2,1)))
      AMT(3,3)=((H(1,1)*H(2,2))-(H(1,2)*H(2,1)))
      AM(1,1)=AMT(1,1)
      AM(1,2)=AMT(2,1)
      AM(1,3)=AMT(3,1)
      AM(2,1)=AMT(1,2)
      AM(2,2)=AMT(2,2)
      AM(2,3)=AMT(3,2)
      AM(3,1)=AMT(1,3)
      AM(3,2)=AMT(2,3)
      AM(3,3)=AMT(3,3)
      PMT=(H(1,1)*((H(2,2)*H(3,3))-(H(2,3)*H(3,2))))-(H(1,2)*((H(2,1)*H(
     13,3))-(H(2,3)*H(3,1))))+(H(1,3)*((H(2,1)*H(3,2))-(H(2,2)*H(3,1))))
      DO 33 N=1,50
      AT11(N)=AM(1,1)/(PMT*EXP(PR(1)*T(N)))
      AT12(N)=AM(1,2)/(PMT*EXP(PR(2)*T(N)))
      AT13(N)=AM(1,3)/(PMT*EXP(PR(3)*T(N)))
      AT21(N)=AM(2,1)/(PMT*EXP(PR(1)*T(N)))
      AT22(N)=AM(2,2)/(PMT*EXP(PR(2)*T(N)))
      AT23(N)=AM(2,3)/(PMT*EXP(PR(3)*T(N)))
      AT31(N)=AM(3,1)/(PMT*EXP(PR(1)*T(N)))
      AT32(N)=AM(3,2)/(PMT*EXP(PR(2)*T(N)))
      AT33(N)=AM(3,3)/(PMT*EXP(PR(3)*T(N)))
33    CONTINUE
      BM11(K)=-HA(2,1)*VO
      BM21(K)=-HA(3,1)*VO
      BM31(K)=-HA(4,1)*VO
      DO 100 N=1,K
      S11(N)=H(1,1)*BM11(K)*(EXP(PR(1)*T(N)))/RP(1)
      S12(N)=H(1,2)*BM21(K)*(EXP(PR(1)*T(N)))/RR(1)
      S13(N)=H(1,3)*BM31(K)*(EXP(PR(1)*T(N)))/RP(1)
      S21(N)=H(2,1)*BM11(K)*(EXP(PR(2)*T(N)))/RP(2)
      S22(N)=H(2,2)*BM21(K)*(EXP(PR(2)*T(N)))/RP(2)
      S23(N)=H(2,3)*BM31(K)*(EXP(PR(2)*T(N)))/RP(2)
      S31(N)=H(3,1)*BM11(K)*(EXP(PR(3)*T(N)))/RP(3)
      S32(N)=H(3,2)*BM21(K)*(EXP(PR(3)*T(N)))/RP(3)
      S33(N)=H(3,3)*BM31(K)*(EXP(PR(3)*T(N)))/RP(3)
      S1(N)=S11(N)+S12(N)+S13(N)
      S2(N)=S21(N)+S22(N)+S23(N)
      S3(N)=S31(N)+S32(N)+S33(N)
      VT1(N)=AT11(N)*S1(N)+AT12(N)*S2(N)+AT13(N)*S3(N)
      VT2(N)=AT21(N)*S1(N)+AT22(N)*S2(N)+AT23(N)*S3(N)
      VT3(N)=AT31(N)*S1(N)+AT32(N)*S2(N)+AT33(N)*S3(N)
      VS1(N)=V1O+VT1(N)
      VS2(N)=V2O+VT2(N)
      VS3(N)=V3O+VT3(N)
100   CONTINUE
      V1P=VT1(K)
      V2P=VT2(K)
      V3P=VT3(K)
      DO 77 N=(K+1),50
101   HM11(N)=(H(1,1)*AT11(N)+H(1,2)*AT21(N)+H(1,3)*AT31(N))
      HM12(N)=(H(1,1)*AT12(N)+H(1,2)*AT22(N)+H(1,3)*AT32(N))
      HM13(N)=(H(1,1)*AT13(N)+H(1,2)*AT23(N)+H(1,3)*AT33(N))
102   HM21(N)=(H(2,1)*AT11(N)+H(2,2)*AT21(N)+H(2,3)*AT31(N))
      HM22(N)=(H(2,1)*AT12(N)+H(2,2)*AT22(N)+H(2,3)*AT32(N))
      HM23(N)=(H(2,1)*AT13(N)+H(2,2)*AT23(N)+H(2,3)*AT33(N))
103   HM31(N)=(H(3,1)*AT11(N)+H(3,2)*AT21(N)+H(3,3)*AT31(N))
      HM32(N)=(H(3,1)*AT12(N)+H(3,2)*AT22(N)+H(3,3)*AT32(N))
      HM33(N)=(H(3,1)*AT13(N)+H(3,2)*AT23(N)+H(3,3)*AT33(N))
      VT11(N)=(V1P*HM11(N)+V2P*HM12(N)+V3P*HM13(N))
      VT12(N)=(V1P*HM21(N)+V2P*HM22(N)+V3P*HM23(N))
      VT13(N)=(V1P*HM31(N)+V2P*HM32(N)+V3P*HM33(N))
```

```
      VS11(N)=V1+VT11(N)
      VS12(N)=V2+VT12(N)
      VS13(N)=V3+VT13(N)
77    CONTINUE
      DO 201 N=1,K
      VB=V0+VP
      Z1(N)=(VB-VST1(N))/(X1-X0)
      Z2(N)=(VST1(N)-VST2(N))/(X2-X1)
      Z3(N)=(VST2(N)-VST3(N))/(X3-X2)
      Z4(N)=VST3(N)/(X4-X3)
201   CONTINUE
      DO 202 N=K+1,50
      Z1(N)=(VB-VS11(N))/(X1-X0)
      Z2(N)=(VS11(N)-VS12(N))/(X2-X1)
      Z3(N)=(VS12(N)-VS13(N))/(X3-X2)
      Z4(N)=VS13(N)/(X4-X3)
202   CONTINUE
      WRITE(6,62)
62    FORMAT(/////////)
      WRITE(6,30)"A,"B,"C,
30    FORMAT(1H ,3E30.5)
      WRITE(6,64)
64    FORMAT(/////)
      WRITE(6,80)(N,T(N),VTT1(N),VTT2(N),VTT3(N),N=1,K)
80    FORMAT(I5 ,5X, 4E20.5,//)
      WRITE(6,122)(N,T(N),VT11(N),VT12(N),VT13(N),N=(K+1),50)
122   FORMAT(I5 ,5X, 4E20.5,//)
      WRITE(6,133)
133   FORMAT(////)
      WRITE(6,203)(N,T(N),Z1(N),Z2(N),Z3(N),Z4(N),N=1,50)
203   FORMAT(I5 ,5X, 5E15.5,//)
      STOP
      END
      FINISH
      $END
```

Program No. 8

```
£FXE/591R/AMOURI/FORT/CST=55000/ST=55000/T=400/LP=6000/PR=1//
      LIST(LP)
      PROGRAM(A591)
      INPUT 5=CRD
      OUTPUT 6=LPO
      COMPRESS INTEGER AND LOGICAL
      TRACE 2
      END
      MASTER CARLES
       DIMENSION AA(7,7),BU(7),X(7),RR(7),UR(7,7),UI(7,7),INT(7),UA(5,8),
     1AT(7,7),RT(7),H(7,7),WKSPACE(10),AH(7,7),T(40),AI11(40),AI12(40),A
     1I13(40),AI14(40),AI15(40),AI16(40),AI17(40),AI21(40),AI22(40),AI23
     1(40),AI24(40),AI25(40),AI26(40),AI27(40),AI31(40),AI32(40),AI33(40
     1),AI34(40),AI35(40),AI36(40),AI37(40),AI41(40),AI42(40),AI43(40),A
     1I44(40),AI45(40),AI46(40),AI47(40),AI51(40),AI52(40),AI53(40),AI54
     1(40),AI55(40),AI56(40),AI57(40),AI61(40),AI62(40),AI63(40),AI64(40
     1),AI65(40)
       DIMENSION  AI66(40),AI67(40),AI71(40),AI72(40),AI73(40),AI74(40),A
     1I75(40),AI76(40),AI77(40),HH11(40),HH12(40),HH13(40),HH14(40),HH15
     1(40),HH16(40),HH17(40),HH21(40),HH22(40),HH23(40),HH24(40),HH25(40
     1),HH26(40),HH27(40),HH31(40),HH32(40),HH33(40),HH34(40),HH35(40),H
     1H36(40),HH37(40),HH41(40),HH42(40),HH43(40),HH44(40),HH45(40),HH46
     1(40),HH47(40),HH51(40),HH52(40),HH53(40),HH54(40),HH55(40),HH56(40
     1),HH57(40),HH61(40),HH62(40),HH63(40),HH64(40),HH65(40),HH66(40),H
     1H67(40),HH71(40),HH72(40),HH73(40),HH74(40),HH75(40),HH76(40),HH77
     1(40),S11(40),S12(40),S13(40),S14(40),S15(40),S16(40),S17(40),S21(4
     10),S22(40),RU11(40),RU21(40),RU51(40),RU51(40),RU41(40),RU71(40),R
     1U41(40)
       DIMENSION  S23(40),S24(40),S25(40),S26(40),S27(40),S31(40),S32(40)
     1,S33(40),S34(40),S35(40),S36(40),S37(40),S41(40),S42(40),S43(40),S
     144(40),S45(40),S46(40),S47(40),S51(40),S52(40),S53(40),S54(40),S55
     1(40),S56(40),S57(40),S61(40),S62(40),S63(40),S64(40),S65(40),S66(4
     10),S67(40),S71(40),S72(40),S73(40),S74(40),S75(40),S76(40),S77(40)
     1,S1(40),S2(40),S3(40),S4(40),S5(40),S6(40),S7(40),VT1(40),VT2(40),
     1VT3(40),VT4(40),VT5(40),VT6(40),VT7(40),SS101(40),SS201(40),SS301(
     140),SS401(40),SS501(40),SS601(40),SS701(40),SS11(40),SS12(40),SS13
     1(40),SS14(40),SS15(40),SS16(40),SS17(40),SS21(40),SS22(40),SS23(40
     1),SS24(40)
       DIMENSION  SS25(40),SS26(40),SS27(40),SS31(40),SS32(40),SS33(40),S
     1S34(40),SS35(40),SS36(40),SS37(40),SS41(40),SS42(40),SS43(40),SS44
     1(40),SS45(40),SS46(40),SS47(40),SS51(40),SS52(40),SS53(40),SS54(40
     1),SS55(40),SS56(40),SS57(40),SS61(40),SS62(40),SS63(40),SS64(40),S
     1S65(40),SS66(40),SS67(40),SS71(40),SS72(40),SS73(40),SS74(40),SS75
     1(40),SS76(40),SS77(40),SS1(40),SS2(40),SS3(40),SS4(40),SS5(40),SS6
     1(40),SS7(40),VT11(40),VT12(40),VT13(40),VT14(40),VT15(40),VT16(40)
     1,VT17(40),VT21(40),VT22(40),VT23(40),VT24(40),VT25(40),VT26(40),VT
     127(40),VTT1(40),VTT2(40),VTT3(40),VTT4(40),VTT5(40),VTT6(40),VTT7(
     140),VST1(40),VST2(40),VST7(40),VST4(40),VST5(40),VST6(40),VST7(40)
     1,Z1(40),Z2(40),Z3(40),Z4(40),Z5(40),Z6(40),Z7(40),Z8(40),VP(40)
      X0=1,42
      X1=1,77
      X2=2,12
      X3=2,47
      X4=2,82
      X5=3,17
      X6=3,52
      X7=3,87
      X8=4,22
      R1=1,157E+14
      R2=1,06E+14
      R3=9,73E+13
      R4=9,132E+13
      R5=8,565E+13
```

```
R6=7,0E+13
R7=7,54E+13
R8=7,165E+13
D1=5,8E-12
D2=7,09E-12
D3=8,374E-12
D4=9,66E-12
D5=1,094E-11
D6=1,222E-11
D7=1,35E-11
D8=1,48E-11
M=7
V0=100,0
AL1=(D1+D2)
AL2=((D2+D3)-(((D2)**2)/AL1))
AL3=((D3+D4)-(((D3)**2)/AL2))
AL4=((D4+D5)-(((D4)**2)/AL3))
AL5=((D5+D6)-(((D5)**2)/AL4))
AL6=((D6+D7)-(((D6)**2)/AL5))
AL7=((D7+D8)-(((D7)**2)/AL6))
D87=(1/AL7)
D86=(D7/AL6)*D87
D85=(D6/AL5)*D86
D84=(D5/AL4)*D85
D83=(D4/AL3)*D84
D82=(D3/AL2)*D83
D81=(D2/AL1)*D82
UA(8,1)=+(D81/R1)
UA(8,2)=+((D81*((R1+R2)/(R1*R2)))-(D82/R2))
UA(8,3)=+((D83/R3)-(D82*(R2+R3)/(R2*R3)))+(D81/R2))
UA(8,4)=+((D83*((R3+R4)/(R3*R4)))-(D84/R4)-(D82/R3))
UA(8,5)=+((D85/R5)-(D84*(R4+R5)/(R4*R5)))+(D83/R4))
UA(8,6)=+((D85*((R5+R6)/(R5*R6)))-(D86/R6)-(D84/R5))
UA(8,7)=+((D87/R7)-(D86*(R6+R7)/(R6*R7)))+(D85/R6))
UA(8,8)=+((D87*(R7+R8)/(R7*R8))-(D86/R7))
D76=(1/AL6)
D75=(D6/AL5)*D76
D74=(D5/AL4)*D75
D73=(D4/AL3)*D74
D72=(D3/AL2)*D73
D71=(D2/AL1)*D72
UA(7,1)=+((D7*UA(8,1)/AL6)+(D71/R1))
UA(7,2)=+((D7*UA(8,2)/AL6)-(D72/R2)+(D71*(R1+R2)/(R1*R2)))
UA(7,3)=+((D7*UA(8,3)/AL6)+(D73/R3)-(D72*(R2+R3)/(R2*R3)))+(D71/R2)
1)
UA(7,4)=+((D7*UA(8,4)/AL6)-(D74/R4)+(D73*(R3+R4)/(R3*R4))-(D72/R3)
1)
UA(7,5)=+((D7*UA(8,5)/AL6)+(D75/R5)-(D74*(R4+R5)/(R4*R5)))+(D73/R4)
1)
UA(7,6)=+((D7*UA(8,6)/AL6)-(D76/R6)+(D75*(R5+R6)/(R5*R6))-(D74/R5)
1)
UA(7,7)=+((D7*UA(8,7)/AL6)-(D76*(R6+R7)/(R6*R7)))+(D75/R6))
UA(7,8)=+((D7*UA(8,8)/AL6)-(D76/R7))
D65=(1/AL5)
D64=(D5/AL4)*D65
D63=(D4/AL3)*D64
D62=(D3/AL2)*D63
D61=(D2/AL1)*D62
UA(6,1)=+((D6*UA(7,1)/AL5)+(D61/R1))
UA(6,2)=+((D6*UA(7,2)/AL5)-(D62/R2)+(D61*(R1+R2)/(R1*R2)))
UA(6,3)=+((D6*UA(7,3)/AL5)+(D63/R3)-(D62*(R2+R3)/(R2*R3)))+(D61/R2)
1)
UA(6,4)=+((D6*UA(7,4)/AL5)-(D64/R4)+(D63*(R3+R4)/(R3*R4))-(D62/R3)
1)
UA(6,5)=+((D6*UA(7,5)/AL5)+(D65/R5)-(D64*(R4+R5)/(R4*R5)))+(D63/R4)
1)
```

```
      UA(6,6)=+((D6*UA(7,6)/AL5)+(D65*(R5+R6)/(R5*R5))-(D64/R5))
      UA(6,7)=+((D6*UA(7,7)/AL5)+(D65/R6))
      UA(6,8)=+(D6*UA(7,8)/AL5)
      D54=(1/AL4)
      D53=(D4/AL3)*D54
      D52=(D3/AL2)*D53
      D51=(D2/AL1)*D52
      UA(5,1)=+((D5*UA(6,1)/AL4)+(D51/R1))
      UA(5,2)=+((D5*UA(6,2)/AL4)-(D52/R2)+(D51*(R1+R2)/(R1*R2)))
      UA(5,3)=+((D5*UA(6,3)/AL4)+(D53/R3)-(D52*(R2+R3)/(R2*R3))+(D51/R2)
     1)
      UA(5,4)=+((D5*UA(6,4)/AL4)-(D54/R4)+(D53*(R3+R4)/(R3*R4))-(D52/R3)
     1)
      UA(5,5)=+((D5*UA(6,5)/AL4)-(D54*(R4+R5)/(R4*R5))+(D53/R4))
      UA(5,6)=+((D5*UA(6,6)/AL4)-(D54/R5))
      UA(5,7)=+(D5*UA(6,7)/AL4)
      UA(5,8)=+(D5*UA(6,8)/AL4)
      D43=(1/AL3)
      D42=(D3/AL2)*D43
      D41=(D2/AL1)*D42
      UA(4,1)=+((D4*UA(5,1)/AL3)+(D41/R1))
      UA(4,2)=+((D4*UA(5,2)/AL3)-(D42/R2)+(D41*(R1+R2)/(R1*R2)))
      UA(4,3)=+((D4*UA(5,3)/AL3)+(D43/R3)-(D42*(R2+R3)/(R2*R3))+(D41/R2)
     1)
      UA(4,4)=+((D4*UA(5,4)/AL3)+(D43*(R3+R4)/(R3*R4))-(D42/R3))
      UA(4,5)=+((D4*UA(5,5)/AL3)+(D43/R4))
      UA(4,6)=+(D4*UA(5,6)/AL3)
      UA(4,7)=+(D4*UA(5,7)/AL3)
      UA(4,8)=+(D4*UA(5,8)/AL3)
      D32=(1/AL2)
      D31=(D2/AL1)*D32
      UA(3,1)=+((D3*UA(4,1)/AL2)+(D31/R1))
      UA(3,2)=+((D3*UA(4,2)/AL2)-(D32/R2)+(D31*(R1+R2)/(R1*R2)))
      UA(3,3)=+((D3*UA(4,3)/AL2)-(D32*(R2+R3)/(R2*R3))+(D31/R2))
      UA(3,4)=+((D3*UA(4,4)/AL2)-(D32/R3))
      UA(3,5)=+(D3*UA(4,5)/AL2)
      UA(3,6)=+(D3*UA(4,6)/AL2)
      UA(3,7)=+(D3*UA(4,7)/AL2)
      UA(3,8)=+(D3*UA(4,8)/AL2)
      D21=(1/AL1)
      UA(2,1)=+((D2*UA(3,1)/AL1)+(D21/R1))
      UA(2,2)=+((D2*UA(3,2)/AL1)+(D21*(R1+R2)/(R1*R2)))
      UA(2,3)=+((D2*UA(3,3)/AL1)+(D21/R2))
      UA(2,4)=+(D2*UA(3,4)/AL1)
      UA(2,5)=+(D2*UA(3,5)/AL1)
      UA(2,6)=+(D2*UA(3,6)/AL1)
      UA(2,7)=+(D2*UA(3,7)/AL1)
      UA(2,8)=+(D2*UA(3,8)/AL1)
      AA(1,1)=-UA(2,2)
      AA(1,2)=UA(2,3)
      AA(1,3)=-UA(2,4)
      AA(1,4)=UA(2,5)
      AA(1,5)=-UA(2,6)
      AA(1,6)=UA(2,7)
      AA(1,7)=-UA(2,8)
      AA(2,1)=-UA(3,2)
      AA(2,2)=UA(3,3)
      AA(2,3)=-UA(3,4)
      AA(2,4)=UA(3,5)
      AA(2,5)=-UA(3,6)
      AA(2,6)=UA(3,7)
      AA(2,7)=-UA(3,8)
      AA(3,1)=-UA(4,2)
      AA(3,2)=UA(4,3)
      AA(3,3)=-UA(4,4)
```

```
AA(3,4)=UA(4,5)
AA(3,5)=-UA(4,6)
AA(3,6)=UA(4,7)
AA(3,7)=-UA(4,8)
AA(4,1)=-UA(5,2)
AA(4,2)=UA(5,3)
AA(4,3)=-UA(5,4)
AA(4,4)=UA(5,5)
AA(4,5)=-UA(5,6)
AA(4,6)=UA(5,7)
AA(4,7)=-UA(5,8)
AA(5,1)=-UA(6,2)
AA(5,2)=UA(6,3)
AA(5,3)=-UA(6,4)
AA(5,4)=UA(6,5)
AA(5,5)=-UA(6,6)
AA(5,6)=UA(6,7)
AA(5,7)=-UA(6,8)
AA(6,1)=-UA(7,2)
AA(6,2)=UA(7,3)
AA(6,3)=-UA(7,4)
AA(6,4)=UA(7,5)
AA(6,5)=-UA(7,6)
AA(6,6)=UA(7,7)
AA(6,7)=-UA(7,8)
AA(7,1)=-UA(8,2)
AA(7,2)=UA(8,3)
AA(7,3)=-UA(8,4)
AA(7,4)=UA(8,5)
AA(7,5)=-UA(8,6)
AA(7,6)=UA(8,7)
AA(7,7)=-UA(8,8)
AT(1,1)=-AA(1,1)
AT(2,1)=-AA(1,2)
AT(3,1)=-AA(1,3)
AT(4,1)=-AA(1,4)
AT(5,1)=-AA(1,5)
AT(6,1)=-AA(1,6)
AT(7,1)=-AA(1,7)
AT(1,2)=-AA(2,1)
AT(2,2)=-AA(2,2)
AT(3,2)=-AA(2,3)
AT(4,2)=-AA(2,4)
AT(5,2)=-AA(2,5)
AT(6,2)=-AA(2,6)
AT(7,2)=-AA(2,7)
AT(1,3)=-AA(3,1)
AT(2,3)=-AA(3,2)
AT(3,3)=-AA(3,3)
AT(4,3)=-AA(3,4)
AT(5,3)=-AA(3,5)
AT(6,3)=-AA(3,6)
AT(7,3)=-AA(3,7)
AT(1,4)=-AA(4,1)
AT(2,4)=-AA(4,2)
AT(3,4)=-AA(4,3)
AT(4,4)=-AA(4,4)
AT(5,4)=-AA(4,5)
AT(6,4)=-AA(4,6)
AT(7,4)=-AA(4,7)
AT(1,5)=-AA(5,1)
AT(2,5)=-AA(5,2)
AT(3,5)=-AA(5,3)
AT(4,5)=-AA(5,4)
AT(5,5)=-AA(5,5)
AT(6,5)=-AA(5,6)
AT(7,5)=-AA(5,7)
```

```
      AT(1,6)=-AA(6,1)
      AT(2,6)=-AA(6,2)
      AT(3,6)=-AA(6,3)
      AT(4,6)=-AA(6,4)
      AT(5,6)=-AA(6,5)
      AT(6,6)=-AA(6,6)
      AT(7,6)=-AA(6,7)
      AT(1,7)=-AA(7,1)
      AT(2,7)=-AA(7,2)
      AT(3,7)=-AA(7,3)
      AT(4,7)=-AA(7,4)
      AT(5,7)=-AA(7,5)
      AT(6,7)=-AA(7,6)
      AT(7,7)=-AA(7,7)
      DO 10 I=1,7
      WRITE(6,11)(AT(I,J),J=1,7)
11    FORMAT(1H ,7E15.3,/)
10    CONTINUE
      IFAIL=0
      IV=7
      CALL F02AGF(AT,IV,R,RR,RI,UR,IV,UI,IV,INT,IFAIL)
      WRITE(6,60)
60    FORMAT(/////)
      DO 12 I=1,7
12    WRITE(6,13)RR(I),RI(I)
13    FORMAT(1H ,2E30.5,/)
      DO 14 I=1,7
      WRITE(6,15)(UR(I,J),J=1,7)
15    FORMAT(1H ,7E15.3)
14    CONTINUE
      DO 41 I=1,7
      WRITE(6,17)(UI(I,J),J=1,7)
17    FORMAT(1H ,7E15.3)
41    CONTINUE
      V10=87.5
      V20=75.0
      V30=62.5
      V40=50.0
      V50=37.5
      V60=25.0
      V70=12.5
      F1=((UR(7,1)/UR(7,7))-(UR(6,1)/UR(6,7)))
      F2=((UR(7,2)/UR(7,7))-(UR(6,2)/UR(6,7)))
      F3=((UR(7,3)/UR(7,7))-(UR(6,3)/UR(6,7)))
      F4=((UR(7,4)/UR(7,7))-(UR(6,4)/UR(6,7)))
      F5=((UR(7,5)/UR(7,7))-(UR(6,5)/UR(6,7)))
      F6=((UR(7,6)/UR(7,7))-(UR(6,6)/UR(6,7)))
      F7=((V70/UR(7,7))-(V60/UR(6,7)))
      F8=((UR(5,1)/UR(5,7))-(UR(4,1)/UR(4,7)))
      F9=((UR(5,2)/UR(5,7))-(UR(4,2)/UR(4,7)))
      F10=((UR(5,3)/UR(5,7))-(UR(4,3)/UR(4,7)))
      F11=((UR(5,4)/UR(5,7))-(UR(4,4)/UR(4,7)))
      F12=((UR(5,5)/UR(5,7))-(UR(4,5)/UR(4,7)))
      F13=((UR(5,6)/UR(5,7))-(UR(4,6)/UR(4,7)))
      F14=((V50/UR(5,7))-(V40/UR(4,7)))
      F15=((UR(3,1)/UR(3,7))-(UR(2,1)/UR(2,7)))
      F16=((UR(3,2)/UR(3,7))-(UR(2,2)/UR(2,7)))
      F17=((UR(3,3)/UR(3,7))-(UR(2,3)/UR(2,7)))
      F18=((UR(3,4)/UR(3,7))-(UR(2,4)/UR(2,7)))
      F19=((UR(3,5)/UR(3,7))-(UR(2,5)/UR(2,7)))
      F20=((UR(3,6)/UR(3,7))-(UR(2,6)/UR(2,7)))
      F21=((V30/UR(3,7))-(V20/UR(2,7)))
      F22=((UR(2,1)/UR(2,7))-(UR(1,1)/UR(1,7)))
      F23=((UR(2,2)/UR(2,7))-(UR(1,2)/UR(1,7)))
      F24=((UR(2,3)/UR(2,7))-(UR(1,3)/UR(1,7)))
      F25=((UR(2,4)/UR(2,7))-(UR(1,4)/UR(1,7)))
```

```
F26=((UR(2,5)/UR(2,7))-(UR(1,5)/UR(1,7)))
F27=((UR(2,6)/UR(2,7))-(UR(1,6)/UR(1,7)))
F28=((V20/UR(2,7))-(V10/UR(1,7)))
F29=((UR(6,1)/UR(6,7))-(UR(1,1)/UR(1,7)))
F30=((UR(6,2)/UR(6,7))-(UR(1,2)/UR(1,7)))
F31=((UR(6,5)/UR(6,7))-(UR(1,3)/UR(1,7)))
F32=((UR(6,4)/UR(6,7))-(UR(1,4)/UR(1,7)))
F33=((UR(6,5)/UR(6,7))-(UR(1,5)/UR(1,7)))
F34=((UR(6,6)/UR(6,7))-(UR(1,6)/UR(1,7)))
F35=((V60/UR(6,7))-(V10/UR(1,7)))
F36=((UR(4,1)/UR(4,7))-(UR(1,1)/UR(1,7)))
F37=((UR(4,2)/UR(4,7))-(UR(1,2)/UR(1,7)))
F38=((UR(4,3)/UR(4,7))-(UR(1,3)/UR(1,7)))
F39=((UR(4,4)/UR(4,7))-(UR(1,4)/UR(1,7)))
F40=((UR(4,5)/UR(4,7))-(UR(1,5)/UR(1,7)))
F41=((UR(4,6)/UR(4,7))-(UR(1,6)/UR(1,7)))
F42=((V40/UR(4,7))-(V10/UR(1,7)))
G1=((F8/F13)-(F1/F6))
G2=((F9/F13)-(F2/F6))
G3=((F10/F13)-(F3/F6))
G4=((F11/F13)-(F4/F6))
G5=((F12/F13)-(F5/F6))
G6=((F14/F13)-(F7/F6))
G7=((F15/F20)-(F1/F6))
G8=((F16/F20)-(F2/F6))
G9=((F17/F20)-(F3/F6))
G10=((F18/F20)-(F4/F6))
G11=((F19/F20)-(F5/F6))
G12=((F21/F20)-(F7/F6))
G13=((F22/F27)-(F1/F6))
G14=((F23/F27)-(F2/F6))
G15=((F24/F27)-(F3/F6))
G16=((F25/F27)-(F4/F6))
G17=((F26/F27)-(F5/F6))
G18=((F28/F27)-(F7/F6))
G19=((F29/F34)-(F1/F6))
G20=((F30/F34)-(F2/F6))
G21=((F31/F34)-(F3/F6))
G22=((F32/F34)-(F4/F6))
G23=((F33/F34)-(F5/F6))
G24=((F35/F34)-(F7/F6))
G25=((F36/F41)-(F1/F6))
G26=((F37/F41)-(F2/F6))
G27=((F38/F41)-(F3/F6))
G28=((F39/F41)-(F4/F6))
G29=((F40/F41)-(F5/F6))
G30=((F42/F41)-(F7/F6))
G31=((G7/G11)-(G1/G5))
G32=((G8/G11)-(G2/G5))
G33=((G9/G11)-(G3/G5))
G34=((G10/G11)-(G4/G5))
G35=((G12/G11)-(G6/G5))
G36=((G13/G17)-(G1/G5))
G37=((G14/G17)-(G2/G5))
G38=((G15/G17)-(G3/G5))
G39=((G16/G17)-(G4/G5))
G40=((G18/G17)-(G6/G5))
G41=((G19/G23)-(G1/G5))
G42=((G20/G23)-(G2/G5))
G43=((G21/G23)-(G3/G5))
G44=((G22/G23)-(G4/G5))
G45=((G24/G23)-(G6/G5))
G46=((G25/G29)-(G1/G5))
G47=((G26/G29)-(G2/G5))
G48=((G27/G29)-(G3/G5))
G49=((G28/G29)-(G4/G5))
```

```
      G50=((G30/G29)-(G6/G5))
      G51=((G35/G39)-(G31/G34))
      G52=((G37/G39)-(G32/G34))
      G53=((G38/G39)-(G33/G34))
      G54=((G40/G39)-(G35/G34))
      G55=((G41/G44)-(G31/G34))
      G56=((G42/G44)-(G32/G34))
      G57=((G43/G44)-(G33/G34))
      G58=((G45/G44)-(G35/G34))
      G59=((G46/G49)-(G31/G34))
      G60=((G47/G49)-(G32/G34))
      G61=((G48/G49)-(G33/G34))
      G62=((G50/G49)-(G35/G34))
      G63=((G55/G57)-(G51/G53))
      G64=((G56/G57)-(G52/G53))
      G65=((G58/G57)-(G54/G53))
      G66=((G59/G61)-(G51/G53))
      G67=((G60/G61)-(G52/G53))
      G68=((G62/G61)-(G54/G53))
      G69=((G66/G67)-(G63/G64))
      G70=((G68/G67)-(G65/G64))
      B1=G70/G69
      B2=(G65-(G63*B1))/G64
      B3=(G54-(G51*B1)-(G52*B2))/G53
      B4=(G50-((G46*B1)+(G47*B2)+(G48*B3)))/G49
      B5=(G30-((G25*B1)+(G26*B2)+(G27*B3)+(G28*B4)))/G29
      B6=(F42-((F36*B1)+(F37*B2)+(F38*B3)+(F39*B4)+(F40*B5)))/F41
      B7=(V10-((UR(1,1)*B1)+(UR(1,2)*B2)+(UR(1,3)*B3)+(UR(1,4)*B4)+(UR(1
     1,5)*B5)+(UR(1,6)*B6)))/UR(1,7)
      WRITE(6,31)B1,B2,B3,B4,B5,B6,B7
   31 FORMAT(1H ,7E10.3)
      H(1,1)=B1*UR(1,1)
      H(1,2)=B1*UR(1,2)
      H(1,3)=B1*UR(1,3)
      H(1,4)=B1*UR(1,4)
      H(1,5)=B1*UR(1,5)
      H(1,6)=B1*UR(1,6)
      H(1,7)=B1*UR(1,7)
      H(2,1)=B2*UR(2,1)
      H(2,2)=B2*UR(2,2)
      H(2,3)=B2*UR(2,3)
      H(2,4)=B2*UR(2,4)
      H(2,5)=B2*UR(2,5)
      H(2,6)=B2*UR(2,6)
      H(2,7)=B2*UR(2,7)
      H(3,1)=B3*UR(3,1)
      H(3,2)=B3*UR(3,2)
      H(3,3)=B3*UR(3,3)
      H(3,4)=B3*UR(3,4)
      H(3,5)=B3*UR(3,5)
      H(3,6)=B3*UR(3,6)
      H(3,7)=B3*UR(3,7)
      H(4,1)=B4*UR(4,1)
      H(4,2)=B4*UR(4,2)
      H(4,3)=B4*UR(4,3)
      H(4,4)=B4*UR(4,4)
      H(4,5)=B4*UR(4,5)
      H(4,6)=B4*UR(4,6)
      H(4,7)=B4*UR(4,7)
      H(5,1)=B5*UR(5,1)
      H(5,2)=B5*UR(5,2)
      H(5,3)=B5*UR(5,3)
      H(5,4)=B5*UR(5,4)
      H(5,5)=B5*UR(5,5)
      H(5,6)=B5*UR(5,6)
```

```
      H(5,7)=B5*UR(5,7)
      H(6,1)=B6*UR(6,1)
      H(6,2)=B6*UR(6,2)
      H(6,3)=B6*UR(6,3)
      H(6,4)=B6*UR(6,4)
      H(6,5)=B6*UR(6,5)
      H(6,6)=B6*UR(6,6)
      H(6,7)=B6*UR(6,7)
      H(7,1)=B7*UR(7,1)
      H(7,2)=B7*UR(7,2)
      H(7,3)=B7*UR(7,3)
      H(7,4)=B7*UR(7,4)
      H(7,5)=B7*UR(7,5)
      H(7,6)=B7*UR(7,6)
      H(7,7)=B7*UR(7,7)
      READ (5,166)(WKSPACE(I),I=1,7)
  166 FORMAT(1H ,7F7.2)
      WRITE(6,200)(WKSPACE(I),I=1,7)
  200 FORMAT(1H ,7F7.2)
      JFAIL=1
      CALL F01AAF(H,7,M,AH,7,WKSPACE,JFAIL)
      IF(JFAIL.EQ.0)GO TO 210
      WRITE(6,201)
  201 FORMAT(1H0,18H FAILURE IN F01AAF)
      STOP
  210 DO 271 I=1,M
      WRITE(6,212)(AH(I,J),J=1,M)
  212 FORMAT(1H ,7E10.7)
  271 CONTINUE
      K=10
      T(1)=12.0
      DO 61 N=2,K
   61 T(N)=T(N-1)+12.0
      DO 91 N=(K+1),40
   91 T(N)=T(N-1)+100.0
      DO 62 N=1,40
      AI11(N)=AH(1,1)/EXP(RR(1)*T(N))
      AI12(N)=AH(1,2)/EXP(RR(2)*T(N))
      AI13(N)=AH(1,3)/EXP(RR(3)*T(N))
      AI14(N)=AH(1,4)/EXP(RR(4)*T(N))
      AI15(N)=AH(1,5)/EXP(RR(5)*T(N))
      AI16(N)=AH(1,6)/EXP(RR(6)*T(N))
      AI17(N)=AH(1,7)/EXP(RR(7)*T(N))
      AI21(N)=AH(2,1)/EXP(RR(1)*T(N))
      AI22(N)=AH(2,2)/EXP(RR(2)*T(N))
      AI23(N)=AH(2,3)/EXP(RR(3)*T(N))
      AI24(N)=AH(2,4)/EXP(RR(4)*T(N))
      AI25(N)=AH(2,5)/EXP(RR(5)*T(N))
      AI26(N)=AH(2,6)/EXP(RR(6)*T(N))
      AI27(N)=AH(2,7)/EXP(RR(7)*T(N))
      AI31(N)=AH(3,1)/EXP(RR(1)*T(N))
      AI32(N)=AH(3,2)/EXP(RR(2)*T(N))
      AI33(N)=AH(3,3)/EXP(RR(3)*T(N))
      AI34(N)=AH(3,4)/EXP(RR(4)*T(N))
      AI35(N)=AH(3,5)/EXP(RR(5)*T(N))
      AI36(N)=AH(3,6)/EXP(RR(6)*T(N))
      AI37(N)=AH(3,7)/EXP(RR(7)*T(N))
      AI41(N)=AH(4,1)/EXP(RR(1)*T(N))
      AI42(N)=AH(4,2)/EXP(RR(2)*T(N))
      AI43(N)=AH(4,3)/EXP(RR(3)*T(N))
      AI44(N)=AH(4,4)/EXP(RR(4)*T(N))
      AI45(N)=AH(4,5)/EXP(RR(5)*T(N))
      AI46(N)=AH(4,6)/EXP(RR(6)*T(N))
      AI47(N)=AH(4,7)/EXP(RR(7)*T(N))
      AI51(N)=AH(5,1)/EXP(RR(1)*T(N))
      AI52(N)=AH(5,2)/EXP(RR(2)*T(N))
      AI53(N)=AH(5,3)/EXP(RR(3)*T(N))
```

```
      AI54(N)=AH(5,4)/EXP(RR(4)*T(N))
      AI55(N)=AH(5,5)/EXP(RR(5)*T(N))
      AI56(N)=AH(5,6)/EXP(RR(6)*T(N))
      AI57(N)=AH(5,7)/EXP(RR(7)*T(N))
      AI61(N)=AH(6,1)/EXP(RR(1)*T(N))
      AI62(N)=AH(6,2)/EXP(RR(2)*T(N))
      AI63(N)=AH(6,3)/EXP(RR(3)*T(N))
      AI64(N)=AH(6,4)/EXP(RR(4)*T(N))
      AI65(N)=AH(6,5)/EXP(RR(5)*T(N))
      AI66(N)=AH(6,6)/EXP(RR(6)*T(N))
      AI67(N)=AH(6,7)/EXP(RR(7)*T(N))
      AI71(N)=AH(7,1)/EXP(RR(1)*T(N))
      AI72(N)=AH(7,2)/EXP(RR(2)*T(N))
      AI73(N)=AH(7,3)/EXP(RR(3)*T(N))
      AI74(N)=AH(7,4)/EXP(RR(4)*T(N))
      AI75(N)=AH(7,5)/EXP(RR(5)*T(N))
      AI76(N)=AH(7,6)/EXP(RR(6)*T(N))
      AI77(N)=AH(7,7)/EXP(RR(7)*T(N))
62    CONTINUE
      DO 77 N=1,40
101   HH11(N)=(H(1,1)*AI11(N)+H(1,2)*AI21(N)+H(1,3)*AI31(N)+H(1,4)*AI41(
     1N)+H(1,5)*AI51(N)+H(1,6)*AI61(N)+H(1,7)*AI71(N))
      HH12(N)=(H(1,1)*AI12(N)+H(1,2)*AI22(N)+H(1,3)*AI32(N)+H(1,4)*AI42(
     1N)+H(1,5)*AI52(N)+H(1,6)*AI62(N)+H(1,7)*AI72(N))
      HH13(N)=(H(1,1)*AI13(N)+H(1,2)*AI23(N)+H(1,3)*AI33(N)+H(1,4)*AI43(
     1N)+H(1,5)*AI53(N)+H(1,6)*AI63(N)+H(1,7)*AI73(N))
      HH14(N)=(H(1,1)*AI14(N)+H(1,2)*AI24(N)+H(1,3)*AI34(N)+H(1,4)*AI44(
     1N)+H(1,5)*AI54(N)+H(1,6)*AI64(N)+H(1,7)*AI74(N))
      HH15(N)=(H(1,1)*AI15(N)+H(1,2)*AI25(N)+H(1,3)*AI35(N)+H(1,4)*AI45(
     1N)+H(1,5)*AI55(N)+H(1,6)*AI65(N)+H(1,7)*AI75(N))
      HH16(N)=(H(1,1)*AI16(N)+H(1,2)*AI26(N)+H(1,3)*AI36(N)+H(1,4)*AI46(
     1N)+H(1,5)*AI56(N)+H(1,6)*AI66(N)+H(1,7)*AI76(N))
      HH17(N)=(H(1,1)*AI17(N)+H(1,2)*AI27(N)+H(1,3)*AI37(N)+H(1,4)*AI47(
     1N)+H(1,5)*AI57(N)+H(1,6)*AI67(N)+H(1,7)*AI77(N))
102   HH21(N)=(H(2,1)*AI11(N)+H(2,2)*AI21(N)+H(2,3)*AI31(N)+H(2,4)*AI41(
     1N)+H(2,5)*AI51(N)+H(2,6)*AI61(N)+H(2,7)*AI71(N))
      HH22(N)=(H(2,1)*AI12(N)+H(2,2)*AI22(N)+H(2,3)*AI32(N)+H(2,4)*AI42(
     1N)+H(2,5)*AI52(N)+H(2,6)*AI62(N)+H(2,7)*AI72(N))
      HH23(N)=(H(2,1)*AI13(N)+H(2,2)*AI23(N)+H(2,3)*AI33(N)+H(2,4)*AI43(
     1N)+H(2,5)*AI53(N)+H(2,6)*AI63(N)+H(2,7)*AI73(N))
      HH24(N)=(H(2,1)*AI14(N)+H(2,2)*AI24(N)+H(2,3)*AI34(N)+H(2,4)*AI44(
     1N)+H(2,5)*AI54(N)+H(2,6)*AI64(N)+H(2,7)*AI74(N))
      HH25(N)=(H(2,1)*AI15(N)+H(2,2)*AI25(N)+H(2,3)*AI35(N)+H(2,4)*AI45(
     1N)+H(2,5)*AI55(N)+H(2,6)*AI65(N)+H(2,7)*AI75(N))
      HH26(N)=(H(2,1)*AI16(N)+H(2,2)*AI26(N)+H(2,3)*AI36(N)+H(2,4)*AI46(
     1N)+H(2,5)*AI56(N)+H(2,6)*AI66(N)+H(2,7)*AI76(N))
      HH27(N)=(H(2,1)*AI17(N)+H(2,2)*AI27(N)+H(2,3)*AI37(N)+H(2,4)*AI47(
     1N)+H(2,5)*AI57(N)+H(2,6)*AI67(N)+H(2,7)*AI77(N))
103   HH31(N)=(H(3,1)*AI11(N)+H(3,2)*AI21(N)+H(3,3)*AI31(N)+H(3,4)*AI41(
     1N)+H(3,5)*AI51(N)+H(3,6)*AI61(N)+H(3,7)*AI71(N))
      HH32(N)=(H(3,1)*AI12(N)+H(3,2)*AI22(N)+H(3,3)*AI32(N)+H(3,4)*AI42(
     1N)+H(3,5)*AI52(N)+H(3,6)*AI62(N)+H(3,7)*AI72(N))
      HH33(N)=(H(3,1)*AI13(N)+H(3,2)*AI23(N)+H(3,3)*AI33(N)+H(3,4)*AI43(
     1N)+H(3,5)*AI53(N)+H(3,6)*AI63(N)+H(3,7)*AI73(N))
      HH34(N)=(H(3,1)*AI14(N)+H(3,2)*AI24(N)+H(3,3)*AI34(N)+H(3,4)*AI44(
     1N)+H(3,5)*AI54(N)+H(3,6)*AI64(N)+H(3,7)*AI74(N))
      HH35(N)=(H(3,1)*AI15(N)+H(3,2)*AI25(N)+H(3,3)*AI35(N)+H(3,4)*AI45(
     1N)+H(3,5)*AI55(N)+H(3,6)*AI65(N)+H(3,7)*AI75(N))
      HH36(N)=(H(3,1)*AI16(N)+H(3,2)*AI26(N)+H(3,3)*AI36(N)+H(3,4)*AI46(
     1N)+H(3,5)*AI56(N)+H(3,6)*AI66(N)+H(3,7)*AI76(N))
      HH37(N)=(H(3,1)*AI17(N)+H(3,2)*AI27(N)+H(3,3)*AI37(N)+H(3,4)*AI47(
     1N)+H(3,5)*AI57(N)+H(3,6)*AI67(N)+H(3,7)*AI77(N))
104   HH41(N)=(H(4,1)*AI11(N)+H(4,2)*AI21(N)+H(4,3)*AI31(N)+H(4,4)*AI41(
     1N)+H(4,5)*AI51(N)+H(4,6)*AI61(N)+H(4,7)*AI71(N))
      HH42(N)=(H(4,1)*AI12(N)+H(4,2)*AI22(N)+H(4,3)*AI32(N)+H(4,4)*AI42(
     1N)+H(4,5)*AI52(N)+H(4,6)*AI62(N)+H(4,7)*AI72(N))
```

```
      HH43(N)=(H(4,1)*AI13(N)+H(4,2)*AI23(N)+H(4,3)*AI33(N)+H(4,4)*AI43(
     1N)+H(4,5)*AI53(N)+H(4,6)*AI63(N)+H(4,7)*AI73(N))
      HH44(N)=(H(4,1)*AI14(N)+H(4,2)*AI24(N)+H(4,3)*AI34(N)+H(4,4)*AI44(
     1N)+H(4,5)*AI54(N)+H(4,6)*AI64(N)+H(4,7)*AI74(N))
      HH45(N)=(H(4,1)*AI15(N)+H(4,2)*AI25(N)+H(4,3)*AI35(N)+H(4,4)*AI45(
     1N)+H(4,5)*AI55(N)+H(4,6)*AI65(N)+H(4,7)*AI75(N))
      HH46(N)=(H(4,1)*AI16(N)+H(4,2)*AI26(N)+H(4,3)*AI36(N)+H(4,4)*AI46(
     1N)+H(4,5)*AI56(N)+H(4,6)*AI66(N)+H(4,7)*AI76(N))
      HH47(N)=(H(4,1)*AI17(N)+H(4,2)*AI27(N)+H(4,3)*AI37(N)+H(4,4)*AI47(
     1N)+H(4,5)*AI57(N)+H(4,6)*AI67(N)+H(4,7)*AI77(N))
105   HH51(N)=(H(5,1)*AI11(N)+H(5,2)*AI21(N)+H(5,3)*AI31(N)+H(5,4)*AI41(
     1N)+H(5,5)*AI51(N)+H(5,6)*AI61(N)+H(5,7)*AI71(N))
      HH52(N)=(H(5,1)*AI12(N)+H(5,2)*AI22(N)+H(5,3)*AI32(N)+H(5,4)*AI42(
     1N)+H(5,5)*AI52(N)+H(5,6)*AI62(N)+H(5,7)*AI72(N))
      HH53(N)=(H(5,1)*AI13(N)+H(5,2)*AI23(N)+H(5,3)*AI33(N)+H(5,4)*AI43(
     1N)+H(5,5)*AI53(N)+H(5,6)*AI63(N)+H(5,7)*AI73(N))
      HH54(N)=(H(5,1)*AI14(N)+H(5,2)*AI24(N)+H(5,3)*AI34(N)+H(5,4)*AI44(
     1N)+H(5,5)*AI54(N)+H(5,6)*AI64(N)+H(5,7)*AI74(N))
      HH55(N)=(H(5,1)*AI15(N)+H(5,2)*AI25(N)+H(5,3)*AI35(N)+H(5,4)*AI45(
     1N)+H(5,5)*AI55(N)+H(5,6)*AI65(N)+H(5,7)*AI75(N))
      HH56(N)=(H(5,1)*AI16(N)+H(5,2)*AI26(N)+H(5,3)*AI36(N)+H(5,4)*AI46(
     1N)+H(5,5)*AI56(N)+H(5,6)*AI66(N)+H(5,7)*AI76(N))
      HH57(N)=(H(5,1)*AI17(N)+H(5,2)*AI27(N)+H(5,3)*AI37(N)+H(5,4)*AI47(
     1N)+H(5,5)*AI57(N)+H(5,6)*AI67(N)+H(5,7)*AI77(N))
106   HH61(N)=(H(6,1)*AI11(N)+H(6,2)*AI21(N)+H(6,3)*AI31(N)+H(6,4)*AI41(
     1N)+H(6,5)*AI51(N)+H(6,6)*AI61(N)+H(6,7)*AI71(N))
      HH62(N)=(H(6,1)*AI12(N)+H(6,2)*AI22(N)+H(6,3)*AI32(N)+H(6,4)*AI42(
     1N)+H(6,5)*AI52(N)+H(6,6)*AI62(N)+H(6,7)*AI72(N))
      HH63(N)=(H(6,1)*AI13(N)+H(6,2)*AI23(N)+H(6,3)*AI33(N)+H(6,4)*AI43(
     1N)+H(6,5)*AI53(N)+H(6,6)*AI63(N)+H(6,7)*AI73(N))
      HH64(N)=(H(6,1)*AI14(N)+H(6,2)*AI24(N)+H(6,3)*AI34(N)+H(6,4)*AI44(
     1N)+H(6,5)*AI54(N)+H(6,6)*AI64(N)+H(6,7)*AI74(N))
      HH65(N)=(H(6,1)*AI15(N)+H(6,2)*AI25(N)+H(6,3)*AI35(N)+H(6,4)*AI45(
     1N)+H(6,5)*AI55(N)+H(6,6)*AI65(N)+H(6,7)*AI75(N))
      HH66(N)=(H(6,1)*AI16(N)+H(6,2)*AI26(N)+H(6,3)*AI36(N)+H(6,4)*AI46(
     1N)+H(6,5)*AI56(N)+H(6,6)*AI66(N)+H(6,7)*AI76(N))
      HH67(N)=(H(6,1)*AI17(N)+H(6,2)*AI27(N)+H(6,3)*AI37(N)+H(6,4)*AI47(
     1N)+H(6,5)*AI57(N)+H(6,6)*AI67(N)+H(6,7)*AI77(N))
107   HH71(N)=(H(7,1)*AI11(N)+H(7,2)*AI21(N)+H(7,3)*AI31(N)+H(7,4)*AI41(
     1N)+H(7,5)*AI51(N)+H(7,6)*AI61(N)+H(7,7)*AI71(N))
      HH72(N)=(H(7,1)*AI12(N)+H(7,2)*AI22(N)+H(7,3)*AI32(N)+H(7,4)*AI42(
     1N)+H(7,5)*AI52(N)+H(7,6)*AI62(N)+H(7,7)*AI72(N))
      HH73(N)=(H(7,1)*AI13(N)+H(7,2)*AI23(N)+H(7,3)*AI33(N)+H(7,4)*AI43(
     1N)+H(7,5)*AI53(N)+H(7,6)*AI63(N)+H(7,7)*AI73(N))
      HH74(N)=(H(7,1)*AI14(N)+H(7,2)*AI24(N)+H(7,3)*AI34(N)+H(7,4)*AI44(
     1N)+H(7,5)*AI54(N)+H(7,6)*AI64(N)+H(7,7)*AI74(N))
      HH75(N)=(H(7,1)*AI15(N)+H(7,2)*AI25(N)+H(7,3)*AI35(N)+H(7,4)*AI45(
     1N)+H(7,5)*AI55(N)+H(7,6)*AI65(N)+H(7,7)*AI75(N))
      HH76(N)=(H(7,1)*AI16(N)+H(7,2)*AI26(N)+H(7,3)*AI36(N)+H(7,4)*AI46(
     1N)+H(7,5)*AI56(N)+H(7,6)*AI66(N)+H(7,7)*AI76(N))
      HH77(N)=(H(7,1)*AI17(N)+H(7,2)*AI27(N)+H(7,3)*AI37(N)+H(7,4)*AI47(
     1N)+H(7,5)*AI57(N)+H(7,6)*AI67(N)+H(7,7)*AI77(N))
      VT11(N)=(V10*HH11(N)+V20*HH12(N)+V30*HH13(N)+V40*HH14(N)+V50*HH15(
     1N)+V60*HH16(N)+V70*HH17(N))
      VT12(N)=(V10*HH21(N)+V20*HH22(N)+V30*HH23(N)+V40*HH24(N)+V50*HH25(
     1N)+V60*HH26(N)+V70*HH27(N))
      VT13(N)=(V10*HH31(N)+V20*HH32(N)+V30*HH33(N)+V40*HH34(N)+V50*HH35(
     1N)+V60*HH36(N)+V70*HH37(N))
      VT14(N)=(V10*HH41(N)+V20*HH42(N)+V30*HH43(N)+V40*HH44(N)+V50*HH45(
     1N)+V60*HH46(N)+V70*HH47(N))
      VT15(N)=(V10*HH51(N)+V20*HH52(N)+V30*HH53(N)+V40*HH54(N)+V50*HH55(
     1N)+V60*HH56(N)+V70*HH57(N))
      VT16(N)=(V10*HH61(N)+V20*HH62(N)+V30*HH63(N)+V40*HH64(N)+V50*HH65(
     1N)+V60*HH66(N)+V70*HH67(N))
      VT17(N)=(V10*HH71(N)+V20*HH72(N)+V30*HH73(N)+V40*HH74(N)+V50*HH75(
     1N)+V60*HH76(N)+V70*HH77(N))
```

```
77    CONTINUE
      DO 90 N=1,K
      VP(N)=(WM*T(N))-VO
      SS101(N)=((((WM*T(N))-VO)*(EXP(RR(1)*T(N))))/RR(1))+(VO/RR(1)))-((WM
     1/(RR(1))**2)*((EXP(RR(1)*T(N)))-1)))
      SS11(N)=H(1,1)*UA(1,1)*SS101(N)
      SS12(N)=H(1,2)*UA(2,1)*SS101(N)
      SS13(N)=H(1,3)*UA(3,1)*SS101(N)
      SS14(N)=H(1,4)*UA(4,1)*SS101(N)
      SS15(N)=H(1,5)*UA(5,1)*SS101(N)
      SS16(N)=H(1,6)*UA(6,1)*SS101(N)
      SS17(N)=H(1,7)*UA(7,1)*SS101(N)
      SS1(N)=SS11(N)+SS12(N)+SS13(N)+SS14(N)+SS15(N)+SS16(N)+SS17(N)
      SS201(N)=((((WM*T(N))-VO)*(EXP(RR(2)*T(N))))/RR(2))+(VO/RR(2)))-((WM
     1/(RR(2))**2)*((EXP(RR(2)*T(N)))-1)))
      SS21(N)=H(2,1)*UA(1,1)*SS201(N)
      SS22(N)=H(2,2)*UA(2,1)*SS201(N)
      SS23(N)=H(2,3)*UA(3,1)*SS201(N)
      SS24(N)=H(2,4)*UA(4,1)*SS201(N)
      SS25(N)=H(2,5)*UA(5,1)*SS201(N)
      SS26(N)=H(2,6)*UA(6,1)*SS201(N)
      SS27(N)=H(2,7)*UA(7,1)*SS201(N)
      SS2(N)=SS21(N)+SS22(N)+SS23(N)+SS24(N)+SS25(N)+SS26(N)+SS27(N)
      SS301(N)=((((WM*T(N))-VO)*(EXP(RR(3)*T(N))))/RR(3))+(VO/RR(3)))-((WM
     1/(RR(3))**2)*((EXP(RR(3)*T(N)))-1)))
      SS31(N)=H(3,1)*UA(1,1)*SS301(N)
      SS32(N)=H(3,2)*UA(2,1)*SS301(N)
      SS33(N)=H(3,3)*UA(3,1)*SS301(N)
      SS34(N)=H(3,4)*UA(4,1)*SS301(N)
      SS35(N)=H(3,5)*UA(5,1)*SS301(N)
      SS36(N)=H(3,6)*UA(6,1)*SS301(N)
      SS37(N)=H(3,7)*UA(7,1)*SS301(N)
      SS3(N)=SS31(N)+SS32(N)+SS33(N)+SS34(N)+SS35(N)+SS36(N)+SS37(N)
      SS401(N)=((((WM*T(N))-VO)*(EXP(RR(4)*T(N))))/RR(4))+(VO/RR(4)))-((WM
     1/(RR(4))**2)*((EXP(RR(4)*T(N)))-1)))
      SS41(N)=H(4,1)*UA(1,1)*SS401(N)
      SS42(N)=H(4,2)*UA(2,1)*SS401(N)
      SS43(N)=H(4,3)*UA(3,1)*SS401(N)
      SS44(N)=H(4,4)*UA(4,1)*SS401(N)
      SS45(N)=H(4,5)*UA(5,1)*SS401(N)
      SS46(N)=H(4,6)*UA(6,1)*SS401(N)
      SS47(N)=H(4,7)*UA(7,1)*SS401(N)
      SS4(N)=SS41(N)+SS42(N)+SS43(N)+SS44(N)+SS45(N)+SS46(N)+SS47(N)
      SS501(N)=((((WM*T(N))-VO)*(EXP(RR(5)*T(N))))/RR(5))+(VO/RR(5)))-((WM
     1/(RR(5))**2)*((EXP(RR(5)*T(N)))-1)))
      SS51(N)=H(5,1)*UA(1,1)*SS501(N)
      SS52(N)=H(5,2)*UA(2,1)*SS501(N)
      SS53(N)=H(5,3)*UA(3,1)*SS501(N)
      SS54(N)=H(5,4)*UA(4,1)*SS501(N)
      SS55(N)=H(5,5)*UA(5,1)*SS501(N)
      SS56(N)=H(5,6)*UA(6,1)*SS501(N)
      SS57(N)=H(5,7)*UA(7,1)*SS501(N)
      SS5(N)=SS51(N)+SS52(N)+SS53(N)+SS54(N)+SS55(N)+SS56(N)+SS57(N)
      SS601(N)=((((WM*T(N))-VO)*(EXP(RR(6)*T(N))))/RR(6))+(VO/RR(6)))-((WM
     1/(RR(6))**2)*((EXP(RR(6)*T(N)))-1)))
      SS61(N)=H(6,1)*UA(1,1)*SS601(N)
      SS62(N)=H(6,2)*UA(2,1)*SS601(N)
      SS63(N)=H(6,3)*UA(3,1)*SS601(N)
      SS64(N)=H(6,4)*UA(4,1)*SS601(N)
      SS65(N)=H(6,5)*UA(5,1)*SS601(N)
      SS66(N)=H(6,6)*UA(6,1)*SS601(N)
      SS67(N)=H(6,7)*UA(7,1)*SS601(N)
      SS6(N)=SS61(N)+SS62(N)+SS63(N)+SS64(N)+SS65(N)+SS66(N)+SS67(N)
      SS701(N)=((((WM*T(N))-VO)*(EXP(RR(7)*T(N))))/RR(7))+(VO/RR(7)))-((WM
     1/(RR(7))**2)*((EXP(RR(7)*T(N)))-1)))
```

```
      SS71(N)=R(7,1)*UA(1,1)*SS701(N)
      SS72(N)=R(7,2)*UA(2,1)*SS701(N)
      SS73(N)=R(7,3)*UA(3,1)*SS701(N)
      SS74(N)=R(7,4)*UA(4,1)*SS701(N)
      SS75(N)=R(7,5)*UA(5,1)*SS701(N)
      SS76(N)=R(7,6)*UA(6,1)*SS701(N)
      SS77(N)=R(7,7)*UA(7,1)*SS701(N)
      SS7(N)=SS71(N)+SS72(N)+SS73(N)+SS74(N)+SS75(N)+SS76(N)+SS77(N)
      VT21(N)=(SS1(N)*AI11(N)+SS2(N)*AI12(N)+SS3(N)*AI13(N)+SS4(N)*AI14(
     1N)+SS5(N)*AI15(N)+SS6(N)*AI16(N)+SS7(N)*AI17(N))
      VT22(N)=(SS1(N)*AI21(N)+SS2(N)*AI22(N)+SS3(N)*AI23(N)+SS4(N)*AI24(
     1N)+SS5(N)*AI25(N)+SS6(N)*AI26(N)+SS7(N)*AI27(N))
      VT23(N)=(SS1(N)*AI31(N)+SS2(N)*AI32(N)+SS3(N)*AI33(N)+SS4(N)*AI34(
     1N)+SS5(N)*AI35(N)+SS6(N)*AI36(N)+SS7(N)*AI37(N))
      VT24(N)=(SS1(N)*AI41(N)+SS2(N)*AI42(N)+SS3(N)*AI43(N)+SS4(N)*AI44(
     1N)+SS5(N)*AI45(N)+SS6(N)*AI46(N)+SS7(N)*AI47(N))
      VT25(N)=(SS1(N)*AI51(N)+SS2(N)*AI52(N)+SS3(N)*AI53(N)+SS4(N)*AI54(
     1N)+SS5(N)*AI55(N)+SS6(N)*AI56(N)+SS7(N)*AI57(N))
      VT26(N)=(SS1(N)*AI61(N)+SS2(N)*AI62(N)+SS3(N)*AI63(N)+SS4(N)*AI64(
     1N)+SS5(N)*AI65(N)+SS6(N)*AI66(N)+SS7(N)*AI67(N))
      VT27(N)=(SS1(N)*AI71(N)+SS2(N)*AI72(N)+SS3(N)*AI73(N)+SS4(N)*AI74(
     1N)+SS5(N)*AI75(N)+SS6(N)*AI76(N)+SS7(N)*AI77(N))
      VT1(N)=VT11(N)+VT21(N)
      VT2(N)=VT12(N)+VT22(N)
      VT3(N)=VT13(N)+VT23(N)
      VT4(N)=VT14(N)+VT24(N)
      VT5(N)=VT15(N)+VT25(N)
      VT6(N)=VT16(N)+VT26(N)
      VT7(N)=VT17(N)+VT27(N)
90    CONTINUE
      BU11(K)=+UA(2,1)*VO
      BU21(K)=+UA(3,1)*VO
      BU31(K)=+UA(4,1)*VO
      BU41(K)=+UA(5,1)*VO
      BU51(K)=+UA(6,1)*VO
      BU61(K)=+UA(7,1)*VO
      BU71(K)=+UA(8,1)*VO
      DO 100 K=K+1,40
      S11(N)=R(1,1)*BU11(K)*(EXP(RR(1)*T(N))-EXP(RR(1)*T(K)))/RR(1)
      S12(N)=R(1,2)*BU21(K)*(EXP(RR(1)*T(N))-EXP(RR(1)*T(K)))/RR(1)
      S13(N)=R(1,3)*BU31(K)*(EXP(RR(1)*T(N))-EXP(RR(1)*T(K)))/RR(1)
      S14(N)=R(1,4)*BU41(K)*(EXP(RR(1)*T(N))-EXP(RR(1)*T(K)))/RR(1)
      S15(N)=R(1,5)*BU51(K)*(EXP(RR(1)*T(N))-EXP(RR(1)*T(K)))/RR(1)
      S16(N)=R(1,6)*BU61(K)*(EXP(RR(1)*T(N))-EXP(RR(1)*T(K)))/RR(1)
      S17(N)=R(1,7)*BU71(K)*(EXP(RR(1)*T(N))-EXP(RR(1)*T(K)))/RR(1)
      S21(N)=R(2,1)*BU11(K)*(EXP(RR(2)*T(N))-EXP(RR(2)*T(K)))/RR(2)
      S22(N)=R(2,2)*BU21(K)*(EXP(RR(2)*T(N))-EXP(RR(2)*T(K)))/RR(2)
      S23(N)=R(2,3)*BU31(K)*(EXP(RR(2)*T(N))-EXP(RR(2)*T(K)))/RR(2)
      S24(N)=R(2,4)*BU41(K)*(EXP(RR(2)*T(N))-EXP(RR(2)*T(K)))/RR(2)
      S25(N)=R(2,5)*BU51(K)*(EXP(RR(2)*T(N))-EXP(RR(2)*T(K)))/RR(2)
      S26(N)=R(2,6)*BU61(K)*(EXP(RR(2)*T(N))-EXP(RR(2)*T(K)))/RR(2)
      S27(N)=R(2,7)*BU71(K)*(EXP(RR(2)*T(N))-EXP(RR(2)*T(K)))/RR(2)
      S31(N)=R(3,1)*BU11(K)*(EXP(RR(3)*T(N))-EXP(RR(3)*T(K)))/RR(3)
      S32(N)=R(3,2)*BU21(K)*(EXP(RR(3)*T(N))-EXP(RR(3)*T(K)))/RR(3)
      S33(N)=R(3,3)*BU31(K)*(EXP(RR(3)*T(N))-EXP(RR(3)*T(K)))/RR(3)
      S34(N)=R(3,4)*BU41(K)*(EXP(RR(3)*T(N))-EXP(RR(3)*T(K)))/RR(3)
      S35(N)=R(3,5)*BU51(K)*(EXP(RR(3)*T(N))-EXP(RR(3)*T(K)))/RR(3)
      S36(N)=R(3,6)*BU61(K)*(EXP(RR(3)*T(N))-EXP(RR(3)*T(K)))/RR(3)
      S37(N)=R(3,7)*BU71(K)*(EXP(RR(3)*T(N))-EXP(RR(3)*T(K)))/RR(3)
      S41(N)=R(4,1)*BU11(K)*(EXP(RR(4)*T(N))-EXP(RR(4)*T(K)))/RR(4)
      S42(N)=R(4,2)*BU21(K)*(EXP(RR(4)*T(N))-EXP(RR(4)*T(K)))/RR(4)
      S43(N)=R(4,3)*BU31(K)*(EXP(RR(4)*T(N))-EXP(RR(4)*T(K)))/RR(4)
      S44(N)=R(4,4)*BU41(K)*(EXP(RR(4)*T(N))-EXP(RR(4)*T(K)))/RR(4)
      S45(N)=R(4,5)*BU51(K)*(EXP(RR(4)*T(N))-EXP(RR(4)*T(K)))/RR(4)
      S46(N)=R(4,6)*BU61(K)*(EXP(RR(4)*T(N))-EXP(RR(4)*T(K)))/RR(4)
      S47(N)=R(4,7)*BU71(K)*(EXP(RR(4)*T(N))-EXP(RR(4)*T(K)))/RR(4)
      S51(N)=R(5,1)*BU11(K)*(EXP(RR(5)*T(N))-EXP(RR(5)*T(K)))/RR(5)
```

```
      S55(N)=B(5,5)*BU51(K)*(EXP(BR(5)*T(N))-EXP(BR(5)*T(K)))/BR(5)
      S56(N)=B(5,6)*BU61(K)*(EXP(BR(5)*T(N))-EXP(BR(5)*T(K)))/BR(5)
      S57(N)=B(5,7)*BU71(K)*(EXP(BR(5)*T(N))-EXP(BR(5)*T(K)))/BR(5)
      S61(N)=B(6,1)*BU11(K)*(EXP(BR(6)*T(N))-EXP(BR(6)*T(K)))/BR(6)
      S62(N)=B(6,2)*BU21(K)*(EXP(BR(6)*T(N))-EXP(BR(6)*T(K)))/BR(6)
      S63(N)=B(6,3)*BU31(K)*(EXP(BR(6)*T(N))-EXP(BR(6)*T(K)))/BR(6)
      S64(N)=B(6,4)*BU41(K)*(EXP(BR(6)*T(N))-EXP(BR(6)*T(K)))/BR(6)
      S65(N)=B(6,5)*BU51(K)*(EXP(BR(6)*T(N))-EXP(BR(6)*T(K)))/BR(6)
      S66(N)=B(6,6)*BU61(K)*(EXP(BR(6)*T(N))-EXP(BR(6)*T(K)))/BR(6)
      S67(N)=B(6,7)*BU71(K)*(EXP(BR(6)*T(N))-EXP(BR(6)*T(K)))/BR(6)
      S1(N)=S11(N)+S12(N)+S13(N)+S14(N)+S15(N)+S16(N)+S17(N)
      S2(N)=S21(N)+S22(N)+S23(N)+S24(N)+S25(N)+S26(N)+S27(N)
      S3(N)=S31(N)+S32(N)+S33(N)+S34(N)+S35(N)+S36(N)+S37(N)
      S4(N)=S41(N)+S42(N)+S43(N)+S44(N)+S45(N)+S46(N)+S47(N)
      S5(N)=S51(N)+S52(N)+S53(N)+S54(N)+S55(N)+S56(N)+S57(N)
      S6(N)=S61(N)+S62(N)+S63(N)+S64(N)+S65(N)+S66(N)+S67(N)
      S7(N)=S71(N)+S72(N)+S73(N)+S74(N)+S75(N)+S76(N)+S77(N)
      VTT1(N)=AI11(N)*S1(N)+AI12(N)*S2(N)+AI13(N)*S3(N)+AI14(N)*S4(N)+AI
     115(N)*S5(N)+AI16(N)*S6(N)+AI17(N)*S7(N)
      VTT2(N)=AI21(N)*S1(N)+AI22(N)*S2(N)+AI23(N)*S3(N)+AI24(N)*S4(N)+AI
     125(N)*S5(N)+AI26(N)*S6(N)+AI27(N)*S7(N)
      VTT3(N)=AI31(N)*S1(N)+AI32(N)*S2(N)+AI33(N)*S3(N)+AI34(N)*S4(N)+AI
     135(N)*S5(N)+AI36(N)*S6(N)+AI37(N)*S7(N)
      VTT4(N)=AI41(N)*S1(N)+AI42(N)*S2(N)+AI43(N)*S3(N)+AI44(N)*S4(N)+AI
     145(N)*S5(N)+AI46(N)*S6(N)+AI47(N)*S7(N)
      VTT4(N)=AI61(N)*S1(N)+AI62(N)*S2(N)+AI63(N)*S3(N)+AI64(N)*S4(N)+AI
     165(N)*S5(N)+AI66(N)*S6(N)+AI67(N)*S7(N)
      VTT7(N)=AI71(N)*S1(N)+AI72(N)*S2(N)+AI73(N)*S3(N)+AI74(N)*S4(N)+AI
     175(N)*S5(N)+AI76(N)*S6(N)+AI77(N)*S7(N)
      VST1(N)=+(VTT1(N)+VT11(N))
      VST2(N)=+(VTT2(N)+VT12(N))
      VST3(N)=+(VTT3(N)+VT13(N))
      VST4(N)=+(VTT4(N)+VT14(N))
      VST5(N)=+(VTT5(N)+VT15(N))
      VST6(N)=+(VTT6(N)+VT16(N))
      VST7(N)=+(VTT7(N)+VT17(N))
  100 CONTINUE
      DO 211 N=1,K
      Z1(N)=(VP(N)-VT1(N))/(X1-X0)
      Z2(N)=(VT1(N)-VT2(N))/(X2-X1)
      Z3(N)=(VT2(N)-VT3(N))/(X3-X2)
      Z4(N)=(VT3(N)-VT4(N))/(X4-X3)
      Z5(N)=(VT4(N)-VT5(N))/(X5-X4)
      Z6(N)=(VT5(N)-VT6(N))/(X6-X5)
      Z7(N)=(VT6(N)-VT7(N))/(X7-X6)
      Z8(N)=VT7(N)/(X8-X7)
  211 CONTINUE
      DO 202 N=K+1,40
      Z1(N)=(V0-VST1(N))/(X1-X0)
      Z2(N)=(VST1(N)-VST2(N))/(X2-X1)
      Z3(N)=(VST2(N)-VST3(N))/(X3-X2)
      Z4(N)=(VST3(N)-VST4(N))/(X4-X3)
      Z5(N)=(VST4(N)-VST5(N))/(X5-X4)
      Z6(N)=(VST5(N)-VST6(N))/(X6-X5)
      Z7(N)=(VST6(N)-VST7(N))/(X7-X6)
      Z8(N)=VST7(N)/(X8-X7)
  202 CONTINUE
      WRITE(6,32)
   32 FORMAT(////////)
   55 WRITE(6,80)(N,T(N),VT1(N),VT2(N),VT3(N),VT4(N),VT5(N),VT6(N),VT7(N
     1),N=1,K)
   80 FORMAT(I5 ,5X, 8E15.3,/)
      WRITE(6,35)(N,T(N),VST1(N),VST2(N),VST3(N),VST4(N),VST5(N),VST6(N)
     1,VST7(N),N=(K+1),40)
   35 FORMAT(I5 ,5X, 8E15.3,/)
      WRITE(6,70)
   70 FORMAT(/////)
   66 WRITE(6,81)(N,T(N),VTT1(N),VTT2(N),VTT3(N),VTT4(N),VTT5(N),VTT6(N)
     1,VTT7(N),N=(K+1),40)
   81 FORMAT(I5 ,5X, 8E15.3,/)
      WRITE(6,133)
  133 FORMAT(////)
      WRITE(6,122)(N,VT11(N),VT12(N),VT13(N),VT14(N),VT15(N),VT16(N),VT1
     17(N),N=1,40)
  122 FORMAT(I5 ,5X, 7E15.3,/)
      WRITE(6,199)
  199 FORMAT(/////)
      WRITE(6,203)(N,T(N),Z1(N),Z2(N),Z3(N),Z4(N),Z5(N),Z6(N),Z7(N
     1),Z8(N),N=1,40)
  203 FORMAT(I5 ,5X, 9E10.2)
      STOP
      END
      FINISH
&DATA
 100.0 100.0  100.0  100.0  100.0  100.0  100.0
&END
```